The Effect of Calcium Interaction and Mineralization on the Properties of Poly(Aspartic Acid) Modified Polyplexes for Gene Delivery

by
Teo Atz Dick

A thesis submitted in partial fulfillment of the requirements for the degree of

Doctor of Philosophy
in
Materials Engineering

Department of Chemical and Materials Engineering

University of Alberta

Abstract

Mineralization is frequently studied as a biomimetic process, owing to the sophisticated architectures and superior mechanical properties of the resultant materials. Bone is a classical example – a nanostructured material with a complex hierarchical architecture that is capable of resisting heavy loads and supporting the biological function necessary for its maintenance. Arguably, gene delivery could also be approached biomimetically, as viruses are the most efficient cell transfecting agents, selected by nature to deliver its genetic material inside cells. The study of synthetic gene carriers as virus inspired materials might therefore bring new ideas for nanoparticle fabrication in gene related applications.

Recently, an unexpected property from viruses have been identified as an evolutionary advantage: the ability to become mineralized. A mineralized virus is more robust, with superior chance of survival when not infecting a host. When infecting a host, better adhesion and protection against the immune system are believed to confer superior infectivity. The new properties from mineralized viruses were proven to be translatable to therapeutic applications with success, generating viral vaccines and gene vectors with superior thermostability, immunization capability and transfection efficiency. However, the use of viral vectors is still unsafe, with many human deaths reported during clinical trials. For this reason, many believe that non-viral vectors could replace viral vectors as a safer option.

In this thesis, a route for the fabrication of a novel non-viral mineralized delivery system was proposed. The non-viral vector used was a polyplex system produced by the self-assembly of a low molecular weight, lipid-modified version of poly(ethylenimine) (PEI), considered by many as the gold standard in non-viral gene delivery. However, polyplexes of this type are highly positively charged and, as a consequence, non-mineralizable. Due to this

fact, poly(aspartic acid) (PAsp), a polyanion commonly used in the study of biomimetic bone mineralization was used to mediate the mineralization of the polyplexes. The mineralization strategy used was tailored for short incubation times necessary for effective gene delivery with polyplexes. Detailed physicochemical studies of every step of the fabrication method proposed were carried with the goal of providing a deep understanding of the phenomena responsible for particle properties. As a result of the approach taken, it was found that not only mineralized polyplexes are promising as new vectors, but also 'calcium incubated polyplexes', a particle that arose as an intermediated step of the fabrication route proposed.

It was found that mineralization with calcium carbonate and calcium phosphate are efficient in promoting transfection efficiency *in vitro* and increased robustness as long as a certain Ca^{2+} excess is given. Calcium incubation can be used to achieve similar effects in transfection efficiency at higher Ca^{2+} concentrations with lower achievement of robustness, depending on polyplex composition. It is proposed that the improved robustness and transfection efficiency provided by means of mineralization and calcium incubation in the presence of PAsp can be used to expand the possible applications of polyplexes in gene therapy.

Preface

Chapter 1 is a review paper published as T.A. Dick, E.D. Sone, H. Uludağ, Mineralized vectors for gene therapy, Acta Biomaterialia. 147 (2022) 1–33. I wrote the document and made the illustrations, and H. Uludag and E.D. Sone reviewed it.

Chapter 2 is published as T. A. Dick, H. Uludağ, Mineralized polyplexes for gene delivery: Improvement of transfection efficiency as a consequence of calcium incubation and not mineralization, Materials Science and Engineering: C. 129 (2021) 112419. I performed the experiments, wrote the document and made the illustrations, and H. Uludag reviewed it.

Chapter 3 is published as T. Atz Dick, H. Uludağ, A Polyplex in a Shell: The Effect of Poly(aspartic acid) Mediated Calcium Carbonate Mineralization on Polyplexes Properties and Transfection Efficiency, Molecular Pharmaceutics. (2022). I performed the experiments, wrote the document and made the illustrations, and H. Uludag reviewed it.

Chapter 4 has not been published yet. I wrote the document and made the illustrations, H. Uludag reviewed it.

This is dedicated to my father, Luis, and my mother, Vera, who sacrificed a lot so I could have a good education; my brothers, Pedro and João, who have always been great friends; and to my wife, Marina, who is always with me, no matter what happens.

Acknowledgements

I would like to thank the financial support from the CAPES funding agency.

I would like to thank Dr. Uludag for giving me the opportunity of doing this research, I'm grateful for that. I think the mixture of backgrounds resulted in something interesting and original.

I would like to thank all my colleagues from the lab.

I would to thank Cezary Kurscharski for giving me all the help needed with cell culture and the good conversations.

I would like to thank Sara Amidian and Dr. Sun from the Cross Cancer Institute, Arlene Oatway from the Biological Sciences Department, and my father Luis F. P. Dick for the information that, when put together, allowed me to prepare my difficult TEM samples.

I would like to thank Aja Rieger for the help with flow cytometry.

Table of Contents

1. Mineralized Vectors for Gene Therapy 3

1.1 Introduction 3

1.2 Background on Theories of Mineralization 5

1.2.1 Classical nucleation theory (CNT) 6
1.2.2 Modern nucleation theories 9
1.2.3 Application of nucleation theory for particle preparation 12

1.3 Gene Therapy and Involvement of Mineralized Vectors in Gene Delivery 14

1.3.1 Controlling Gene Expression 14
1.3.2 Endocytosis of NPs 16
1.3.3 Intracellular trafficking and calcium phosphate NP endosomal escape 17
1.3.4 Effect of NPs Physicochemical Properties in Biological Interactions 19

1.4 Fabrication of Nanoparticulate Mineral Vectors by co-Precipitation 27

1.4.1 Traditional co-precipitation method for NP vectors 27
1.4.2 Polymer-coated co-precipitated vectors 35
1.4.3 NP vectors by reverse micro-emulsion co-precipitation 45
1.4.4 Co-precipitation with simulated body fluid (SBF) 56

1.5 Co-Precipitation Formed Mineralized Surfaces for Gene Therapy 58

1.6 NPs from Non-Co-precipitated Systems 64

1.6.1 Solid core and multi-shell NPs 64
1.6.2 Mineralized pre-assembled NPs 72

1.7 Conclusion and Future Perspectives 81

1.8 References 87

2. Mineralized polyplexes for gene delivery: Improvement of transfection efficiency as a consequence of calcium incubation and not mineralization 119

2.1 Introduction 119

2.2 Materials and Methods 122

2.2.1 Materials 122
2.2.2 Particle Fabrication 123
2.2.3 Physicochemical and Morphological Characterization 124
2.2.4 DNA Binding Efficiency 125
2.2.5 Cell Culture 125
2.2.6 Flow Cytometry for Cell Uptake and Transfection Efficiency of Polyplexes 126
2.2.7 Statistical Analysis 127

2.3 Results 127

2.3.1 Binding and Dissociation of Polyplexes. 127
2.3.2 Particle Hydrodynamic Size and Zeta-potential Analysis 130
2.3.3 Particle Morphology Analysis 131
2.3.4 Particle Phase Analysis 134
2.3.5 Transfection Efficiency 135

2.4 Discussion 140

2.5 Conclusions 151

2.6 References 151

3. A Polyplex in a Shell: The Effect of Poly(aspartic acid)-Mediated Calcium Carbonate Mineralization on Polyplexes Properties and Transfection Efficiency 158

3.1 Introduction 158

3.2 Materials and Methods 160

3.2.1 Materials 160
3.2.2 Poly(aspartic acid) mediated mineralization of polyplexes 160
3.2.3 Particle size and z-potential analysis by light scattering 162
3.2.4 Transmission electron microscopy 163
3.2.5 Energy dispersive x-ray spectroscopy 163
3.2.6 Agarose gel retardation assay 163
3.2.7 Cell Culture and transfection efficiency studies using flow cytometry 164
3.2.8 Statistical Analysis 165

3.3 Results and Discussion 165

3.3.1 Initial characterization of pAsp-coated polyplexes 165
3.3.2 Calcium incubation and mineralization of polyplexes 171
3.3.3 Transfection Studies 183

3.4 Conclusions 188

3.5 References 189

4. General Discussion and Conclusions 195

4.1 The importance of surface charge for nucleation and materials fabrication 198

4.2 Future perspectives and studies 201

4.3 References 207

References 214

Chapter 1 214

Chapter 2 245

Chapter 3 251

Chapter 4 256

List of Tables

Table 1-1 Targeting ligands employed on mineralized vectors. 26
Table 1-2 Benefits and limitations of each mineralized delivery vector reviewed 30
Table 1-3 Main in vivo studies reviewed published after 2010. SC: Subcutaneous, IV: Intravenous, IM: Intramuscular, IP: Intraperitoneal 31
Table 1-4 Main factors affecting the transfection efficiency from mineral layers 63
Table 1-5 Solid core/multi-shell NP size as a consequence of functionalization/extra-mineral layers. 71
Table 2-1 Composition of the polyplexes submitted to treatment. 124
Table 4-1 A summary of properties as a consequence of each step of the fabrication process. 196

List of Figures

Figure 1.1 Nucleation according to the CNT. An energy barrier is a result of a negative bulk free energy and a positive interface free energy. Due to density fluctuations, cluster forms and dissolve until a metastable nucleus is achieved, with critical radius r. The barriers for heterogeneous and homogeneous nucleation are represented as* ΔGhet* *and* ΔGhom* 7
Figure 1.2 Nucleation models for CaCO3 as proposed by [33] (top) and [32] (bottom) 11
Figure 1.3 DNA mineralization. (a) The negatively charged phosphate groups in DNA attract the free calcium ions in solution; (b) With the addition of a phosphate or carbonate salt, nucleation of a mineral phase takes place in association with DNA; (c) With the growth of the mineral phase, co-precipitation occurs, and DNA can be encapsulated inside a mineralized NP. 14
Figure 1.4 Mineralized NP uptake by endocytosis. Acidification of the endosome triggers NP dissolution as a result of increased mineral solubility, releasing the polynucleotide and increasing osmotic pressure in the endosome. Endosome rupture results in polynucleotide escape into the cytoplasm. 19
Figure 1.5 Summary of physicochemical properties affecting NP uptake. 21
Figure 1.6 Two methods for stabilizing co-precipitated NPs. Method I: a PEG-polyanion conjugate is present during co-precipitation, binding to Ca^{+2} *before nucleation. Method II: a bisphosphonate-PEG conjugate is added after co-precipitation and binds to* Ca^{+2} *at the particle surface. Both methods result in PEG-stabilized NPs.* 37
Figure 1.7 Effect of polymeric additives on the transfection efficiency of siRNA polyplexes. Polyplexes were formed with 1.2 kDa lipid-grafted PEI, and a fixed ratio of HA was added to the polyplexes during complex formation. The numbers on the horizontal axis indicate HA:siRNA ratio used for polyplex formation. The specific siRNA against CDC20 is used to inhibit the growth of breast cancer cells in this study. Note that at optimal HA:siRNA ratios (i.e., 0.1 to 2), increased inhibition of cell growth was seen with CDC20 siRNA, while the control scrambled siRNA (CsiRNA) did not show any growth inhibition. Data adapted from[198]. 45
Figure 1.8 NP fabrication by microemulsion. After two separate microemulsions are mixed, the formation of dimers by droplet coalescence results in solution exchange and nucleation. Growth can occur by coalescence or coagulation. 47
Figure 1.9 Fabrication of lipid-coated NPs (adapted from [40]) 50
Figure 1.10 Mineralized surfaces incorporating DNA can be produced by exposing a surface with appropriate nucleation sites to SBF in the presence of DNA (top). NPs can be produced from suitable templates (e.g., DNA) using short incubation times, avoiding aggregation (bottom) 59
Figure 1.11 Effect of grain size and solubility in the release of DNA from a mineralized layer. (a) Larger, more soluble crystals as a consequence of higher Mg^{2+} *content result in the release of DNA unprotected. (b) Small, less soluble crystals in the absence of* Mg^{2+} *and increased* Ca^{2+} *content result in the release of mineralized DNA NPs [240]* 61
Figure 1.12 Different types of multi-shell NPs. (a) CaP/pDNA/PEI[104,259]. (b) CaP/pDNA/Protamine/CaP[162,270] . (c) CaP/PEI/pDNA/Silica[271]. 67
Figure 1.13 (a) TEM image of mineralized stPEI/DNA complexes without indication of the presence of heterogeneous morphology. (b) Gel electrophoresis shows a decrease in the robustness of mineralized complexes[301]. TEM of (c) nonmineralized (HA-NP) and (d) mineralized hyaluronic acid nanoparticles (MHA-NP) carrying doxorubicin, with the indication of successful controlled particle mineralization by heterogeneous morphology of particles. In (e), the cumulative release of HA-NP and MHA-NP at different pH indicates increased robustness as a consequence of mineralization at pH 7.4 and 6.5 [282]. 79
Figure 1.14 Mineralization of lipid-modified PEI/pDNA polyplexes mediated by poly(aspartic acid) (PAsp) from [155]. ***1.*** *Polyplexes are positively charged.* ***2.*** *PAsp adsorption shifts the surface charge to negative and enables the chelation of* Ca^{2+}. ***3.*** *Mineralization occurs at the surface of the polyplexes by the addition of a phosphate salt (*Na_3PO_4*). The resultant nanoarchitecture is believed to be a polyplex inside a mineral shell (top right), which is in accordance with the TEM image from the polyplexes (bottom). The shell-core morphology observed is a consequence of the contrast between the less dense organic core (polyplex) and the dense mineral shell [155].* 81
Figure 2.1 Electrophoretic gel mobility assay for mineralized and unmineralized samples at various $CaCl_2$ *and* Na_3PO_4 *concentrations. (a) Electrophoretic gel mobility assay for mineralized samples with the final concentration of 0.047 µg/µL ALL-Fect. (b) Electrophoretic gel mobility assay for mineralized samples with*

the final concentration of 0.047 µg/µL ALL-Fect after incubation with heparin for 1 h. (c) Electrophoretic gel mobility assay for mineralized samples with the final concentration of 0.063 µg/µL ALL-Fect. (d) Electrophoretic gel mobility assay for mineralized samples with the final concentration of 0.063 µg/µL ALL-Fect after incubation with heparin for 1 h. (e) Electrophoretic gel mobility assay for calcium incubated samples. (f) Electrophoretic gel mobility assay for calcium incubated samples after incubation with heparin for 1h. *128*
Figure 2.2 Hydrodynamic size, PDI and z-potential after each step of the particle fabrication process. (a) Hydrodynamic size, (b) PDI, and (c) z-potential after polyplex formation, PAsp coating, $CaCl_2$ incubation and mineralization at 0.047 µg/µL ALL-Fect. (d) Hydrodynamic size, (e) PDI, and (f) z-potential after polyplex formation, PAsp coating, $CaCl_2$ incubation and Mineralization at 0.063 µg/µL ALL-Fect. *131*
Figure 2.3 TEM images of (a)PAsp coated polyplexes, (b) CaCl2 incubated, PAsp coated polyplexes. and (c) mineralized PAsp coated polyplexes at ALL-Fect concentration of 0.047µg/µL. Size distribution diagram for PAsp coated polyplexes (d), and (e) mineralized PAsp coated polyplexes. *132*
Figure 2.4 TEM images of (a) PAsp coated polyplexes, (b) $CaCl_2$ incubated, PAsp coated polyplexes. and (c) mineralized PAsp coated polyplexes at ALL-Fect concentration of 0.063 µg/µL. Size distribution diagram for PAsp coated polyplexes (d), and (e) mineralized PAsp coated polyplexes. *134*
*Figure 2.5 X-ray diffraction analysis of the mineralized polyplexes and the control (precipitation reaction without polyplexes) at 10 mM $CaCl_2$ and 1.1 Na_3PO_4. Peaks relative to the substrate are indicated with *.* *135*
*Figure 2.6 Transfection efficiency of $CaCl_2$ incubated and mineralized polyplexes carrying pDNA encoding for GFP: (a) GFP-positive population and median fluorescence intensity of MC3T3-E1 cells transfected. (b) Fluorescence images from MC3T3-E1 cells with different Ca^{2+} and PO_4^{3-} contents. *p<0.05 compared with calcium incubated sample (0 mM $PO4^{3-}$) with same calcium concentration.* *137*
*Figure 2.7 Transfection efficiency of $CaCl_2$ incubated and mineralized polyplexes carrying pDNA encoding for GFP: (a) GFP-positive population and median fluorescence intensity of MC3T3-E1 cells transfected. (b) Fluorescence images from MC3T3-E1 cells with various Ca^{2+} and PO_4^{3-} contents. *p<0.05 compared with calcium incubated sample (0 mM $PO4^{3-}$) with same calcium concentration.* *138*
*Figure 2.8 Uptake of $CaCl_2$ incubated and mineralized polyplexes carrying Cy3-labeled pDNA: (a) Cy3-positive population and (b) MFI of transfected MC3T3-E1 cells. *p<05 compared with calcium incubated sample (0 mM $PO4^{3-}$) with same calcium concentration.* *139*
Figure 2.9 GFP transfection efficiency (MFI) at days 4 and 9 of unmineralized negatively charged polyplexes, calcium incubated polyplexes and mineralized polyplexes in MC3T3-E1 cells *140*
Figure 2.10 Steps leading to final structure of mineralized polyplexes: 1 – Positively charged polyplexes are formed by complexation of pDNA and the cationic PEI; 2 – Coating polyplexes with PAsp changes zeta-potential to negative, preparing particles to interact with Ca^{2+}, and leads to particle rearrangement and increase in PDI; 3 – Interaction with Ca^{2+} neutralizes part of the negative charges leading to aggregation of particles and increase in size and PDI, and concentration of Ca^{2+} around the particles ensures PAsp associated precipitation; 4 – Ionic reaction with PO_4^{3-} leads to calcium phosphate precipitation in association with the PAsp layer, increased negative surface charge and aggregation. The resulting morphology is schematically represented in the right *147*
Figure 3.1 Scheme of the fabrication process of mineralized $CaCO_3$ mineralized polyplexes *162*
Figure 3.2 Effect of pAsp content analyzed by DLS and ELS: (a) Intensity weighted particle size distribution of polyplexes with ALL-Fect/pDNA=7.5 and pAsp/pDNA=(0.5–3); (b) Intensity weighted particle size distribution ALL-Fect/pDNA=10 and pAsp/pDNA=(0.5–3); (c) Hydrodynamic diameter and PDI of polyplexes with ALL-Fect/pDNA=7.5 and pAsp/pDNA=(0.5-3); (d) Hydrodynamic diameter and PDI of polyplexes with ALL-Fect/pDNA=10 and pAsp/pDNA=(0.5-3); (e) z-potential of ALL-Fect:pDNA=7.5 and pAsp/pDNA=(0.5-3) and (f) z-potential of ALL-Fect/pDNA=10 and pAsp/pDNA=(0.5-3) *166*
Figure 3.3 TEM images of :(a) uncoated polyplexes with pDNA:ALL-Fect=1:7.5 (stained); (b) pAsp coated polyplexes with pDNA:ALL-Fect:pAsp=1:7.5:1 (P1); (c) uncoated polyplexes with pDNA:ALL-Fect=1:10 (stained); and (b) pAsp coated polyplexes with pDNA:ALL-Fect:pAsp=1:10:2 (P2). *169*
Figure 3.4 Effect of $CaCl_2$ incubation on pAsp coated polyplexes analyzed by ELS and DLS: (a) Intensity weighted particle size distribution of polyplexes with P1; (b) Intensity weighted particle size distribution of P2; (c) Hydrodynamic diameter and PDI of polyplexes with ALL-P1; (d) P2; (e) z-potential of P1; and (f) z-potential of P2. ..... *172*
Figure 3.5 TEM of calcium incubated P1 (pDNA:ALL-Fect:pAsp=1:7.5:1) *174*

Figure 3.6 Effect of mineralized content on pAsp coated polyplexes analyzed by ELS and DLS: (a) Intensity weighted particle size distribution of P1; (b) Intensity weighted particle size distribution P2; (c) Hydrodynamic diameter and PDI of P1; (d) Hydrodynamic diameter and PDI of P2; (e) z-potential of P1; and (f) z-potential of P2 175
Figure 3.7Effect of mineralized content in the protection against heparin induced dissociation (0.7 mg/mL) analyzed by gel electrophoresis 177
Figure 3.8 (a) Scanning Electron Microscopy (SEM) of particles prepared with pDNA:ALL-Fect:pAsp = 1:7.5:1 and mineralized with 10 mM $CaCl_2$ and 1.1 mM Na_2CO_3. Scale bars = 10 µm (lower magnification image) and = 1 µM (higher magnification image). (b) Electron dispersive x-ray spectroscopy (EDS) of the area highlighted on the higher magnification image and substrate without particles. Mass ratios of the elements are indicated. 179
Figure 3.9 TEM images of polyplexes mineralized with 5 mM $CaCl_2$ and 0.7 mM Na_2PO_4: (a) P1 and particle sizes measured on the same image; and (b) P2 and particle sizes measured on the same image. Scale bars = 1 µm 180
Figure 3.10 TEM images of mineralization using 5 mM $CaCl_2$ and 0.7 mM Na_2CO_3 of: (a) P1 (scale bar = 200 nm); (b) P1 at higher magnification (scale bar = 200 nm); (c) Inverse of Z-contrast values from the selected area in previous figure; (d) P2 (scale bar = 500 nm); (e) P2 at higher magnification (scale bar = 200 nm); (c) Inverse of Z-contrast values from the selected area in previous figure. 181
Figure 3.11 Proposed mechanism for mineralization 183
*Figure 3.12 Transfection efficiency of mineralized polyplexes on MC3T3 cells as the GFP positive population (top graphs) and the mean fluorescence intensity. (MFI, bottom graphs). The specific rations for the complexes prepared with pDNA, ALL-Fect and pAsp are indicated on top of each graph. $p \leq 0.05$ is indicated as *, $p \leq 0.001$ as ***, and $p \leq 0.0001$ as ****.* 185
*Figure 3.13 Transfection efficiency of mineralized polyplexes on MDA-MB 231 cells as the GFP positive population (top graphs) and the mean fluorescence intensity. (MFI, bottom graphs). The specific rations for the complexes prepared with pDNA, ALL-Fect and pAsp are indicated on top of each graph. $p \leq 0.05$ is indicated as *, $p \leq 0.001$ as ***, and $p \leq 0.0001$ as ****.* 185
Figure 4.1 Fabrication of a PEG, targeting ligand-functionalized mineralized polyplex for gene delivery.. 204

Scope

In this thesis, the effect of mineralization on polyplexes as non-viral gene delivery vectors is investigated. Polyplexes tend to be the most effective when they are positively charged. However, mineralization demands a highly negative surface charge to occur at the surface of particles. Mineralization at low supersaturations with the help of nucleators is necessary for a controlled mineralization process.

A comprehensive review of the literature regarding the application of mineralization in gene delivery is presented in Chapter 1. The very basic fundamentals that are necessary to understand the extensive body of work was reviewed. Classical nucleation theory, with a focus on phase transition from ionic solutions, and the most accepted modern mineralization theories, were reviewed. Cell uptake mechanisms and the influence of nanoparticle properties on uptake were also discussed. Although the number of applications employing mineralization in gene delivery is extensive, a clear look over the whole field was possible by categorizing the literature in terms of the resultant nanoarchitecture of the mineralized vectors, which were recognized to be just a few. Vector properties were related to the many medical applications, and when possible, qualitative and quantitate data were discussed. Finally, a future perspective of the field was given, presenting the current challenges for reaching the clinical application using mineralized vectors and proposing solutions based on the potential of the state-of-the-art technologies reviewed.

Chapters 2 and 3 contain the experimental investigation of the effects of mineralization of polyplexes for gene delivery. In Chapter 2, calcium phosphate mineralized polyplexes were studied. The aim of this study is to test the hypothesis that polyplexes can be mineralized by polyplex charge manipulation and to study the effect of mineralization on polyplex

properties. Calcium incubated polyplexes were used as controls to isolate the effect of mineralization. After proving that the mineralization was achieved, it was observed that while mineralization could protect the polyplexes against dissociation, mineralization was not capable of inducing superior transfection efficiency compared to calcium incubation.

In chapter 3, a mineralization strategy was developed based on polyplex mineralization by calcium carbonate. In this study, a buffer was not used due to the high ionic content, which resulted in increased agglomeration and growth of the nanoparticles in the previous study. Also, avoiding the use of a buffer during mineralization allows for studying the effect of calcium incubation and mineralization without the confounding effect of the components of the buffer. In this chapter, the effect of poly(aspartic acid) over the polyplex properties and calcium incubation was studied in-depth, and ideal poly(aspartic acid) coated polyplex formulations for reduced size after mineralization were proposed. An in-depth study of the morphology of the polyplexes was performed, and a basic polyplex mineralization mechanism was proposed.

Chapter 4 is the conclusions of the thesis, considering what was found in Chapters 2 and 3. Future perspectives for the application of the technology developed are given, and future studies are proposed based on the knowledge generated in this thesis.

1. Mineralized Vectors for Gene Therapy

1.1 Introduction

The history of medicine is marked by changes in the approach to illness and disease in response to discoveries and developments of new materials and technologies. Some of these technologies have such broad applicability that they impact multiple fields of study. Gene therapy represents such a significant breakthrough for treating several human diseases. In gene therapy, concepts of cell biology and materials chemistry are condensed to develop strategies for the delivery of gene medicines in the treatment of a wide range of medical conditions, including cancer treatment[1], tissue engineering[2], genetic disorders, and infectious diseases[3].

Almost 50 years ago, gene therapy piqued the interest of researchers due to the promising and straightforward principle upon which it was founded[4]: a disease could be treated by delivering functional genes to a cell and inducing the expression of the desired protein, correcting a defective gene. Later, the inhibition of gene expression also became a possibility by the discovery of RNA interference[5–7]. The application of these principles in clinical practice, however, is complicated: the delivery of polynucleotides to specific cells necessitates the development of vectors (or carriers) with specific tissue targetability, the ability to protect polynucleotides from degradation by nucleases, and low immunogenicity[8]. Viral vectors became a predominant option since viruses naturally present many features necessary for the highly efficient delivery of their genetic cargo. The gene therapy field was propelled in the following decade with a successful first clinical trial in 1990 using a viral vector. However, many patients were observed to develop adverse

effects with the more widespread use of viruses. In 1999, a patient died after suffering multiple organ failure as a consequence of a robust systemic inflammatory response to the virus capsid[9]. This, in addition to other casualties, raised severe concerns for the safety of gene therapy, especially with the use of viral vectors, illustrated by an abrupt decline in investments that lasted almost a decade[10]. Such unexpected tragedies propelled the research for the development of safe and effective vectors from non-viral means.

Non-viral vectors offer many advantages over viral vectors. Made up of well-characterized, usually synthetic materials, they display low immunogenicity, low production cost, and properties that can be precisely controlled by tuning the material composition and structure. However, non-viral vectors are still less efficient than their viral counterparts. Various synthetic vectors have been tried in gene therapy: gold nanoparticles (NPs)[11], carbon nanotubes[12], magnetic particles[13], cationic lipids[14] and calcium phosphate (CaP) are a few example[15]. Among these, CaP and other mineralized vectors are probably the safest options. With the negligible toxicity of its constituents, CaP is well tolerated in the body, being the main component of bones and teeth, and frequently used in bone tissue regeneration therapy due to its bioactivity and safety[16]. Furthermore, CaP NPs encapsulating polynucleotides can be easily synthesized by wet chemical synthesis using calcium and phosphate salts in a co-precipitation method[17]. The same is true for other mineralized vectors, such as calcium carbonate[18,19] and magnesium phosphate[20,21]. However, without a rigorous optimization, the traditional co-precipitation method to create CP materials presents serious disadvantages compared to other non-viral vectors, such as lack of control over particle size under storage, low reproducibility, and high dependence of

efficiency on the details of the synthesis reaction, which frequently results in low efficiency compared to other non-viral vectors cationic lipids and polycations[22].

Fortunately, over the last two decades, innovations in inorganic materials synthesis allowed researchers to experiment with new methods for the production of mineralized vectors. Once adapted to the production of mineralized gene vectors, these could be used to overcome the main drawbacks of the co-precipitation method, starting a new era of *in vitro* studies that eventually led to numerous successful attempts *in vivo* [23–26]. Part of this success comes from the modification of NP synthesis processes in a way that organic molecules could be added to the surface of materials, generating hybrid vectors capable of synergic actions with other transfection reagents and targetability to specific cell types.

Distinct from the times when traditional co-precipitation was the sole option available for CaP particle fabrication, the scientific scene now is marked by various mineralized delivery systems for gene therapy, each presenting a characteristic nanoarchitecture as a fingerprint of its fabrication method. Here, confident that the renaissance of mineralized vectors emerged as a consequence of new fabrication methods, we propose a different perspective for categorizing recently emerging literature based on the mineralization strategy and, therefore, resultant nanoarchitecture. The focus of this review is maintained on CaP since this is the most utilized material among the mineralized vectors; however, when possible, other mineralized vectors of importance are discussed. Therapeutic applications of gene therapy using Ca/P surfaces and NPs are presented below with an eye on structure-function relationships.

1.2 Background on Theories of Mineralization

All transfection systems discussed in this review concern the synthesis of solid precipitates in aqueous solutions that contain the ions and form a solid. Precipitation involves the process of nucleation (start of the new phase), followed by the growth of the nucleated phase. In this work, when discussing the literature, we used the term mineralization for the heterogeneous or molecular templated nucleation of a mineral followed growth. The term 'biomimetic' was used to describe mineralization performed with the idea of mimicking a biological process, when this term was used by the authors of the work cited. In this section, we review the main concepts of the classical nucleation theory, modern theories of nucleation, and their applications.

1.2.1 Classical nucleation theory (CNT)

The classical nucleation theory is founded on the works of Becker and Doring[27], Frenkel[28], and Volmer and Weber[29]. According to the CNT, the energy barrier for nucleation results from opposing energetic contributions that arise when clusters form in solution. In solution before nucleation, the constituent atoms or molecules that form the solid have a higher degree of freedom, which results in density fluctuations. Upon collision, these components are joined in close-packed, short-lived clusters with an atomic organization that coincides with that of the crystal phase. Upon the formation of the new cluster, there is a formation of a new solid-liquid interface, which is accompanied by an increase in the interfacial energy of the new phase proportional to the square of the radius (r) of the cluster (Fig. 1.1). Accordingly, a decrease in the free energy related to the bulk of the new phase is observed, which is proportional to r^3. In Eq. 1, the total free energy ΔG is given as the sum of these two contributions, where γ is the surface free energy and ΔG_v is the bulk free energy.

The bulk free energy is dependent on the Boltzmann constant k_B, temperature T, supersaturation S and the crystal volume v (Eq. 2)

$$\Delta G = 4\pi r^2 \gamma + \frac{4}{3}\pi r^3 \Delta G_v \quad (1)$$

$$\Delta G_v = \frac{-k_B T \ln(S)}{v} \quad (2)$$

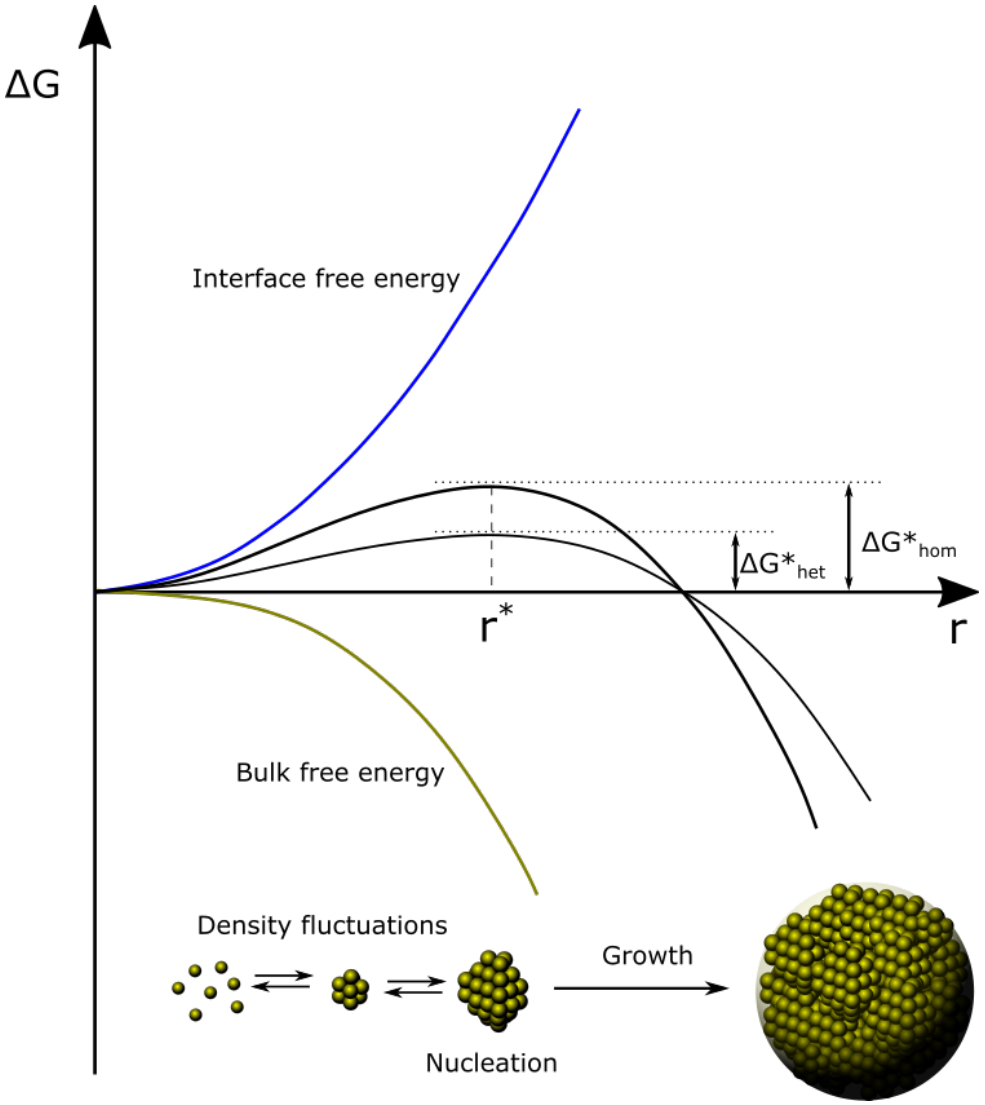

Figure 1.1 Nucleation according to the CNT. An energy barrier is a result of a negative bulk free energy and a positive interface free energy. Due to density fluctuations, cluster forms and dissolve until a metastable nucleus is achieved, with critical radius r. The barriers for heterogeneous and homogeneous nucleation are represented as ΔG^*_{het} and ΔG^*_{hom}.*

These opposing contributions create what is known as the nucleation barrier for nucleation, related to a critical radius r^*. At r^*, a metastable state is achieved ($d\Delta G/dr = 0$, $d^2\Delta G/dr^2 < 0$), and this is known as the critical nucleus. The free energy of the system is lowered by the dissolution of subcritical clusters. At the same time, for any infinitesimal increase in size beyond the critical cluster size, the decrease in free energy is achieved by the growth of nuclei and the formation of the solid phase. The free energy related to the critical nucleus ΔG^* is the energy barrier for nucleation, given in Eq. 3, while the critical radius r^*, is given in Eq. 4.

$$\Delta G^* = \frac{4}{3}\pi\gamma r^{*2} \quad (3$$

$$r^* = \frac{-2\gamma}{\Delta G_v} = \frac{2\gamma v}{k_B T\ lnS} \quad (4)$$

With the system reaching supersaturation and, therefore, sufficient thermodynamic driving force, nucleation occurs. The nucleation rate J represents the number of new nuclei per unit time per unit volume and is expressed in an Arrhenius type equation (Eqs 5 and 6):

$$J = A\ exp\left(-\frac{\Delta G^*}{k_B T}\right) \quad (5)$$

$$J = A\ exp\left(-\frac{16\pi\gamma^3 v^2}{3k_B^3 T^3 (\ln S)^2}\right) \quad (6)$$

where A is the pre-exponential factor specific to the material investigated. From Eq. (6), the only experimental parameters that can be varied are temperature, supersaturation, and surface energy. This means that at a fixed temperature for a given material, which is the most common experimental setup, supersaturation is the main parameter influencing nucleation.

The ability to accelerate or slow nucleation by controlling supersaturation is especially useful when the energy barrier for nucleation can be lowered by introducing heterogeneous nucleation. When the probability of formation of the nuclei is evenly distributed in the system, 'homogeneous' nucleation results. Otherwise, 'heterogeneous' nucleation occurs, which indicates specific conditions in the system capable of lowering the nucleation barrier for the same critical radius among the nucleating species. The energy barrier for homogeneous nucleation can be seen as an upper energetic limit for nucleation, while the heterogeneous nucleation barrier represents a lowering of the energy barrier by agents that are capable of facilitating nucleation. Heterogeneous nucleation can be caused by diverse agents from the environment, including unwanted species, such as bubbles, dust, or the walls of the reaction vessels. However, agents with high affinity towards the constituents in the solution can be added to significantly facilitate nucleation compared to unavoidable factors. We can correlate the homogeneous and heterogeneous nucleations by:

$$\Delta G^*_{het} = \Delta G^*_{hom}\, f(m)$$

where f(m) is the correlation factor that describes the lowering of the nucleation barrier caused by the nucleating agent, and m is a function of the interfacial free energy. f(m) assumes values between 0 and 1; the closer to 0, the better match and the larger the lowering of the nucleation barrier.

1.2.2 Modern nucleation theories

From the material synthesis perspective, the concept of an energy barrier that can be lowered by the use of specific agents is crucial for the design of hybrid materials with control at the nanoscale. However, the CNT in its pure form fails to explain many of the

experimental observations at the early stages of nucleation, such as the formation of amorphous solid intermediates instead of the most thermodynamically stable crystal [30]. Additionally, the assumption made within the CNT that the nucleating clusters are pseudo phases with similar interfacial energetics to the stable crystal leads to miscalculations of the energy barrier for nucleation and, as a consequence, the inability to correctly predict nucleation rates [31]. The CaP and carbonate systems are good examples in which amorphous intermediates can nucleate prior to the most thermodynamically stable crystal, depending on the synthesis parameters [32]. The nucleation in these two systems has been a source of great debate in recent publications, in which two approaches seem to be pursued. The first approach is dedicated to correcting discrepancies or over-simplifications of the CNT, preserving the main theoretical framework and concepts [30,33]. The second approach proposes a non-classical nucleation pathway, in which the idea of a metastable cluster as nucleation species is abolished [34].

In mid-1970s, the idea of nucleation by cluster aggregation had been already proposed by Posner and Betts for CaP formation [35]. Posner postulated that small close-packed clusters with a $Ca_9(PO_4)_6$ configuration would aggregate to form the amorphous calcium phosphate (ACP) precursor, which would later transform into hydroxyapatite (HAp). Precursors coinciding with Posner's model would later be reported by others [36,37]. In 2008, Gebauer and co-workers [34] proposed a nucleation path for $CaCO_3$ based on the aggregation of stable pre-nucleation clusters (PNC) (Fig. 1.2). With titration under stable pH with ion-selective electrodes and analytical ultracentrifugation, it was observed that ~75% of calcium was bound before nucleation in what was described as stable nanometric species. According to this definition, PNCs do not present interfacial energy with the liquid, being

considered stable solutes [32]. PNC would also be present in undersaturated solutions. Under super-saturation, the PNCs would aggregate to form an amorphous precursor, which later would transform into the stable crystal phase.

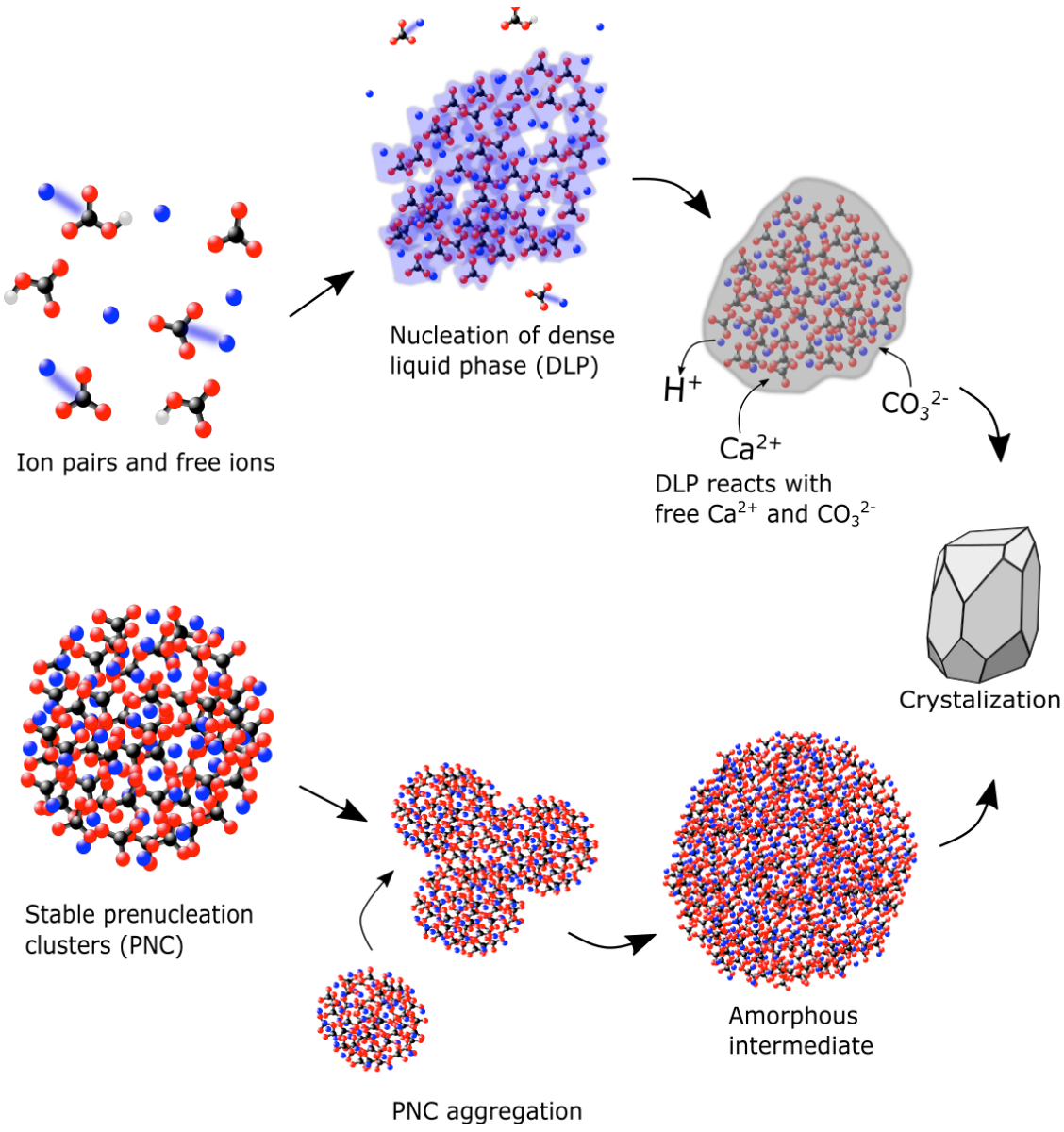

Figure 1.2 Nucleation models for CaCO3 as proposed by [33] (top) and [32] (bottom).

Other authors proposed mechanisms that are framed around classical concepts. Smeets and co-workers[33] performed a comprehensive study in $CaCO_3$ nucleation, revisiting the

techniques employed by Gebauer, in addition to cryo-TEM and computer simulations [33]. Indeed, most calcium ions were found to be bound before nucleation, in agreement with Gebauer results [34]. However, based on dynamic light scattering results and computer simulations, it was proposed that the pre-nucleation species are free ions and ion pairs, with more complex ionic structures being the consequence of density fluctuations.[33]. TEM analysis showed the presence of a submicrometric dense liquid-like phase prior to solid formation. The authors proposed a nucleation mechanism explained by classical concepts, in which liquid-liquid separation by nucleation and growth within the binodal regimen would originate a dense amorphous liquid phase (DLP) and a lean ionic solution both containing ion pairs alongside free ions (Fig. 1.2). A growth mechanism involving intermediate phases would lead to dehydration of the dense liquid phase and vaterite formation. Single calcium ion associates were also proposed for CaP as pre-nucleation species in the form of $[Ca(PO_4)_3]^{4-}$[30]. TEM analysis showed inorganic polymeric structures, which were proposed to form by the association of clusters. A correction of the CNT, in which interfacial free energy dependence with particle size is taken into account, was used to explain the polymeric structures and to re-calculate the energy barrier for nucleation, placing the energy barrier for ACP at lower values than the energy barrier for apatite, indicating the formation of ACP as the first solid phase. The degree of validity of the CNT and the exact mechanism of nucleation seem to be an open debate.

1.2.3 Application of nucleation theory for particle preparation

The fabrication of mineralized particulate systems for gene therapy greatly depends on the correct understanding of the effect of macromolecules on nucleation and growth control.

The nucleation process can be seen as a "yes or no" process; 'yes' if super-saturation is high enough for driving nucleation and 'no' if it is not. However, the possibility of lowering the energy barrier for nucleation transforms the nucleation process into a "yes or no, and where" process, opening the possibility to fabricate materials with complex nanoarchitecture. This comes from the fact that when species concentration is kept low enough to inhibit homogeneous nucleation, the lowering of the energy barrier at specific locations by adding nucleation sites can locally generate a supersaturated status, limiting nucleation to specific sites through heterogeneous nucleation. Negatively charged chemical groups in macromolecules and surfaces can work as sites for heterogeneous nucleation for calcium minerals. For instance, in polynucleotide mineralization, the negatively charged phosphate groups in polynucleotides strongly interact with calcium in solution. With the addition of a phosphate or carbonate salt to a polynucleotide/calcium salt solution, CaP or $CaCO_3$ can be co-precipitated with the polynucleotide, forming NPs capable of transfecting cells[38][39] (DNA mineralization is represented in Fig. 1.3).

With nucleation, supersaturation is abruptly reduced, and with the use of strategies to limit the access of free ions to the particle surface, growth and aggregation can be controlled. Removing the particles from solution by centrifugation[40] or removing free ions by dialysis[41] are commonly used methods to control growth; however, most applications demand a tight control over size, which can be done by methods that confine the synthesized particles. Particles can be confined by the use of block copolymers (displaying a combination of distinct features), which can be present during or immediately after nucleation, adsorbing to the particle surface, and occupying the available sites for growth[25]. Methods using reverse microemulsion confine the particle inside a droplet in a hydrophobic solvent, limiting

growth by the size of the droplet and by surfactant adsorption[42,43]. Confinement can also be exerted by a gas phase, as in spray pyrolysis[44].

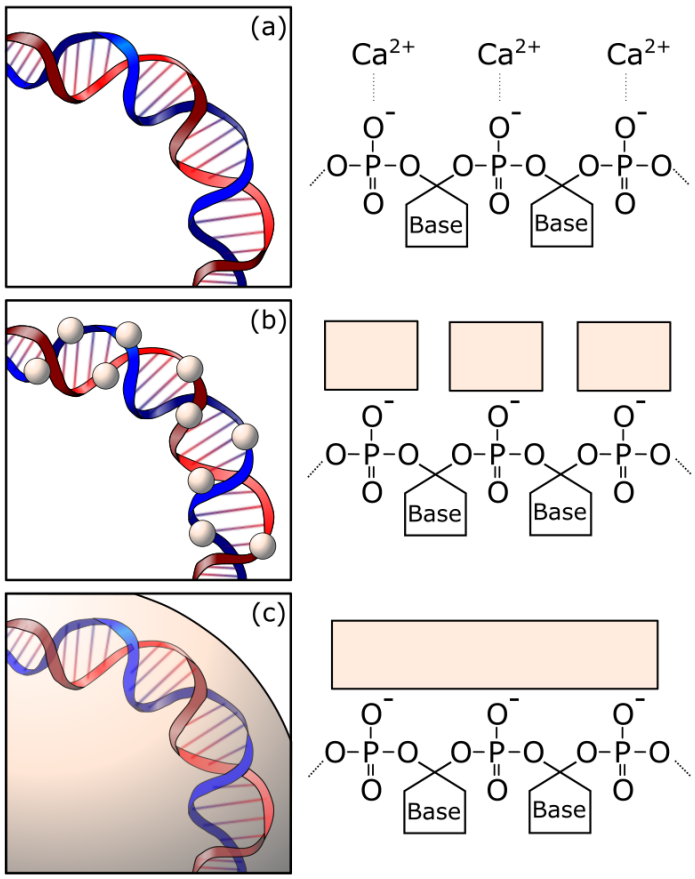

Figure 1.3 DNA mineralization. (a) The negatively charged phosphate groups in DNA attract the free calcium ions in solution; (b) With the addition of a phosphate or carbonate salt, nucleation of a mineral phase takes place in association with DNA; (c) With the growth of the mineral phase, co-precipitation occurs, and DNA can be encapsulated inside a mineralized NP.

1.3 Gene Therapy and Involvement of Mineralized Vectors in Gene Delivery

1.3.1 Controlling Gene Expression

Gene therapy is a versatile option to treat many conditions using cells' own machinery to control protein production by promotion or inhibition of gene expression. In both cases, for appreciable efficiency of treatment, the polynucleotide cargo must be protected and

delivered intracellularly. Protein production takes place in two steps: transcription, which takes place in the nucleus, and translation, which takes place in the cytoplasm. Accordingly, depending on the polynucleotide cargo and in which step it acts, the intracellular target might vary[45,46]. Promotion of expression is done by delivering DNA (or, more recently, mRNA) intracellularly in its different forms, such as plasmids, minicircles, or minivectors, and others[8,47,48]. We encourage the reader to consult the effect of DNA vector properties on transfection efficiency in references [8,49,50]. The transcription of the exogenous DNA sequence depends on the cell's own machinery inside the nucleus. This demands protection of the cargo against the cell's natural defenses upon endosomal uptake, effective endosomal escape, and unpacking that allows for transcription inside the nucleus. Molecular entry inside the nucleus happens through the nuclear pore complex. It is not very well understood how to target specific parts of the cell or what is the nature of the species after endosomal scape; however, it seems like entry is affected by the original size of the NPs and the presence of nuclear localization sequences[51]. The diameter of the central nuclear pore complex core is thought to be ~30 nm. However, particles significantly larger than that – or the reminiscent species after endosomal scape – are found to be taken up inside the nucleus once tagged with nuclear delivery sequences [52]. It is also reported that NPs can reach the nucleus during cell mitosis, which would explain the nuclear delivery of larger particles[53].

Inhibition of expression, or gene silencing, on the other hand, could happen at the post-transcriptional step of the protein production process. It is most frequently executed by means of ribonucleic acid interference (RNAi) using small interfering RNA (siRNA) or micro RNA (miRNA)[54]. These are short RNA molecules that possess binding sequences on target messenger RNA (mRNA) by base paring, and with the help of the RNA-induced

silencing complex (RISC), inhibit translation of the mRNA into a protein. siRNA and miRNA differ in the degree of specificity towards the mRNA target: while siRNA targets a specific sequence by full complementarity, the miRNA is partially complementary to the target mRNA and can target multiple mRNAs[54]. Since translation happens on the cytoplasm of the cells, the technologies used to deliver the RNA do not need to reach the nucleus of the cell, which might demand different properties from the carrier[46].

1.3.2 Endocytosis of NPs

When a NP reaches a cell and interacts with its membrane, there is the opportunity of internalization by endocytosis. In endocytosis, the NP is surrounded by the cell membrane and engulfed, joining the vesicle trafficking machinery inside the cell. The membrane bending necessary for endocytosis can happen by many different energy-driven mechanisms[55]. The most relevant endocytic pathways for NP uptake include phagocytosis, micropinocytosis, clathrin- and caveolae-mediated endocytosis.

Phagocytosis occurs mainly in professional phagocytes as an integral part of their host defense functions and during the clearance of dead cells and debris[56]. Depending on the NP physicochemical properties, the particles can be coated by opsonins, a family of proteins responsible for enhancing phagocytosis[57]. Phagocytosis is then triggered by receptor-ligand interactions, which results in cell surface extensions that engulf and internalize particles, forming a phagosome[56]. Phagocytic cell lines have been shown to better take up large particles, which explains the faster clearance from blood[58,59]. Another important pathway for larger particles is macropinocytosis, which shares with phagocytosis its dependence on the actin polymerization machinery for creating large membrane extensions

for engulfment[60–62]. Macropinocytosis, however, is a non-specific, growth factor-induced endocytic pathway that is present in most cells[60,63]. At the smaller scale (<200 nm), bending the membrane for uptake demands specific membrane machinery. Clathrin- and caveolae-mediated endocytosis are important NP uptake pathways that fall in this category[64–66]. Both these pathways depend on the assembly of proteins as coatings for vesicle formation. In clathrin-mediated endocytosis, the recruitment and assembly of clathrin form a coat on the cell membrane inner leaflet that bends the plasma membrane around the NP, forming a clathrin-coated vesicle[64,66] Caveolin is another membrane coat at the cell surface, being directly bound to membrane cholesterol. Upon assembly, caveolin forms the caveolae, 50-100 nm flask-shaped structures at the cell membrane. There are three caveolin isoforms, and they have varied functions and abundancy dependent on cell type. However, the expression of caveolin-1 is recognized as the main marker for caveolae formation in cells[65,66]. Notably, endothelial cells express high levels of caveolin-1 and contain a large number of caveolae. In both clathrin- and caveolae-mediated endocytosis, the scission of the coated vesicle is promoted by dynamin[66].

1.3.3 Intracellular trafficking and calcium phosphate NP endosomal escape

After scission and de-coating (in the case of clathrin- or caveolin-coated) of the endocytic vesicles, they fuse with the early endosomes[67,68]. The intracellular trafficking of NPs is then guided by the early endosomes to different locations inside the cell, which upon maturation to late endosomes can result in exocytosis by fusion with the cell membrane, or fusion with the lysosomes, which exposes the NP to a variety of degradation enzymes. At any given point, NPs that carry specific mechanisms for endosomal

interactions, often triggered by acidification of the endosomal compartment, can escape to the cytoplasm and reach other locations inside the cell[67,68]. Inside the endosomes and lysosomes, endocytosed NPs are subjected to acidic pH[69]. This property ensures that when CaP particles carrying polynucleotides enter cells by clathrin- and caveolae-dependent pathways, they are completely dissolved into non-toxic products inside the endosomes[70]. It is believed that the buffering effect of Pi ions is responsible for the pumping of additional H^+ inside the endosome, which is accompanied by the influx of Cl^- counter ions, leading to osmotic swelling of endosomes[71]. This "proton sponge effect"[72], in addition to the increase in internal calcium ion concentration[71], will result in rupture of the endosomes and release of the delivered polynucleotide (Fig. 1.4). However, the exact dissolution mechanism of CaP carrying nucleic acid cargo is not completely understood. It was proposed that the initial hydration of phosphates followed by hydrogenation triggers Ca^{+2} detachment in multiple independent centers at the surface[38]. Dissolution initiated by localized pits is also a reported mechanism[73].

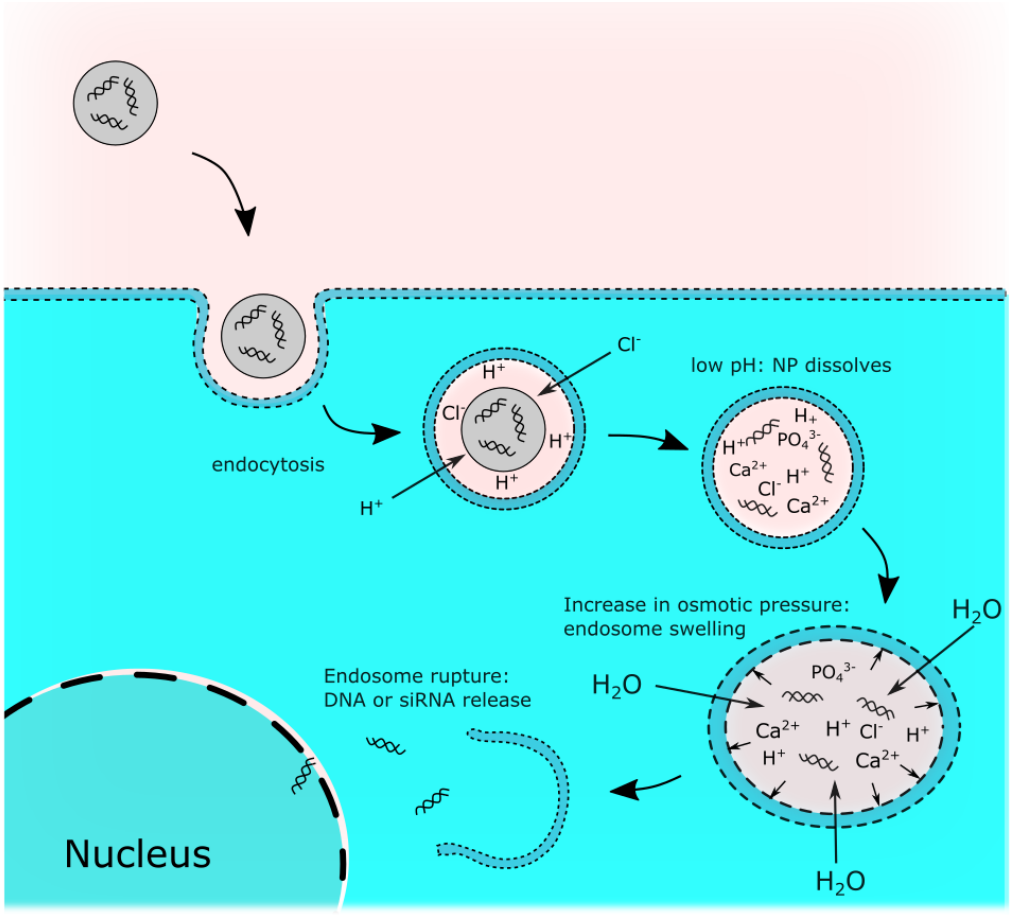

Figure 1.4 Mineralized NP uptake by endocytosis. Acidification of the endosome triggers NP dissolution as a result of increased mineral solubility, releasing the polynucleotide and increasing osmotic pressure in the endosome. Endosome rupture results in polynucleotide escape into the cytoplasm.

1.3.4 Effect of NPs Physicochemical Properties in Biological Interactions

Biological Identity

The NP biological interactions in biological fluids start influencing particle fate long before any cell/particle interaction occurs. Once administered, NPs immediately start interacting with many components of biological fluids, such as proteins, electrolytes, and other biomolecules[74]. Such interactions result in the decoration of NPs by a so-called "protein corona". The properties of the protein corona have a substantial effect on how NPs interact with cells, which can determine their fate[75–77]. For instance, silica NPs were

reported to lose their specific targeting capabilities due to corona formation[78]. It is also observed that pharmacokinetics and cytotoxicity can be significantly affected by corona formation[79], as well as biodistribution[80]. While the environment will determine the availability of proteins regarding their type and abundancy, the physicochemical properties of the particles (size, shape, surface charge, hydrophobicity) regulate which proteins will be adsorbed and the conformation upon adsorption[74,81,82]. Accordingly, the route of NP entry (intravenous injection, oral ingestion, inhalation) will likely affect the protein corona composition and final NP properties and, as a consequence, biodistribution and uptake efficiency[74,80,83]. It was found that when NPs switch from one biological medium to another, the protein corona evolves, building a footprint of the different biological environments it navigated[84]. In short, the nano-bio interactions happen in a way that when the NP finally reaches a cell, it possesses a unique biological identity, influenced by its original properties and carrying information of its journey to that point inside the cellular universe [68].

Effect of physicochemical properties in NP uptake

The NP uptake by a cell is greatly influenced by the initial NP physicochemical properties. Morphological properties, such as size and shape, as well as NP surface chemistry, responsible for controlling surface charge and hydrophobicity/hydrophilicity, will be briefly discussed in this section. A summary of the properties discussed in this section can be found in Fig. 1.5.

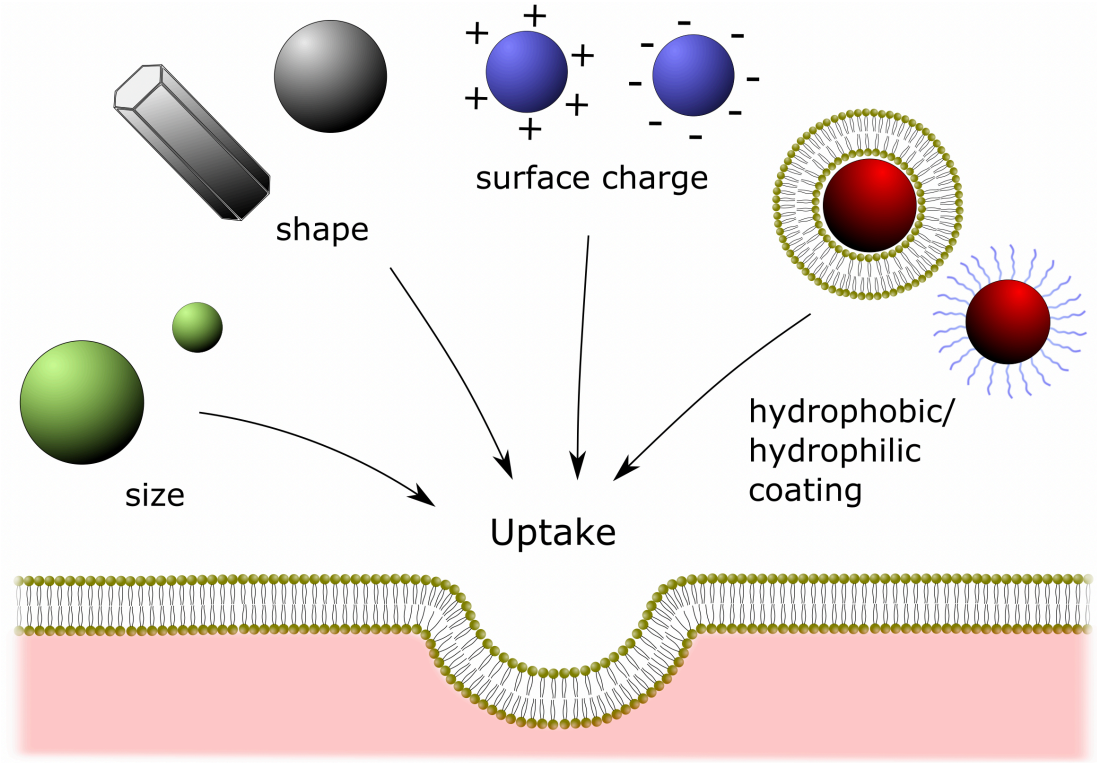

Figure 1.5 Summary of physicochemical properties affecting NP uptake.

Effect of size and shape

In order for endocytosis to occur, the energy necessary to drive the NP across a cell membrane must be balanced by favorable cell/NP interactions[85,86]. Particles that are too small would not bind enough receptors to balance the energy necessary for wrapping the NP. On the other hand, particles that are too large would compete for a finite number of surface receptors, which upon depletion would limit the binding energy gained to overcome the large membrane bending. The optimal value of ~50 nm seems to be recurrent in theoretical and experimental studies [85,87–90]. It was observed experimentally that particles that are bigger than the optimal value for uptake get stuck to the cell surface due to incomplete membrane folding while smaller NPs undergo aggregation for endocytosis [85,91]. The size is also known to influence the type of endocytic pathway[92]. For Ag NPs, clathrin-mediated

endocytosis seems to be a shared pathway for NPs with sizes ranging from 5 nm to 100 nm. However, caveolin-mediated endocytosis is predominant on uptake of NP smaller than 50 nm and macropinocytosis for NPs with 50 nm and 100 nm. Also, it is observed that larger particles are more easily taken up by phagocytes *in vitro*, and *in vivo,* they are more rapidly cleared from the bloodstream due to being more susceptible to the binding of opsonins, and hence, phagocytosis[58,59]. Biodistribution is highly influenced by particle size, and the increased circulation time of small particles frequently results in superior tumor accumulation [59,81,93,94].

However, achieving efficient treatment involving intracellular delivery is not as simple as achieving a specific optimal size for uptake. For instance, the superior accumulation of NP with small or optimal sizes at tumor sites does not necessarily translate into superior treatment compared to bigger particles and can increase toxicity[94]. Additionally, reports of superior transfection efficiency of polyplexes *in vitro* and *in vivo* with sizes close to the micrometer range raise attention to the importance of probing the uptake mechanisms of large particles [61,95]. It seems like large polyplexes might show increased transfection efficiency due to superior DNA release inside the cells [61]. There is also evidence of the interplay between different sizes of NPs in which larger NPs promote the uptake of small NPs, while small NPs inhibit the uptake of larger NPs[96]. This gives insight into what could be a complex mechanism in play on the uptake of particles with certain particle distribution.

The shape can additionally influence uptake efficiency and pathway[97–99] toxicity and biodistribution[87,100]. However, it is difficult to draw definitive conclusions regarding optimal shape for uptake across different materials and even across different groups' studies on the same material. Gold NPs perhaps serve as a good example, in which many authors

report spheres as being superior in terms of uptake[87,90,101]. Reports of higher uptake of nanorods are also present in the literature[82]. Nanorods might also present benefits regarding tumor accumulation *in vivo* due to decreased uptake by macrophages[102]. A few studies also looked into the effect of shape on the endocytic pathway. PEGylated mesoporous silica NPs in the form of long rods were taken up mainly by caveolae-mediated endocytosis and spheres by clathrin-mediated endocytosis[97]. Cylindrical hydrogel NP prepared by a top-down lithographic method showed a shared uptake mechanism between clathrin- and caveolae-mediated endocytosis, and interestingly, an increase in aspect ratio from 1 to 3 resulted in a 4 times faster uptake rate[99].

Effect of surface chemistry.

Surface chemistry is another highly influential factor in NP uptake efficiency, being able to influence particle surface charge, hydrophobicity, and addition of targeting ligands to NPs surface and hence directly affecting the interactions of NPs with cell membranes. In general, surface charge and hydrophobicity will govern non-specific binding forces with the cell membrane, while the presence of functionalities capable of receptor-ligand interactions will lead to receptor-mediated endocytosis[74]. For most cases, cationic surface charge correlates with considerably higher cellular uptake and toxicity in non-phagocytic cell lines compared to anionic particles[14,103–105]. Both cationic and anionic particles interact with lipid membranes and induce local structural changes[106]. However, the strong attraction between cationic particles and the anionic cell membrane allows utilization of non-endocytic pathways that are not experienced by negatively charged particles, such as entry by disruption and hole creation in the cell membranes[107]. The membrane disruption, along

with alteration of cell membrane potential and intracellular calcium content, is responsible for high cell toxicity [103,108,109]. *In vivo*, both highly anionic or cationic particles seem to be more prone to phagocytosis and clearance by the reticuloendothelial system (RES). However, many authors find that a slight negative zeta potential leads to increased circulation time and superior tumor accumulation by limiting non-specific cell-particle interactions[59,102,110,111].

The balance of hydrophilicity-hydrophobicity of NPs influences particle stability and cell-membrane interactions. Good NP colloidal stability and increased circulation time in biological applications are important features that demand the use of hydrophilic coatings[57]. Furthermore, a high degree of hydrophobicity might elicit cytotoxicity[112,113], high immune system activation, and poor biodistribution[114]. However, hydrophobicity might be important for encouraging uptake by NP-membrane interactions. For instance, poly(lactic acid) NP showed a 60% increase in uptake by HeLa cells when hydrophobicity was increased by co-polymerization with membrane lipids[115]. Due to the variable demands in terms of hydrophobicity during particle application *in vivo*, many authors develop systems that are based on the combination of hydrophilic and hydrophobic components. For example, the coating with hydrophilic and hydrophobic functionalities can potentially benefit uptake by rearrangements of the components during membrane crossing due to maximization of hydrophilic and hydrophobic interactions at a separate portion of the particle surface as it crosses a lipid bilayer[116]. Maximization of hydrophilic and hydrophobic interactions can also trigger a change in conformation of co-polymer coatings that expose hydrophilic or hydrophobic portions of the chain[112].

Targeting ligands

Even with optimization of NPs features for uptake in a given application, a high degree of targetability of NP towards a specific site of disease or cell type is a considerable challenge. Modifying the NPs surface with targeting ligands that bind to surface receptors on target cells is the most fruitful approach to specific targeting and increased uptake. This strategy is especially useful when the target cell over-expresses specific receptors that are not expressed to the same extent in other cell types, reducing unwanted side effects due to off-targeting[117–122]. There are many well-known examples of effective ligands that have successfully been used to modify NPs surfaces, such as hyaluronic acid[117,118], folic acid[119–121], peptides[122], and antibodies[123]. It is also important to modulate NPs

features to work in conjunction with targeting ligands. However, one should carefully interpret results from *in vitro* studies since these represent a less complex scenario than the *in vivo* application. From a gene therapy perspective, highly efficient hydrophobic cationic NPs that transfect a wide range of cell phenotypes might be indeed very appropriate for *in vitro* cell modification. However, the lack of specificity and considerable toxicity due to the strong interaction with cell membranes are highly undesirable features *in vivo*. For *in vivo* targeting, the size, shape, surface charge, and hydrophobicity should be carefully modulated to optimize targeted uptake and to minimize all biological interactions other than receptor-mediated endocytosis triggered by the specific targeting ligand. This also demands surface chemistry that avoids interference of targetability by protein corona composition[78]. Reducing unspecific biological interactions is not an objective commonly pursued in *in vitro* studies using non-targeted particles, as this would literally mean achieving negative results. A contrary example is found with CaP NPs having hyaluronic acid coatings for targeting

cells overexpressing CD44 receptors[124,125]. Hyaluronic acid coatings rendered hydrophilic anionic NPs with high uptake *in vitro* when CD44 receptors are available. However, when CD44 receptors are saturated, uptake decreases dramatically, revealing that the NPs properties on their own do not favor uptake by other endocytic pathways[124,125]. The targeted NPs using mineralization strategies discussed during this review have been summarized in Table 1.

Table 1-1 Targeting ligands employed on mineralized vectors.

Particle type	Targeting ligand	Target	Cell targeted	Application	Ref.
Polymer Coated	3,4-dihydroxy-L-phenylalanine-conjugated Hyaluronic acid	CD44 receptor	HT29	*In vivo* luciferase inhibition in tumors	[125]
			hMSCs	*In vitro* osteogenesis by BMP-2 pDNA delivery	[126]
	Alendronate conjugated hyaluronic acid	CD44 receptor	A549	*In vivo* EGFR silencing in tumor xenograft	[25]
	D-SS-crosslinked Hyaluronic acid	CD44 receptor	B16F10- In vitro and in vivo	*In vivo* luciferase and BCL-2 silencing in tumor xenograft	[124]
Lipid coated	Lipid-PEG-conjugated anisamide	Sigma receptors	H460 human lung cancer cells in vivo	*In vivo* luciferase silencing in tumor xenograft	[40]
			A549 and H460	*In vivo* MDM2, c-Myc, and VEGF silencing in tumors	[127]
			B16F10	*In vivo* MDM2, c-Myc, and VEGF silencing in a metastatic tumor model	[128]
	Lipid-PEG-conjugated ABX-EGF scFv/folic acid	EGFR and folate receptors	MDA-MB-468 (Triple-negative breast cancer)	*In vivo* CD-siRNA delivery to tumor xenograft	[43]
	Lipid-PEG aminoethyl anisamide	Sigma 1 receptor	Stellate hepatic cells	*In vivo* relaxin gene delivery in metastatic liver cancer model	[129]
	Lipid-conjugated Galactose	D-galactose receptor	Stellate hepatic cells	Inhibition of CXCL12/ CXCR	[130]

				in a liver metastatic cancer model	
	Lipid-conjugated β-D-galactoside	Asialoglycoprotein receptor	Hepatocytes and hepatocellular carcinoma cells	*In vivo* VEGF silencing in liver cancer	[24]
	SP94 peptide	n/a	Hepatocellular carcinoma cells	*In vivo* TRAIL gene therapy and protamine delivery to liver	[131]
			Hepatocellular carcinoma cells	*In vivo* IL-2 pDNA and PD-L1 siRNA	[132]
	Folic acid	Folate receptor	B16F0 melanoma cells	*In vitro* co-delivery of cell death siRNA and α-tocopheryl succinate	[133]
Multi-shell (CaP/PEI/poly(I:C)/SiO$_2$)	anti-CD146, anti-IgG1, and anti-IgG2	CD146, IgG1and IgG2	THP-1 cells, Kupffer cells (KC), and liver sinusoidal endothelial cells	*In vivo* toll-like-receptor ligand-3 to the liver.	[134]
	TLR9 ligand	TLR9	CD8+ T cells	HIV-1 vaccination *in vivo*	[135]

1.4 Fabrication of Nanoparticulate Mineral Vectors by co-Precipitation

1.4.1 Traditional co-precipitation method for NP vectors

The use of CaP as a vector for the transfection of mammalian cells was introduced in the early 1970s with Graham's pioneering paper[136], and as in many discoveries in chemistry, by the recognition of an unintended chemical reaction, as described one decade later by Graham himself[137]. At the time of this discovery, the only available transfection option was the inefficient diethyl aminoethyl (DEAE)-dextran method. Graham, motivated by the effect of divalent ions binding to DNA, tried new ionic combinations with DEAE-dextran in buffered media. When $CaCl_2$ was used in conjunction with a phosphate buffer, an unusually high transfection efficiency was observed, which was later related to the presence

of a fine precipitate or co-precipitate, since the mineral was nucleated in association with DNA. Numerous papers have since been published on the CaP precipitation method, which led to further optimization of the technique[17,70,138–141].

Solubility is a key property of CaPs. It controls precipitation, dissolution, hydrolysis, phase transition[142,143] and even bioactivity[144] of the mineral. Not surprisingly, it is important to optimize the parameters controlling solubility in order to achieve efficient transfection. Precursor concentration, pH, and incubation time are vital to be optimized[17,138,141]. A Ca molar concentration in excess of as much as 170-fold of Pi is frequently used to assure complete calcium/DNA binding before co-precipitation. A low Pi salt supersaturation, on the other hand, limits excessive precipitation and particle growth, while incubation times are rarely longer than 5 minutes. With everything else fixed, pH is the key parameter to control the solubility of the resultant Ca/P. At acidic pH, CaP is not easily precipitated, while at close to neutral pH, small increases can cause uncontrollable precipitation, drastically decreasing transfection efficiency[17,138,141].

CaP precipitation and dissolution is an ongoing process inside our bodies. In bone remodeling, osteoblasts create new bone by performing appropriate steps for calcium precipitation, while osteoclasts degrade bone by local acidification[145]. Thus, it is not a surprise that a material naturally produced and degraded by the body (biodegradable) presents considerable bioactivity and is well accepted by the body, including in its synthetic form. CaP synthetic materials are recognized as being extremely safe options in clinical practice, often showing negligible toxicity to cells in gene therapy applications[25,146,147]. Additionally, CaP can be produced using cheap reactants via easy chemical routes. One interesting addition to the co-precipitation method is the option of using other minerals. With

similar properties to CaP mineral regarding safety, bioactivity and acid triggered dissolution, calcium carbonate[148] and magnesium phosphate[149] became promising options for the delivery of polynucleotides. Perhaps even more appealing is the control of properties of the vectors by combining different mineralizing solutions. The combination of calcium carbonate and phosphate[39] and calcium phosphate and silicate[146] presented superior pDNA transfection efficiency *in vitro* compared to unmodified NPs.

A major concern of the co-precipitation method is its low reproducibility. Rather than a characteristic of CaP itself, the reproducibility issue is a consequence of the processes used for synthesis in this practice. Different from other synthetic vectors in which the synthesis can be performed in a more automated way for big batches for several repeated transfection experiments, CaP synthesis is normally undertaken before every transfection experiment by manually mixing the components[17,140]. This makes it impossible to have strict control over temperature, mixing rate, or rate of addition of reactants, all of which are known to affect the reaction rate. In a study in which these factors were controlled, the different rates could be compared and were shown to be highly influential in transfection efficiency, and a higher degree of reproducibility was achieved[140]. However, the continuous growth and aggregation of particles precipitated in solution is still a major drawback. *In vitro*, this effect can be partially

overcome by adding the particles to cells immediately after precipitation. However, *in vivo* applications demand very stable systems and, depending on the treatment, targetability to specific cell types might be altered. It is clear that in order to achieve the clinical practice with mineralized vectors, the co-precipitation method needs to be adapted to incorporate better control of particle features and surface insertion of functional groups for cell targeting.

Studies approaching these topics are summarized and discussed in the following sections. The main advantages and disadvantages of each delivery method involving mineralization are summarized in Table 2 and the *in vivo* studies reviewed can be found in Table 3.

Table 1-2 Benefits and limitations of each mineralized delivery vector reviewed.

Delivery method	Brief description	Benefits	Limitations
Particles by traditional co-precipitation	Nucleotide/mineral co-precipitates are synthesized in water without control over NP growth[136].	This method is straightforward, clean, and cost-effective.	The excessive growth and lack of surface functionalization limit this process to only a few *in vitro* applications.
Polymer coated NPs	Co-precipitate growth is limited by surface insertion of a block copolymer with a strong calcium affinity during or immediately after precipitation[150,151].	Stable NPs can be synthesized in a straightforward method.	A block copolymer with a portion responsible for co-precipitate dispersion and another portion responsible for calcium binding needs to be designed and synthesized.
Lipid coated NP	The co-precipitation reaction is carried inside micelles in a reverse microemulsion method. Growth is inhibited by the micelle diameter and the adsorption of hydrophobic functionalities at the water/oil interface [152].	The reverse emulsion method allows high control over particle size and low PDI. The hydrophobic coating allows functionalization with lipid-modified PEG for dispersion and targeting ligands via adsorption.	The reverse microemulsion method and the hydrophobic nature of the NPs demand the use of organic solvents and multiple washing steps.
Mineralized surfaces	A surface is mineralized by a metastable solution in the presence of DNA. DNA is entrapped inside the mineral layer during the process[153].	Entrapment of DNA inside the mineral surface allows reverse transfection on a coated surface. The transfection can be tuned by modifications in the ionic content of the mineralizing solution.	DNA delivery is limited to cells attached to the mineral layer, possibly restricting this method to tissue engineering applications *in vivo*.
Multi-shell NPs	Adsorption of nucleotides and functional polymers around a homogeneous core is intercalated by precipitated mineral shells[154].	Multiple functional molecules can be added to the same particle. Specific interaction between functional molecules can be explored (e.g., two	The multiple precipitation reactions might result in increased particle size compared to other methods.

		molecules can be adsorbed to the same layer or separated by a mineral layer).	
Mineralized pre-assembled NPs	Delivery vectors (e.g., viral particles, polyplexes) are coated by a mineral shell[155,156].	A mineral layer over the delivery vector can exert increased protection of the cargo and improve transfection efficiency *in vivo*.	NPs must be negatively charged to be mineralized, which might require surface functionalization of the delivery vector.

Table 1-3 Main in vivo studies reviewed published after 2010. SC: Subcutaneous, IV: Intravenous, IM: Intramuscular, IP: Intraperitoneal

Technology	Nature	Delivery strategy	Treatment	Animal model	Dose	Outcome	Ref.
Polymer coated co-precipitated NPs	siRNA/CaP/ PEG-Charge reversible polymer.	Charge reversible mechanism.	VEGF silencing	Mice with SC BxPC3 tumor (pancreatic cancer)	25 μg siRNA in 200 μL per injection were injected into the tail vein four times at days 2, 5, 8 and 12	Statistical significance observed for tumors treated with the siVEGF NPs with reduced tumor volume (66%) on day.	[151]
	siRNA/CaP/ 3,4-dihydroxy-L-phenyl alanine (dopa)hyaluronic acid.	CD44 targeting.	Luciferase silencing	Mice with SC HT29-Luc tumor (human colorectal adenocarcinoma)	A single injection into the tail vein (0.6 mg/kg).	CAP/siRNA/dopa –HA containing luciferase siRNA significantly suppressed the expression of the target gene in the tumor xenograft 24h after a single dose.	[125]
	siRNA/CaP/ PEG-charge reversible polymer	Charge reversible mechanism.	Luciferase silencing	Mice with spontaneous bioluminescent pancreatic adenocarcinoma.	A single IV injection (200 μL, 20 μg siRNA).	Significant gene silencing and reduced siRNA-Luc tumor accumulation after 24h	[157]
	sirna/CaP/ alendronate-hyaluronan graft polymer.	CD44 targeting.	EGFR silencing	Mice with SC A549 tumor (lung cancer)	Five doses of 1mg/kg on days 1, 3, 5, 8, and 11 IV	Significant tumor size reduction five days after the last injection	[25]
	siRNA/pluronic/CaP/PEI-colesterol/DOPE.	-	VEGF silencing, DOX	Mice with MCF-7 SC tumor	0.5 nM siRNA, 100 μL, twice a week for 28	After 28 days, relative tumor reduction (weight)	[158]

				(breast cancer).	days into tumor and IP DOX injections once a week (1.2 mg/kg)	compared to saline control was ~72% (siRNA), ~84% (DOX) and ~91% (DOX+siRNA).	
	siRNA/CaP/ hyaluronic acid crosslinked with disulfide bonds.	CD44 targeting.	BCL-2	Mice with B16F10 SC tumor (melanoma)	IV injection of 1.2 mg/kg of siRNA on days 0, 2, 4, 6, and 8.	After ten days, tumor mass was 25% of the mass of saline control (80% volume reduction).	[124]
	pDNA/CaP/a lendronate-PEG.	-	GFP expression	Mice with 4T1 SC tumor (breast cancer).	Three 2 μg pDNA doses were injected into the tumor every other day for one week.	High GFP expression in vitro but weak GFP expression *in vivo*.	[159]
Lipid coated/ microemulsion	siRNA/CaP/ DOTAP/DS PE-PEG/cholest erol/glycolip id/L4 ligand.	L4 targeting.	VEGF	Mice with orthotopic HCA-1 tumor (human endocervical adenocarcin oma).	0.7 mg/kg/dose, three doses per week, two weeks IV.	Significant inhibition of tumor growth and lung metastasis after 2 weeks— significative tumor growth inhibition with targeted particles.	[24]
	siRNA/CaP/ DSPE-PEG-folate/ single chain fragment antibody.	EGFR and folate receptor targeting.	siRNA *in vitro*, Cy5-dsDNA *in vivo*	Mice with MDA-MB-468 tumor (breast cancer)	3 μM Cy5-dsDNA in a single dose.	Significant tumor accumulation in vivo from 4-24h post-injection with targeted nanoparticles.	[43]
	siRNA/CaP/ cholesterol-charge reversible polymer.	Charge reversible polymer.	BCL-2	Mice with A549 SC tumors (lung cancer)	IV injection of 0.1 mg/kg and 0.2 mg/kg siRNA every three days seven times.	Increased tumor accumulation after 24h of injection and considerable tumor growth inhibition.	[160]
	siRNA/CaP/ DOPA/PEG-phospholipid /anisamide.	Sigma receptors targeting.	Luciferase siRNA, Cy3- siRNA	Mice with H460 SC tumors (lung cancer)	0.6 mg/kg injected into the tail vein	Significant tumor accumulation and gene silencing after 4h.	[40]
	siRNA/CaP/ DOPA/PEG-phospholipid /anisamide.	Sigma receptors targeting.	HDM2, c-myc, and VEFG	Mice with H460 or A549	0.36 mg/kg every third day for 15 days (H460	Significant tumor size reduction for both models after the period tested.	[127]

				tumors (lung cancer).	tumor) and every fifth day for 31 days (A549).		
Multi-shell NPs	CaP/PEI/pDNA/TLR9 ligand/silica.	TLR9 targeting.	Native-like trimeric HIV-1 antigen expression.	Mice	Mice were immunized with 100 μg of pDNA three times over a week SC or IM.	Enhanced immunization with pDNA vaccine vs. naked pDNA and significantly higher levels of IFN-γ, CD8+ T cells, and CTL-mediated killing activity for SC vs. IM injection.	[135]
	CaP/PEI/dsRNA/SiO_2-CD146 antibody.	CD146.	Poly(I:C): TLR3-targeting adjuvant	Mice	14.4 mg of poly (I:C) IV.	Targeting of CD146 did not enhance uptake efficiency *in vivo*. Uptake in lung and liver, 1 and 3 h after the injection.	[134]
	CaP/siRNA/PLGA/PEI.	-	Local silencing of inflammatory cytokines	Mice with chronic colonic inflammation	Single intrarectal application with 50 μg of siRNA.	Significant silencing of target genes in colonic biopsies and mesenteric lymph nodes. Local inflammation was reduced (histological analysis).	[161]
	CaP/pDNA+protamine/CaP/protamine in a collagen scaffold.	Gene activated matrix.	BMP-2 expression (bone regeneration).	Rats	9.6 μg of pDNA implanted into SC tissue on the back of rats for 28 days.	BMP-2 release from scaffolds with CaP was more extended than that of scaffolds immersed in BMP-2 solution.	[162]
	CaP/siRNA/PEI-galactose/siRNA/PEI-galactose.	Targeting of asialoglycoprotein receptors.	Luciferase	Mice with SC A549-Luc tumor (lung cancer).	Systemic injection of 25 μg siRNA every two days for 14 days.	Significant lowering of tumor bioluminescence starting on day 9. Targeted particles accumulated in the liver compared to non-targeted particles.	[163]

Mineralized surfaces	PEI/pDNA polyplexes embedded into carbonate apatite surfaces over collagen sponges.	Gene activated matrix.	FGF-2 and BMP-2 expression (bone regeneration).	Calvarial defects in rats	25 μg pDNA implanted into calvarial defects for 6 days.	Increased bone tissue formation with pBMP-2 delivery and pBMP-2+pFGF-2 delivery compared to mineralized implants without genes.	[164]
	pDNA and fibronectin embedded into carbonate apatite over Hap disks.	Gene activated matrix.	BMP-2 expression (bone regeneration).	Cranial defect in rats.	pDNA concentration in mineralizing solution at 40 μL/mL.	pBMP-2 significantly increased BMP-2 concentration in bone defects. The presence of fibronectin efficiently increased this effect.	[165]
Mineralized viruses	RNA chimeric dengue virus vaccine/CaP.	-	Vaccination against DENV-2 (dengue) virus.	Mice	Two doses administered 16 days apart intranasally with 10^4 plaque-forming units (PFU) of the vaccine.	The mineralized vaccine induced significant higher levels of secretory mucosal IgA against DENV2. Higher antigen-specific systemic humoral and cellular immune response with mineralized vaccine.	[166]
	Oncolytic adenovirus (OA)/($MnCO_3$+$CaCO_3$).	-	Cell lysis by OA replication. Mn^{2+} delivery for increased OA replication, enhanced T1 signal for MRA and photoacoustic imaging.	Mice with SC 4T1-tumors (breast cancer).	100 µL of viral suspension with $1x10^{10}$ VPs/mL on day 0, 2, 4, and 6.	Photoacoustic signal drastically increased compared to PBS injection and non mineralized OA. Mineralization significantly reduced the immune response to OA, increased circulation time, increased half-life 10-fold. $CaCO_3$ mineralization increased anti-tumor efficacy, and (Mn+Ca)CO_3 further increased this effect.	[156]

	Oncolytic adenovirus (OA)/CaP/(lipids+PEG).	-	Cell lysis by OA replication	Mice with SC Huh-7 tumor	A low dose ($7.5x10^9$ VPs) or a high dose ($1.5x10^{10}$) every other day. 4 total applications.	Mineralization increased circulation time and tumor accumulation of particles. Tumor to liver GFP expression of the mineralized virus was 560-602 fold higher compared to the unmineralized virus. Anti-tumor efficacy was significantly increased by mineralization	[26]

1.4.2 Polymer-coated co-precipitated vectors

The major challenge with the traditional co-precipitation technique is to exert satisfactory control over the size and morphology of the particles. While it is possible to partially overcome this issue by transfecting the cells immediately after the precipitation reaction for *in vitro* studies, *in vivo* applications demand stability of particle size for prolonged periods of time, which makes the standard CaP co-precipitation method not appropriate for *in vivo* applications. Modified precipitation strategies using polymer additives designed for the specific task of stabilizing the co-precipitate could be an effective strategy. In most cases, the utilized polymers carry a functional group with a strong affinity towards Ca^{+2} and a long hydrophilic chain responsible for the dispersion of the particles, avoiding aggregation and excessive growth[167].

Since the co-precipitation is performed by a simple reaction between the two precursors, there are only a limited number of possibilities for introducing the polymer additive to the reaction mixture. It can be added to (i) Ca precursor, (ii) Pi precursor, or (iii) precipitation reaction solution after the two precursors are mixed[147]. It is not clear from

the current literature what is the most effective method, but it most probably depends on the properties of the group used for Ca^{2+} binding, precursor concentrations, and specific application. Polymers with groups bearing multiple phosphates with very strong Ca affinity, such as bisphosphonates, are normally added immediately after the precipitation reaction[147,159,168]. On the other hand, polymers presenting –COOH groups have been added during the NP precipitation with effective results[157,167]. It is not clear, however, why authors chose the specific protocols; presumably, better size control is the main advantage of the additives, while any changes in morphology (that may impact transfection efficiency) remain to be explored.

One of the first efforts for producing stabilized CaP systems was made by the Kataoka group[169]. The group produced a series of polyethylene glycol (PEG)-polyanion block copolymers capable of stabilizing the size of CaP NPs carrying nucleotides with core-shell architectures (Fig. 1.6, Method I). PEG is a non-ionic hydrophilic polymer with a great capacity of preventing particle aggregation by steric stabilization, which yields to formulations with increased stabilities over long storage times[170]. Furthermore, PEG is capable of decreasing non-specific interactions *in vivo*, leading to a prolonged blood circulation time, thereby increasing the chances of the cargo reaching the target site[171]. The polymers produced were variations of the block copolymers of PEG-*block*-poly(aspartic acid) (PEG-PAsp) with great capability to stabilize the CaP NPs for long periods of time and maintain a narrow size distribution. [151,157,169,172–174] The P(Asp) portion of the macromolecule was involved in the early steps of particle formation, probably being incorporated in the CaP core, while the non-reactive PEG chain is responsible for steric repulsion and, consequently, the colloidal stability.

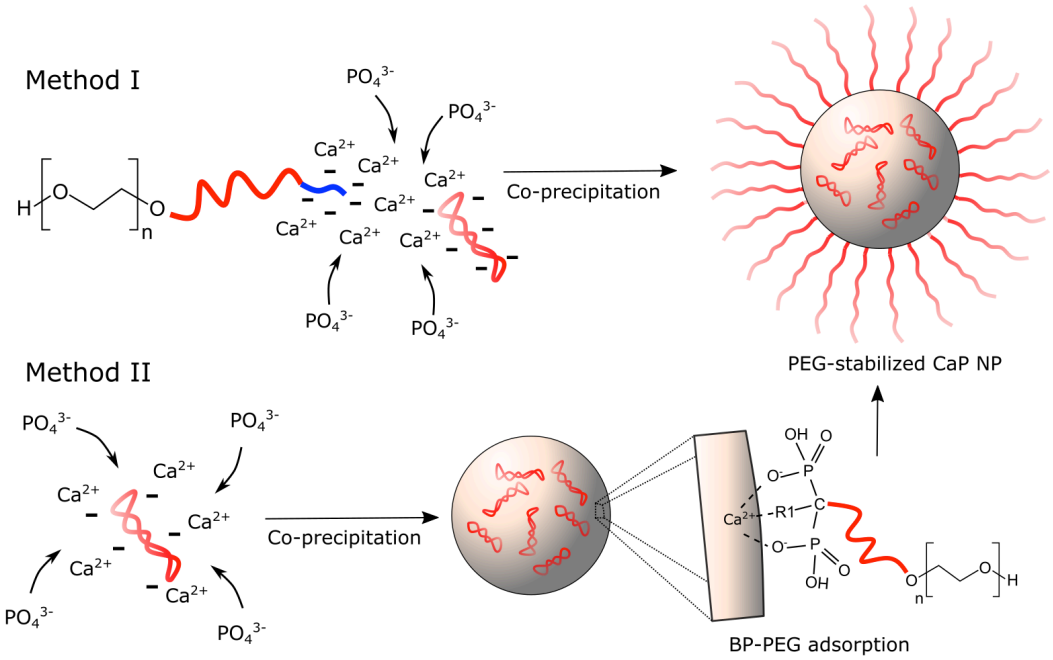

Figure 1.6 Two methods for stabilizing co-precipitated NPs. Method I: a PEG-polyanion conjugate is present during co-precipitation, binding to Ca^{+2} before nucleation. Method II: a bisphosphonate-PEG conjugate is added after co-precipitation and binds to Ca^{+2} at the particle surface. Both methods result in PEG-stabilized NPs.

The presence of P(Asp) also allows further modifications, such as the addition of functionalities. Charge conversional polymers were produced by functionalizing the PAsp with diethylenetriamine producing a polyaspartamide derivative, poly{*N*′-[*N*-(2-aminoethyl)-2-aminoethyl] aspartamide} (PAsp(DET)), followed by the addition of an acid cleavable cis-aconitylamide moiety (PAsp(ACO)). These polymers were used to fabricate hybrid NPs carrying siRNA with negligible cytotoxicity. Before entering the cells, the particles were <100 nm with a small negative charge, which supposedly does not cause membrane disrupting toxicity that is seen in traditional cationic polymers such as polyethylenimine (PEI) [105,175]. At the endosomal pH of ~5.5, the disassembly of the NP is triggered, and the polymer bearing the cis-aconitylamide group gets cleaved into the

aspartamide parental cationic polymer, generating a facilitated endosomal scape by the proton sponge effect, in addition to the already present escape mechanism of the CaP. The fact that the additional escape mechanism was conducive to increasing the efficiency of the particles while maintaining the same surface charge is an indication that part of the issues regarding CaP co-precipitate transfection might be related to the effectiveness of its endosomal escape ability. The polymer was used in a series of studies evaluating the hybrid NPs in the treatment of pancreatic cancer[151,157,173,174]. The effect of the acid-labile group on endosomal escape was evaluated by confocal laser microscopy; the NPs made with polymers with charge conversion properties underwent early endosomal scape compared to NPs stabilized by a corresponding control polymer without the same mechanism[173]. The charge conversional polymer improved the siRNA knockdown of vascular endothelial growth factor (VEGF) in human pancreatic panC-1 cancer cells compared to the control group without charge conversion[173]. The same polymer showed a reduction of VEGF mRNA and tumor volume upon intravenous treatment of mice bearing subcutaneous BxPC3 (human pancreatic adenocarcinoma) cell xenografts. Notably, NPs purified by microfiltration and redispersed in an extracellular buffer performed slightly better than non-purified NPs[151]. The NPs were also tested in spontaneous pancreatic tumors[157]. Analysis of tumor histology and biodistribution with microscopy confirmed the accumulation of labeled siRNA in the tumor with the use of the hybrid NPs compared to naked siRNA. The NPs had negligible cytotoxicity *in vitro* and no signs of change in hematological parameters[157]. The importance of the charge conversional mechanism in the gene silencing was further reinforced by a study comparing PEGylated polymers bearing a moderate acid hydrolysis sensitivity, a rapid acid hydrolysis sensitivity, and no sensitivity

(i.e., charge conversion)[174]. The faster charge conversion mechanism was correlated to early endosomal escape and greater gene silencing in human ovarian SKOV3 cancer cells expressing firefly luciferase, presumably by a superior endosomal escape mechanism.

Mello and co-workers explored the PEG-polyanion methoxy-PEG-block-(poly(L-glutamic-acid) in the stabilization of CaP NPs and knockdown of anti-apoptotic BCL-2 and BCL-xL genes[167]. These anti-apoptotic genes are over-expressed in most cancers, being a key factor in tumor growth, and inhibition of their expression has been shown to decrease tumor growth and work synergistically with other drug treatments[176–178]. The siRNA-loaded NPs were effective in decreasing the expression of BCL-2 and BCL-xL. The knockdown of the genes did not cause apoptosis by itself, but it decreased the concentration of doxorubicin necessary for 50% cytotoxicity (IC_{50}) in breast cancer MCF-7 cells.

One possible disadvantage of using a polyanion-PEG copolymer for particle stabilization during polynucleotide/CaP NP precipitation is that the polyanion component of the copolymer competes with the polynucleotide for calcium binding; therefore, polynucleotide encapsulation efficiency might be hindered. As a solution, an alternative stabilization strategy was proposed for producing siRNA/CaP NPs using a boroxole-containing block polymer, PEG-b-poly(benzoxaborole) (PEG-PBO), which forms pH-responsive boronic ester bonds with the ribose rings of siRNA[179]. At pH 7.4, the crosslinking between PEG-PBO and siRNA resulted in template structures that were mineralized by simple CaP precipitation. The PEG-PBO/siRNA interaction was shown to increase siRNA incorporation. At mildly acidic pH, such as that of the ribosome, the boronic ester bonds are broken, and CaP dissolution is triggered, releasing the cargo. Additionally, the particles were efficient in inducing apoptosis by Bcl-2 inhibition in human lung

adenocarcinoma A549 cells.

PEG polymers bearing Ca chelating groups can also be used to produce stable NPs for the delivery of polynucleotides. Bisphosphonates (BPs) such as alendronate are a good example of molecules that present a strong affinity towards the Ca^{2+} and CaP surfaces[180]. When these strong chelators are used in mineralized delivery systems, they are usually added immediately after the precipitation as particle stabilizers[147,150,159,168] (Fig. 1.6, Method II). However, a recent study compared BP-modified PEG (BP-PEG) addition before and after precipitation[147]. The addition of BP-PEG before nucleation led to well-dispersed 40 nm amorphous particles that, after a few hours, turned into 80 nm needle-like hydroxyapatite, while addition after nucleation led to amorphous aggregates of 200 nm spherical particles. The aggregated 200 nm particles had significantly higher DNA transfection efficiency in hepatoma HepG2 cells. Interestingly, cellular uptake was not influenced by the change in morphology from spherical to needle-like particles over the storage time[147].

In another study, two other polymers constituted by a 2 kDa PEG linked to either alendronate or pentakisphosphate were used for stabilization of CaP particles for siRNA delivery to prostate adenocarcinoma PC-3 cells[150]. The polymer bearing the pentakisphosphate had a 2.5-fold lower uptake than the one bearing alendronate, probably because of the excessive stabilization of the particles, since pentakisphosphate presents higher Ca chelating power compared to alendronate. On the other hand, the particles stabilized by alendronate-PEG had BCL-2 inhibition similar to the conventional liposome Lipofectamine™. It is also worth noting that BP such as alendronate displays pharmacological activity and has been used as bone anti-resorptive agents to treat

osteoporosis by acting on osteoclasts and adsorbing to Hap to inhibit resorption[181,182]. It is well established that BPs increase tumor apoptotic cell death by interfering with the mevalonate pathway[183–185]. There has also been evidence that BPs contribute to the anti-tumor effect by increased apoptosis of tumor-associated macrophages (TAM) and reversal of macrophage phenotype from pro-tumoral to tumoricidal[186]. *In vitro*, in addition to high transfections, the dual delivery of siRNA/DNA with BPs conjugated to PEG has resulted in strong inhibition of the mevalonate pathway and selective toxicity towards macrophages[150,159]. The mineralized NP approach also opens the possibility of delivering BP intracellularly, using lower doses and avoiding non-specific spread to undesired locations in the body[182].

An alternative to PEG-based polymers as particle stabilizers is the use of hyaluronic acid (HA) polymers. HA can be used with similar outcomes to PEG regarding particle stabilization with the additional benefit of targeting CD44 receptors[187]. Moreover, HA has outstanding biological properties and is used in many clinical applications[188]. The affinity towards CD44 can be used to prepare particle systems targeted towards the cell types that overexpress this receptor, in particular mesenchymal stem cells[118,189] and cancer cells[187]. Of high clinical importance, the CD44 mediated uptake using CaP particles was observed in multiple cancer cells, indicating that these particles can be targeted to tumor tissue when administered systemically[25,124,125]. A 3,4-dihydroxy-L-phenyalanine-HA (Dopa-HA) conjugate was developed for the stabilization of siRNA/CaP NPs[125]. Dopa is an important component of mussel adhesive proteins, with strong adhesive properties towards various materials, including CaP[190]. With increasing Dopa-HA concentration, the particles varied in size from 273 to 63 nm, and -potential varied from approximately -20

to -60 mV. Additionally, the particles were effective in silencing luciferase expression in animals bearing HT29-luc tumor xenografts[125]. In another study, similar NPs were used for delivery of the cancer drug doxorubicin[191], which indicates the flexibility of the CaP strategies in accommodating different cargos. This may be important for combinational strategies, in which drugs and polynucleotides are delivered by the same particles. The Dopa-HA conjugate interaction with CD44 receptors was also used to deliver the BMP-2 gene to human mesenchymal stem cells (hMSCs)[189][192]. The NPs were efficient in increasing levels of osteogenic markers in hMSCs, including alkaline phosphatase, osteocalcin, osteonectin, and osteopontin, compared to 25 kDa PEI and unmodified CaP. Transfection efficiency decreased after pretreatment with HA, revealing that not only the increased particle stability but also the CD44 mediated uptake was important in enhancing transfection efficiency.

Qiu and coworkers used alendronate-functionalized HA to fabricate 170 nm spherical particles with core-shell morphology, low PDI, and negative -potential (-12 mV)[25]. Cell uptake *in vitro* was significantly decreased when A549 cells were pre-treated with free HA, revealing the contribution of CD44 mediated uptake. The fabricated NPs accumulated in A549 xenografts and were efficient in decreasing tumor size by epidermal growth factor receptor (EGFR) downregulation. Considering the multiple reports of *in vitro* CD44 mediated uptake and resultant targeted delivery to tumors, BP-HA polymers might be an option to overcome the issue of targetability observed when using BP-PEG polymers in CaP systems[159].

Zhou and coworkers performed an elaborate siRNA/CaP NP synthesis strategy using redox-responsive thiolated HA (HA-SH). The polymer was present during the nucleation of

siRNA/CaP NPs, and particle stabilization was achieved by an additional crosslinking step by exposure of formed NPs to O_2, forming a disulfide-HA (HA-SS-HA) layer. The anionic NPs were stable, and a decrease in size from 216.3 to 168.9 nm was seen after 12 h, which reportedly was an effect of oxidation of thiols and tightening of the crosslinks. The NPs had an efficient inhibition of luciferase and BCL-2 expression in murine melanoma B16F10 cells *in vitro* and reduced the size of B16F10 xenografts via BCL-2 inhibition[124].

Multiple-step coating strategies using oppositely charged components is another promising approach to creating surface-tailored NPs. Zhang *et al*. performed the synthesis of siRNA/CaP co-precipitates in the presence of a surfactant, followed by citrate stabilization, which reversed the charge of the particles to negative[193]. Anionic particles were then coated by a PEI-cholesterol mixture, generating 260 nm hybrid particles with close to neutral -potential. The hybrid particles showed superior GFP silencing in MCF-7 cells compared to cationic liposomes alone. Moreover, the hybrid particles also showed superior buffering capability, which could have been responsible for more efficient endosomal escape by the proton sponge effect or increased Ca^{+2} concentration. The same effect was observed in cationic lipid/CaP hybrid NPs prepared in a reverse microemulsion method[71]. Recently, un-modified alendronate was used to stabilize CaP/pDNA coprecipitates[194], turning the surface charge of the particles to positive (-potential = 20 mV) due to charged amino groups in alendronate. The positive surface charge facilitated albumin adsorption, turning the -potential to -10 mV and further increasing the stability of the NPs. The alendronate/albumin-coated particles efficiently transfected macrophages *in vitro* with slight cytotoxicity compared to unmodified particles. The multiple-step coating using a non-conjugated stabilizer might be a simple way of preparing stable vectors without demanding

prior organic synthesis. Additionally, due to the simpler fabrication process, comparative studies (e.g., comparing multiple outside coating layers for a fixed inside coating layer, and vice-versa) would be greatly facilitated.

The charge of the additive could also be important, although this is a scarcely investigated issue. Khan[141] compared the anionic citrate with the cationic poly(l-lysine) additive in the transfection of MC3T3-E1 preosteoblasts. Poly(l-lysine) did not have an immediate effect on transfection; however, a delayed increase over time was observed. Citrate, on the other hand, immediately increased efficiency by increased dispersion and control over the size. When high concentrations of citrate were added, particles were highly dispersed with reduced size, and transfection efficiency was decreased abruptly. The authors proposed that the decrease in efficiency was a consequence of the highly dispersed nature of the particulate, and slight aggregation might be needed for CaP transfection. Larger sizes also help with sedimentation in culture and increased contact with cells. Considering the fact that highly dispersed systems with particles sizes as small as 40 nm have been shown to be highly efficient in gene delivery[195], it is possible that other factors might be responsible for this effect, such as competition between DNA and citrate for CaP nucleation. Nucleation is known to be facilitated by appropriate molecular templates, and different chemical groups present different capabilities to nucleate minerals;[196] therefore, there would be a competition towards binding among additives with different potential towards nucleation. This effect was well exposed by Baillargeon *et al*.[197], in which DNA aptamers with enhanced capability for CaP formation could be selected from aptamers with less capability by co-precipitation. As already discussed, the method proposed by Zhou[179] in which the

polynucleotide is previously crosslinked forming templates for mineralization was specifically designed to avoid siRNA/polyanion competition for binding.

While the role(s) of additive polymers in these studies are usually explored in the context of CaP mineralization, it is important to realize that such additives are also beneficial for transfection, even in the absence of CaP. As a prototypical example, the use of HA has increased the transfection efficiency of both plasmid DNA (pDNA) and siRNA-based NPs when using purely polyplex NPs without the involvement of any mineral (see Fig. 1.7 for siRNA studies). This beneficial effect was attributed to better dissociation of polyplexes as well as better uptake of the polyplexes at times. The former mechanism (i.e., improved dissociation of the bioactive polynucleotide from CaP vector) in particular might be still operational with CaP particles so that beneficial effects of additive polymers in CaP NP formulations should be probed in more detail.

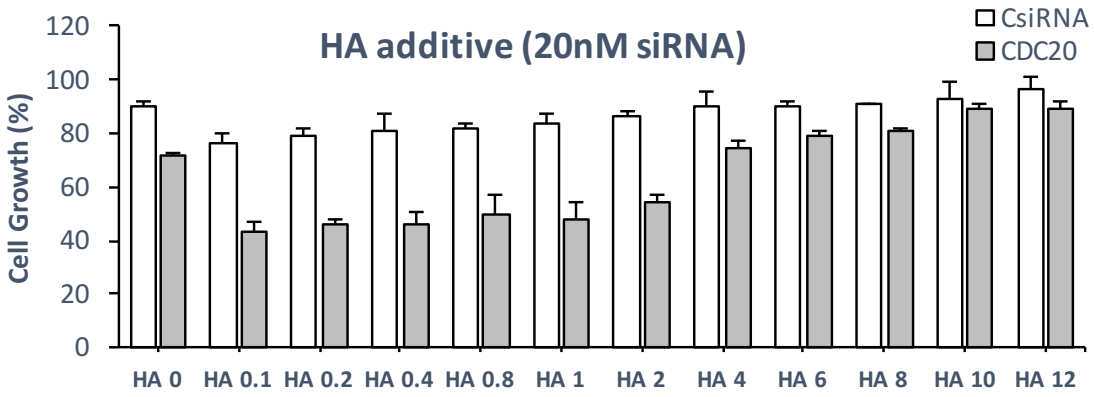

Figure 1.7 Effect of polymeric additives on the transfection efficiency of siRNA polyplexes. Polyplexes were formed with 1.2 kDa lipid-grafted PEI, and a fixed ratio of HA was added to the polyplexes during complex formation. The numbers on the horizontal axis indicate HA:siRNA ratio used for polyplex formation. The specific siRNA against CDC20 is used to inhibit the growth of breast cancer cells in this study. Note that at optimal HA:siRNA ratios (i.e., 0.1 to 2), increased inhibition of cell growth was seen with CDC20 siRNA, while the control scrambled siRNA (CsiRNA) did not show any growth inhibition. Data adapted from[198].

1.4.3 NP vectors by reverse micro-emulsion co-precipitation

The reverse microemulsion co-precipitation is an elaborate method used to fabricate inorganic NPs with good dispersion, homogeneous size, and good reproducibility[199]. In this process, two water-in-oil microemulsions are prepared and mixed together, each one bearing one of the precursors. The co-precipitation reaction is therefore limited to the compartment of the water phase, which works as a reactor at the nano-scale. By having the chemical reaction separated in small compartments, nucleation and growth become physically separated processes, as they depend on coalescence and redispersion events. Nucleation can occur with the coalescence of two droplets carrying the reactants. With redispersion of the short-lived droplet dimer, two daughter droplets are formed carrying reacted and unreacted products. Growth of particles is limited by the decrease in supersaturation inside the droplet caused by nucleation, unless there is coalescence with a new droplet carrying unreacted products (coalescence-exchange led growth) or another NP (coagulation-led growth)[200,201]. It has been proposed that coalescence-exchange is the primary growth mechanism at the early stages of particle formation. In contrast, when the number of NPs becomes sufficiently large, the coagulation of particles during droplet coalescence becomes the primary determinant of final NP size. However, growth is not unrestricted. Maximal particle size is limited by the size of an individual droplet, as head groups of surfactant molecules surrounding the droplet adsorb on the NP surface [200–202]. Thus, the growth limitation in water-in-oil microemulsions is attractive for the production of controlled size vectors. A representation of mechanisms involved in microemulsion precipitation is presented in Fig. 1.8.

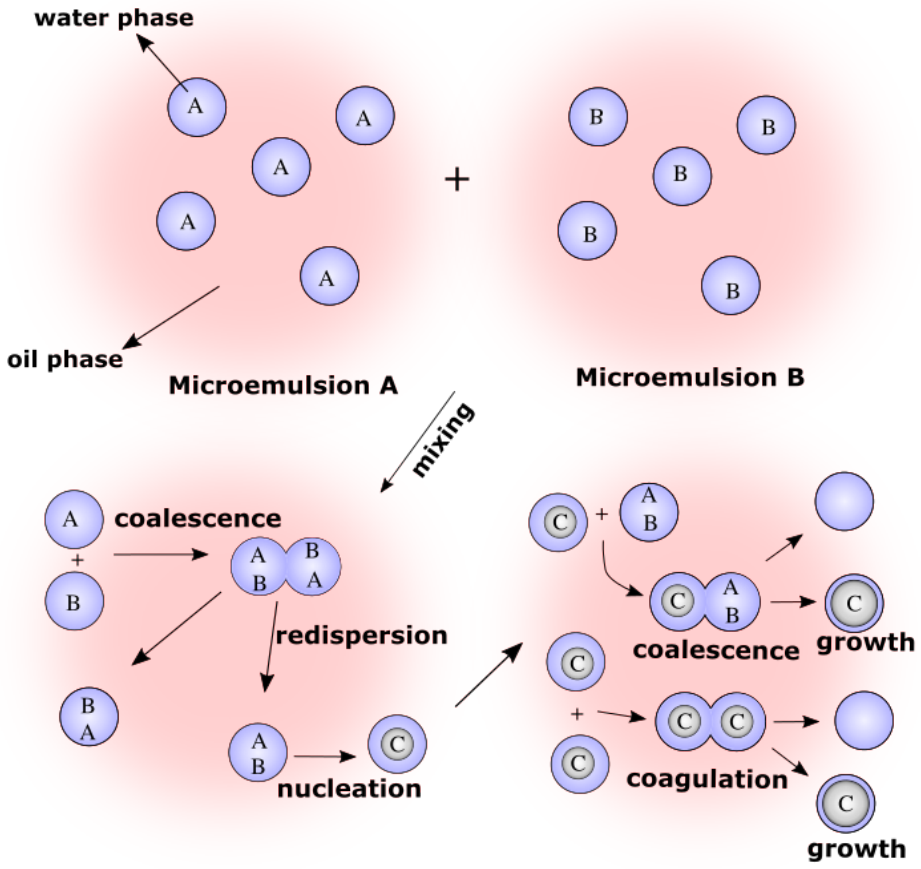

Figure 1.8 NP fabrication by microemulsion. After two separate microemulsions are mixed, the formation of dimers by droplet coalescence results in solution exchange and nucleation. Growth can occur by coalescence or coagulation.

The traditional polynucleotide co-precipitation method can be easily adapted to reverse microemulsion configuration. CaP[43,128,195,203,204], calcium carbonate[18,133,205], and magnesium phosphate[20,21,206] carriers have been synthesized with promising *in vitro* and *in vivo* results for gene therapy and drug delivery. For CaP NPs, two microemulsions are prepared and mixed, each containing the Ca^{+2} and Pi precursors, with the polynucleotide being added to the Ca^{+2} precursor solution. The synthesis of calcium carbonate and magnesium phosphate particles follows a similar reaction between two microemulsions. With the restricted particle growth, co-precipitates produced by this

method are frequently smaller than the ones produced by other co-precipitation methods, with sizes in the range of 40 to 80 nm being reported in early studies[203,207]. The pDNA entrapment efficiency seems to increase with reaction time, with reports of 85% entrapment after 6 h of reaction[207] and >99% after 12 h of reaction[203]; however, a noticeable size increase was seen with reaction time. In more recent studies, efficient entrapment could be achieved for shorter reactions time (i.e., preserving size) by optimization of precursor concentrations and their ratio[195]. Additionally, the Ca/P molar ratio has been shown to influence particle size, ζ-potential, siRNA loading efficiency, siRNA protection against enzyme degradation, and after optimization, better control of breast cancer cell growth was achieved[195]. Surfactant type and concentration can also influence the size and structure of the NPs[208,209]. Various surfactants have been used as emulsion stabilizers in microemulsion fabrication, such as bis(2-ethylhexyl)sulphosuccinate[203], ethylene glycol monobutyl ether[210] and Igepal CO-520[195]. Cyclohexane or hexane is frequently used as the oil phase of microemulsions[152,203,207]. Using toxic solvents and surfactants requires additional steps for purification, such as silica column chromatography, centrifugation, and dialysis. This could be seen as a disadvantage of reverse microemulsion synthesis[168]. However, more-precisely controlled precipitation methods such as the polymer-stabilized co-precipitation require the synthesis of special polymers for growth control [125,159,167,211]. The feasibility of scaling up reverse microemulsion methods to the industrial application is also worthy of note[212].

After the initial studies that settled the foundations of the technique, meaningful innovations were conducted related to the implementation of organic coatings to NPs. In that regard, the coating of CaP NPs by lipids (lipid-coated NPs, LC-NPs) is one of the most

successful strategies with numerous *in vivo* studies for cancer therapy [24,43,213]. LC-NPs can be prepared by adding a sodium citrate solution after mixing the precursor emulsions to avoid the aggregation and insert negative charges to the particle surface, and after NP purification and resuspension in water, a cationic liposome coating is applied by opposite charge attraction. Another option is to use lipids with phosphatidic groups, such as dioleoyl phosphatidic acid, as a stabilizer[40]. In this case, dioleoyl phosphatidic acid is added to the phosphate emulsion and is present at the oil-water boundary when nucleation occurs, interacting with CaP through its phosphate headgroup. These particles were reported to be hollow at the center (from TEM analysis), indicating that nucleation could have been started by dioleoyl phosphatidic acid at the droplet wall. The dioleoyl phosphatidic acid stabilized cores are smaller than the citrate stabilized ones (25-30 nm compared to 60-80 nm). After particle purification, a second lipid layer is added (1,2-Dioleoyl-sn-glycero-3-phosphocholine, DOPC), and further functionalization strategies can be employed to increase the targetability of particles and circulation time (Fig. 1.9). PEG, anisamide [128,152], galactose derivatives[24,206], and folic acid[43,133] are a few examples of the molecules that have been used for the coating of LC-NPs for targeting strategies.

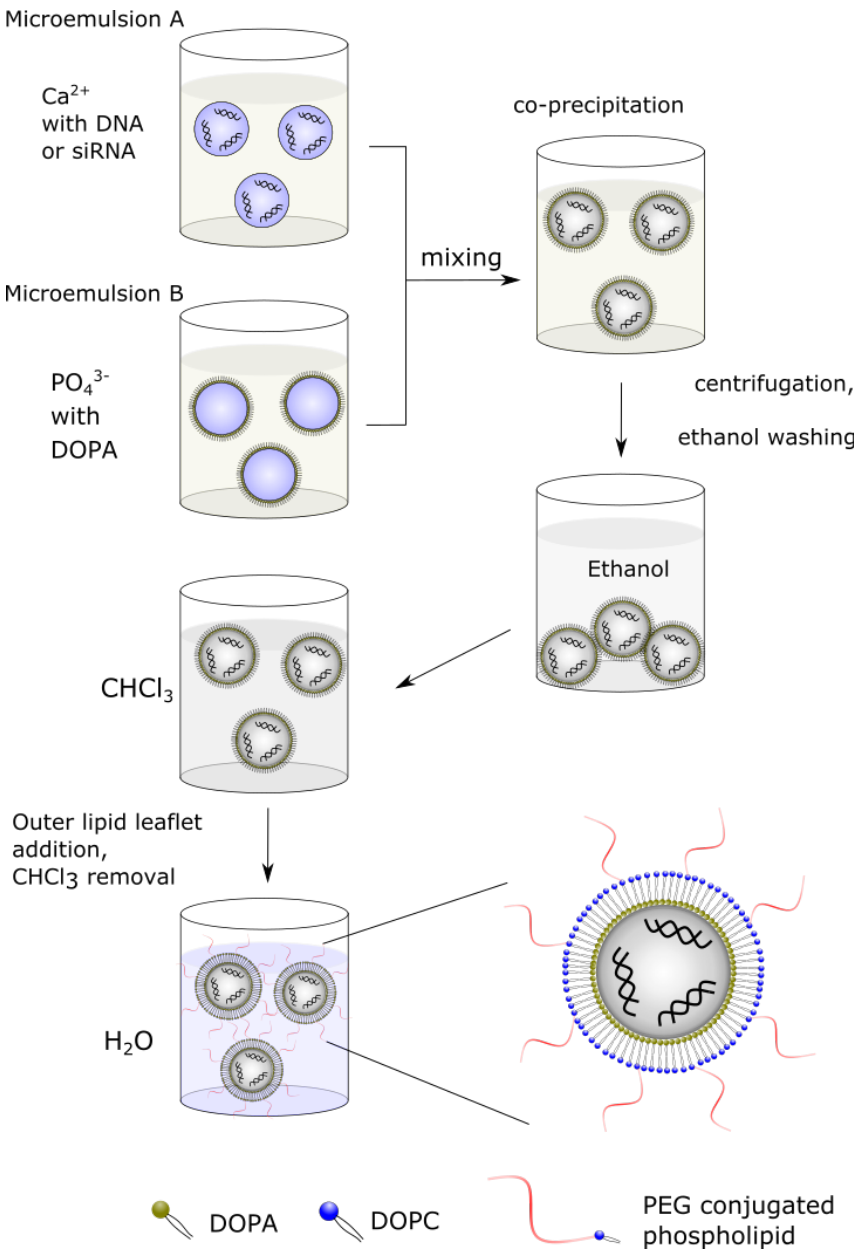

Figure 1.9 Fabrication of lipid-coated NPs (adapted from [40]).

Most of the studies employing LC-NPs concern RNAi therapies to treat various types of cancers. In human lung cancer cells (NCI-H-460), for the same lipid-PEG-anisamide coating, the substitution of a lipid NP core by a CaP core caused a 40-fold higher *in vitro* and 4-fold higher *in vivo* silencing of the luciferase gene[40]. The targeting ligand anisamide

has been shown to have an important role in the efficiency of the particles in lung and metastatic lung cancer by targeting sigma receptors. A 9-fold higher efficiency was found in siRNA delivery to A549 cells when anisamide was present on the surface of LC-NPs [127,128]. The LC-PEG-anisamide NPs were also used to co-deliver pDNA and siRNA targeting the oncogenes MDM2, c-myc, and VEGF, impairing tumor proliferation and angiogenesis and inducing tumor apoptosis. This strategy was efficient in knocking down the targeted genes and impairing A549 and H460 human xenograft growth *in vivo*[127]. The same particles were also capable of significantly reducing the expression of the oncogenes in cancer nodules and reducing lung metastasis by 70-80%[128]. The coating of a pH-triggered charge reversible cholesterol-aminocaproic acid-citraconic conjugate to LC-NPs increased liposomal escape in A549 cells reducing Bcl-2 expression and tumor size *in vivo* when delivered intravenously[160]. The particle charge conversion from anionic at physiological pH to cationic at endosomal pH is thought to increase endosomal escape for CaP with decreased toxicity by other synthesis methods as well, with a faster charge conversion mechanism leading to faster escape[157,173,174].

LC-NPs are also promising delivery agents for breast cancer treatment. Recently, PLGA-PEG stabilized LC-NPs were used to deliver an RNA inhibitor for miRNA-221 and miRNA-222 (miR-221/222) and the chemotherapy drug paclitaxel to triple-negative breast cancer (TNBC) cells[214]. TNBC is a highly aggressive breast cancer, and miRNA-221/222 has been described as being crucial for breast cancer development, progression, and resistance to common therapies, as well as being overexpressed in TNBC[215]. The encapsulation of the hydrophilic miRs by CaP core and the interaction of lipid coating with the hydrophobic paclitaxel, followed by co-encapsulation with PLGA-PEG, ensures the

delivery of both RNA and paclitaxel to the same cells (at defined ratios) and synergistic actions for better outcomes. The NPs were formed by multiple inorganic hollow cores stabilized by the lipid coating and PLGA-PEG as the same entity. With efficient knockdown of miR-221/222, upregulation of the tumor suppressors p27kip1 and TIMP3 was reported, and a synergistic decrease in cell viability was seen for the combinational treatment. In another study, the delivery of siRNA (cell death siRNA) to TNBC cell line MDA-MB-468 was performed by using LC-NPs coated with targeting ligands ABX-EGF scFv [216] and folic acid (FA)[120,121], targeting EGFR and folate receptors, both of which are overexpressed in TNBC [43]. The *in vitro* uptake of NPs bearing optimized amounts of both targeting ligands was moderately reduced by saturating the cells with individual free ligands and drastically reduced with the saturation of both ligands simultaneously, indicating uptake mediated by the specific receptors. The targeted strategy led to improved antitumor activity *in vitro* and increased tumor accumulation *in vivo* compared to non-targeted controls[43]. Untargeted LCP-NPs, on the other hand, have been used in an *ex-vivo* expansion-based therapy. The therapy consisted of knocking down PD-1 in tumor-infiltrating lymphocytes (TILs) from breast cancer patients and PD-L1 in MCF7 breast cancer cells[217]. The combined treatment was responsible for increased tumor toxicity of TILS compared to either of the treatments alone.

Targeted strategies are also critical for new experimental treatments for metastatic cancers in the liver. Stellate hepatic cells seem to have an important role in metastasis establishment and survival of metastasized cells in the liver[218], and two studies highlight novel strategies of treatment with a focus on interfering with mechanisms mediated by these cells[129,130]. Aminoethyl anisamide functionalized LC-NPs were used to study the repair

mechanism of fibrosis in the liver mediated by relaxin expression and its effect in metastatic cancer treatment[129]. Liver fibrosis triggered by metastatic colonization forms a favorable microenvironment for tumor cell survival[218] and limits T-cell mobility and penetration into the tumor area[219]. The aminoethyl anisamide ligand was used to target sigma-1 receptors in activated hepatic stellate cells, which are the main mediators of fibrosis in the liver[218]. Relaxin expression seems to be responsible for an endogenous repair mechanism that reverses fibrosis, which could, in turn, be used as an antitumor therapy[220]. In animal models of late-stage liver metastatic breast, pancreatic, and colorectal cancers, the delivery of the relaxin gene resulted in prolongation of survival by significant inhibition of metastasis progression and increased T-cell infiltration using the targeted LC-NPs [129]. The T-cell infiltration allowed the application of combined treatment with PD-L1 immunotherapy, prolonging survival by 2-fold, which was not effective without induction of relaxin expression. In a different treatment strategy, galactose-coated LC-NPs were used to target the liver to avoid metastasis by disrupting the CXCL12/CXCR4 axis[130]. Stellate hepatic cells have a central role by endogenously expressing high amounts of CXCL12, which leads to the recruitment of immunosuppressive lymphocytes and helps establish the metastasized cells[221]. The CXCL12/CXCR4 axis is vital in the immune system[222]; accordingly, a targeted therapy to the liver is especially important in this case. The strategy consisted of delivering a gene for an antibody-like protein capable of entrapping CXCL12 in colorectal and breast cancer models. The treatment was reported to act by directly inhibiting the CXCL12/CXCR4 stimulation and by reducing the recruitment of $CXCR4^{+}$ immunosuppressive cells. Transient expression lasted 4 days, and with multiple treatments,

test groups presented decreased incidence of liver metastasis and longer survival, with no significant expression outside the liver[130].

Liver targeting with LC-NPs was also used for hepatocellular carcinoma treatment. The uptake mediated by the asialoglycoprotein receptor, predominantly found in hepatocytes and hepatocellular carcinoma cells[223], was studied using 8 different galactose derivatives[24]. A phenyl β-D-galactoside-decorated LC-NP showed the highest uptake between the targeting ligands produced and used for VEGF inhibition by siRNA locally in the liver. Efficient VEGF inhibition *in vivo* led to a decrease in vessel density in the tumor microenvironment, reducing tumor sizes and the extent of metastasis to the lung. The success was highly dependent on the choice of the correct galactoside derivative. In another study, hepatocellular carcinoma cells (HCC) were targeted using SP94 peptide in the tumor necrosis factor-related apoptosis-inducing ligand (TRAIL) gene therapy, with co-delivery of protamine[131]. TRAIL can bind to death receptors inducing apoptosis in cancer cells, being a promising treatment strategy[224]. However, TRAIL resistance was an important reason for underwhelming clinical results. The SP94-mediated delivery showed superior TRAIL expression and apoptosis, which was further increased by the concomitant treatment with sorafenib. The treatment also reduced fibrotic tissue production mediated by hepatic stellate cells. Furthermore, the intracellular release of Ca^{2+} from the CaP core might have helped to de-sensitize hepatic cancer cells to TRAIL through CaM-KII activation and DR5 upregulation[131]. Ca^{2+} intracellular modulation seems to be important for TRAIL toxicity, although this effect is not well understood, with pro-death and pro-survival function depending on experimental conditions[225,226]. The Ca-rich mineralized NPs might be useful for synergistic action for TRAIL-mediated therapies. The SP94 peptide to target HCC

was also used for dual-targeted immunotherapy, using pDNA encoding cytokines to modulate the immunosuppressive tumor environment and activate immune effector cells (IL-2 pDNA) and siRNA against immunosuppressive factors (PD-L1 siRNA)[132]. A thymine-capped polyamidopamine (PAMAM) dendrimer was loaded at the CaP core along with pDNA and siRNA in order to improve the endosomal escape and nuclear entry of pDNA. NPs accumulated predominantly in tumors and liver, and uptake and transfection efficiency were ligand and dendrimer dependent. Additionally, co-treatment with PD-L1 siRNA and IL-2 pDNA showed an increased tumor growth suppression and inhibition of distal lung metastasis compared to either of the treatments alone.

Other than exploring different coatings on CaP NPs, optimizing the mineral composition also represents an opportunity for controlling NP properties. In a study comparing different carbonate to phosphate ratios in CaP/$CaCO_3$ LC-NPs, the dsDNA release rate could be significantly increased by increasing the carbonate to phosphate ratio[18]. However, at carbonate to phosphate ratios >3, dsDNA loading efficiency decreased considerably, and a size increase from 39 nm to 58 nm was observed after 2 days of incubation in cell culture conditions (DMEM with 10% FBS at 37 ºC). In a subsequent study from the same group, NPs with a similar CaP/$CaCO_3$ core at carbonate to phosphate ratio of 1/3 were studied for CD (cell death) siRNA delivery to melanoma cells with an elaborate coating[133]. In addition to the lipid coating, cholesterol, PEG, folic acid (FA), and α-tocopheryl succinate (α-TOS) were added to the outer layer of the NP. The FA is a widely employed targeting ligand expressed in a range of transformed cells, including melanoma cells[119], while α-TOS is the most effective form of vitamin E for adjuvant cancer treatment[227]. B16F0 melanoma cells internalized the NPs via FA-mediated

pathway in a dose-dependent manner until saturation, while CD siRNA and α-TOS synergistically inhibited cell growth[133].

Phosphates of other divalent ions have also been explored for mineralized vectors. NPs with similar in size (<100 nm) and properties to CaP regarding toxicity and dissolution in endosomal pH have been reported. Uncoated MgP and MnP NPs were as efficient as the commercial transfection reagent Polyfect in the transfection of HeLa cells[149]. Coated MgP NPs were efficient in protecting pDNA *in vivo*, and a galactose coating (*p*-aminophenyl-1-thio-β-D-galacto-pyranoside) was more efficient than a PEG coating in concentrating β-galactosidase expression in the liver compared to spleen and lung after IV, IP and IM injections[206]. With a considerable promotion of expression in the immunologically relevant spleen and thymus, the PEGylated MgP NP were also employed as DNA vaccines, eliciting both humoral and cell-mediated responses with considerably low total effective doses administered to animals (1 – 2 μg)[21]. For the sake of comparison, 50 μg per animal were delivered by chitosan NPs to elicit robust T-cell response[228]. More recently, lipid-coated MgP NPs were used as an intracellular delivery agent for a model cargo protein, showing that MgP can be as versatile as CaP in terms of the diversity of its cargo molecules[20].

1.4.4 Co-precipitation with simulated body fluid (SBF)

The mineralization of macroscopic biomaterials by the use of SBF is a traditional 'biomimetic' preparation method employed in biomaterials engineering. Initially described as a tool for evaluating bioactivity of biomaterials[229], SBF has later shown to be valuable in materials synthesis[230–232] and *in situ* mechanistic studies[233]. Surfaces and scaffolds

can become osteoconductive (i.e., support bone growth) by the precipitation of a mineral layer composed of carbonated apatite in SBF[234]. This mineralization process is frequently described as biomimetic because of the similar preparation conditions (in pH, the ionic composition of the solution involved, and temperature) to the physiological mineralization process. Controlled physiological mineralization yields materials with highly complex structures such as bones, shells, teeth, coral, and exoskeletons[235], resulting from the induction of a metastable state and lowering the energy barrier for nucleation with appropriate nucleation sites. In practice, 'biomimetic' mineralization is performed by soaking a material presenting nucleation sites in SBF. Mineralization is therefore controlled by features of the original material, which is very appealing from a materials synthesis standpoint. Another important feature of this process is the possibility of incorporating bioactive molecules such as proteins and polynucleotides inside the mineral layer[234]. This yields materials that are not just biocompatible but also excellent delivery tools, opening new applications for mineralized materials.

During the fabrication of NPs in SBF, nucleation is triggered by the addition of the material or molecule to be mineralized in a premade solution. This is different from the co-precipitation methods relying on the mixing of a polynucleotide/calcium salt and a phosphate salt solution. As in any particulate system, excessive aggregation should be avoided. Recently, strontium doped particles with a diameter of ~300 nm were produced by incubating pDNA for 40 min in a modified SBF containing strontium[236]. Particles were amorphous and spherical with a low polydispersity index. This contrasts with the biomimetic needle-like apatite layers obtained when surfaces are mineralized in SBF at longer incubation times (see below). An increase in strontium content slightly increased particle

size, and when Sr/(Sr+Ca) percentage were greater than 20 in the solid product, transfection efficiency in human fetal osteoblastic hFOB1.19 cells were greatly reduced as a consequence of decreased uptake. While the addition of Sr to SBF did not result in an increased transfection efficiency compared to undoped particle control, a significant increase in ALP activity was observed for all samples containing Sr, indicating the additional benefit of Sr on the osteogenic activity of stem and pre-osteoblastic cells. Indeed, Sr is reported to stimulate osteogenesis and cell proliferation in the form of ranelate salt when present in osteogenic culture medium[237] and when released from hydrogels[238] or bioceramics[239].

1.5 Co-Precipitation Formed Mineralized Surfaces for Gene Therapy

The aggregation that is considered detrimental in particulate fabrication systems might well be advantageous with surface-mineralized configurations. The aggregated state of crystals on surfaces mineralized by supersaturated solutions can be useful to take advantage of the bioactivity and surface-related interactions with cells. Differences between the process of fabrication of particles and surfaces using SBF are presented in Fig. 1.10. The gene transfection from DNA-doped mineralized surfaces, pioneered by Shen[240], is a good example of a strategy that achieves high transfection efficiency by modulation of materials features, showing that aggregation of NPs might not be an impediment to effective gene transfer if the DNA is localized to cell-attachment conducive surfaces. For biomolecule incorporation, nucleation must also be induced by the biomolecule and not just the material surface. This can allow modulating transfection by tuning specific features of mineralized

layers to optimize gene transfer. The main findings using mineral layers for gene delivery are exposed in Table 2.

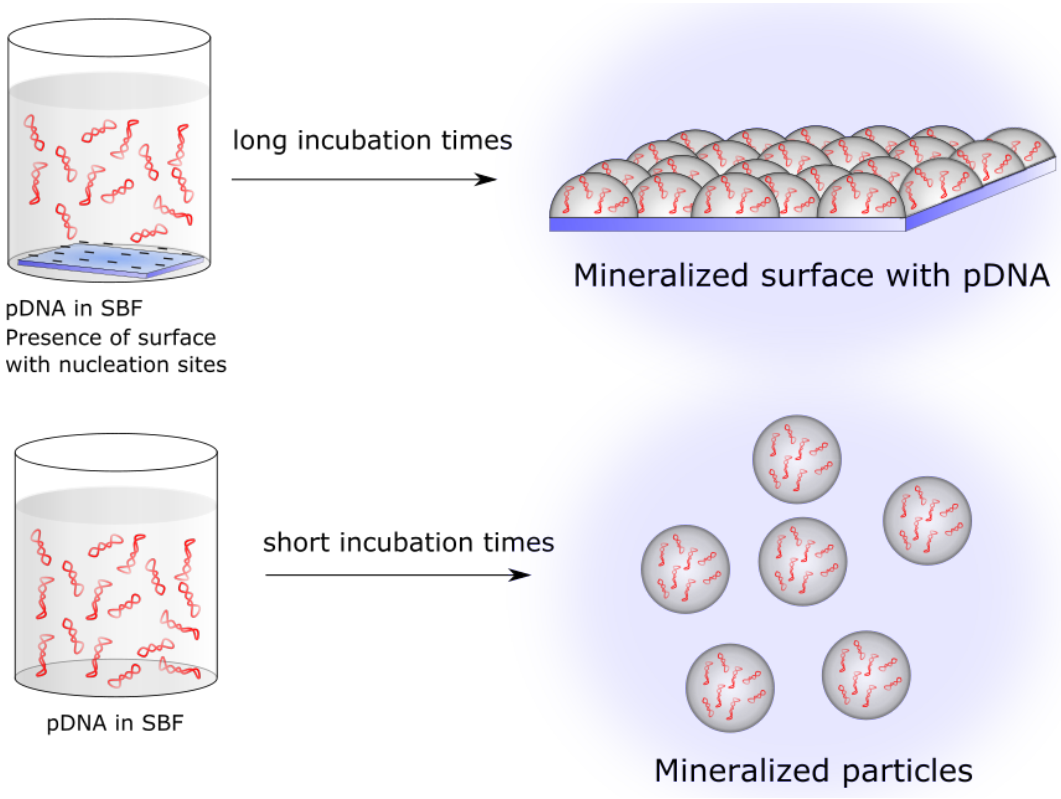

Figure 1.10 Mineralized surfaces incorporating DNA can be produced by exposing a surface with appropriate nucleation sites to SBF in the presence of DNA (top). NPs can be produced from suitable templates (e.g., DNA) using short incubation times, avoiding aggregation (bottom).

Composition and morphology can be treated as interlinked features affecting the efficiency of gene transfer via different delivery mechanisms. Modification of the composition of the mineralization solution led to DNA-doped mineral layers presenting different morphologies and gene transfer efficiencies[240–243]. For example, a formulation without Mg^{2+} induced plate-like crystals with sizes <500 nm, while a Mg^{2+} rich formulation presented big (>500 nm) round crystals. The Mg^{2+} rich formulation led to the highest DNA release efficiency in culture media, and with the removal of Mg^{2+} and increase in the concentration of Ca^{2+}, the lowest release efficiency was achieved. Surprisingly, the

formulation with the highest release efficiency caused the lowest transfection efficiency, while the lowest release efficiency favored transfection. Perhaps fast release from the mineralized surface resulted in a premature release before internalization of the mineralized DNA (since free DNA is not likely to be internalized on its own). Also, the mineral layer with the lowest release efficiency was more sensitive to changes in gene transfer efficiency by changes in DNA doping concentration. It is thought that the plate-like structure can dissolve and deliver DNA inside a nanocrystal, being taken up by cells due to the small crystal size, while the structure with bigger round crystals would dissolve faster and release DNA in a less protected way[240](Fig. 1.11). This fact demonstrates that transfection is, in fact, surface-mediated and therefore related to characteristics of the environment close to the surface, which makes this method particularly translatable to medical device applications[244]. Tuning the solubility of the mineral layer by adding ions known to be related to cell proliferation and differentiation, such as F and Sr, was used to fabricate surfaces that are directed to specific cell types. It was found that for cell types with less discrepancy between phagosomal pH and pH_{50} (the pH at which 50% of calcium ions from the mineral layer are released), higher transfection efficiency is seen. Depending on the composition and cell type, gene delivery from a mineralized DNA-doped layer was more efficient than common lipidic reagent Lipofectamine 2000[241].

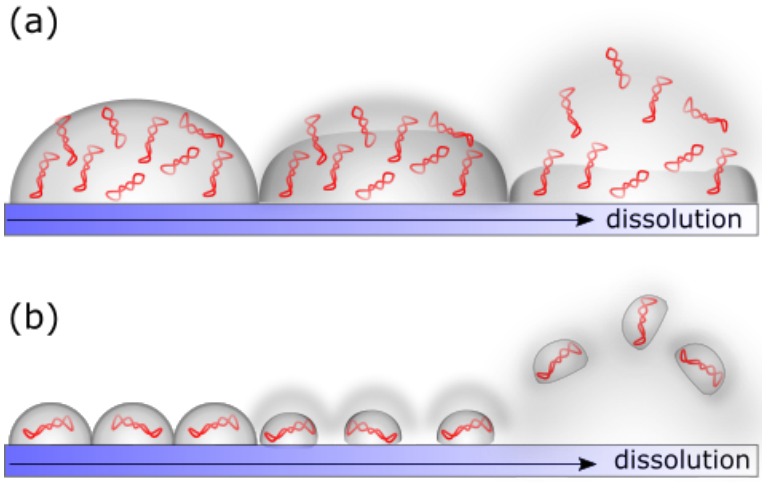

Figure 1.11 Effect of grain size and solubility in the release of DNA from a mineralized layer. (a) Larger, more soluble crystals as a consequence of higher Mg^{2+} content result in the release of DNA unprotected. (b) Small, less soluble crystals in the absence of Mg^{2+} and increased Ca^{2+} content result in the release of mineralized DNA NPs [240].

The chemical groups used to nucleate the mineral layer over the material surface also appear to modulate the DNA transfer[245]. The ability to induce mineralization by anionic groups from supersaturated solutions is known to follow the order $H_2PO_4^-$ > SO^{3-} > COO^- > OH[246–249]. The OH group is considered a weak mineralization promoter, but it induces higher DNA concentration inside cells and transfection efficiency. It was proposed that the weak attraction to the substrate creates a layer that is more easily detached, and the delivery of DNA-bearing particles from the substrate is facilitated[245]. With weaker nucleation by the substrate and DNA being a strong nucleator, the resultant surface could be more DNA dense.

The incorporation of cationic lipids is also a valuable approach for increasing the transfection efficiencies of DNA-doped mineralized surfaces. In this strategy, DNA and cationic lipids are incubated together to form lipoplexes and then subjected to mineralization

in the presence of a supersaturated solution[153,243,250]. This method was more efficient than the delivery of adsorbed lipoplexes from mineralized surfaces and the delivery of mineralized naked DNA. There was co-localization of cationic lipids and DNA in mineralized layers by fluorescent staining, which indicates the incorporation of lipoplexes as intact particles [239]. The incorporation of lipoplexes inside the mineralized layer led to a slow, sustained release profile, while the adsorbed complexes were released in short bursts [251,252]. In the same way as DNA-doped mineralized surfaces, lipoplex composite mineral layers have been shown to have their gene transfer efficiency modulated by the composition of the mineral layer[242]. Detailed studies assessing the effect of the surface charge of the polyplexes on the incorporation in the mineralized layer were not conducted. However, some studies show that the higher lipid/DNA ratio at the same DNA quantity decreases the incorporation of DNA inside the mineral layer, probably because of the increased charge of lipoplexes[242,250,251], which may facilitate increased solubilization and/or steric repulsion. Therefore, it is possible that anionic particles could be more efficiently incorporated into mineral layers.

The delivery of DNA from a mineralized layer is ideal for bone tissue engineering applications. Mineralized surfaces have been shown to induce osteoblastic differentiation in progenitor cells resulting in desired bone-inducing and bone-bonding properties *in vivo*[253]. Tissue engineering relies on the combination of materials, bioactive molecules, and cells to create new functional tissues[254]. Cell adhesion molecules incorporated in the mineral layer can be effective in increasing the affinity of cells to the mineral layer, resulting in improved gene transfection efficiency[165,255]. The adhesion molecules are added to mineralizing solutions to be incorporated during mineralization. The delivery of the BMP-2

gene from mineralized surfaces containing immobilized adhesion molecules laminin[255] and fibronectin[165] have been shown to increase the expression of BMP-2 and increase alkaline phosphatase activity and osteocalcin synthesis *in vitro,* and increased bone formation in vivo[165]. The ability to limit genes inside a mineral layer has also been used to perform area-specific dual gene transfer[256]. Promoter genes for VEGF and BMP-2 were incorporated separately into separate samples that were joined inside the same wells, resulting in area-specific gene transfer, with fibronectin being used to enhance adhesion. The different proteins were expressed spatially confined inside the same well.

Table 1-4 Main factors affecting the transfection efficiency from mineral layers

Main findings	**Biological model**	**Ref.**
Mineral composition can be optimized for transfection of specific cell lines due to ideal nanotopography and/or solubility.	CHO, MG-63, and Saos-2	[240]
	MG-63, Hela, EMT6, Caco-2, TC1, B53, HepG2	[241]
	CHO-K1	[257]
	Human mesenchymal stem cells (HMSCs), C3H10T1/2, and human umbilical vein endothelial cells (HUVECs).	[244]
Complexation of pDNA with a delivery agent before mineralization is superior to other methods (mineralized naked DNA, adsorbed complexes, and traditional transfection with complexes).	C3H10T1/2	[242]
	EMT-6 and B35	[241]
	CHO-K1	[258]
The composition of mineral layer affects expression of intracellular	HEK-293, J774A.1, and mouse embryonic fibroblasts	[243]

DNA sensors and inflammatory cytokines.		
Nucleation of mineral layer by weak nucleators increases transfection efficiency.	HEK-293	[245]
Presence of a cell adhesion molecule on the mineral increases transfection efficiency.	MG-63, HeLa, CHO-K1, and BHK-21 cells	[255]
	MC3T3-E1, HeLa, C3H10T1/2, and *in vivo*	[165]
	CHO-K1	[257]
Synergy in cell differentiation or mineralization markers in bone tissue engineering applications by delivery of bone growth factors from mineral layer.	Human mesenchymal stem cells (HMSCs)	[164]
	Human mesenchymal stem cells (HMSCs)	[244]
	MC3T3, C3H10T1/2 and *in vivo* animal model.	[165]

1.6 NPs from Non-Co-precipitated Systems

1.6.1 Solid core and multi-shell NPs

In all vectors discussed so far, the polynucleotide cargo is incorporated inside the mineralized carriers in variations of the traditional co-precipitation method. These methods frequently demand the use of additional and sometimes elaborate strategies to inhibit excessive particle growth, which can be time-consuming or require the design of special polymers for this function. However, polynucleotides have many of the characteristics of the substances routinely used to stabilize mineral NPs, such as long hydrophilic chains and, in the case of DNA, strong interactions with Ca^{+2}. Therefore, the Ca^{+2}-DNA binding can be exploited as a growth control and/or dispersion strategy, making DNA a particle stabilizer in addition to its therapeutic function.

This is simple to achieve experimentally. The polynucleotide is added after particle synthesis to a suspension of particles[259–261]. The resultant nanoarchitecture consists of a solid core decorated with the polynucleotide. The particles can be synthesized with more flexibility since the polynucleotide is not present during the fabrication process. For example, high-temperature aqueous precipitation[163] and flame spray synthesis[44] could be performed, and the polynucleotide can be added after room temperature, and other appropriate parameters are achieved. This allows more flexibility to experiment with different particle crystallinities and morphologies, such as nanorod, needle, and flower-like mineral morphologies[262]. If the synthesis is performed at room temperature, polynucleotides can be added immediately after nucleation to take advantage of growth inhibition induced by surface adsorption[104,259]. Indeed, the loading of the polynucleotide occurs at the NP surface, which creates a new configuration in which loading is governed by surface adsorption (and not ionic interactions in solution as in CNT), and the polynucleotide is somehow exposed to the medium. Loading capacity and efficiency will likely be limited by surface saturation. Studies performed on double-stranded DNA adsorption to HAp show that DNA binding strength and conformation greatly vary depending on the plane of adsorption[262,263]. Moreover, needle-like particles with a higher proportion of Ca^{2+} rich planes presented more efficient siRNA binding[264]. The salt composition can also affect the dynamics of DNA binding on a solid substrate. For example, on DNA adsorbed to a mica surface, different divalent cations caused different DNA conformations, while adsorption of DNA on a monovalent cation medium was not possible[265]. Furthermore, it was proposed that the presence of Ca^{2+} can have a positive effect on transfection efficiency by inducing conformational changes in DNA decorated NPs[266,267]. The exposure of the

polynucleotide to aqueous media is a concern due to the possibility of degradation by nucleases, and many strategies have been used to address it, such as coating the NPs with additional mineral layers[104,268] or protection by polymer coatings[163].

One of the first reported variations of the solid core NPs involved adding an extra mineral layer after DNA adsorption by subsequent precipitation. DNA on the surface of the original core serves as the nucleator for the new layer[161,259,269]. This process can be repeated multiple times, producing a particle with multiple shells (multi-shell particles), where the final layer could be an organic coating layer[104,259]. Multi-shell NPs presenting PEI as coating layer (CaP/DNA/CaP/PEI) (Fig. 1.12(a)) had better pDNA transfection in multiple cell lines compared to pDNA coated multi-shell NPs[104,259], probably due to increased cationic charge. However, toxicity was also high depending on the concentration used, and this requires careful optimization of efficiency vs. toxicity features as in other multi-shell NPs[154,161].

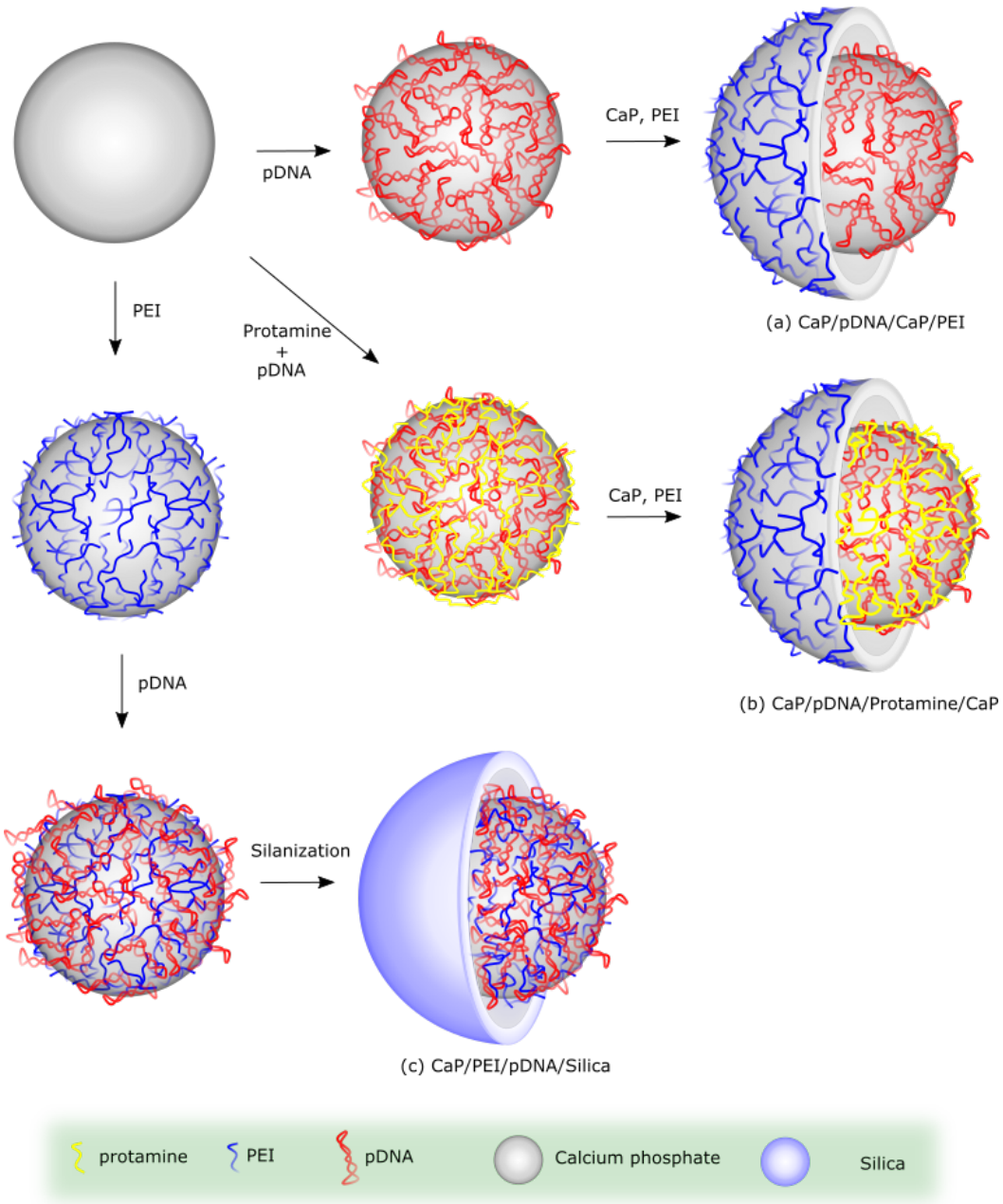

Figure 1.12 Different types of multi-shell NPs. (a) CaP/pDNA/PEI[104,259]. (b) CaP/pDNA/Protamine/CaP[162,270] . (c) CaP/PEI/pDNA/Silica[271].

Multi-shell NPs were used for induction of osteochondral regeneration in MSCs inside an enzyme crosslinked scaffold[268]. Different multi-shell architectures were produced by intercalating CaP, pDNA, and branched PEI (25 kDa). Interestingly CaP/pDNA and

CaP/pDNA/PEI had similar reporter gene (i.e., GFP) expression in hMSCs while the intercalation of a calcium layer between pDNA and PEI (CaP/pDNA/CaP/PEI) more than doubled the GFP expression. It is possible that while PEI is important for increased delivery into the cells, its direct interaction with pDNA might be detrimental (e.g., by minimizing DNA release inside cells), and the precipitation of the acid-labile mineral layer between these two components decreased such interactions. The CaP/pDNA/CaP/PEI particles were then used for delivery of TGF-β3 and BMP-2 genes to hMSCs, stimulating chondrogenic and osteogenic differentiation with spatial control (each lineage occupying a specific portion of the scaffold) with long term transgene expression[268].

After the first multi-shell approaches were published, several variations of the technique were reported. A few comparative studies shed light on the relative efficiency and cell viability of these particles. A study compared CaP/DNA/CaP/PEI particles with different protamine addition methods for gene delivery to hMSCs using a collagen scaffold[270]. Protamine was either added with DNA between the two CaP layers or after the PEI adsorption. When protamine was added with DNA, an increase in transfection efficiency, BMP-2 (transgene) concentration, and cell viability was achieved (Fig. 1.12(b)). This is a promising result since most studies on multi-shell particles reported an increased transfection accompanied by increased toxicity. When optimized protamine-modified multi-shell NPs were combined with mineralized collagen scaffolds, enhanced local expression of BMP-2 and ectopic tissue formation were achieved *in vivo*[162]. In another study, octa-arginine was added as a finishing layer to the multi-shell NPs, and then these particles were compared with protamine- and PEI-finished multi-shell NPs, and the simple DNA adsorbed CaP NPs[272]. The PEI-finished multi-shell particles were superior to protamine and octa-

arginine coated particles in HeLa and SAOS-2 cells. However, octa-arginine was superior to PEI in hMSCs and human osteoblasts. Particles in this study had minimal toxicities, especially the PEI-finished particles. This effect was attributed to the removal of excess polymer and additional purification steps by centrifugation. The simple DNA-adsorbed CaP cores showed high cell viabilities but low transfection efficiencies. However, the authors did not perform DNA incubation with Ca^{+2} before adsorption onto inorganic cores, which is reported as being strictly necessary for efficient transfection with this simple particle formulation[23,44,267]. Interestingly, unlike other groups, the octa-arginine-finished particles presented high transfection efficiency even when cells were treated with amiloride[272], an inhibitor of macro-pinocytosis and Na^{+}/H^{+} exchange[273], presumably indicating a direct penetration mechanism for these NPs. However, this phenomenon was not studied in more detail.

An interesting variation on the multi-shell approach consists of stabilization of CaP core with PEI, followed by DNA adsorption. The CaP/PEI/DNA particle is then submitted to a silanization process by hydrolysis of tetraethoxysilane, forming a silica-coated particle (Fig. 1.12(c)). Particles with a silica shell functionalized by thiols were used to induce osteogenesis in MC3T3-E1 preosteoblasts with low toxicity[271], but these particles were not compared with other types of particles built around a CaP core. In another study, the CaP/PEI/DNA/silica particles were compared to CaP/DNA/CaP/PEI particles and the commercial vector Lipofectamine in 10 different cell lines. Results were highly dependent on cell type, and for each cell type, higher efficiency was correlated with higher toxicity, i.e., efficiency did not seem to be correlated with particle fabrication strategy[154]. Perhaps, the most elaborate version of the silica-coated particles involved the attachment of targeting

antibodies, which was facilitated by the thiol-terminated silica shell[134]. Following this strategy, conjugation of anti-CD146, anti-IgG1, and anti-IgG2 was used to deliver toll-like-receptor ligand-3 to the liver in order to enhance inflammatory response as a possible immunization tool. Particles were mainly concentrated in the liver and lungs after intravenous injection, and hepatocytes gave an increased expression of IFN-α/β, TNF-α, IL-6, and IP-10 with targeting. Similar particles were also used as DNA-based vaccines against HIV-1 functionalized with the TLR9 ligand for T-cell activation, inducing an effective humoral immune response compared to naked DNA [135].

However, the necessity of the multi-shell approach has been questioned. Pedraza *et al*. proposed that rather than the additional mineralized layers, what causes the increase in transfection efficiency is simply the presence of calcium salt, and mineralization would not be necessary as a last step, i.e., a solid core stabilized particle would be as efficient as a multi-shell particle[267]. Using MC3T3 and NIH/3T3 cells, the counter ion in the calcium precursor was also of great importance for the transfection efficiency, with other calcium salts not being effective in comparison to $CaCl_2$ for increasing transfection. In fact, efficient gene silencing was also possible with particles that were not finished by a protecting layer[274]. The same type of supposedly unprotected particles was used for cardiac delivery of siRNA in vivo[23]. Hybrid tricalcium phosphate/Fe_2O_3 particles prepared by flame spray synthesis decorated with DNA in the presence of $CaCl_2$ were also efficient in delivery, with the added benefit of being magnetically deliverable[44]. These results raise the question of how important additional layers are for delivery efficiency and which kind of finishing layer is most appropriate for each application or cell type.

An alternative to the multi-shell approach is to elaborate the polymer coatings after polynucleotide adsorption to the solid core. Porous spherical $CaCO_3$ particles prepared in the presence of arginine carrying a p53 expression system had improved transfection by an additional PEI layer in multiple cancer cell lines. The high porosity provided by the arginine-mediated synthesis ensured high loading, while the PEI coating was responsible for high uptake in the cells[275]. It seems like the intercalation of multiple layers of polymer and polynucleotide is also a possible strategy to increase the total loading of particles[163]. In another approach, multiple CaP NPs carrying siRNA were encapsulated by poly(D, L-lactide-*co*-glycolide) in a water in oil emulsion method and then coated by PEI[161,269]. The presence of the CaP cores was shown to increase the loading of siRNA inside the PLGA particles. This particle formulation was used for the knockdown of multiple inflammatory genes in local delivery approaches to the lungs[269] and colon[161]. A summary of NP size by TEM and DLS as a consequence of the layers around a homogeneous solid core is shown in Table 4.

Table 1-5 Solid core/multi-shell NP size as a consequence of functionalization/extra-mineral layers.

Ref.	Layers/composition	TEM	DLS
[267]	CaP/pDNA	20–150 nm	116.00 ± 23.78 nm
[259]	CaP/pDNA	-	152 nm
[259]	CaP/pDNA/CaP	-	415 nm
[259]	CaP/pDNA/CaP/pDNA	-	216 nm
[104]	CaP/pDNA/CaP/PEI	-	285 nm (PEI 0.1 mL) 150 nm (PEI 0.5 mL)
[276]	CaP/PEI/pDNA/SiO_2.	40–120 nm	482 nm
[274]	CaP/siRNA	100-200 nm	-

[163]	CaP/siRNA/PEI-gal/siRNA/PEI-gal.	50-60 nm	56-60
[44]	Fe_2O_3/CaP/pDNA.	25 nm	121 nm
[161]	Cap/siRNA/PLGA/PEI.	150 nm	151
[275]	($CaCO_3$+Arginine)/PEI/pDNA.	900 nm	-
[272]	CaP/pDNA/CaP/Octa-arginine.	-	200-500 nm
[277]	CaP/siRNA/PEG-destran-3,4-dihydroxy-l-phenylalanine (dopa) conjugate.	-	150-250 nm
[135]	CaP/PEI/CpG (TLR9 ligand)/DNA/silica.	~100 nm	158.8 ± 1.93 nm

1.6.2 Mineralized pre-assembled NPs

Another strategy for gene vector design consists of assembling organic NPs encapsulating the cargo and subsequently performing a mineralization reaction. This method borrows knowledge from the vast literature concerning the mineralization of polymer NPs for intracellular delivery of chemotherapy drugs[278–287]. The mineralization of pre-assembled particles provides an extra acid-labile protection layer to crosslinking techniques of the shell, in which stimuli-labile crosslinks are introduced to polymer NPs, making it stable at extracellular conditions. Upon stimuli, the labile crosslinks can be cleaved, increasing the efficacy of drug delivery due to protection against drug leakage in the extracellular environment[288]. However, the breaking of the crosslinks may be accompanied by changes in the polymer structures leading to undefined species as well as

the generation of toxic by-products[289]. Therefore, many authors relied on mineralization as a safe way for preserving the nanocarrier structure until intracellular delivery. The rapid dissolution of mineralized materials such as CaPs or $CaCO_3$ at mildly acidic pH makes them responsive in intracellular environments such as the endosome and lysosome or at the low pH extracellular matrix of tumor tissue[278–287].

Pioneering methods for mineralization of organic particles, such as the ones developed by Antonietti[278], Schmidt[279] and Perking[280], follow the basic fundaments of the CNT. Low supersaturations in combination with excess nucleation sites over the particles are used to assure a controlled mineralization process. The nucleation sites, in this case, are ionizable anionic groups in sections of the polymer molecules that form the polymer shell. Ca^{+2} in solution bind to carboxylate groups in polyaspartic acid[281], hyaluronic acid[282] or methylcarboxylated chitosan[285] of fabricated particles, and when a solution carrying phosphate salts is added, precipitation occurs in association with such polymers. Studies can be divided between those using a single step mineralization reaction with long incubation times[281,283,285,286] or those using a sequential addition of Ca^{+2} and Pi solutions with certain intervals (e.g., 10 min) between each step that causes a gradual increase in supersaturation[282,284,287]. Mineralization does not appear to have a noticeable effect on the size of the NP when reasonable supersaturations are used (i.e., the template NP size dictates the final size). On the contrary, for HA polymers, the mineralization actually decreased the particle size, which can be a consequence of conformational changes induced by Ca^{2+}[282,284,287]. The mineralized delivery systems are frequently referred to as being "robust" or "reinforced" as a reference to their improved ability to retain the cargo at the extracellular environment and release it at the acidic pH of tumor tissue or

endosomes[282,285,286]. As a result, *in vivo* studies typically show an increased concentration of particles in tumor tissue compared to unmineralized NPs, and consequently, more effective treatment[283,284,287]. A successful mineralization process is accompanied by increased cargo retention at the physiologic pH.

Compared to the wider field of intracellular delivery using mineralized particles, the applications in the field of gene therapy is relatively scarce based on the few reported studies. However, studies highlighting the importance of the mineralization mechanism of viruses in survival and infection shed light on what could be a strong strategy in the development of new vectors for vaccines and gene therapy[166,290,291]. Zhou and coworkers proposed that the high calcium concentration in Aves's digestive system could mineralize influenza viruses and be a key factor in the initial Aves to human contamination[292]. They performed mineralization in a simulated avian gastric fluid. Mineralization was accompanied by a change in ζ-potential from negative to slightly positive and a drastic increase in adsorption to A549 cells surface (as high as 10-fold compared to unmineralized viruses depending on virus type). Differently from cellular systems that can actively control self-mineralization, viruses are passively mineralized as they can only exert some kind of control over their mineralization by expressing proteins carrying appropriate chemical groups for nucleation sites[293]. An uptake mechanism highly dependent on endocytosis was observed only in mineralized viruses, such as in the case of CaP vectors[70]. It is thought that mineralization might overcome low infectivity in the absence of specific receptor interactions between non-adapted avian viruses and human cells[294]. BALB/c mice infected intranasally with the mineralized H1N1 presented a 10-fold higher viral load compared to those infected by native H1N1, which led to mortality of 100% with mineralized H1N1 compared to 40% with the

unmineralized virus after 12 days[292]. Mineralization might also be responsible for protecting the viruses against high temperature and dissociation when not infecting an organism, which could help the spread of viruses without a host[293] as well as protecting the virus when infecting a host when there is a pre-existing immunity[290].

Most of the properties that viruses acquire when mineralized are attractive for therapeutic applications. Interestingly, the realization that mineralization is a powerful therapeutic strategy using viruses seems to have occurred before the idea of mineralization as a natural mechanism in interspecies infectivity[295]. Earlier papers on the subject of mineralized viruses did not perform controlled mineralizations, and resultant images indicated excess precipitation and particle growth, probably due to the use of excessive supersaturations[41,291,296]. The improved adhesion to epithelia caused by the mineralized shell showed promise in gene transfer to blood vessels[297] and airways[295]. In more recent studies, more careful mineralization processes were performed, being capable of preserving the nanometric size of the viral particles[26,166,298], which probably plays an important role in the efficiency of treatment. In the case of delivery to airways, particles with sizes smaller than 300 nm have been shown to be able to perform a longer-lasting drug delivery by less interaction with mucus[299]. An oncolytic adenovirus was mineralized and surface coated with a lipid bilayer and PEG for cancer therapy[26]. Results showed improved tumor delivery *in vivo* with the mineralized particle as a consequence of the decrease in hepatic sequestration and immune response. It is proposed that mineralization would not inhibit receptor-mediated delivery since the shell can dissolve at mildly acidic pH of the tumor environment. In another study, an oncolytic adenovirus was mineralized by a combination of $MnCO_3$ and $CaCO_3$. The mineral layer conferred increased circulation time

when administered intravenously in mice due to lower immune response, which resulted in considerably higher tumor concentration in mice with 4T1 xenografts. The Mn^{2+} released from the mineral shell triggered O_2 production in the cancer cells, which is an important factor to induce enhanced oncolytic adenovirus replication and cancer cell lysis. As a result, the combination of $MnCO_3$ and $CaCO_3$ resulted in an accentuated oncolytic effect. Also, the free Mn^{2+} and higher O_2 intracellular concentration in the tumor resulted in increased signal for magnetic resonance and photoacoustic imaging.

Mineralization is also relevant for the development of vaccines. An effective mineralized needle-free intranasal immunization against the dengue virus was elaborated; the increased adhesion to the mucosa and receptor-independent uptake generated an efficient local IgA response and systemic antibody response, neutralizing the virus[166]. The increased thermal stability due to the mineral layer is also a property of interest for vaccines. Mineralized vaccines were shown to be effective after 9 days of storage at 26 ºC, while unmineralized vaccines lost efficacy after 3 days. This property is especially important in reducing the cost of vaccination programs, in which the vaccines must frequently be maintained in non-urbanized locations that do not have appropriate refrigeration. The expression of peptides capable of nucleating CaP with anionic chemical groups was also important, with viruses specifically engineered to undergo effective mineralization being much more resistant to temperature increases during storage due to more efficient mineralization[298]. Another appealing property that comes with mineralization is that mineralized viral particles can be concentrated by traditional centrifugation, while native viral particles demand ultracentrifugation under complicated conditions for appropriate concentration[41,298].

The delivery of genes by mineralized pre-assembled NPs presents properties such as decreased toxicity, sustained gene expression, increased transfection efficiency, and increased loading efficiency[300]. Ito and coworkers fabricated cationic PEI/pDNA NPs and charged-reversed the NPs to anionic by adsorption of HA[300]. Bearing the appropriate nucleation sites, the particles could be mineralized by overnight incubation in a supersaturated metastable solution at a low temperature (4 ºC). The adsorption of negatively charged polymers to positive particles is a simple way of adding nucleation sites without the necessity of fabrication of special polymers, and it also has been shown to increase transfection efficiency by loosening PEI/DNA complexes[118]. SEM showed aggregated 200 nm spherical particles. Although TEM images were not published for this study, which precludes the verification of the organic/inorganic interaction, gel electrophoresis showed an increase in dissociation robustness of particles after mineralization, a hallmark of mineralized particles. The conjunction of attractive features caused by mineralization, such as prevention of DNA release at the physiological pH and a delayed and sustained DNA expression *in vitro,* makes the proposed process an interesting option to better adapt the use of polyplexes to clinical treatment. Mineralization resulted in an improved tumor growth suppression compared to controls when the suspension of particles was injected directly into the tumor[300].

More recently, Chen and co-workers prepared NPs formed by stearic acid-modified PEI (PEI-StA) and minicircle DNA (mcDNA) and submitted the particles to $CaCl_2$ incubation followed by precipitation of CaP by the addition of a buffered solution[301]. The CaP constituted the outer layer of the nanocomplexes forming hybrid particles. However, most of the particle features showed otherwise. The particles that were submitted to

mineralization were cationic, which is an indication that these particles lack the primordial requirement for nucleating CaP and form a hybrid structure. TEM images show overgrown homogeneous structures (~1 μm) without any indication of heterogeneity (i.e., purely inorganic-looking particles). Heterogeneity of phases is highly characteristic of mineralized organic NPs and self-evident in TEM analysis, even without the use of staining techniques. For example, mineralized poly(aspartic acid)-based NPs presented hollow cores and an identifiable coating layer[281], while HA presented multiple solid cores inside the same particle[282,284] or multiple denser spots in a less dense matrix[287]. Additionally, mineralized particles prepared by Chen and coworkers had weaker DNA binding capacity than the unmineralized particles in gel electrophoresis, which is unlike the expectation from mineralized particles. In Fig. 1.13, Chen's TEM and gel electrophoresis (Fig. 1.13a and b) results are compared with TEM results and cumulative release of mineralized hyaluronic acid particles carrying doxorubicin from reference [282]. A heterogeneous morphology was obtained after mineralization, indicating a successful process, with increased robustness of mineralized particles (Fig. 1.13c, d, and e). Even with the strong indications that the particles were not successfully coated by CaP in Chen's study, the treated particles were much more effective than untreated particles in inducing GFP expression in HEK293T cells and secretion of bispecific T-cell engaging antibodies in HepG2 cells for immunotherapy, which raises the idea of some kind of secondary interaction(s) leading to increased effectiveness. It is possible that the increase in transfection efficiency is merely a consequence of the ionic content of the buffer solution used for CaP precipitation, including the free Ca^{+2} content. There are multiple studies showing that $CaCl_2$ by itself can increase the transfection efficiency of polyplexes[302,303]. Another possibility is the presence of some kind of

surface interaction between the complexes and the CaP surface that increases transfection efficiency. Mineralized surfaces have been shown to be helpful in mediating PEI/DNA transfection to MSCs by increased uptake in reverse transfection[304], but it is unknown if particulate systems can exert the same effect.

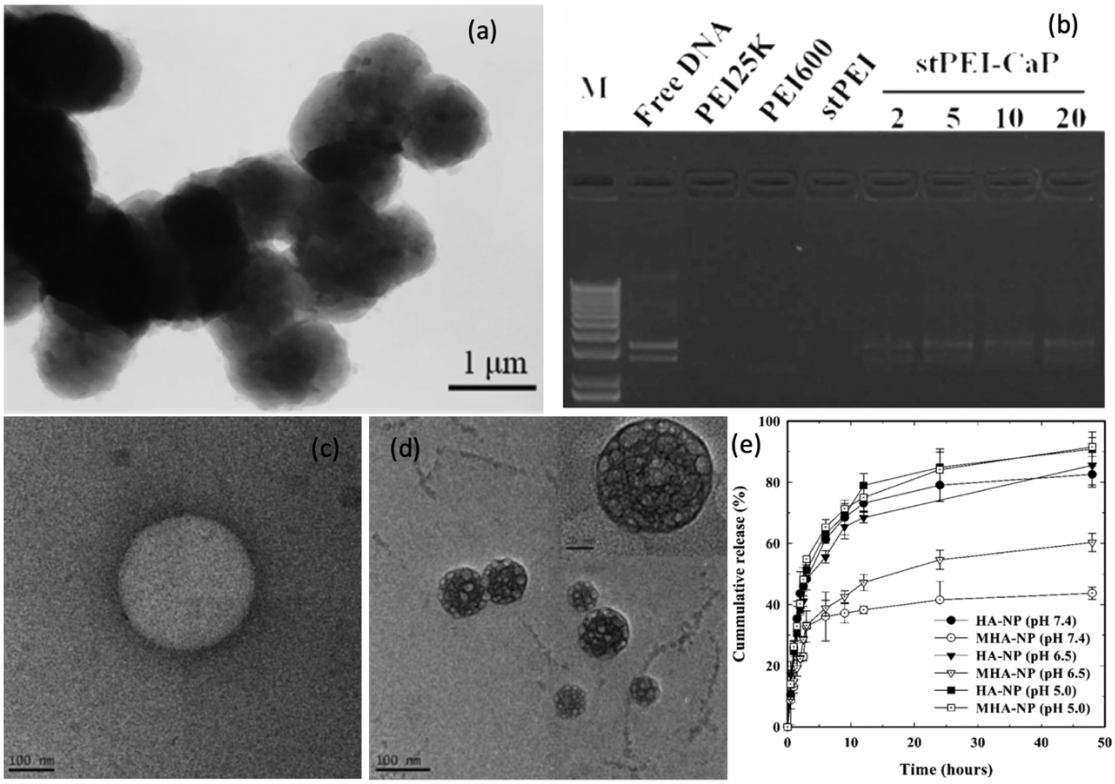

Figure 1.13 (a) TEM image of mineralized stPEI/DNA complexes without indication of the presence of heterogeneous morphology. (b) Gel electrophoresis shows a decrease in the robustness of mineralized complexes[301]. TEM of (c) nonmineralized (HA-NP) and (d) mineralized hyaluronic acid nanoparticles (MHA-NP) carrying doxorubicin, with the indication of successful controlled particle mineralization by heterogeneous morphology of particles. In (e), the cumulative release of HA-NP and MHA-NP at different pH indicates increased robustness as a consequence of mineralization at pH 7.4 and 6.5 [282].

We performed the mineralization of polyplexes with CaP mediated by poly(aspartic acid) [155]. The positively charged polyplexes could be mineralized due to the shift in surface charge by poly(aspartic acid) adsorption (Fig. 1.14). The complex formed by Ca^{2+} and negatively charged polyelectrolytes is proposed to be an intermediate species in templated mineralization [305]. Accordingly, after the coating with PAsp, the polyplexes

were submitted to incubation with $CaCl_2$ for 30 min to increase Ca^{2+} sequestration and then mineralization with Na_3PO_4 for another 30 min. The chemical reaction took 1h, which is a lot shorter than the time needed for mineralization reactions using metastable solutions such as SBF. In figure 1.14, we show the fabrication process used, and a TEM image of the mineralized polyplexes, showing a shell-core morphology (observed as rings), indicating a less dense organic core, believed to be the polyplex, coated by CaP. The size of the NPs ranged from approximately 100-300 nm. Convincing TEM in conjunction with a strong increase in robustness are good indicators of a successful mineralization reaction. *In vitro* transfection studies showed that both calcium incubation and mineralization could enhance transfection efficiency [155].

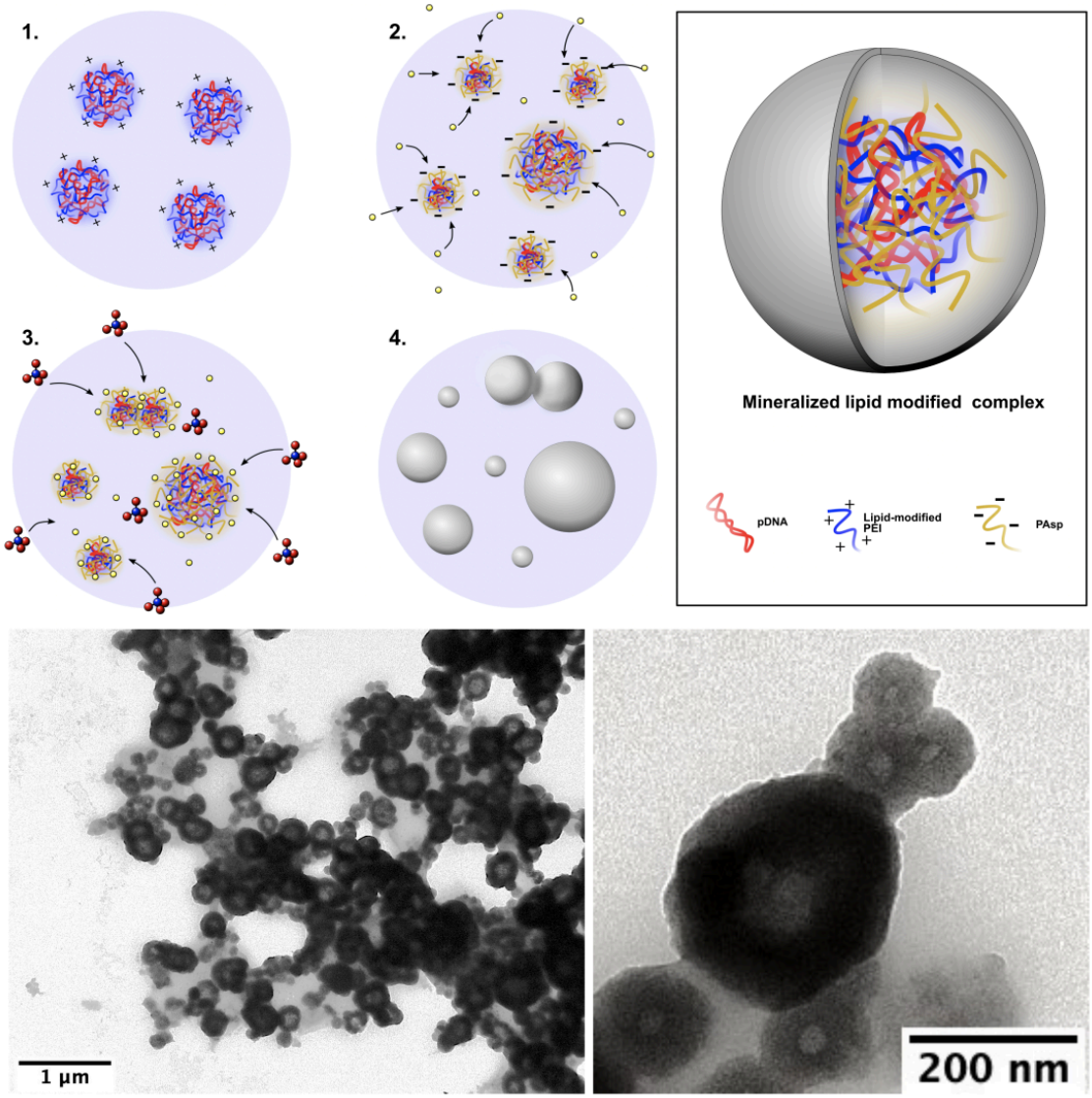

*Figure 1.14 Mineralization of lipid-modified PEI/pDNA polyplexes mediated by poly(aspartic acid) (PAsp) from [155]. **1.** Polyplexes are positively charged. **2.** PAsp adsorption shifts the surface charge to negative and enables the chelation of Ca^{2+}. **3.** Mineralization occurs at the surface of the polyplexes by the addition of a phosphate salt (Na_3PO_4). The resultant nanoarchitecture is believed to be a polyplex inside a mineral shell (top right), which is in accordance with the TEM image from the polyplexes (bottom). The shell-core morphology observed is a consequence of the contrast between the less dense organic core (polyplex) and the dense mineral shell [155].*

1.7 Conclusion and Future Perspectives

Calcium phosphates and carbonates, and other minerals reviewed here, have been demonstrated over the last decades to be safe in a wide range of medical applications. Perhaps due to well-established clinical use in medicine and dentistry in bone-related

applications, calcium phosphates are the most studied materials of its class for fabrication of gene vectors. Calcium carbonates, currently a common product in the food industry, is also gaining popularity as a delivery vector. Efficient incorporation of polynucleotides during mineral precipitation is clearly beneficial to minimize the volume of applied exogeneous mineral. The mineralization protocols reviewed here are straightforward and can be used in both DNA and RNA delivery with minimal adaptations, which also allows the possibility for co-delivery of these agents. The dissolution of minerals under acidic conditions can lead to efficient nucleotide protection against natural defenses while facilitating intracellular release at the endosomal pH with benign degradation products indistinguishable from physiological ions. These inherent attractive properties, however, cannot propel the use of mineralized vectors to clinical practice alone. Efforts are needed to overcome the continuous particle growth and lack of specific cell/organ targetability.

Polymer and lipid-coated NPs are closer to clinical practice than the mineralized NPs. Both techniques are highly promising to offer NPs with low polydispersity and specific targeting. Polymer-coated mineral NPs have their growth limited by the attachment of hydrophilic moieties with strong interactions with Ca^{2+}, which allows for a clean and straightforward precipitation method in water, with NP size being a consequence of the macromolecule used as well as reaction concentrations. Lipid-coated NPs are fabricated in reverse microemulsions and, as a consequence, have the drawbacks of demanding multiple washing steps to remove organic solvents and surfactants, followed by redispersion in chloroform for the attachment of functional molecules before the NPs can be redispersed in water. However, the reverse microemulsion method offers impressive control over the size and the polydispersity attained, and the lipid-coated core can be easily modified by

incorporating lipids carrying PEG and ligands. Due to the advanced size control and efficient cancer cell targeting, lipid and polymer-coated NPs are featured more frequently in *in vivo* (animal) studies than the mineralized vectors, which indicates better proximity to the clinical practice. Based on the review of the current literature here, we predict both technologies having their first use in cancer treatments employing RNAi. Precipitation in water is clearly a cleaner and cheaper process, but the high level of reproducibility of the reverse microemulsion method provides a higher potential for scalability. Perhaps each fabrication technique will naturally find a role based on the requirements of the application. It would be desirable, however, to seek adaptations to the reverse microemulsion method resulting in a cleaner method.

Studies on multi-shell NPs, on the other hand, seem to still focus on achieving optimal composition and fabrication strategy, not being on the same level as polymer or lipid-coated NPs with respect to the extent of preclinical animal studies. Perhaps, this is due to the fact that research with multi-shell NPs focused on achieving cationic NPs, which indeed results in high *in vitro* transfections. However, those might not be appropriate for cancer applications. Incorporation of the NPs in scaffolds that are attractive to specific cell types might be the most appropriate *in vivo* application for cationic non-targeted strategies and hold promise in tissue engineering studies. Of note, studies on multi-shell NPs reveal that component interactions are likely influenced by their distribution along the layers forming the shell of the particle. For example, better transfection efficiency was achieved when an extra mineral layer was precipitated between pDNA and PEI, probably by reducing binding between PEI and DNA[268]. Protamine, on the other hand, only enhanced transfection efficiency when directly bound with DNA on the same layer[270,306]. For silica NPs, it

appears that the nature and strength of interaction between polymeric carriers and the particle surface can affect binding with pDNA after particle dissolution[307]. A strong particle/PEI interaction is thought to lower the PEI/pDNA binding after endosome escape, which is expected to enhance the bioavailability of pDNA. Design of mineralized vectors can be undertaken in this way to minimize binding and enhance polymer release from the nucleic acid cargo (or mineral release from nucleic acid). If nuclear targeting is needed for pDNA cargo, carriers designed for nuclear import should remain entrapped in the cytoplasm, while the siRNA could be released in free form into the cytoplasm where it is needed. Carrier details need to be tailored accordingly, and a better understanding of the effects of variable binding strength between components will be beneficial.

Mineralized matrices make an interesting case in which the continuous properties of the mineral phase is taken advantage of, and used for reverse transfection. This method holds great promise in tissue engineering, and further improvement could be achieved by exploring the mineralized matrix as an active participant in gene therapies. For instance, Sr-containing matrices are capable of increasing osteogenic differentiation[308]. One can therefore envision other roles of the mineralized matrix to control cell physiology. For example, certain nHap formulations promoted better osteogenesis from MSC compared to other vectors – even though their reporter gene expression efficiency was similar; therefore, inherently more conducive for cellular differentiation[309]. Progress in this direction could possibly be incorporated in any of the fabrication methods discussed here. Considering that mineralization techniques are widely used to prepare materials used in contact with bone (e.g., Hap coated titanium implants), the possibility of adding functional DNA delivery from mineralized materials might represent the next step in the direction of achieving high

bioactivity and bone healing rates. Additionally, the triggering of gene delivery by cell adhesion seems to be a very useful tool for delivering DNA selectively to the cells that interact with mineralized layers. Considering this, the next step in the use of mineralized surfaces might be the adaptation of the current mineralization technique to 'practical' materials, i.e., mineralized materials that are already in use could be turned into DNA-mineralized materials. This will demand adaptation of mineralization techniques and a better understanding of the effect of DNA as an additive during the mineralization process in the presence of varied substrates and the effect of the substrate itself in the efficiency of transfection. Ti alloy substrates might be a good start for making the next step in that direction since Ti alloys are widely used as bone implants [310]. With Ti alloy substrates, TiO_2 surface morphologies such as nanopores or nanotube arrays with a varying specific surface area can be prepared by anodization [311]. Recently, it was shown that under controlled mineralization, the nanotube morphology could be preserved and transposed to the mineral layer, generating a synergistic effect on pre-osteoblast differentiation compared to the presence of TiO_2 nanotubes mineralization alone [312]. Therefore, "forcing" a specific morphology onto the mineral layer by a nucleating substrate seems to be a fruitful possibility. Importantly, considering the surface-mediated delivery process, increasing the effective surface area under each cell might result in increased uptake and transfection rates by the increased availability of mineralized area (and nucleic acid cargo) per cell. Moreover, a better understanding of intracellular events as a response to nanotopography might help with designing better transfection substrates. For example, in the case of Si nanosheets, the aspect ratio (wall height/width) showed a critical effect on transfection efficiency and was shown to correlate with integrin activation[313]. In short, there might be direct (increased

nucleotide availability per cell due to increased surface area) and indirect factors (intracellular events) favoring transfection efficiency by the use of complex nucleating substrate nanotopographies compared to flat surfaces.

The mineralization of pre-assembled NPs is emerging as a promising strategy to give new properties to particles that already have inherent therapeutic applications. Increased robustness that can be turned off by mildly acidic pH is the most obvious benefit in therapeutic applications. Additionally, it is possible that properties acquired by viruses and therapeutic viral vectors when mineralized, such as increased mucosal adhesion and more resistance to increased temperatures, could be explored in mineralized non-viral vectors. Despite its great promise, this hypothesis remains to be confirmed. It can be anticipated that increased robustness might be useful for introducing delivery vectors inside dense materials before their fabrication, which could be useful for exploring novel delivery methods. In electrospinning, for example, when non-viral vectors are added to polymer solution before the spinning process, they are subjected to conditions that are not optimal for NP stability needed for the transfection process, such as shear forces, high ionic strength, and the drying process inside the fibers[314]. In such cases, mineralization could help to preserve the original properties of the delivery vector.

Considering the current situation with the global COVID-19 pandemic caused by the SARS-CoV-2 virus, the possibility of applying mineralized vaccines for COVID-19 (and other viral) treatment is appealing. The current non-viral mRNA vaccines proved to be safe and effective in this pandemic, which, in addition to financial stimulus from governments, increased demand from markets, and lowering of mRNA manufacturing costs, is likely to propel the number of studies concerning mRNA vaccination and other treatments using non-

viral technologies. As we reviewed here, mineralization is capable of preparing vaccines for application through airways, which is efficient in inducing local mucosal immunity and believed to be ideal for airway infections[315]. This adhesive effect towards mucosa is likely a property from the mineral layer itself, meaning that all nanoarchitectures reviewed here could potentially offer such a benefit. The main mRNA vaccine drawback compared to pDNA seems to be its lower stability. If the same protective effect used to create thermostable DNA vaccines could be applied to the mRNA vaccines, increased availability to the public would result if costs related to the cold chain and storage are reduced. The techniques reviewed here represent the effort of many researchers to bring highly safe materials to a field that suffered from uncertainties regarding safety. Looking ahead, the available opportunities for mineralization in the fabrication of vectors for nucleotide delivery are varied and impactful.

1.8 References

[1] M.H. Amer, Gene therapy for cancer: present status and future perspective, Molecular and Cellular Therapies. 2 (2014) 27. https://doi.org/10.1186/2052-8426-2-27.

[2] M. Cucchiarini, A.L. McNulty, R.L. Mauck, L.A. Setton, F. Guilak, H. Madry, Advances in combining gene therapy with cell and tissue engineering-based approaches to enhance healing of the meniscus, Osteoarthritis and Cartilage. 24 (2016) 1330–1339. https://doi.org/https://doi.org/10.1016/j.joca.2016.03.018.

[3] C.E. Dunbar, K.A. High, J.K. Joung, D.B. Kohn, K. Ozawa, M. Sadelain, Gene therapy comes of age, Science. 359 (2018) eaan4672. https://doi.org/10.1126/science.aan4672.

[4] T. Friedmann, R. Roblin, Gene Therapy for Human Genetic Disease?, Science. 175 (1972) 949 LP – 955. https://doi.org/10.1126/science.175.4025.949.

[5] S.M. Elbashir, J. Harborth, W. Lendeckel, A. Yalcin, K. Weber, T. Tuschl, Duplexes of 21-nucleotide RNAs mediate RNA interference in cultured

mammalian cells, Nature. 411 (2001) 494–498. https://doi.org/10.1038/35078107.

[6] A.P. McCaffrey, L. Meuse, T.-T.T. Pham, D.S. Conklin, G.J. Hannon, M.A. Kay, RNA interference in adult mice, Nature. 418 (2002) 38–39. https://doi.org/10.1038/418038a.

[7] D. Grimm, M.A. Kay, Therapeutic application of RNAi: is mRNA targeting finally ready for prime time?, The Journal of Clinical Investigation. 117 (2007) 3633–3641. https://doi.org/10.1172/JCI34129.

[8] C.L. Hardee, L.M. Arévalo-Soliz, B.D. Hornstein, L. Zechiedrich, Advances in Non-Viral DNA Vectors for Gene Therapy, Genes. 8 (2017) 65. https://doi.org/10.3390/genes8020065.

[9] S.E. Raper, N. Chirmule, F.S. Lee, N.A. Wivel, A. Bagg, G. Gao, J.M. Wilson, M.L. Batshaw, Fatal systemic inflammatory response syndrome in a ornithine transcarbamylase deficient patient following adenoviral gene transfer, Molecular Genetics and Metabolism. 80 (2003) 148–158. https://doi.org/https://doi.org/10.1016/j.ymgme.2003.08.016.

[10] V. Picanço-Castro, C.G. Pereira, D.T. Covas, G.S. Porto, A. Athanassiadou, M.L. Figueiredo, Emerging patent landscape for non-viral vectors used for gene therapy, Nature Biotechnology. 38 (2020) 151–157. https://doi.org/10.1038/s41587-019-0402-x.

[11] Z. Xiong, C.S. Alves, J. Wang, A. Li, J. Liu, M. Shen, J. Rodrigues, H. Tomás, X. Shi, Zwitterion-functionalized dendrimer-entrapped gold nanoparticles for serum-enhanced gene delivery to inhibit cancer cell metastasis, Acta Biomaterialia. 99 (2019) 320–329. https://doi.org/10.1016/j.actbio.2019.09.005.

[12] K. Bates, K. Kostarelos, Carbon nanotubes as vectors for gene therapy: Past achievements, present challenges and future goals, Advanced Drug Delivery Reviews. 65 (2013) 2023–2033. https://doi.org/https://doi.org/10.1016/j.addr.2013.10.003.

[13] J. Dobson, Gene therapy progress and prospects: magnetic nanoparticle-based gene delivery, Gene Therapy. 13 (2006) 283–287. https://doi.org/10.1038/sj.gt.3302720.

[14] H. Lv, S. Zhang, B. Wang, S. Cui, J. Yan, Toxicity of cationic lipids and cationic polymers in gene delivery, Journal of Controlled Release. 114 (2006) 100–109. https://doi.org/https://doi.org/10.1016/j.jconrel.2006.04.014.

[15] R. Khalifehzadeh, H. Arami, Biodegradable calcium phosphate nanoparticles for cancer therapy, Advances in Colloid and Interface Science. 279 (2020). https://doi.org/10.1016/j.cis.2020.102157.

[16] W. Habraken, P. Habibovic, M. Epple, M. Bohner, Calcium phosphates in biomedical applications: materials for the future?, Materials Today. 19 (2016) 69–

87. https://doi.org/https://doi.org/10.1016/j.mattod.2015.10.008.

[17] L. Guo, L. Wang, R. Yang, R. Feng, Z. Li, X. Zhou, Z. Dong, G. Ghartey-Kwansah, M. Xu, M. Nishi, Q. Zhang, W. Isaacs, J. Ma, X. Xu, Optimizing conditions for calcium phosphate mediated transient transfection, Saudi Journal of Biological Sciences. 24 (2017) 622–629. https://doi.org/https://doi.org/10.1016/j.sjbs.2017.01.034.

[18] Y. Wu, W. Gu, J. Tang, Z.P. Xu, Devising new lipid-coated calcium phosphate/carbonate hybrid nanoparticles for controlled release in endosomes for efficient gene delivery, Journal of Materials Chemistry B. 5 (2017) 7194–7203. https://doi.org/10.1039/c7tb01635b.

[19] C.-Q. Wang, M.-Q. Gong, J.-L. Wu, R.-X. Zhuo, S.-X. Cheng, Dual-functionalized calcium carbonate based gene delivery system for efficient gene delivery, RSC Advances. 4 (2014) 38623–38629. https://doi.org/10.1039/C4RA05468G.

[20] Y. Fang, M. Vadlamudi, Y. Huang, X. Guo, Lipid-Coated, pH-Sensitive Magnesium Phosphate Particles for Intracellular Protein Delivery, Pharmaceutical Research. 36 (2019) 81. https://doi.org/10.1007/s11095-019-2607-6.

[21] G. Bhakta, V. Nurcombe, A. Maitra, A. Shrivastava, DNA-encapsulated magnesium phosphate nanoparticles elicit both humoral and cellular immune responses in mice, Results in Immunology. 4 (2014) 46–53. https://doi.org/10.1016/j.rinim.2014.04.001.

[22] L. Jin, X. Zeng, M. Liu, Y. Deng, N. He, Current Progress in Gene Delivery Technology Based on Chemical Methods and Nano-carriers, Theranostics. 4 (2014) 240–255. https://doi.org/10.7150/thno.6914.

[23] V. Di Mauro, M. Iafisco, N. Salvarani, M. Vacchiano, P. Carullo, G.B. Ramírez-Rodríguez, T. Patrício, A. Tampieri, M. Miragoli, D. Catalucci, Bioinspired negatively charged calcium phosphate nanocarriers for cardiac delivery of MicroRNAs, Nanomedicine. 11 (2016) 891–906. https://doi.org/10.2217/nnm.16.26.

[24] K.-W. Huang, Y.-T. Lai, G.-J. Chern, S.-F. Huang, C.-L. Tsai, Y.-C. Sung, C.-C. Chiang, P.-B. Hwang, T.-L. Ho, R.-L. Huang, T.-Y. Shiue, Y. Chen, S.-K. Wang, Galactose Derivative-Modified Nanoparticles for Efficient siRNA Delivery to Hepatocellular Carcinoma, Biomacromolecules. 19 (2018) 2330–2339. https://doi.org/10.1021/acs.biomac.8b00358.

[25] C. Qiu, W. Wei, J. Sun, H.-T. Zhang, J.-S. Ding, J.-C. Wang, Q. Zhang, Systemic delivery of siRNA by hyaluronan-functionalized calcium phosphate nanoparticles for tumor-targeted therapy, Nanoscale. 8 (2016) 13033–13044. https://doi.org/10.1039/C6NR04034A.

[26] J. Chen, P. Gao, S. Yuan, R. Li, A. Ni, L. Chu, L. Ding, Y. Sun, X.-Y. Liu, Y. Duan,

Oncolytic Adenovirus Complexes Coated with Lipids and Calcium Phosphate for Cancer Gene Therapy, ACS Nano. 10 (2016) 11548–11560. https://doi.org/10.1021/acsnano.6b06182.

[27] R. Becker, W. Döring, Kinetische Behandlung der Keimbildung in übersättigten Dämpfen, Annalen Der Physik. 416 (1935) 719–752. https://doi.org/10.1002/andp.19354160806.

[28] J. Frenkel, A General Theory of Heterophase Fluctuations and Pretransition Phenomena, The Journal of Chemical Physics. 7 (1939) 538–547. https://doi.org/10.1063/1.1750484.

[29] M. Volmer, A. Weber, Keimbildung in übersättigten Gebilden, Zeitschrift Für Physikalische Chemie. 119U (1926) 277–301. https://doi.org/https://doi.org/10.1515/zpch-1926-11927.

[30] W.J.E.M. Habraken, J. Tao, L.J. Brylka, H. Friedrich, L. Bertinetti, A.S. Schenk, A. Verch, V. Dmitrovic, P.H.H. Bomans, P.M. Frederik, J. Laven, P. van der Schoot, B. Aichmayer, G. de With, J.J. DeYoreo, N.A.J.M. Sommerdijk, Ion-association complexes unite classical and non-classical theories for the biomimetic nucleation of calcium phosphate, Nature Communications. 4 (2013) 1507. https://doi.org/10.1038/ncomms2490.

[31] P.G. Vekilov, The two-step mechanism of nucleation of crystals in solution, Nanoscale. 2 (2010) 2346–2357. https://doi.org/10.1039/C0NR00628A.

[32] D. Gebauer, M. Kellermeier, J.D. Gale, L. Bergström, H. Cölfen, Pre-nucleation clusters as solute precursors in crystallisation, Chemical Society Reviews. 43 (2014) 2348–2371. https://doi.org/10.1039/C3CS60451A.

[33] P.J.M. Smeets, A.R. Finney, W.J.E.M. Habraken, F. Nudelman, H. Friedrich, J. Laven, J.J. De Yoreo, P.M. Rodger, N.A.J.M. Sommerdijk, A classical view on nonclassical nucleation, Proceedings of the National Academy of Sciences. 114 (2017) E7882 LP-E7890. https://doi.org/10.1073/pnas.1700342114.

[34] D. Gebauer, A. Völkel, H. Cölfen, Stable Prenucleation Calcium Carbonate Clusters, Science. 322 (2008) 1819 LP – 1822. https://doi.org/10.1126/science.1164271.

[35] A.S. Posner, F. Betts, Synthetic amorphous calcium phosphate and its relation to bone mineral structure, Accounts of Chemical Research. 8 (1975) 273–281. https://doi.org/10.1021/ar50092a003.

[36] A. Dey, P.H.H. Bomans, F.A. Müller, J. Will, P.M. Frederik, G. de With, N.A.J.M. Sommerdijk, The role of prenucleation clusters in surface-induced calcium phosphate crystallization, Nature Materials. 9 (2010) 1010–1014. https://doi.org/10.1038/nmat2900.

[37] K. Onuma, A. Ito, Cluster Growth Model for Hydroxyapatite, Chemistry of Materials. 10 (1998) 3346–3351. https://doi.org/10.1021/cm980062c.

[38] O. Bertran, G. Revilla-López, J. Casanovas, L.J. del Valle, P. Turon, J. Puiggalí, C. Alemán, Dissolving Hydroxyolite: A DNA Molecule into Its Hydroxyapatite Mold, Chemistry – A European Journal. 22 (2016) 6631–6636. https://doi.org/10.1002/chem.201600703.

[39] D. Zhao, C.-Q. Wang, R.-X. Zhuo, S.-X. Cheng, Modification of nanostructured calcium carbonate for efficient gene delivery, Colloids and Surfaces B: Biointerfaces. 118 (2014) 111–116. https://doi.org/https://doi.org/10.1016/j.colsurfb.2014.03.007.

[40] J. Li, Y. Yang, L. Huang, Calcium phosphate nanoparticles with an asymmetric lipid bilayer coating for siRNA delivery to the tumor, Journal of Controlled Release. 158 (2012) 108–114. https://doi.org/https://doi.org/10.1016/j.jconrel.2011.10.020.

[41] L. Pham, H. Ye, F.-L. Cosset, S.J. Russell, K.-W. Peng, Concentration of viral vectors by co-precipitation with calcium phosphate, The Journal of Gene Medicine. 3 (2001) 188–194. https://doi.org/10.1002/1521-2254(2000)9999:9999<::AID-JGM159>3.0.CO;2-9.

[42] J. Zhao, P. Chen, G. Chen, X.J. Pang, P. Huang, X. Hou, Z. Wang, C.-Y. He, Z.-Y. Chen, Controllable synthesis of calcium silicate nanoparticles through one-step microemulsion method for drug and gene delivery, Nanoscience and Nanotechnology Letters. 9 (2017) 1720–1723. https://doi.org/10.1166/nnl.2017.2391.

[43] J. Tang, C.B. Howard, S.M. Mahler, K.J. Thurecht, L. Huang, Z.P. Xu, Enhanced delivery of siRNA to triple negative breast cancer cells in vitro and in vivo through functionalizing lipid-coated calcium phosphate nanoparticles with dual target ligands, Nanoscale. 10 (2018) 4258–4266. https://doi.org/10.1039/C7NR08644J.

[44] M. Puddu, N. Broguiere, D. Mohn, M. Zenobi-Wong, W.J. Stark, R.N. Grass, Magnetically deliverable calcium phosphate nanoparticles for localized gene expression, RSC Advances. 5 (2015) 9997–10004. https://doi.org/10.1039/C4RA13413C.

[45] C. Zelmer, L.P. Zweifel, L.E. Kapinos, I. Craciun, Z.P. Güven, C.G. Palivan, R.Y.H. Lim, Organelle-specific targeting of polymersomes into the cell nucleus, Proceedings of the National Academy of Sciences. 117 (2020) 2770 LP – 2778. https://doi.org/10.1073/pnas.1916395117.

[46] Y. Zeng, B.R. Cullen, RNA interference in human cells is restricted to the cytoplasm, RNA (New York, N.Y.). 8 (2002) 855–860. https://doi.org/10.1017/s1355838202020071.

[47] M.M. Munye, A.D. Tagalakis, J.L. Barnes, R.E. Brown, R.J. McAnulty, S.J. Howe, S.L. Hart, Minicircle DNA Provides Enhanced and Prolonged Transgene Expression Following Airway Gene Transfer, Scientific Reports. 6 (2016) 23125. https://doi.org/10.1038/srep23125.

[48] B.D. Hornstein, D. Roman, L.M. Arévalo-Soliz, M.A. Engevik, L. Zechiedrich, Effects of Circular DNA Length on Transfection Efficiency by Electroporation into HeLa Cells, PLOS ONE. 11 (2016) e0167537. https://doi.org/10.1371/journal.pone.0167537.

[49] P. Kreiss, P. Mailhe, D. Scherman, B. Pitard, B. Cameron, R. Rangara, O. Aguerre-Charriol, M. Airiau, J. Crouzet, Plasmid DNA size does not affect the physicochemical properties of lipoplexes but modulates gene transfer efficiency, Nucleic Acids Research. 27 (1999) 3792–3798. https://doi.org/10.1093/nar/27.19.3792.

[50] J. Mairhofer, R. Grabherr, Rational Vector Design for Efficient Non-viral Gene Delivery: Challenges Facing the Use of Plasmid DNA, Molecular Biotechnology. 39 (2008) 97–104. https://doi.org/10.1007/s12033-008-9046-7.

[51] S.N. Tammam, H.M.E. Azzazy, H.G. Breitinger, A. Lamprecht, Chitosan Nanoparticles for Nuclear Targeting: The Effect of Nanoparticle Size and Nuclear Localization Sequence Density, Molecular Pharmaceutics. 12 (2015) 4277–4289. https://doi.org/10.1021/acs.molpharmaceut.5b00478.

[52] S.N. Tammam, H.M.E. Azzazy, A. Lamprecht, How successful is nuclear targeting by nanocarriers?, Journal of Controlled Release. 229 (2016) 140–153. https://doi.org/https://doi.org/10.1016/j.jconrel.2016.03.022.

[53] J.D. Larsen, N.L. Ross, M.O. Sullivan, Requirements for the nuclear entry of polyplexes and nanoparticles during mitosis, The Journal of Gene Medicine. 14 (2012) 580–589. https://doi.org/10.1002/jgm.2669.

[54] J.K.W. Lam, M.Y.T. Chow, Y. Zhang, S.W.S. Leung, siRNA Versus miRNA as Therapeutics for Gene Silencing, Molecular Therapy. Nucleic Acids. 4 (2015) e252–e252. https://doi.org/10.1038/mtna.2015.23.

[55] G. Sahay, D.Y. Alakhova, A. V Kabanov, Endocytosis of nanomedicines, Journal of Controlled Release : Official Journal of the Controlled Release Society. 145 (2010) 182–195. https://doi.org/10.1016/j.jconrel.2010.01.036.

[56] F. Niedergang, Phagocytosis, in: R.A. Bradshaw, P.D.B.T.-E. of C.B. Stahl (Eds.), Academic Press, Waltham, 2016: pp. 751–757. https://doi.org/https://doi.org/10.1016/B978-0-12-394447-4.20073-4.

[57] T.U. Wani, S.N. Raza, N.A. Khan, Nanoparticle opsonization: forces involved and protection by long chain polymers, Polymer Bulletin. 77 (2020) 3865–3889. https://doi.org/10.1007/s00289-019-02924-7.

[58] J.A. Champion, A. Walker, S. Mitragotri, Role of particle size in phagocytosis of polymeric microspheres, Pharmaceutical Research. 25 (2008) 1815–1821. https://doi.org/10.1007/s11095-008-9562-y.

[59] C. He, Y. Hu, L. Yin, C. Tang, C. Yin, Effects of particle size and surface charge on cellular uptake and biodistribution of polymeric nanoparticles, Biomaterials. 31 (2010) 3657–3666. https://doi.org/https://doi.org/10.1016/j.biomaterials.2010.01.065.

[60] J.A. Swanson, S. Yoshida, Macropinocytosis, in: R.A. Bradshaw, P.D.B.T.-E. of C.B. Stahl (Eds.), Academic Press, Waltham, 2016: pp. 758–765. https://doi.org/https://doi.org/10.1016/B978-0-12-394447-4.20084-9.

[61] W. Zhang, X. Kang, B. Yuan, H. Wang, T. Zhang, M. Shi, Z. Zheng, Y. Zhang, C. Peng, X. Fan, H. Yang, Y. Shen, Y. Huang, Nano-Structural Effects on Gene Transfection: Large, Botryoid-Shaped Nanoparticles Enhance DNA Delivery via Macropinocytosis and Effective Dissociation, Theranostics. 9 (2019) 1580–1598. https://doi.org/10.7150/thno.30302.

[62] X.-Y. Sun, Q.-Z. Gan, J.-M. Ouyang, Size-dependent cellular uptake mechanism and cytotoxicity toward calcium oxalate on Vero cells, Scientific Reports. 7 (2017) 41949. https://doi.org/10.1038/srep41949.

[63] J. Mercer, A. Helenius, Virus entry by macropinocytosis, Nature Cell Biology. 11 (2009) 510–520. https://doi.org/10.1038/ncb0509-510.

[64] M. Kaksonen, A. Roux, Mechanisms of clathrin-mediated endocytosis, Nature Reviews Molecular Cell Biology. 19 (2018) 313–326. https://doi.org/10.1038/nrm.2017.132.

[65] F.P. G., W.S. E., P.D. S., L.M. P., Caveolin, Caveolae, and Endothelial Cell Function, Arteriosclerosis, Thrombosis, and Vascular Biology. 23 (2003) 1161–1168. https://doi.org/10.1161/01.ATV.0000070546.16946.3A.

[66] S. Kumari, S. MG, S. Mayor, Endocytosis unplugged: multiple ways to enter the cell, Cell Research. 20 (2010) 256–275. https://doi.org/10.1038/cr.2010.19.

[67] P. Foroozandeh, A.A. Aziz, Insight into Cellular Uptake and Intracellular Trafficking of Nanoparticles, Nanoscale Research Letters. 13 (2018) 339. https://doi.org/10.1186/s11671-018-2728-6.

[68] S. Behzadi, V. Serpooshan, W. Tao, M.A. Hamaly, M.Y. Alkawareek, E.C. Dreaden, D. Brown, A.M. Alkilany, O.C. Farokhzad, M. Mahmoudi, Cellular uptake of nanoparticles: journey inside the cell, Chemical Society Reviews. 46 (2017) 4218–4244. https://doi.org/10.1039/C6CS00636A.

[69] Y.-B. Hu, E.B. Dammer, R.-J. Ren, G. Wang, The endosomal-lysosomal system: from acidification and cargo sorting to neurodegeneration, Translational

Neurodegeneration. 4 (2015) 18. https://doi.org/10.1186/s40035-015-0041-1.

[70] D.Y.E. Olton, J.M. Close, C.S. Sfeir, P.N. Kumta, Intracellular trafficking pathways involved in the gene transfer of nano-structured calcium phosphate-DNA particles, Biomaterials. 32 (2011) 7662–7670. https://doi.org/https://doi.org/10.1016/j.biomaterials.2011.01.043.

[71] C. Zhou, B. Yu, X. Yang, T. Huo, L.J. Lee, R.F. Barth, R.J. Lee, Lipid-coated nano-calcium-phosphate (LNCP) for gene delivery, International Journal of Pharmaceutics. 392 (2010) 201–208. https://doi.org/10.1016/j.ijpharm.2010.03.012.

[72] L.M.P. Vermeulen, S.C. De Smedt, K. Remaut, K. Braeckmans, The proton sponge hypothesis: Fable or fact?, European Journal of Pharmaceutics and Biopharmaceutics. 129 (2018) 184–190. https://doi.org/https://doi.org/10.1016/j.ejpb.2018.05.034.

[73] L. Wang, J. Lu, F. Xu, F. Zhang, Dynamics of crystallization and dissolution of calcium orthophosphates at the near-molecular level, Chinese Science Bulletin. 56 (2011) 713–721. https://doi.org/10.1007/s11434-010-4184-2.

[74] A.E. Nel, L. Mädler, D. Velegol, T. Xia, E.M. V Hoek, P. Somasundaran, F. Klaessig, V. Castranova, M. Thompson, Understanding biophysicochemical interactions at the nano–bio interface, Nature Materials. 8 (2009) 543–557. https://doi.org/10.1038/nmat2442.

[75] W. Hu, C. Peng, M. Lv, X. Li, Y. Zhang, N. Chen, C. Fan, Q. Huang, Protein Corona-Mediated Mitigation of Cytotoxicity of Graphene Oxide, ACS Nano. 5 (2011) 3693–3700. https://doi.org/10.1021/nn200021j.

[76] V. Serpooshan, M. Mahmoudi, M. Zhao, K. Wei, S. Sivanesan, K. Motamedchaboki, A. V Malkovskiy, A.B. Goldstone, J.E. Cohen, P.C. Yang, J. Rajadas, D. Bernstein, Y.J. Woo, P. Ruiz-Lozano, Protein Corona Influences Cell–Biomaterial Interactions in Nanostructured Tissue Engineering Scaffolds, Advanced Functional Materials. 25 (2015) 4379–4389. https://doi.org/10.1002/adfm.201500875.

[77] M.P. Monopoli, C. Åberg, A. Salvati, K.A. Dawson, Biomolecular coronas provide the biological identity of nanosized materials, Nature Nanotechnology. 7 (2012) 779–786. https://doi.org/10.1038/nnano.2012.207.

[78] A. Salvati, A.S. Pitek, M.P. Monopoli, K. Prapainop, F.B. Bombelli, D.R. Hristov, P.M. Kelly, C. Åberg, E. Mahon, K.A. Dawson, Transferrin-functionalized nanoparticles lose their targeting capabilities when a biomolecule corona adsorbs on the surface, Nature Nanotechnology. 8 (2013) 137–143. https://doi.org/10.1038/nnano.2012.237.

[79] S. Tenzer, D. Docter, J. Kuharev, A. Musyanovych, V. Fetz, R. Hecht, F. Schlenk,

D. Fischer, K. Kiouptsi, C. Reinhardt, K. Landfester, H. Schild, M. Maskos, S.K. Knauer, R.H. Stauber, Rapid formation of plasma protein corona critically affects nanoparticle pathophysiology, Nature Nanotechnology. 8 (2013) 772–781. https://doi.org/10.1038/nnano.2013.181.

[80] F.S.M. Tekie, M. Hajiramezanali, P. Geramifar, M. Raoufi, R. Dinarvand, M. Soleimani, F. Atyabi, Controlling evolution of protein corona: a prosperous approach to improve chitosan-based nanoparticle biodistribution and half-life, Scientific Reports. 10 (2020) 9664. https://doi.org/10.1038/s41598-020-66572-y.

[81] S. Kaga, N.P. Truong, L. Esser, D. Senyschyn, A. Sanyal, R. Sanyal, J.F. Quinn, T.P. Davis, L.M. Kaminskas, M.R. Whittaker, Influence of Size and Shape on the Biodistribution of Nanoparticles Prepared by Polymerization-Induced Self-Assembly, Biomacromolecules. 18 (2017) 3963–3970. https://doi.org/10.1021/acs.biomac.7b00995.

[82] C. Carnovale, G. Bryant, R. Shukla, V. Bansal, Identifying Trends in Gold Nanoparticle Toxicity and Uptake: Size, Shape, Capping Ligand, and Biological Corona, ACS Omega. 4 (2019) 242–256. https://doi.org/10.1021/acsomega.8b03227.

[83] A. Lesniak, F. Fenaroli, M.P. Monopoli, C. Åberg, K.A. Dawson, A. Salvati, Effects of the Presence or Absence of a Protein Corona on Silica Nanoparticle Uptake and Impact on Cells, ACS Nano. 6 (2012) 5845–5857. https://doi.org/10.1021/nn300223w.

[84] M. Lundqvist, J. Stigler, T. Cedervall, T. Berggård, M.B. Flanagan, I. Lynch, G. Elia, K. Dawson, The Evolution of the Protein Corona around Nanoparticles: A Test Study, ACS Nano. 5 (2011) 7503–7509. https://doi.org/10.1021/nn202458g.

[85] S. Zhang, J. Li, G. Lykotrafitis, G. Bao, S. Suresh, Size-Dependent Endocytosis of Nanoparticles, Advanced Materials. 21 (2009) 419–424. https://doi.org/10.1002/adma.200801393.

[86] H. Yuan, C. Huang, S. Zhang, Virus-inspired design principles of nanoparticle-based bioagents, PloS One. 5 (2010) e13495–e13495. https://doi.org/10.1371/journal.pone.0013495.

[87] B.D. Chithrani, A.A. Ghazani, W.C.W. Chan, Determining the Size and Shape Dependence of Gold Nanoparticle Uptake into Mammalian Cells, Nano Letters. 6 (2006) 662–668. https://doi.org/10.1021/nl052396o.

[88] F. Osaki, T. Kanamori, S. Sando, T. Sera, Y. Aoyama, A Quantum Dot Conjugated Sugar Ball and Its Cellular Uptake. On the Size Effects of Endocytosis in the Subviral Region, Journal of the American Chemical Society. 126 (2004) 6520–6521. https://doi.org/10.1021/ja048792a.

[89] F. Lu, S.-H. Wu, Y. Hung, C.-Y. Mou, Size Effect on Cell Uptake in Well-

Suspended, Uniform Mesoporous Silica Nanoparticles, Small. 5 (2009) 1408–1413. https://doi.org/10.1002/smll.200900005.

[90] B.D. Chithrani, W.C.W. Chan, Elucidating the Mechanism of Cellular Uptake and Removal of Protein-Coated Gold Nanoparticles of Different Sizes and Shapes, Nano Letters. 7 (2007) 1542–1550. https://doi.org/10.1021/nl070363y.

[91] S.-H. Wang, C.-W. Lee, A. Chiou, P.-K. Wei, Size-dependent endocytosis of gold nanoparticles studied by three-dimensional mapping of plasmonic scattering images, Journal of Nanobiotechnology. 8 (2010) 33. https://doi.org/10.1186/1477-3155-8-33.

[92] M. Wu, H. Guo, L. Liu, Y. Liu, L. Xie, Size-dependent cellular uptake and localization profiles of silver nanoparticles, International Journal of Nanomedicine. 14 (2019) 4247–4259. https://doi.org/10.2147/IJN.S201107.

[93] N. Hoshyar, S. Gray, H. Han, G. Bao, The effect of nanoparticle size on in vivo pharmacokinetics and cellular interaction, Nanomedicine. 11 (2016) 673–692. https://doi.org/10.2217/nnm.16.5.

[94] J.M. Caster, S.K. Yu, A.N. Patel, N.J. Newman, Z.J. Lee, S.B. Warner, K.T. Wagner, K.C. Roche, X. Tian, Y. Min, A.Z. Wang, Effect of particle size on the biodistribution, toxicity, and efficacy of drug-loaded polymeric nanoparticles in chemoradiotherapy, Nanomedicine: Nanotechnology, Biology and Medicine. 13 (2017) 1673–1683. https://doi.org/https://doi.org/10.1016/j.nano.2017.03.002.

[95] D. Pezzoli, E. Giupponi, D. Mantovani, G. Candiani, Size matters for in vitro gene delivery: investigating the relationships among complexation protocol, transfection medium, size and sedimentation, Scientific Reports. 7 (2017) 44134. https://doi.org/10.1038/srep44134.

[96] L. Li, W.-S. Xi, Q. Su, Y. Li, G.-H. Yan, Y. Liu, H. Wang, A. Cao, Unexpected Size Effect: The Interplay between Different-Sized Nanoparticles in Their Cellular Uptake, Small. 15 (2019) 1901687. https://doi.org/10.1002/smll.201901687.

[97] N. Hao, L. Li, Q. Zhang, X. Huang, X. Meng, Y. Zhang, D. Chen, F. Tang, L. Li, The shape effect of PEGylated mesoporous silica nanoparticles on cellular uptake pathway in Hela cells, Microporous and Mesoporous Materials. 162 (2012) 14–23. https://doi.org/https://doi.org/10.1016/j.micromeso.2012.05.040.

[98] X. Xie, J. Liao, X. Shao, Q. Li, Y. Lin, The Effect of shape on Cellular Uptake of Gold Nanoparticles in the forms of Stars, Rods, and Triangles, Scientific Reports. 7 (2017) 3827. https://doi.org/10.1038/s41598-017-04229-z.

[99] S.E.A. Gratton, P.A. Ropp, P.D. Pohlhaus, J.C. Luft, V.J. Madden, M.E. Napier, J.M. DeSimone, The effect of particle design on cellular internalization pathways, Proceedings of the National Academy of Sciences. 105 (2008) 11613 LP – 11618. https://doi.org/10.1073/pnas.0801763105.

[100] P.M. Favi, M. Gao, L. Johana Sepúlveda Arango, S.P. Ospina, M. Morales, J.J. Pavon, T.J. Webster, Shape and surface effects on the cytotoxicity of nanoparticles: Gold nanospheres versus gold nanostars, Journal of Biomedical Materials Research Part A. 103 (2015) 3449–3462. https://doi.org/10.1002/jbm.a.35491.

[101] Arnida, A. Malugin, H. Ghandehari, Cellular uptake and toxicity of gold nanoparticles in prostate cancer cells: a comparative study of rods and spheres, Journal of Applied Toxicology. 30 (2010) 212–217. https://doi.org/10.1002/jat.1486.

[102] Arnida, M.M. Janát-Amsbury, A. Ray, C.M. Peterson, H. Ghandehari, Geometry and surface characteristics of gold nanoparticles influence their biodistribution and uptake by macrophages, European Journal of Pharmaceutics and Biopharmaceutics. 77 (2011) 417–423. https://doi.org/https://doi.org/10.1016/j.ejpb.2010.11.010.

[103] E. Fröhlich, The role of surface charge in cellular uptake and cytotoxicity of medical nanoparticles, International Journal of Nanomedicine. 7 (2012) 5577–5591. https://doi.org/10.2147/IJN.S36111.

[104] V. Sokolova, S. Neumann, A. Kovtun, S. Chernousova, R. Heumann, M. Epple, An outer shell of positively charged poly(ethyleneimine) strongly increases the transfection efficiency of calcium phosphate/DNA nanoparticles, Journal of Materials Science. 45 (2010) 4952–4957. https://doi.org/10.1007/s10853-009-4159-3.

[105] S.M. Moghimi, P. Symonds, J.C. Murray, A.C. Hunter, G. Debska, A. Szewczyk, A two-stage poly(ethylenimine)-mediated cytotoxicity: implications for gene transfer/therapy, Molecular Therapy. 11 (2005) 990–995. https://doi.org/https://doi.org/10.1016/j.ymthe.2005.02.010.

[106] B. Wang, L. Zhang, S.C. Bae, S. Granick, Nanoparticle-induced surface reconstruction of phospholipid membranes, Proceedings of the National Academy of Sciences. 105 (2008) 18171 LP – 18175. https://doi.org/10.1073/pnas.0807296105.

[107] E.C. Cho, J. Xie, P.A. Wurm, Y. Xia, Understanding the Role of Surface Charges in Cellular Adsorption versus Internalization by Selectively Removing Gold Nanoparticles on the Cell Surface with a I2/KI Etchant, Nano Letters. 9 (2009) 1080–1084. https://doi.org/10.1021/nl803487r.

[108] J. Lin, H. Zhang, Z. Chen, Y. Zheng, Penetration of Lipid Membranes by Gold Nanoparticles: Insights into Cellular Uptake, Cytotoxicity, and Their Relationship, ACS Nano. 4 (2010) 5421–5429. https://doi.org/10.1021/nn1010792.

[109] T. Wang, J. Bai, X. Jiang, G.U. Nienhaus, Cellular Uptake of Nanoparticles by Membrane Penetration: A Study Combining Confocal Microscopy with FTIR Spectroelectrochemistry, ACS Nano. 6 (2012) 1251–1259. https://doi.org/10.1021/nn203892h.

[110] K. Xiao, Y. Li, J. Luo, J.S. Lee, W. Xiao, A.M. Gonik, R.G. Agarwal, K.S. Lam, The effect of surface charge on in vivo biodistribution of PEG-oligocholic acid based micellar nanoparticles, Biomaterials. 32 (2011) 3435–3446. https://doi.org/10.1016/j.biomaterials.2011.01.021.

[111] Y. Yamamoto, Y. Nagasaki, Y. Kato, Y. Sugiyama, K. Kataoka, Long-circulating poly(ethylene glycol)–poly(d,l-lactide) block copolymer micelles with modulated surface charge, Journal of Controlled Release. 77 (2001) 27–38. https://doi.org/https://doi.org/10.1016/S0168-3659(01)00451-5.

[112] K. Kobayashi, J. Wei, R. Iida, K. Ijiro, K. Niikura, Surface engineering of nanoparticles for therapeutic applications, Polymer Journal. 46 (2014) 460–468. https://doi.org/10.1038/pj.2014.40.

[113] S.T. Kim, K. Saha, C. Kim, V.M. Rotello, The Role of Surface Functionality in Determining Nanoparticle Cytotoxicity, Accounts of Chemical Research. 46 (2013) 681–691. https://doi.org/10.1021/ar3000647.

[114] D.F. Moyano, M. Goldsmith, D.J. Solfiell, D. Landesman-Milo, O.R. Miranda, D. Peer, V.M. Rotello, Nanoparticle hydrophobicity dictates immune response, Journal of the American Chemical Society. 134 (2012) 1520–5126.

[115] M. Samadi Moghaddam, M. Heiny, V.P. Shastri, Enhanced cellular uptake of nanoparticles by increasing the hydrophobicity of poly(lactic acid) through copolymerization with cell-membrane-lipid components, Chemical Communications. 51 (2015) 14605–14608. https://doi.org/10.1039/C5CC06397C.

[116] H.-Y. Lee, S.H.R. Shin, L.L. Abezgauz, S.A. Lewis, A.M. Chirsan, D.D. Danino, K.J.M. Bishop, Integration of Gold Nanoparticles into Bilayer Structures via Adaptive Surface Chemistry, Journal of the American Chemical Society. 135 (2013) 5950–5953. https://doi.org/10.1021/ja400225n.

[117] Z. Luo, Y. Dai, H. Gao, Development and application of hyaluronic acid in tumor targeting drug delivery, Acta Pharmaceutica Sinica. B. 9 (2019) 1099–1112. https://doi.org/10.1016/j.apsb.2019.06.004.

[118] R.B. KC, C. Kucharski, H. Uludağ, Additive nanocomplexes of cationic lipopolymers for improved non-viral gene delivery to mesenchymal stem cells, Journal of Materials Chemistry B. 3 (2015) 3972–3982. https://doi.org/10.1039/C4TB02101K.

[119] L. Sánchez-del-Campo, M.F. Montenegro, J. Cabezas-Herrera, J.N. Rodríguez-López, The critical role of alpha-folate receptor in the resistance of melanoma to methotrexate, Pigment Cell & Melanoma Research. 22 (2009) 588–600. https://doi.org/10.1111/j.1755-148X.2009.00586.x.

[120] G.L. Zwicke, G. Ali Mansoori, C.J. Jeffery, Utilizing the folate receptor for active targeting of cancer nanotherapeutics, Nano Reviews. 3 (2012) 18496.

https://doi.org/10.3402/nano.v3i0.18496.

[121] B. Frigerio, C. Bizzoni, G. Jansen, C.P. Leamon, G.J. Peters, P.S. Low, L.H. Matherly, M. Figini, Folate receptors and transporters: biological role and diagnostic/therapeutic targets in cancer and other diseases, Journal of Experimental & Clinical Cancer Research. 38 (2019) 125. https://doi.org/10.1186/s13046-019-1123-1.

[122] Z. Jiang, J. Guan, J. Qian, C. Zhan, Peptide ligand-mediated targeted drug delivery of nanomedicines, Biomaterials Science. 7 (2019) 461–471. https://doi.org/10.1039/C8BM01340C.

[123] D.A. Richards, A. Maruani, V. Chudasama, Antibody fragments as nanoparticle targeting ligands: a step in the right direction, Chemical Science. 8 (2017) 63–77. https://doi.org/10.1039/C6SC02403C.

[124] Z. Zhou, H. Li, K. Wang, Q. Guo, C. Li, H. Jiang, Y. Hu, D. Oupicky, M. Sun, Bioreducible Cross-Linked Hyaluronic Acid/Calcium Phosphate Hybrid Nanoparticles for Specific Delivery of siRNA in Melanoma Tumor Therapy, ACS Applied Materials & Interfaces. 9 (2017) 14576–14589. https://doi.org/10.1021/acsami.6b15347.

[125] M.S. Lee, J.E. Lee, E. Byun, N.W. Kim, K. Lee, H. Lee, S.J. Sim, D.S. Lee, J.H. Jeong, Target-specific delivery of siRNA by stabilized calcium phosphate nanoparticles using dopa–hyaluronic acid conjugate, Journal of Controlled Release. 192 (2014) 122–130. https://doi.org/https://doi.org/10.1016/j.jconrel.2014.06.049.

[126] J.E. Lee, Y. Yin, S.Y. Lim, E.S. Kim, J. Jung, D. Kim, J.W. Park, M.S. Lee, J.H. Jeong, J.E. Lee, Y. Yin, S.Y. Lim, E.S. Kim, J. Jung, D. Kim, J.W. Park, M.S. Lee, J.H. Jeong, Enhanced Transfection of Human Mesenchymal Stem Cells Using a Hyaluronic Acid/Calcium Phosphate Hybrid Gene Delivery System, Polymers. 11 (2019) 798. https://doi.org/10.3390/polym11050798.

[127] Y. Yang, Y. Hu, Y. Wang, J. Li, F. Liu, L. Huang, Nanoparticle Delivery of Pooled siRNA for Effective Treatment of Non-Small Cell Lung Caner, Molecular Pharmaceutics. 9 (2012) 2280–2289. https://doi.org/10.1021/mp300152v.

[128] Y. Yang, J. Li, F. Liu, L. Huang, Systemic delivery of siRNA via LCP nanoparticle efficiently inhibits lung metastasis, Molecular Therapy. 20 (2012) 609–615. https://doi.org/10.1038/mt.2011.270.

[129] M. Hu, Y. Wang, L. Xu, S. An, Y. Tang, X. Zhou, J. Li, R. Liu, L. Huang, Relaxin gene delivery mitigates liver metastasis and synergizes with check point therapy, Nature Communications. 10 (2019). https://doi.org/10.1038/s41467-019-10893-8.

[130] T.J. Goodwin, Y. Zhou, S.N. Musetti, R. Liu, L. Huang, Local and transient gene expression primes the liver to resist cancer metastasis, Science Translational Medicine. 8 (2016) 364ra153 LP-364ra153.

https://doi.org/10.1126/scitranslmed.aag2306.

[131] C.-H. Liu, G.-J. Chern, F.-F. Hsu, K.-W. Huang, Y.-C. Sung, H.-C. Huang, J.T. Qiu, S.-K. Wang, C.-C. Lin, C.-H. Wu, H.-C. Wu, J.-Y. Liu, Y. Chen, A multifunctional nanocarrier for efficient TRAIL-based gene therapy against hepatocellular carcinoma with desmoplasia in mice, Hepatology. 67 (2018) 899–913. https://doi.org/10.1002/hep.29513.

[132] K.-W. Huang, F.-F. Hsu, J.T. Qiu, G.-J. Chern, Y.-A. Lee, C.-C. Chang, Y.-T. Huang, Y.-C. Sung, C.-C. Chiang, R.-L. Huang, C.-C. Lin, T.K. Dinh, H.-C. Huang, Y.-C. Shih, D. Alson, C.-Y. Lin, Y.-C. Lin, P.-C. Chang, S.-Y. Lin, Y. Chen, Highly efficient and tumor-selective nanoparticles for dual-targeted immunogene therapy against cancer, Science Advances. 6 (2020) eaax5032. https://doi.org/10.1126/sciadv.aax5032.

[133] Y. Wu, W. Gu, Z.P. Xu, Enhanced combination cancer therapy using lipid-calcium carbonate/phosphate nanoparticles as a targeted delivery platform, Nanomedicine. 14 (2019) 77–92. https://doi.org/10.2217/nnm-2018-0252.

[134] V. Sokolova, Z. Shi, S. Huang, Y. Du, M. Kopp, A. Frede, T. Knuschke, J. Buer, D. Yang, J. Wu, A.M. Westendorf, M. Epple, Delivery of the TLR ligand poly(I:C) to liver cells in vitro and in vivo by calcium phosphate nanoparticles leads to a pronounced immunostimulation, Acta Biomaterialia. 64 (2017) 401–410. https://doi.org/10.1016/j.actbio.2017.09.037.

[135] S. Li, B. Wang, S. Jiang, Y. Pan, Y. Shi, W. Kong, Y. Shan, Surface-Functionalized Silica-Coated Calcium Phosphate Nanoparticles Efficiently Deliver DNA-Based HIV-1 Trimeric Envelope Vaccines against HIV-1, ACS Applied Materials & Interfaces. 13 (2021) 53630–53645. https://doi.org/10.1021/acsami.1c16989.

[136] F.L. Graham, A.J. van der Eb, A new technique for the assay of infectivity of human adenovirus 5 DNA, Virology. 52 (1973) 456–467. https://doi.org/https://doi.org/10.1016/0042-6822(73)90341-3.

[137] F.L. Graham, This Week's Citation Classic - A new technique for the assay of infectivity of human adenovirus 5 DNA., (1988) 1. http://garfield.library.upenn.edu/classics1988/A1988Q713500001.pdf.

[138] M. Jordan, A. Schallhorn, F.M. Wurm, Transfecting Mammalian Cells: Optimization of Critical Parameters Affecting Calcium-Phosphate Precipitate Formation, Nucleic Acids Research. 24 (1996) 596–601. https://doi.org/10.1093/nar/24.4.596.

[139] B. Goetze, B. Grunewald, S. Baldassa, M. Kiebler, Chemically controlled formation of a DNA/calcium phosphate coprecipitate: Application for transfection of mature hippocampal neurons, Journal of Neurobiology. 60 (2004) 517–525. https://doi.org/10.1002/neu.20073.

[140] D. Olton, J. Li, M.E. Wilson, T. Rogers, J. Close, L. Huang, P.N. Kumta, C. Sfeir, Nanostructured calcium phosphates (NanoCaPs) for non-viral gene delivery: Influence of the synthesis parameters on transfection efficiency, Biomaterials. 28 (2007) 1267–1279. https://doi.org/https://doi.org/10.1016/j.biomaterials.2006.10.026.

[141] M.A. Khan, V.M. Wu, S. Ghosh, V. Uskoković, Gene delivery using calcium phosphate nanoparticles: Optimization of the transfection process and the effects of citrate and poly(l-lysine) as additives, Journal of Colloid and Interface Science. 471 (2016) 48–58. https://doi.org/https://doi.org/10.1016/j.jcis.2016.03.007.

[142] L. Wang, G.H. Nancollas, Calcium orthophosphates: crystallization and dissolution, Chemical Reviews. 108 (2008) 4628–4669. https://doi.org/10.1021/cr0782574.

[143] H.-B. Pan, B.W. Darvell, Calcium Phosphate Solubility: The Need for Re-Evaluation, Crystal Growth & Design. 9 (2009) 639–645. https://doi.org/10.1021/cg801118v.

[144] J. Jeong, J.H. Kim, J.H. Shim, N.S. Hwang, C.Y. Heo, Bioactive calcium phosphate materials and applications in bone regeneration, Biomaterials Research. 23 (2019) 4. https://doi.org/10.1186/s40824-018-0149-3.

[145] D.J. HADJIDAKIS, I.I. ANDROULAKIS, Bone Remodeling, Annals of the New York Academy of Sciences. 1092 (2006) 385–396. https://doi.org/10.1196/annals.1365.035.

[146] S. Shekhar, A. Roy, D. Hong, P.N. Kumta, Nanostructured silicate substituted calcium phosphate (NanoSiCaPs) nanoparticles — Efficient calcium phosphate based non-viral gene delivery systems, Materials Science and Engineering: C. 69 (2016) 486–495. https://doi.org/https://doi.org/10.1016/j.msec.2016.06.076.

[147] X. Huang, D. Andina, J. Ge, A. Labarre, J.-C. Leroux, B. Castagner, Characterization of Calcium Phosphate Nanoparticles Based on a PEGylated Chelator for Gene Delivery, ACS Applied Materials & Interfaces. 9 (2017) 10435–10445. https://doi.org/10.1021/acsami.6b15925.

[148] S. Chen, F. Li, R.-X. Zhuo, S.-X. Cheng, Efficient non-viral gene delivery mediated by nanostructured calcium carbonate in solution-based transfection and solid-phase transfection, Molecular BioSystems. 7 (2011) 2841–2847. https://doi.org/10.1039/C1MB05147D.

[149] G. Bhakta, S. Mitra, A. Maitra, DNA encapsulated magnesium and manganous phosphate nanoparticles: potential non-viral vectors for gene delivery, Biomaterials. 26 (2005) 2157–2163. https://doi.org/https://doi.org/10.1016/j.biomaterials.2004.06.039.

[150] E. V Giger, B. Castagner, J. Räikkönen, J. Mönkkönen, J.-C. Leroux, siRNA

Transfection with Calcium Phosphate Nanoparticles Stabilized with PEGylated Chelators, Advanced Healthcare Materials. 2 (2013) 134–144. https://doi.org/10.1002/adhm.201200088.

[151] F. Pittella, K. Miyata, Y. Maeda, T. Suma, S. Watanabe, Q. Chen, R.J. Christie, K. Osada, N. Nishiyama, K. Kataoka, Pancreatic cancer therapy by systemic administration of VEGF siRNA contained in calcium phosphate/charge-conversional polymer hybrid nanoparticles, Journal of Controlled Release. 161 (2012) 868–874. https://doi.org/https://doi.org/10.1016/j.jconrel.2012.05.005.

[152] J. Li, Y.-C. Chen, Y.-C. Tseng, S. Mozumdar, L. Huang, Biodegradable calcium phosphate nanoparticle with lipid coating for systemic siRNA delivery, Journal of Controlled Release. 142 (2010) 416–421. https://doi.org/https://doi.org/10.1016/j.jconrel.2009.11.008.

[153] B. Sun, K.K. Tran, H. Shen, Enabling customization of non-viral gene delivery systems for individual cell types by surface-induced mineralization, Biomaterials. 30 (2009) 6386–6393. https://doi.org/https://doi.org/10.1016/j.biomaterials.2009.08.006.

[154] B. Neuhaus, B. Tosun, O. Rotan, A. Frede, A.M. Westendorf, M. Epple, Nanoparticles as transfection agents: a comprehensive study with ten different cell lines, RSC Advances. 6 (2016) 18102–18112. https://doi.org/10.1039/C5RA25333K.

[155] T. A. Dick, H. Uludağ, Mineralized polyplexes for gene delivery: Improvement of transfection efficiency as a consequence of calcium incubation and not mineralization, Materials Science and Engineering: C. 129 (2021) 112419. https://doi.org/https://doi.org/10.1016/j.msec.2021.112419.

[156] L.-L. Huang, X. Li, J. Zhang, Q.R. Zhao, M.J. Zhang, A.-A. Liu, D.-W. Pang, H.-Y. Xie, MnCaCs-Biomineralized Oncolytic Virus for Bimodal Imaging-Guided and Synergistically Enhanced Anticancer Therapy, Nano Letters. 19 (2019) 8002–8009. https://doi.org/10.1021/acs.nanolett.9b03193.

[157] F. Pittella, H. Cabral, Y. Maeda, P. Mi, S. Watanabe, H. Takemoto, H.J. Kim, N. Nishiyama, K. Miyata, K. Kataoka, Systemic siRNA delivery to a spontaneous pancreatic tumor model in transgenic mice by PEGylated calcium phosphate hybrid micelles, Journal of Controlled Release. 178 (2014) 18–24. https://doi.org/https://doi.org/10.1016/j.jconrel.2014.01.008.

[158] J. Chen, X. Sun, R. Shao, Y. Xu, J. Gao, W. Liang, VEGF siRNA delivered by polycation liposome-encapsulated calcium phosphate nanoparticles for tumor angiogenesis inhibition in breast cancer, International Journal of Nanomedicine. 12 (2017) 6075–6088. https://doi.org/10.2147/IJN.S142739.

[159] S. Bisso, S. Mura, B. Castagner, P. Couvreur, J.-C. Leroux, Dual delivery of nucleic acids and PEGylated-bisphosphonates via calcium phosphate nanoparticles,

BioRxiv. (2019) 621102. https://doi.org/10.1101/621102.

[160] R.-Q. Cai, D.-Z. Liu, H. Cui, Y. Cheng, M. Liu, B.-L. Zhang, Q.-B. Mei, S.-Y. Zhou, Charge reversible calcium phosphate lipid hybrid nanoparticle for siRNA delivery, Oncotarget; Vol 8, No 26. (2017). https://www.oncotarget.com/article/17484/text/.

[161] A. Frede, B. Neuhaus, R. Klopfleisch, C. Walker, J. Buer, W. Müller, M. Epple, A.M. Westendorf, Colonic gene silencing using siRNA-loaded calcium phosphate/PLGA nanoparticles ameliorates intestinal inflammation in vivo, Journal of Controlled Release. 222 (2016) 86–96. https://doi.org/https://doi.org/10.1016/j.jconrel.2015.12.021.

[162] T. Tenkumo, J.R. Vanegas Sáenz, K. Nakamura, Y. Shimizu, V. Sokolova, M. Epple, Y. Kamano, H. Egusa, T. Sugaya, K. Sasaki, Prolonged release of bone morphogenetic protein-2 in vivo by gene transfection with DNA-functionalized calcium phosphate nanoparticle-loaded collagen scaffolds, Materials Science and Engineering: C. 92 (2018) 172–183. https://doi.org/10.1016/J.MSEC.2018.06.047.

[163] T. Devarasu, R. Saad, A. Ouadi, B. Frisch, E. Robinet, P. Laquerriere, J.-C. Voegel, T. Baumert, J. Ogier, F. Meyer, Potent calcium phosphate nanoparticle surface coating for in vitro and in vivo siRNA delivery: a step toward multifunctional nanovectors, Journal of Materials Chemistry B. 1 (2013) 4692–4700. https://doi.org/10.1039/C3TB20557F.

[164] T. Acri, N. Laird, L. Jaidev, D. Meyerholz, A. Salem, K. Shin, Nonviral Gene Delivery Embedded in Biomimetically Mineralized Matrices for Bone Tissue Engineering, Tissue Engineering Part A. 27 (2021) 1074–1083.

[165] W. Zhang, H. Tsurushima, A. Oyane, Y. Yazaki, Y. Sogo, A. Ito, A. Matsumura, BMP-2 gene-fibronectin-apatite composite layer enhances bone formation, Journal of Biomedical Science. 18 (2011) 62. https://doi.org/10.1186/1423-0127-18-62.

[166] X. Wang, D. Yang, S. Li, X. Xu, C.-F. Qin, R. Tang, Biomineralized vaccine nanohybrid for needle-free intranasal immunization, Biomaterials. 106 (2016) 286–294. https://doi.org/https://doi.org/10.1016/j.biomaterials.2016.08.035.

[167] L.J. de Mello, G.R.R. Souza, E. Winter, A.H. Silva, F. Pittella, T.B. Creczynski-Pasa, Knockdown of antiapoptotic genes in breast cancer cells by siRNA loaded into hybrid nanoparticles, Nanotechnology. 28 (2017) 175101. https://doi.org/10.1088/1361-6528/aa6283.

[168] E. V Giger, J. Puigmartí-Luis, R. Schlatter, B. Castagner, P.S. Dittrich, J.-C. Leroux, Gene delivery with bisphosphonate-stabilized calcium phosphate nanoparticles, Journal of Controlled Release. 150 (2011) 87–93. https://doi.org/https://doi.org/10.1016/j.jconrel.2010.11.012.

[169] Y. Kakizawa, K. Kataoka, Block Copolymer Self-Assembly into Monodispersive

Nanoparticles with Hybrid Core of Antisense DNA and Calcium Phosphate, Langmuir. 18 (2002) 4539–4543. https://doi.org/10.1021/la011736s.

[170] J.S. Suk, Q. Xu, N. Kim, J. Hanes, L.M. Ensign, PEGylation as a strategy for improving nanoparticle-based drug and gene delivery, Advanced Drug Delivery Reviews. 99 (2016) 28–51. https://doi.org/https://doi.org/10.1016/j.addr.2015.09.012.

[171] K. Knop, R. Hoogenboom, D. Fischer, U.S. Schubert, Poly(ethylene glycol) in Drug Delivery: Pros and Cons as Well as Potential Alternatives, Angewandte Chemie International Edition. 49 (2010) 6288–6308. https://doi.org/10.1002/anie.200902672.

[172] Y. Kakizawa, K. Miyata, S. Furukawa, K. Kataoka, Size-Controlled Formation of a Calcium Phosphate-Based Organic–Inorganic Hybrid Vector for Gene Delivery Using Poly(ethylene glycol)-block-poly(aspartic acid), Advanced Materials. 16 (2004) 699–702. https://doi.org/10.1002/adma.200305782.

[173] F. Pittella, M. Zhang, Y. Lee, H.J. Kim, T. Tockary, K. Osada, T. Ishii, K. Miyata, N. Nishiyama, K. Kataoka, Enhanced endosomal escape of siRNA-incorporating hybrid nanoparticles from calcium phosphate and PEG-block charge-conversional polymer for efficient gene knockdown with negligible cytotoxicity, Biomaterials. 32 (2011) 3106–3114. https://doi.org/https://doi.org/10.1016/j.biomaterials.2010.12.057.

[174] Y. Maeda, F. Pittella, T. Nomoto, H. Takemoto, N. Nishiyama, K. Miyata, K. Kataoka, Fine-Tuning of Charge-Conversion Polymer Structure for Efficient Endosomal Escape of siRNA-Loaded Calcium Phosphate Hybrid Micelles, Macromolecular Rapid Communications. 35 (2014) 1211–1215. https://doi.org/10.1002/marc.201400049.

[175] M. Khansarizadeh, A. Mokhtarzadeh, M. Rashedinia, S.M. Taghdisi, P. Lari, K.H. Abnous, M. Ramezani, Identification of possible cytotoxicity mechanism of polyethylenimine by proteomics analysis, Human & Experimental Toxicology. 35 (2015) 377–387. https://doi.org/10.1177/0960327115591371.

[176] M.-E. Halatsch, R.E. Kast, A. Dwucet, M. Hlavac, T. Heiland, M.-A. Westhoff, K.-M. Debatin, C.R. Wirtz, M.D. Siegelin, G. Karpel-Massler, Bcl-2/Bcl-xL inhibition predominantly synergistically enhances the anti-neoplastic activity of a low-dose CUSP9 repurposed drug regime against glioblastoma, British Journal of Pharmacology. 176 (2019) 3681–3694. https://doi.org/10.1111/bph.14773.

[177] M.-E. Halatsch, R.E. Kast, A. Dwucet, C.R. Wirtz, M. Siegelin, G. Karpel-Massler, EXTH-54. Bcl-2/Bcl-xL INHIBITION SYNERGISTICALLY ENHANCES THE ANTI-NEOPLASTIC ACTIVITY OF CUSP9 AGAINST GLIOBLASTOMA CELLS IN VITRO, Neuro-Oncology. 20 (2018) vi96–vi96. https://doi.org/10.1093/neuonc/noy148.402.

[178] S. Kehr, T. Haydn, A. Bierbrauer, B. Irmer, M. Vogler, S. Fulda, Targeting BCL-2 proteins in pediatric cancer: Dual inhibition of BCL-XL and MCL-1 leads to rapid induction of intrinsic apoptosis, Cancer Letters. (2020). https://doi.org/https://doi.org/10.1016/j.canlet.2020.02.041.

[179] Q. Zhou, Y. Wang, J. Xiang, Y. Piao, Z. Zhou, J. Tang, X. Liu, Y. Shen, Stabilized calcium phosphate hybrid nanocomposite using a benzoxaborole-containing polymer for pH-responsive siRNA delivery, Biomaterials Science. 6 (2018) 3178–3188. https://doi.org/10.1039/c8bm00575c.

[180] L. Forte, S. Sarda, P. Torricelli, C. Combes, F. Brouillet, O. Marsan, F. Salamanna, M. Fini, E. Boanini, A. Bigi, Multifunctionalization Modulates Hydroxyapatite Surface Interaction with Bisphosphonate: Antiosteoporotic and Antioxidative Stress Materials, ACS Biomaterials Science & Engineering. 5 (2019) 3429–3439. https://doi.org/10.1021/acsbiomaterials.9b00795.

[181] M.T. Drake, B.L. Clarke, S. Khosla, Bisphosphonates: mechanism of action and role in clinical practice, Mayo Clinic Proceedings. 83 (2008) 1032–1045. https://doi.org/10.4065/83.9.1032.

[182] S. Cremers, M.T. Drake, F.H. Ebetino, J.P. Bilezikian, R.G.G. Russell, Pharmacology of bisphosphonates, British Journal of Clinical Pharmacology. 85 (2019) 1052–1062. https://doi.org/10.1111/bcp.13867.

[183] D.D. Waller, J. Park, Y.S. Tsantrizos, Inhibition of farnesyl pyrophosphate (FPP) and/or geranylgeranyl pyrophosphate (GGPP) biosynthesis and its implication in the treatment of cancers, Critical Reviews in Biochemistry and Molecular Biology. 54 (2019) 41–60. https://doi.org/10.1080/10409238.2019.1568964.

[184] S.S. Virtanen, H.K. Väänänen, P.L. Härkönen, P.T. Lakkakorpi, Alendronate Inhibits Invasion of PC-3 Prostate Cancer Cells by Affecting the Mevalonate Pathway, Cancer Research. 62 (2002) 2708 LP – 2714. http://cancerres.aacrjournals.org/content/62/9/2708.abstract.

[185] Y. Liu, C. Du, Y. Zhang, S. Zhao, L. Zhao, P. Li, F. Hu, L. Zhu, Y. Liu, D. Pang, Y. Zhao, Bisphosphonate and risk of cancer recurrence: protocol for a systematic review, meta-analysis and trial sequential analysis of randomised controlled trials, BMJ Open. 5 (2015) e007215–e007215. https://doi.org/10.1136/bmjopen-2014-007215.

[186] T.L. Rogers, I. Holen, Tumour macrophages as potential targets of bisphosphonates, Journal of Translational Medicine. 9 (2011) 177. https://doi.org/10.1186/1479-5876-9-177.

[187] G. Mattheolabakis, L. Milane, A. Singh, M.M. Amiji, Hyaluronic acid targeting of CD44 for cancer therapy: from receptor biology to nanomedicine, Journal of Drug Targeting. 23 (2015) 605–618. https://doi.org/10.3109/1061186X.2015.1052072.

[188] A. Fakhari, C. Berkland, Applications and emerging trends of hyaluronic acid in tissue engineering, as a dermal filler and in osteoarthritis treatment, Acta Biomaterialia. 9 (2013) 7081–7092. https://doi.org/https://doi.org/10.1016/j.actbio.2013.03.005.

[189] J.. Lee, J.E.; Yin, Y.; Lim, S.Y.; Kim, E.S.; Jung, J.; Kim, D.; Park, J.W.; Lee, M.S.; Jeong, Enhanced Transfection of Human Mesenchymal Stem Cells Using a Hyaluronic Acid/Calcium Phosphate Hybrid Gene Delivery System, Polymers. 11 (2019) 798.

[190] A.H. Hofman, I.A. van Hees, J. Yang, M. Kamperman, Bioinspired Underwater Adhesives by Using the Supramolecular Toolbox, Advanced Materials. 30 (2018) 1704640. https://doi.org/10.1002/adma.201704640.

[191] H.Y. Nam, K.H. Min, D.E. Kim, J.R. Choi, H.J. Lee, S.C. Lee, Mussel-inspired poly(L-DOPA)-templated mineralization for calcium phosphate-assembled intracellular nanocarriers, Colloids and Surfaces B: Biointerfaces. 157 (2017) 215–222. https://www.scopus.com/inward/record.uri?eid=2-s2.0-85020258647&doi=10.1016%2Fj.colsurfb.2017.05.077&partnerID=40&md5=e8ec80d84e58d34fc8f985fbcb24a1fd.

[192] M. Ullah, D.D. Liu, A.S. Thakor, Mesenchymal Stromal Cell Homing: Mechanisms and Strategies for Improvement, IScience. 15 (2019) 421–438. https://doi.org/10.1016/j.isci.2019.05.004.

[193] J. Zhang, X. Sun, R. Shao, W. Liang, J. Gao, J. Chen, Polycation liposomes combined with calcium phosphate nanoparticles as a non-viral carrier for siRNA delivery, Journal of Drug Delivery Science and Technology. 30 (2015) 1–6. https://doi.org/https://doi.org/10.1016/j.jddst.2015.09.005.

[194] B. Sun, M. Gillard, Y. Wu, P. Wu, Z.P. Xu, W. Gu, Bisphosphonate Stabilized Calcium Phosphate Nanoparticles for Effective Delivery of Plasmid DNA to Macrophages, ACS Applied Bio Materials. 3 (2020) 986–996. https://doi.org/10.1021/acsabm.9b00994.

[195] J. Tang, L. Li, C.B. Howard, S.M. Mahler, L. Huang, Z.P. Xu, Preparation of optimized lipid-coated calcium phosphate nanoparticles for enhanced in vitro gene delivery to breast cancer cells, Journal of Materials Chemistry B. 3 (2015) 6805–6812. https://doi.org/10.1039/C5TB00912J.

[196] S. Karthika, T.K. Radhakrishnan, P. Kalaichelvi, A Review of Classical and Nonclassical Nucleation Theories, Crystal Growth & Design. 16 (2016) 6663–6681. https://doi.org/10.1021/acs.cgd.6b00794.

[197] K.R. Baillargeon, K. Meserve, S. Faulkner, S. Watson, H. Butts, P. Deighan, A.E. Gerdon, Precipitation SELEX: identification of DNA aptamers for calcium phosphate materials synthesis, Chemical Communications. 53 (2017) 1092–1095. https://doi.org/10.1039/c6cc08687j.

[198] M.B. Parmar, D.N. Meenakshi Sundaram, R.B. K.C., R. Maranchuk, H. Montazeri Aliabadi, J.C. Hugh, R. Löbenberg, H. Uludağ, Combinational siRNA delivery using hyaluronic acid modified amphiphilic polyplexes against cell cycle and phosphatase proteins to inhibit growth and migration of triple-negative breast cancer cells, Acta Biomaterialia. 66 (2018) 294–309. https://doi.org/https://doi.org/10.1016/j.actbio.2017.11.036.

[199] M.A. López-Quintela, Synthesis of nanomaterials in microemulsions: formation mechanisms and growth control, Current Opinion in Colloid & Interface Science. 8 (2003) 137–144. https://doi.org/https://doi.org/10.1016/S1359-0294(03)00019-0.

[200] M. de Dios, F. Barroso, C. Tojo, M.A. López-Quintela, Simulation of the kinetics of nanoparticle formation in microemulsions, Journal of Colloid and Interface Science. 333 (2009) 741–748. https://doi.org/https://doi.org/10.1016/j.jcis.2009.01.032.

[201] R. Jain, D. Shukla, A. Mehra, Coagulation of Nanoparticles in Reverse Micellar Systems: A Monte Carlo Model, Langmuir. 21 (2005) 11528–11533. https://doi.org/10.1021/la0523208.

[202] T. Hirai, H. Sato, I. Komasawa, Mechanism of Formation of CdS and ZnS Ultrafine Particles in Reverse Micelles, Industrial & Engineering Chemistry Research. 33 (1994) 3262–3266. https://doi.org/10.1021/ie00036a048.

[203] S. Bisht, G. Bhakta, S. Mitra, A. Maitra, pDNA loaded calcium phosphate nanoparticles: highly efficient non-viral vector for gene delivery, International Journal of Pharmaceutics. 288 (2005) 157–168. https://doi.org/https://doi.org/10.1016/j.ijpharm.2004.07.035.

[204] N.I. Ponomareva, T.D. Poprygina, S.I. Karpov, M. V Lesovoi, B.L. Agapov, Microemulsion method for producing hydroxyapatite, Russian Journal of General Chemistry. 80 (2010) 905–908. https://doi.org/10.1134/S1070363210050063.

[205] X. He, T. Liu, Y. Chen, D. Cheng, X. Li, Y. Xiao, Y. Feng, Calcium carbonate nanoparticle delivering vascular endothelial growth factor-C siRNA effectively inhibits lymphangiogenesis and growth of gastric cancer in vivo, Cancer Gene Therapy. 15 (2008) 193–202. https://doi.org/10.1038/sj.cgt.7701122.

[206] G. Bhakta, A. Shrivastava, A. Maitra, Magnesium phosphate nanoparticles can be efficiently used in vitro and in vivo as non-viral vectors for targeted gene delivery, Journal of Biomedical Nanotechnology. 5 (2009) 106–114. https://doi.org/10.1166/jbn.2009.029.

[207] I. Roy, S. Mitra, A. Maitra, S. Mozumdar, Calcium phosphate nanoparticles as novel non-viral vectors for targeted gene delivery, International Journal of Pharmaceutics. 250 (2003) 25–33. https://doi.org/https://doi.org/10.1016/S0378-5173(02)00452-0.

[208] C. Tojo, M. de Dios, F. Barroso, Surfactant Effects on Microemulsion-Based Nanoparticle Synthesis, Materials (Basel, Switzerland). 4 (2010) 55–72. https://doi.org/10.3390/ma4010055.

[209] M. Soleimani Zohr Shiri, W. Henderson, M.R. Mucalo, A Review of The Lesser-Studied Microemulsion-Based Synthesis Methodologies Used for Preparing Nanoparticle Systems of The Noble Metals, Os, Re, Ir and Rh, Materials (Basel, Switzerland). 12 (2019) 1896. https://doi.org/10.3390/ma12121896.

[210] S. Hou, H. Ma, Y. Ji, W. Hou, N. Jia, A Calcium Phosphate Nanoparticle-Based Biocarrier for Efficient Cellular Delivery of Antisense Oligodeoxynucleotides, ACS Applied Materials & Interfaces. 5 (2013) 1131–1136. https://doi.org/10.1021/am3028926.

[211] K. Lee, M.H. Oh, M.S. Lee, Y.S. Nam, T.G. Park, J.H. Jeong, Stabilized calcium phosphate nano-aggregates using a dopa-chitosan conjugate for gene delivery, International Journal of Pharmaceutics. 445 (2013) 196–202. https://doi.org/https://doi.org/10.1016/j.ijpharm.2013.01.014.

[212] R. Paliwal, R.J. Babu, S. Palakurthi, Nanomedicine Scale-up Technologies: Feasibilities and Challenges, AAPS PharmSciTech. 15 (2014) 1527–1534. https://doi.org/10.1208/s12249-014-0177-9.

[213] Y. Wu, W. Gu, L. Li, C. Chen, Z.P. Xu, Enhancing PD-1 gene silence in T lymphocytes by comparing the delivery performance of two inorganic nanoparticle platforms, Nanomaterials. 9 (2019). https://doi.org/10.3390/nano9020159.

[214] Z. Zhou, C. Kennell, J.-Y. Lee, Y.-K. Leung, P. Tarapore, Calcium phosphate-polymer hybrid nanoparticles for enhanced triple negative breast cancer treatment via co-delivery of paclitaxel and miR-221/222 inhibitors, Nanomedicine: Nanotechnology, Biology and Medicine. 13 (2017) 403–410. https://doi.org/https://doi.org/10.1016/j.nano.2016.07.016.

[215] S. Li, Q. Li, J. Lü, Q. Zhao, D. Li, L. Shen, Z. Wang, J. Liu, D. Xie, W.C. Cho, S. Xu, Z. Yu, Targeted Inhibition of miR-221/222 Promotes Cell Sensitivity to Cisplatin in Triple-Negative Breast Cancer MDA-MB-231 Cells , Frontiers in Genetics . 10 (2020) 1278. https://www.frontiersin.org/article/10.3389/fgene.2019.01278.

[216] K. Taylor, C.B. Howard, M.L. Jones, I. Sedliarou, J. MacDiarmid, H. Brahmbhatt, T.P. Munro, S.M. Mahler, Nanocell targeting using engineered bispecific antibodies, MAbs. 7 (2015) 53–65. https://doi.org/10.4161/19420862.2014.985952.

[217] Y. Wu, W. Gu, J. Li, C. Chen, Z.P. Xu, Silencing PD-1 and PD-L1 with nanoparticle-delivered small interfering RNA increases cytotoxicity of tumor-infiltrating lymphocytes, Nanomedicine. 14 (2019) 955–967. https://doi.org/10.2217/nnm-2018-0237.

[218] N. Kang, G.J. Gores, V.H. Shah, Hepatic stellate cells: partners in crime for liver metastases?, Hepatology (Baltimore, Md.). 54 (2011) 707–713. https://doi.org/10.1002/hep.24384.

[219] S.J. Turley, V. Cremasco, J.L. Astarita, Immunological hallmarks of stromal cells in the tumour microenvironment, Nature Reviews Immunology. 15 (2015) 669–682. https://doi.org/10.1038/nri3902.

[220] D.F. Mardhian, G. Storm, R. Bansal, J. Prakash, Nano-targeted relaxin impairs fibrosis and tumor growth in pancreatic cancer and improves the efficacy of gemcitabine in vivo, Journal of Controlled Release. 290 (2018) 1–10. https://doi.org/https://doi.org/10.1016/j.jconrel.2018.09.031.

[221] I.S. Zeelenberg, L. Ruuls-Van Stalle, E. Roos, The Chemokine Receptor CXCR4 Is Required for Outgrowth of Colon Carcinoma Micrometastases, Cancer Research. 63 (2003) 3833 LP – 3839. http://cancerres.aacrjournals.org/content/63/13/3833.abstract.

[222] E.M. García-Cuesta, C.A. Santiago, J. Vallejo-Díaz, Y. Juarranz, J.M. Rodríguez-Frade, M. Mellado, The Role of the CXCL12/CXCR4/ACKR3 Axis in Autoimmune Diseases, Frontiers in Endocrinology. 10 (2019) 585. https://doi.org/10.3389/fendo.2019.00585.

[223] A.A. D'Souza, P. V Devarajan, Asialoglycoprotein receptor mediated hepatocyte targeting — Strategies and applications, Journal of Controlled Release. 203 (2015) 126–139. https://doi.org/https://doi.org/10.1016/j.jconrel.2015.02.022.

[224] S. von Karstedt, A. Montinaro, H. Walczak, Exploring the TRAILs less travelled: TRAIL in cancer biology and therapy, Nature Reviews Cancer. 17 (2017) 352–366. https://doi.org/10.1038/nrc.2017.28.

[225] N. Takata, Y. Ohshima, M. Suzuki-Karasaki, Y. Yoshida, Y. Tokuhashi, Y. Suzuki-Karasaki, Mitochondrial Ca2+ removal amplifies TRAIL cytotoxicity toward apoptosis-resistant tumor cells via promotion of multiple cell death modalities, International Journal of Oncology. 51 (2017) 193–203. https://doi.org/10.3892/ijo.2017.4020.

[226] Y. Ohshima, N. Takata, Suzuki-Karasaki, Y. M., Yoshida, Y. Tokuhashi, Y. Suzuki-Karasaki, Disrupting mitochondrial Ca2+ homeostasis causes tumor-selective TRAIL sensitization through mitochondrial network abnormalities, International Journal of Oncology. 51 (2017) 1146–1158.

[227] K.N. Prasad, B. Kumar, X.-D. Yan, A.J. Hanson, W.C. Cole, α-Tocopheryl Succinate, the Most Effective Form of Vitamin E for Adjuvant Cancer Treatment: A Review, Journal of the American College of Nutrition. 22 (2003) 108–117. https://doi.org/10.1080/07315724.2003.10719283.

[228] J. Meerak, S.P. Wanichwecharungruang, T. Palaga, Enhancement of immune

response to a DNA vaccine against Mycobacterium tuberculosis Ag85B by incorporation of an autophagy inducing system, Vaccine. 31 (2013) 784–790. https://doi.org/https://doi.org/10.1016/j.vaccine.2012.11.075.

[229] T. Kokubo, H. Takadama, How useful is SBF in predicting in vivo bone bioactivity?, Biomaterials. 27 (2006) 2907–2915. https://doi.org/https://doi.org/10.1016/j.biomaterials.2006.01.017.

[230] J. Si, Z. Cui, Q. Wang, Q. Liu, C. Liu, Biomimetic composite scaffolds based on mineralization of hydroxyapatite on electrospun poly(ε-caprolactone)/nanocellulose fibers, Carbohydrate Polymers. 143 (2016) 270–278. https://doi.org/10.1016/j.carbpol.2016.02.015.

[231] Z. Xu, L. Shi, D. Hu, B. Hu, M. Yang, L. Zhu, Formation of hierarchical bone-like apatites on silk microfiber templates: Via biomineralization, RSC Advances. 6 (2016) 76426–76433. https://doi.org/10.1039/c6ra17199k.

[232] K.H. Park, S.-J. Kim, Y.-H. Jeong, H.-J. Moon, H.-J. Song, Y.-J. Park, Fabrication and biological properties of calcium phosphate/chitosan composite coating on titanium in modified SBF, Materials Science and Engineering: C. 90 (2018) 113–118. https://doi.org/https://doi.org/10.1016/j.msec.2018.04.060.

[233] X. Wang, J. Yang, C.M. Andrei, L. Soleymani, K. Grandfield, Biomineralization of calcium phosphate revealed by in situ liquid-phase electron microscopy, Communications Chemistry. 1 (2018) 80. https://doi.org/10.1038/s42004-018-0081-4.

[234] K. Shin, T. Acri, S. Geary, A.K. Salem, Biomimetic Mineralization of Biomaterials Using Simulated Body Fluids for Bone Tissue Engineering and Regenerative Medicine<sup/>, Tissue Engineering. Part A. 23 (2017) 1169–1180. https://doi.org/10.1089/ten.TEA.2016.0556.

[235] F. Nudelman, N.A.J.M. Sommerdijk, Biomineralization as an Inspiration for Materials Chemistry, Angewandte Chemie International Edition. 51 (2012) 6582–6596. https://doi.org/10.1002/anie.201106715.

[236] R. Khalifehzadeh, H. Arami, DNA-Templated Strontium-Doped Calcium Phosphate Nanoparticles for Gene Delivery in Bone Cells, ACS Biomaterials Science and Engineering. 5 (2019) 3201–3211. https://doi.org/10.1021/acsbiomaterials.8b01587.

[237] A. Aimaiti, A. Maimaitiyiming, X. Boyong, K. Aji, C. Li, L. Cui, Low-dose strontium stimulates osteogenesis but high-dose doses cause apoptosis in human adipose-derived stem cells via regulation of the ERK1/2 signaling pathway, Stem Cell Research & Therapy. 8 (2017) 282. https://doi.org/10.1186/s13287-017-0726-8.

[238] V. Nardone, S. Fabbri, F. Marini, R. Zonefrati, G. Galli, A. Carossino, A. Tanini,

M.L. Brandi, Osteodifferentiation of Human Preadipocytes Induced by Strontium Released from Hydrogels, International Journal of Biomaterials. 2012 (2012) 865291. https://doi.org/10.1155/2012/865291.

[239] B.G. Mohan, S. Suresh Babu, H.K. Varma, A. John, In vitro evaluation of bioactive strontium-based ceramic with rabbit adipose-derived stem cells for bone tissue regeneration, Journal of Materials Science: Materials in Medicine. 24 (2013) 2831–2844. https://doi.org/10.1007/s10856-013-5018-y.

[240] H. Shen, J. Tan, W.M. Saltzman, Surface-mediated gene transfer from nanocomposites of controlled texture, Nature Materials. 3 (2004) 569–574. https://doi.org/10.1038/nmat1179.

[241] B. Sun, K.K. Tran, H. Shen, Enabling customization of non-viral gene delivery systems for individual cell types by surface-induced mineralization, Biomaterials. 30 (2009) 6386–6393. https://doi.org/10.1016/j.biomaterials.2009.08.006.

[242] L.N. Luong, K.M. McFalls, D.H. Kohn, Gene delivery via DNA incorporation within a biomimetic apatite coating, Biomaterials. 30 (2009) 6996–7004. https://doi.org/https://doi.org/10.1016/j.biomaterials.2009.09.001.

[243] B. Sun, H. Shen, Correlation of the composition of biominerals with their ability of stimulating intracellular DNA sensors and inflammatory cytokines, Biomaterials. 54 (2015) 106–115. https://doi.org/https://doi.org/10.1016/j.biomaterials.2015.03.013.

[244] S. Choi, X. Yu, L. Jongpaiboonkit, S.J. Hollister, W.L. Murphy, Inorganic coatings for optimized non-viral transfection of stem cells, Scientific Reports. 3 (2013) 1567. https://doi.org/10.1038/srep01567.

[245] B. Sun, M. Yi, C.C. Yacoob, H.T. Nguyen, H. Shen, Effect of surface chemistry on gene transfer efficiency mediated by surface-induced DNA-doped nanocomposites, Acta Biomaterialia. 8 (2012) 1109–1116. https://doi.org/https://doi.org/10.1016/j.actbio.2011.12.005.

[246] M. Tanahashi, T. Matsuda, Surface functional group dependence on apatite formation on self-assembled monolayers in a simulated body fluid, Journal of Biomedical Materials Research. 34 (1997) 305–315. https://doi.org/10.1002/(SICI)1097-4636(19970305)34:3<305::AID-JBM5>3.0.CO;2-O.

[247] J. Aizenberg, A.J. Black, G.M. Whitesides, Oriented Growth of Calcite Controlled by Self-Assembled Monolayers of Functionalized Alkanethiols Supported on Gold and Silver, Journal of the American Chemical Society. 121 (1999) 4500–4509. https://doi.org/10.1021/ja984254k.

[248] I. HIRATA, M. AKAMATSU, E. FUJII, S. POOLTHONG, M. OKAZAKI, Chemical analyses of hydroxyapatite formation on SAM surfaces modified with

COOH, NH₂, CH₃, and OH functions, Dental Materials Journal. 29 (2010) 438–445. https://doi.org/10.4012/dmj.2010-017.

[249] G.K. Toworfe, R.J. Composto, I.M. Shapiro, P. Ducheyne, Nucleation and growth of calcium phosphate on amine-, carboxyl- and hydroxyl-silane self-assembled monolayers, Biomaterials. 27 (2006) 631–642. https://doi.org/https://doi.org/10.1016/j.biomaterials.2005.06.017.

[250] Y. Yazaki, A. Oyane, H. Tsurushima, H. Araki, Y. Sogo, A. Ito, A. Yamazaki, Improved gene transfer efficiency of a DNA-lipid-apatite composite layer by controlling the layer molecular composition, Colloids and Surfaces B: Biointerfaces. 122 (2014) 465–471. https://doi.org/https://doi.org/10.1016/j.colsurfb.2014.07.001.

[251] B. Sun, H. Shen, Controlling Surface-Induced Nanocomposites by Lipoplexes for Enhanced Gene Transfer, Journal of Nanomaterials. 2015 (2015) 784836. https://doi.org/10.1155/2015/784836.

[252] A. Oyane, Y. Yazaki, H. Araki, Y. Sogo, A. Ito, A. Yamazaki, H. Tsurushima, Fabrication of a DNA-lipid-apatite composite layer for efficient and area-specific gene transfer, Journal of Materials Science: Materials in Medicine. 23 (2012) 1011–1019. https://doi.org/10.1007/s10856-012-4581-y.

[253] C. Gao, S. Peng, P. Feng, C. Shuai, Bone biomaterials and interactions with stem cells, Bone Research. 5 (2017) 17059. https://doi.org/10.1038/boneres.2017.59.

[254] R. Langer, J.P. Vacanti, Tissue engineering, Science. 260 (1993) 920 LP – 926. https://doi.org/10.1126/science.8493529.

[255] A. Oyane, H. Tsurushima, A. Ito, Novel gene-transferring scaffolds having a cell adhesion molecule–DNA–apatite nanocomposite surface, Gene Therapy. 14 (2007) 1750–1753. https://doi.org/10.1038/sj.gt.3303041.

[256] Y. Yazaki, A. Oyane, Y. Sogo, A. Ito, A. Yamazaki, H. Tsurushima, Area-Specific Cell Stimulation via Surface-Mediated Gene Transfer Using Apatite-Based Composite Layers, International Journal of Molecular Sciences . 16 (2015). https://doi.org/10.3390/ijms16048294.

[257] Y. Yazaki, A. Oyane, Y. Sogo, A. Ito, A. Yamazaki, H. Tsurushima, Control of gene transfer on a DNA–fibronectin–apatite composite layer by the incorporation of carbonate and fluoride ions, Biomaterials. 32 (2011) 4896–4902. https://doi.org/https://doi.org/10.1016/j.biomaterials.2011.03.021.

[258] Y. Yazaki, A. Oyane, H. Tsurushima, H. Araki, Y. Sogo, A. Ito, A. Yamazaki, Coprecipitation of DNA-lipid complexes with apatite and comparison with superficial adsorption for gene transfer applications, Journal of Biomaterials Applications. 28 (2013) 937–945. https://doi.org/10.1177/0885328213486706.

[259] V. V Sokolova, I. Radtke, R. Heumann, M. Epple, Effective transfection of cells with multi-shell calcium phosphate-DNA nanoparticles, Biomaterials. 27 (2006) 3147–3153. https://doi.org/https://doi.org/10.1016/j.biomaterials.2005.12.030.

[260] V. Sokolova, L. Rojas-Sánchez, N. Białas, N. Schulze, M. Epple, Calcium phosphate nanoparticle-mediated transfection in 2D and 3D mono- and co-culture cell models, Acta Biomaterialia. 84 (2019) 391–401. https://doi.org/10.1016/J.ACTBIO.2018.11.051.

[261] T. Tenkumo, J.R. Vanegas Sáenz, K. Nakamura, Y. Shimizu, V. Sokolova, M. Epple, Y. Kamano, H. Egusa, T. Sugaya, K. Sasaki, Prolonged release of bone morphogenetic protein-2 in vivo by gene transfection with DNA-functionalized calcium phosphate nanoparticle-loaded collagen scaffolds, Materials Science and Engineering: C. 92 (2018) 172–183. https://doi.org/https://doi.org/10.1016/j.msec.2018.06.047.

[262] L.J. del Valle, O. Bertran, G. Chaves, G. Revilla-López, M. Rivas, M.T. Casas, J. Casanovas, P. Turon, J. Puiggalí, C. Alemán, DNA adsorbed on hydroxyapatite surfaces, Journal of Materials Chemistry B. 2 (2014) 6953–6966. https://doi.org/10.1039/C4TB01184H.

[263] M. Okazaki, Y. Yoshida, S. Yamaguchi, M. Kaneno, J.C. Elliott, Affinity binding phenomena of DNA onto apatite crystals, Biomaterials. 22 (2001) 2459–2464. https://doi.org/10.1016/S0142-9612(00)00433-6.

[264] F. Bakan, G. Kara, M. Cokol Cakmak, M. Cokol, E.B. Denkbas, Synthesis and characterization of amino acid-functionalized calcium phosphate nanoparticles for siRNA delivery, Colloids and Surfaces B: Biointerfaces. 158 (2017) 175–181. https://doi.org/https://doi.org/10.1016/j.colsurfb.2017.06.028.

[265] Y. Kan, Q. Tan, G. Wu, W. Si, Y. Chen, Study of DNA adsorption on mica surfaces using a surface force apparatus, Scientific Reports. 5 (2015) 8442. https://doi.org/10.1038/srep08442.

[266] M. Banik, T. Basu, Calcium phosphate nanoparticles: a study of their synthesis, characterization and mode of interaction with salmon testis DNA, Dalton Transactions. 43 (2014) 3244–3259. https://doi.org/10.1039/C3DT52522H.

[267] C.E. Pedraza, D.C. Bassett, M.D. McKee, V. Nelea, U. Gbureck, J.E. Barralet, The importance of particle size and DNA condensation salt for calcium phosphate nanoparticle transfection, Biomaterials. 29 (2008) 3384–3392. https://doi.org/https://doi.org/10.1016/j.biomaterials.2008.04.043.

[268] Y.-H. Lee, H.-C. Wu, C.-W. Yeh, C.-H. Kuan, H.-T. Liao, H.-C. Hsu, J.-C. Tsai, J.-S. Sun, T.-W. Wang, Enzyme-crosslinked gene-activated matrix for the induction of mesenchymal stem cells in osteochondral tissue regeneration, Acta Biomaterialia. 63 (2017) 210–226. https://doi.org/https://doi.org/10.1016/j.actbio.2017.09.008.

[269] A. Frede, B. Neuhaus, T. Knuschke, M. Wadwa, S. Kollenda, R. Klopfleisch, W. Hansen, J. Buer, D. Bruder, M. Epple, A.M. Westendorf, Local delivery of siRNA-loaded calcium phosphate nanoparticles abates pulmonary inflammation, Nanomedicine: Nanotechnology, Biology and Medicine. 13 (2017) 2395–2403. https://doi.org/https://doi.org/10.1016/j.nano.2017.08.001.

[270] T. Tenkumo, J.R. Vanegas Sáenz, Y. Takada, M. Takahashi, O. Rotan, V. Sokolova, M. Epple, K. Sasaki, Gene transfection of human mesenchymal stem cells with a nano-hydroxyapatite–collagen scaffold containing DNA-functionalized calcium phosphate nanoparticles, Genes to Cells. 21 (2016) 682–695. https://doi.org/10.1111/gtc.12374.

[271] C. Hadjicharalambous, D. Kozlova, V. Sokolova, M. Epple, M. Chatzinikolaidou, Calcium phosphate nanoparticles carrying BMP-7 plasmid DNA induce an osteogenic response in MC3T3-E1 pre-osteoblasts, Journal of Biomedical Materials Research Part A. 103 (2015) 3834–3842. https://doi.org/10.1002/jbm.a.35527.

[272] J.R. Vanegas Sáenz, T. Tenkumo, Y. Kamano, H. Egusa, K. Sasaki, Amiloride-enhanced gene transfection of octa-arginine functionalized calcium phosphate nanoparticles, PLOS ONE. 12 (2017) e0188347. https://doi.org/10.1371/journal.pone.0188347.

[273] D. Dutta, J.G. Donaldson, Search for inhibitors of endocytosis: Intended specificity and unintended consequences, Cellular Logistics. 2 (2012) 203–208. https://doi.org/10.4161/cl.23967.

[274] L. Qin, Y. Sun, P. Liu, Q. Wang, B. Han, Y. Duan, F127/Calcium phosphate hybrid nanoparticles: a promising vector for improving siRNA delivery and gene silencing, Journal of Biomaterials Science, Polymer Edition. 24 (2013) 1757–1766. https://doi.org/10.1080/09205063.2013.801702.

[275] C. Chen, H. Han, W. Yang, X. Ren, X. Kong, Polyethyleneimine-modified calcium carbonate nanoparticles for p53 gene delivery , Regenerative Biomaterials. 3 (2016) 57–63. https://doi.org/10.1093/rb/rbv029.

[276] D. Kozlova, S. Chernousova, T. Knuschke, J. Buer, A.M. Westendorf, M. Epple, Cell targeting by antibody-functionalized calcium phosphate nanoparticles, Journal of Materials Chemistry. 22 (2012) 396–404. https://doi.org/10.1039/C1JM14683A.

[277] Y. Yin, M.S. Lee, J.E. Lee, S.Y. Lim, E.S. Kim, J. Jeong, D. Kim, J. Kim, D.S. Lee, J.H. Jeong, Effective systemic siRNA delivery using dual-layer protected long-circulating nanohydrogel containing an inorganic core, Biomaterials Science. 7 (2019) 3297–3306. https://doi.org/10.1039/c9bm00369j.

[278] M. Antonietti, M. Breulmann, C.G. Göltner, H. Cölfen, K.K.W. Wong, D. Walsh, S. Mann, Inorganic/Organic Mesostructures with Complex Architectures: Precipitation of Calcium Phosphate in the Presence of Double-Hydrophilic Block

Copolymers, Chemistry – A European Journal. 4 (1998) 2493–2500. https://doi.org/10.1002/(SICI)1521-3765(19981204)4:12<2493::AID-CHEM2493>3.0.CO;2-V.

[279] H.T. Schmidt, A.E. Ostafin, Liposome Directed Growth of Calcium Phosphate Nanoshells, Advanced Materials. 14 (2002) 532–535. https://doi.org/10.1002/1521-4095(20020404)14:7<532::AID-ADMA532>3.0.CO;2-4.

[280] K.K. Perkin, J.L. Turner, K.L. Wooley, S. Mann, Fabrication of Hybrid Nanocapsules by Calcium Phosphate Mineralization of Shell Cross-Linked Polymer Micelles and Nanocages, Nano Letters. 5 (2005) 1457–1461. https://doi.org/10.1021/nl050817w.

[281] H.J. Lee, S.E. Kim, I.K. Kwon, C. Park, C. Kim, J. Yang, S.C. Lee, Spatially mineralized self-assembled polymeric nanocarriers with enhanced robustness and controlled drug-releasing property, Chemical Communications. 46 (2010) 377–379. https://doi.org/10.1039/B913732G.

[282] S.-Y. Han, H.S. Han, S.C. Lee, Y.M. Kang, I.-S. Kim, J.H. Park, Mineralized hyaluronic acid nanoparticles as a robust drug carrier, Journal of Materials Chemistry. 21 (2011) 7996–8001. https://doi.org/10.1039/C1JM10466G.

[283] K.H. Min, H.J. Lee, K. Kim, I.C. Kwon, S.Y. Jeong, S.C. Lee, The tumor accumulation and therapeutic efficacy of doxorubicin carried in calcium phosphate-reinforced polymer nanoparticles, Biomaterials. 33 (2012) 5788–5797. https://doi.org/https://doi.org/10.1016/j.biomaterials.2012.04.057.

[284] H.S. Han, J. Lee, H.R. Kim, S.Y. Chae, M. Kim, G. Saravanakumar, H.Y. Yoon, D.G. You, H. Ko, K. Kim, I.C. Kwon, J.C. Park, J.H. Park, Robust PEGylated hyaluronic acid nanoparticles as the carrier of doxorubicin: Mineralization and its effect on tumor targetability in vivo, Journal of Controlled Release. 168 (2013) 105–114. https://doi.org/https://doi.org/10.1016/j.jconrel.2013.02.022.

[285] Y. Lv, H. Huang, B. Yang, H. Liu, Y. Li, J. Wang, A robust pH-sensitive drug carrier: Aqueous micelles mineralized by calcium phosphate based on chitosan, Carbohydrate Polymers. 111 (2014) 101–107. https://doi.org/https://doi.org/10.1016/j.carbpol.2014.04.082.

[286] B.J. Kim, K.H. Min, G.H. Hwang, H.J. Lee, S.Y. Jeong, E.-C. Kim, S.C. Lee, Calcium carbonate-mineralized polymer nanoparticles for pH-responsive robust nanocarriers of docetaxel, Macromolecular Research. 23 (2015) 111–117. https://doi.org/10.1007/s13233-015-3020-6.

[287] B. Deng, M. Xia, J. Qian, R. Li, L. Li, J. Shen, G. Li, Y. Xie, Calcium Phosphate-Reinforced Reduction-Sensitive Hyaluronic Acid Micelles for Delivering Paclitaxel in Cancer Therapy, Molecular Pharmaceutics. 14 (2017) 1938–1949. https://doi.org/10.1021/acs.molpharmaceut.7b00025.

[288] Y. Li, K. Xiao, W. Zhu, W. Deng, K.S. Lam, Stimuli-responsive cross-linked micelles for on-demand drug delivery against cancers, Advanced Drug Delivery Reviews. 66 (2014) 58–73. https://doi.org/https://doi.org/10.1016/j.addr.2013.09.008.

[289] S.J. Lee, K.H. Min, H.J. Lee, A.N. Koo, H.P. Rim, B.J. Jeon, S.Y. Jeong, J.S. Heo, S.C. Lee, Ketal Cross-Linked Poly(ethylene glycol)-Poly(amino acid)s Copolymer Micelles for Efficient Intracellular Delivery of Doxorubicin, Biomacromolecules. 12 (2011) 1224–1233. https://doi.org/10.1021/bm101517x.

[290] X. Wang, Y. Deng, S. Li, G. Wang, E. Qin, X. Xu, R. Tang, C. Qin, Biomineralization-Based Virus Shell-Engineering: Towards Neutralization Escape and Tropism Expansion, Advanced Healthcare Materials. 1 (2012) 443–449. https://doi.org/10.1002/adhm.201200034.

[291] T. Sakoda, N. Kasahara, L. Kedes, M. Ohyanagi, Calcium phosphate coprecipitation greatly enhances transduction of cardiac myocytes and vascular smooth muscle cells by lentivirus vectors, Experimental and Clinical Cardiology. 12 (2007) 133–138. https://pubmed.ncbi.nlm.nih.gov/18650994.

[292] H. Zhou, G. Wang, X. Wang, Z. Song, R. Tang, Mineralized State of the Avian Influenza Virus in the Environment, Angewandte Chemie International Edition. 56 (2017) 12908–12912. https://doi.org/10.1002/anie.201705769.

[293] X. Wang, X. Liu, Y. Xiao, H. Hao, Y. Zhang, R. Tang, Biomineralization State of Viruses and Their Biological Potential, Chemistry – A European Journal. 24 (2018) 11518–11529. https://doi.org/10.1002/chem.201705936.

[294] H. Zhou, X. Wang, R. Tang, Could a mineralized state of avian flu virus be dangerous to humans?, Future Virology. 13 (2018) 79–81. https://doi.org/10.2217/fvl-2017-0142.

[295] A. Fasbender, J.H. Lee, R.W. Walters, T.O. Moninger, J. Zabner, M.J. Welsh, Incorporation of adenovirus in calcium phosphate precipitates enhances gene transfer to airway epithelia in vitro and in vivo., The Journal of Clinical Investigation. 102 (1998) 184–193. https://doi.org/10.1172/JCI2732.

[296] Y.-W. Yang, C.-K. Chao, Incorporation of calcium phosphate enhances recombinant adeno-associated virus-mediated gene therapy in diabetic mice, The Journal of Gene Medicine. 5 (2003) 417–424. https://doi.org/10.1002/jgm.353.

[297] K. Toyoda, J.J. Andresen, J. Zabner, F.M. Faraci, D.D. Heistad, Calcium phosphate precipitates augment adenovirus-mediated gene transfer to blood vessels in vitro and in vivo, Gene Therapy. 7 (2000) 1284–1291. https://doi.org/10.1038/sj.gt.3301214.

[298] G. Wang, R.-Y. Cao, R. Chen, L. Mo, J.-F. Han, X. Wang, X. Xu, T. Jiang, Y.-Q. Deng, K. Lyu, S.-Y. Zhu, E.-D. Qin, R. Tang, C.-F. Qin, Rational design of

thermostable vaccines by engineered peptide-induced virus self-biomineralization under physiological conditions, Proceedings of the National Academy of Sciences. 110 (2013) 7619 LP – 7624. https://doi.org/10.1073/pnas.1300233110.

[299] C.S. Schneider, Q. Xu, N.J. Boylan, J. Chisholm, B.C. Tang, B.S. Schuster, A. Henning, L.M. Ensign, E. Lee, P. Adstamongkonkul, B.W. Simons, S.-Y.S. Wang, X. Gong, T. Yu, M.P. Boyle, J.S. Suk, J. Hanes, Nanoparticles that do not adhere to mucus provide uniform and long-lasting drug delivery to airways following inhalation, Science Advances. 3 (2017) e1601556. https://doi.org/10.1126/sciadv.1601556.

[300] T. Ito, Y. Koyama, M. Otsuka, Preparation of Calcium Phosphate Nanocapsule Including Deoxyribonucleic Acid–Polyethyleneimine–Hyaluronic Acid Ternary Complex for Durable Gene Delivery, Journal of Pharmaceutical Sciences. 103 (2014) 179–184. https://doi.org/10.1002/jps.23768.

[301] P. Chen, Y. Liu, J. Zhao, X. Pang, P. Zhang, X. Hou, P. Chen, C. He, Z. Wang, Z. Chen, The synthesis of amphiphilic polyethyleneimine/calcium phosphate composites for bispecific T-cell engager based immunogene therapy, Biomaterials Science. 6 (2018) 633–641. https://doi.org/10.1039/C7BM01143A.

[302] T.M. Acri, N.Z. Laird, S.M. Geary, A.K. Salem, K. Shin, Effects of calcium concentration on nonviral gene delivery to bone marrow-derived stem cells, Journal of Tissue Engineering and Regenerative Medicine. 13 (2019) 2256–2265. https://doi.org/10.1002/term.2971.

[303] S.-X. Xie, A.A. Baoum, N.A. Alhakamy, C.J. Berkland, Calcium enhances gene expression when using low molecular weight poly-l-lysine delivery vehicles, International Journal of Pharmaceutics. 547 (2018) 274–281. https://doi.org/https://doi.org/10.1016/j.ijpharm.2018.05.067.

[304] R.R. Rao, J. He, J.K. Leach, Biomineralized composite substrates increase gene expression with nonviral delivery, Journal of Biomedical Materials Research Part A. 94A (2010) 344–354. https://doi.org/10.1002/jbm.a.32690.

[305] Z. Zhou, L. Zhang, J. Li, Y. Shi, Z. Wu, H. Zheng, Z. Wang, W. Zhao, H. Pan, Q. Wang, X. Jin, X. Zhang, R. Tang, B. Fu, Polyelectrolyte-calcium Complexes as a Pre-precursor Induce Biomimetic Mineralization of Collagen, Nanoscale. (2020). https://doi.org/10.1039/D0NR05640E.

[306] T. TENKUMO, O. ROTAN, V. SOKOLOVA, M. EPPLE, Protamine Increases Transfection Efficiency and Cell Viability after Transfection with Calcium Phosphate Nanoparticles, Nano Biomedicine. 5 (2013) 64–74. https://doi.org/10.11344/nano.5.64.

[307] X. Wang, S. Masse, G. Laurent, C. Hélary, T. Coradin, Impact of Polyethylenimine Conjugation Mode on the Cell Transfection Efficiency of Silica Nanovectors, Langmuir. 31 (2015) 11078–11085. https://doi.org/10.1021/acs.langmuir.5b02616.

[308] F. Yang, J. Yang D FAU - Tu, Q. Tu J FAU - Zheng, L. Zheng Q FAU - Cai, L. Cai L FAU - Wang, L. Wang, Strontium enhances osteogenic differentiation of mesenchymal stem cells and in vivo bone formation by activating Wnt/catenin signaling., STEM CELLS. 29 (2011) 981–991. 10.1002/stem.646.

[309] T. Gonzalez-Fernandez, B.N. Sathy, C. Hobbs, G.M. Cunniffe, H.O. McCarthy, N.J. Dunne, V. Nicolosi, F.J. O'Brien, D.J. Kelly, Mesenchymal stem cell fate following non-viral gene transfection strongly depends on the choice of delivery vector, Acta Biomaterialia. 55 (2017) 226–238. https://doi.org/https://doi.org/10.1016/j.actbio.2017.03.044.

[310] Y. Li, C. Yang, H. Zhao, S. Qu, X. Li, Y. Li, New Developments of Ti-Based Alloys for Biomedical Applications, Materials (Basel, Switzerland). 7 (2014) 1709–1800. https://doi.org/10.3390/ma7031709.

[311] K. Indira, U.K. Mudali, T. Nishimura, N. Rajendran, A Review on TiO2 Nanotubes: Influence of Anodization Parameters, Formation Mechanism, Properties, Corrosion Behavior, and Biomedical Applications, Journal of Bio- and Tribo-Corrosion. 1 (2015) 28. https://doi.org/10.1007/s40735-015-0024-x.

[312] J. Yun, J. Wu, C. Aparicio, J.K. Hon Tsoi, Y. Wang, A. Fok, Enzyme-Mediated Mineralization of TiO2 Nanotubes Subjected to Different Heat Treatments, Crystal Growth & Design. 19 (2019) 7112–7121. https://doi.org/10.1021/acs.cgd.9b00966.

[313] N.-C. Huang, Q. Ji, T. Yamazaki, W. Nakanishi, N. Hanagata, K. Ariga, S. Hsu, Gene transfer on inorganic/organic hybrid silica nanosheets, Physical Chemistry Chemical Physics. 17 (2015) 25455–25462. https://doi.org/10.1039/C5CP03483C.

[314] P. Pankongadisak, E. Tsekoura, O. Suwantong, H. Uludağ, Electrospun gelatin matrices with bioactive pDNA polyplexes, International Journal of Biological Macromolecules. 149 (2020) 296–308. https://doi.org/https://doi.org/10.1016/j.ijbiomac.2020.01.252.

[315] M. Hellfritzsch, R. Scherließ, Mucosal Vaccination via the Respiratory Tract, Pharmaceutics. 11 (2019) 375. https://doi.org/10.3390/pharmaceutics11080375.

2. Mineralized polyplexes for gene delivery: Improvement of transfection efficiency as a consequence of calcium incubation and not mineralization

2.1 Introduction

Gene therapy is a promising medical technology that uses nucleic acids to engage the cellular transcription and/or translation processes to produce desired proteins. Accordingly, gene therapy can be used for manipulation of gene expression, resulting in control over protein synthesis using the cells' own machinery[1–4]. Such a powerful principle allows for development of treatments for many disease conditions, including cancer[1], infectious diseases[2], tissue injuries[3], and otherwise intractable genetic diseases[4], making gene therapy a highly encouraging field of medicine. As a cell-based therapy, gene therapy can only be effective if the nucleic acid reaches specific cellular sites for efficient treatment[5,6]. This task is accomplished by the association of the nucleic acid with carriers that protect and hold the nucleic outside the cell and, once inside the cell, release the nucleic acid and provide escape mechanisms against cell defenses in the endo-lysosomal compartment[7].

Arguably, one of the struggles in gene therapy concerns the development of highly specialized carriers capable of fitting the envisioned ground-breaking biological applications. There are two main categories of carriers, namely viral and non-viral. Due to effectiveness, viral vectors were the first choice in clinical trials[8]. Viruses naturally evolved to show many of the critical properties desired on an effective gene carrier, allowing the modification of diseased cells by genetic manipulation[8]. However, after the death of a

teenager from an immune reaction in a 1999 clinical trial for treatment of a non-life threatening disease [9], valid safety concerns have been raised, which was intensified after the very recent deaths of two boys in a Phase 2 clinical trial using an adeno-associated virus-8 (AAV8) vector for the treatment of a skeletal muscle disorder[10]. On the other hand, non-viral carriers from synthetic materials are relatively easy and inexpensive to fabricate, and given appropriate materials selection and design, they are safe[11]. However, non-viral vectors have lower transfection efficiency than viral vectors, which stimulated various nanofabrication methods capable of improving the carrier efficiency.

Calcium phosphate (CaP), well known for its osteoconductive properties[12], was one of the first materials used to deliver DNA to cells in culture. The fast co-precipitation with DNA at very high Ca/P ratios was firstly reported in the mid-1970s [13], and it has been widely used since then, mainly due to the simplicity and effectiveness of this method[14–16]. However, due to the lack of control over particle size, the classical co-precipitation method shows poor reproducibility between experiments and very low transfection efficiency compared to viral vectors, mostly being considered for easy-to-transfect cells *in vitro*[14–16]. Arguably, the increasing interest in CaP due to its outstanding role in tissue engineering applications, and the development of new precipitation techniques capable of very high control over particle size, stimulated re-emergence of CaP in gene therapy delivery over the last two decades. New nanofabrication techniques using controlled mineralization to produce hybrid organic-inorganic carriers made CaP a viable option for many *in vivo* applications[17–20]. Among the new technologies employing mineralization, lipid-coated calcium phosphate nanoparticles by microemulsions[21–23], self-assembly of nucleic acid-calcium phosphate/copolymer hybrid

particles[24–26], and mineralization for production of composite nucleic-acid/CaP surfaces for reverse transfection[27–29] are a few notable examples.

It is also reported that viral and non-viral pre-assembled nanoparticles can acquire new properties due to the controlled mineralization with CaP, such as improved resistance to temperature-related degradation[30,31], better adhesion to epithelial tissue and mucosa[32–35], and direct improvement of transfection efficiency of non-viral vectors[36–40]. However, the reason(s) for improvement of transfection efficiency in non-viral vectors is not always clear and if mineralization is indeed required for an increase in transfection efficiency has been debated. The case of DNA coated solid core CaP nanoparticles for nucleic acid delivery is a good example. One group reported the necessity of the precipitation of an external CaP coating layer for improved transfection efficiency by performing a precipitation reaction at the surface of the particle[36,41,42]. In contrast, other groups reported that calcium incubation was enough to improve transfection efficiency[43,44]. This fact was pointed out by Pedraza et al.[43], however, there was never, to our knowledge, a study comparing both techniques.

Recently, we recognized a similar controversial situation regarding the mineralization of polyplexes. Some authors reported improved transfection efficiency through mineralization[39,40]; however, there is an emerging literature reporting similar effects solely with the incubation in water-soluble calcium salts such as $CaCl_2$[45,46]. Considering that calcium salts are obligatorily used as reagents in mineralization reactions, it is very plausible to propose that some of the positive effects reported to come from mineralization can be purely a consequence of calcium incubation, especially considering the fact that in mineralization studies, controls submitted to calcium incubation were never used, at least to our knowledge. Therefore, an open question remains: is mineralization responsible for

achieving high transfection efficiency, or calcium incubation alone is sufficient for this purpose?

Due to inconclusive data on this issue, this study compared the effect of mineralization vs. Ca^{+2} incubation for the pre-assembled particles. We fabricated anionic tri-component polyplexes by self-assembly of pDNA and a lipid-modified polyethylenimine (PEI) followed by coating with poly(aspartic acid) (PAsp). This strategy resulted in polyplexes that allow for efficient interaction with calcium and mineralization due to the presence of PAsp[47–49], and, if efficiently taken up by cells, the PEI should provide an endosomal escape mechanism[50]. Mineralization was performed under low supersaturations by a chemical precipitation method carefully designed to permit easy comparison between calcium incubated and mineralized polyplexes. Additionally, we compared the effects of mineralization and calcium incubation on the physicochemical properties, particle size, and morphology of the polyplexes. Finally, we compared the calcium incubated and mineralized polyplexes in terms of transfection and uptake efficiency using MC3T3-E1 mouse osteoblastic cells *in vitro*.

2.2 Materials and Methods

2.2.1 Materials

The lipid-modified PEI used to make polyplexes was provided by RJH Biosciences (Edmonton, AB) under the trade name ALL-Fect. Poly(aspartic acid) (PAsp) was purchased from Alamanda Polymers (Huntsville, Alabama, US). The gWIZ plasmid (with no protein expression) and Green Fluorescent Protein (GFP)-expressing gWIZ-GFP plasmid were purchased from Aldevron (Fargo, ND). Cy3 used for pDNA labeling was from Mirus

(Madison, WI). The nuclease-free water, Hank's Balanced Salt Solution (HBSS), tissue culture media DMEM and F12, SYBR Green I nucleic acid gel stain, and antibiotic solutions Penicillin and Streptomycin were from Life Technologies (ThermoFisher). NaCl, $CaCl_2$, Na_3PO_4, and HEPES were also purchased from Life Technologies (ThermoFisher).

2.2.2 Particle Fabrication

The polyplexes were fabricated in a two-step incubation method followed by calcium incubation and, for mineralized samples, a reaction with a phosphate salt. The first complexation step consisted of mixing the lipid-modified PEI (ALL-Fect) solution (1 mg/ml) with a pDNA solution (0.4 mg/mL) in sterile water in an Eppendorf tube with the pipette for 15 seconds. After incubation for 30 min, a PAsp solution (1 mg/mL) was added under mixing with the pipette for 15 seconds, followed by another 30 min of incubation. This bulk solution containing coated polyplexes was used to produce all samples. The calcium incubation step was performed by adding the desired volume of a 250 mM $CaCl_2$ solution to the polyplexes, followed by 30 min incubation. Immediately after that, samples had their volume doubled with a 2X HEPES buffer saline (HBS) with a pH of 7.0 without the presence of any phosphate precursor (150 mM NaCl, 50 mM HEPES). For mineralized samples, a similar process was used, however, in this case, the 2X HBS contained Na_3PO_4 to form CaP. Finally, after incubation for 30 minutes for the precipitation reaction to occur, samples were studied. Calcium and phosphate concentrations ranged from 5–20 mM and 0.7–1.9 mM, respectively, depending on the experiment performed. The $CaCl_2$ concentrations chosen result in Ca/P ratios higher than the usual 1.5-1.67 ratios for hydroxyapatite synthesis. These concentrations were chosen as an effort to minimize the time for achieving adsorption of Ca^{2+} onto PAsp by increasing the initial ionic concentration,

which in low Ca^{2+} methods (0.3-2.5 mM) can take up to 12h[40], and to test a wider range of Ca^{2+} concentrations without inducing excessive CaP precipitation. Accordingly, low Na_3PO_4 concentrations were used as an effort to limit the excessive growth of the precipitated inorganic phase. All samples, mineralized or not, were dispersed in 1X HBS (without any source of phosphate, unless mentioned) with pH 7.0 at the end of the preparation method. Two polyplex compositions were submitted to calcium incubation and the mineralization processes, differing only on ALL-Fect concentration during complexation. The final pDNA, PAsp, and ALL-Fect concentrations of the two polyplex compositions submitted to treatment can be found in Table 1.

Table 2-1 Composition of the polyplexes submitted to treatment.

Sample	pDNA (µg/µL)	PAsp (µg/µL)	ALL-Fect (µg/µL)
1	0.0033	0.0066	0.047
2	0.0033	0.0066	0.063

2.2.3 Physicochemical and Morphological Characterization

Hydrodynamic size by dynamic light scattering and zeta potential measurements of polyplexes were assessed using a Zetasizer Nano ZS (Malvern Instruments, UK). The original nanoparticle suspensions dispersed in HBS were diluted to 1 mL in deionized water to increase sample volume and decrease ionic concentration and measured in triplicate. Transmission electron microscopy (TEM) was performed using a Philips/FEI EM208S electron microscope. Samples for TEM were prepared by subsequently dripping and drying the particle suspension over a carbon-coated grid. Particle size distribution was done by analyzing the size of >250 particles with the Fiji-ImageJ software. A Rigaku Ultima IV X-

ray diffraction analyser was used for phase analysis of the mineralized materials. Product from multiple synthesis reactions were accumulated over a glass slide until enough material for intense enough signal was achieved due to the low yield of the synthesis reaction. The samples were analysed between 20 and 50 degrees with a step size of 0.02º and a scan speed of 1.00º/min. Data was converted using the JADE MDI 9.6 software and the DIFFRAC.EVA software with the 2021 ICDD PDF 4+ databases was used for phase identification.

2.2.4 DNA Binding Efficiency

An agarose gel retardation assay was used to assess the stability and unpacking ability of the polyplexes as a consequence of formulation features, $CaCl_2$, and Na_3PO_4 concentration. The samples were loaded in a 0.8% agarose gel in TAE buffer containing SYBR Green I (10 µl) and electrophoresed for 30 min under 100 mV at 0.3 µg of pDNA per well. Samples were also analyzed after incubation with 0.7 µg/µl of heparin, a commonly used agent to dissociate polyplexes [51]. The fluorescent SYBR Green I-DNA complex allows the observation of dislocation of bands in case of pDNA release from particles. Gels were photographed using an Alpha imager HP with SYBR green photographic filter under UV light in complete darkness.

2.2.5 Cell Culture

MC3T3-E1 cells were used to investigate the effect of mineralization and calcium incubation over the polyplexes in transfection efficiency and uptake. Cells were cultured in a flask with Dulbecco's Modified Eagle Medium:F12 medium (DMEM:F12=1:1) with 10% Fetal Bovine Serum (FBS), 0.1% Glutramax-1, 0.1% MEM NEAA, Penicillin (100 U/mL) and Streptomycin (100 µg/mL). The cells were kept in a humidified atmosphere with 95%

air and 5% CO_2 at 37 ºC. Cells were plated into 24-well plates when reaching 75% confluence for transfection experiments.

2.2.6 Flow Cytometry for Cell Uptake and Transfection Efficiency of Polyplexes

In vitro transfection and uptake efficiency of the calcium incubated and mineralized polyplexes in preosteoblastic MC3T3-E1 cells was assessed using an Attune NxT Flow Cytometer (Thermo Fisher Scientific, US). This cell line was chosen since mineralized polyplexes is ideal for use on gene therapy efforts on mineralized tissues. In both types of experiments, cells were seeded in 24-well plates, and after ~50% confluence was reached, they were treated with different types of particles in HBS (unmodified, calcium incubated, and mineralized polyplexes) by addition of a volume of the suspension to reach 0.25 μg of pDNA per well. Transfection efficiency was quantified after 48 h according to the positive population and median fluorescence intensity (MFI) due to green fluorescent protein (GFP) expression using a gWIZ-GFP expression vector under the CMV promoter. The uptake efficiency through the positive population and MFI was measured after overnight incubation using Cy3-labeled pDNA without protein expression. In either case, fluorescence imaging was used as an additional characterization tool. Samples for flow cytometry were prepared by trypsinization and neutralization in complete culture medium with 10% FBS, fixation with a formaldehyde solution in the cold for 20 min, and final suspension in PBS, with appropriate washing in-between steps by suspension in PBS and centrifugation. Calcium incubated samples were used as positive controls for the mineralized samples with the same $CaCl_2$ concentration to evaluate the effect of different concentrations of Na_3PO_4 in a multicolumn analysis, while pDNA in HBS and unmodified polyplexes were used as untreated controls.

2.2.7 Statistical Analysis

Experiments were performed independently (n=3) and results represented as means ± standard deviation. The means of different groups were compared using one-way ANOVA followed by a Tukey-Kramer test. Means were considered significantly different when $p<0.05$.

2.3 Results

2.3.1 Binding and Dissociation of Polyplexes.

The binding efficiency and heparin-induced dissociation of the polyplexes at different stages of the fabrication process (before and after PAsp coating, after $CaCl_2$ incubation, and after mineralization) were evaluated through an electrophoretic gel mobility assay (Figure 2.1). The polyanion heparin was used for dissociating polycation/DNA polyplexes by competitive binding[51,52] that permits evaluation of the robustness of the particles after mineralization or calcium incubation. For a specific sample, a visible fluorescent band shift such as the one found in the pDNA control means pDNA is released from the particle, since the SYBR Green I dye binds specific to pDNA and forms a fluorescent complex. By comparing band shifts from mineralized and unmineralized samples with same composition, it is possible to infer about robustness gained by mineralization against heparin dissociation. Species with lower negative charge/mass ratio will experience less shift towards the positive pole of the applied current. Therefore, less shifted bands (in comparison to the pDNA control) are likely resultant of incomplete polyplex dissociation, as the resultant species will be less charged and have more mass than the free pDNA.

In Figure 2.1(a), the results for the polyplexes fabricated with 0.047 μg/μl ALL-Fect (pDNA:ALL-Fect ratio of 1:7) during complexation without heparin incubation are shown. At this polycation concentration, the pDNA showed complete binding. However, when the PAsp is added as a coating to the polyplexes (0 mM $CaCl_2$), incomplete pDNA binding was evident due to presence of free pDNA on the gels, observed as a fluorescent band shift.

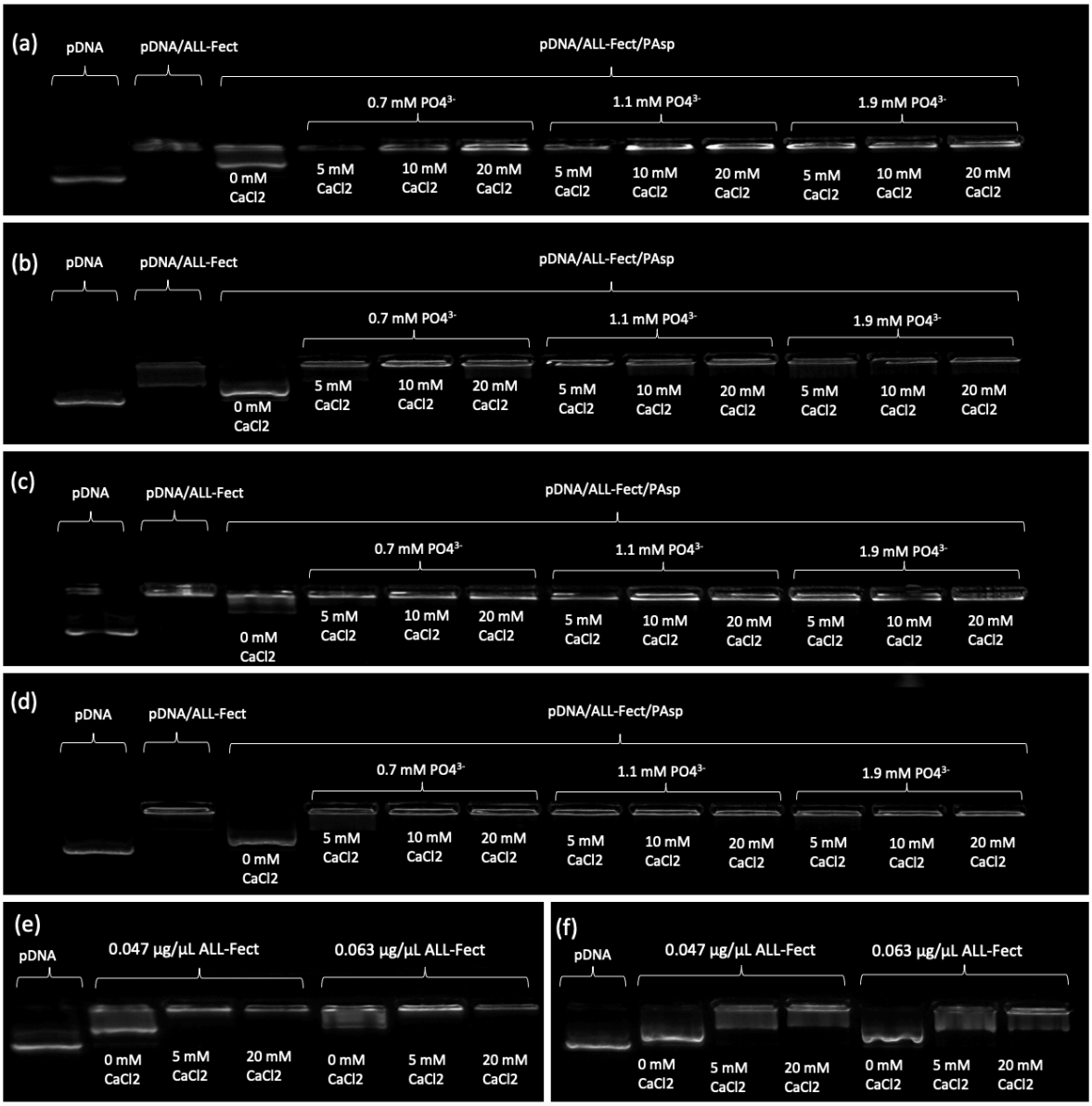

Figure 2.1 Electrophoretic gel mobility assay for mineralized and unmineralized samples at various $CaCl_2$ and Na_3PO_4 concentrations. (a) Electrophoretic gel mobility assay for mineralized samples with the final concentration of 0.047 µg/µL ALL-Fect. (b) Electrophoretic gel mobility assay for mineralized samples with the final concentration of 0.047 µg/µL ALL-Fect after incubation with heparin for 1 h. (c) Electrophoretic gel

mobility assay for mineralized samples with the final concentration of 0.063 µg/µL ALL-Fect. (d) Electrophoretic gel mobility assay for mineralized samples with the final concentration of 0.063 µg/µL ALL-Fect after incubation with heparin for 1 h. (e) Electrophoretic gel mobility assay for calcium incubated samples. (f) Electrophoretic gel mobility assay for calcium incubated samples after incubation with heparin for 1h.

Mineralization with 5, 10 and, 20 mM $CaCl_2$ and 0.7, 1.1, and 1.9 mM Na_3PO_4 generated a stabilizing effect over the PAsp coated polyplexes since no dissociated pDNA was observed even at the lowest concentration of the ions used (5 mM $CaCl_2$ and 0.7 mM Na_3PO_4). Figure 2.1(b) shows the heparin-induced dissociation for same samples used in Figure 2.1(a). The presence of heparin did not affect the band observed for the pDNA control but the polyplexes underwent partial dissociation, which was evident by a free pDNA band. The PAsp coated polyplexes, on the other hand, were completely dissociated by heparin. The mineralization reaction provided no pDNA dissociation since no free pDNA band was observed for any of the mineralized samples.

Figures 2.1(c) and Fig 2.1(d) show polyplex samples prepared with an increased concentration of ALL-Fect (0.063 μg/μL, pDNA;ALL-Fect ratio of 1:10) without and with heparin incubation, respectively. While the polyplexes with PAsp again showed incomplete binding, heparin incubation resulted in a complete dissociation band comparable to that of free pDNA (Figure 2.1 (d)). Similar to the mineralized polyplexes with lower polycation content, mineralized samples showed increased binding of pDNA, with no indication of pDNA release after heparin incubation.

To differentiate the effects of Ca^{2+} interaction with polyplexes vs. mineralization, we performed gel electrophoresis of samples that were Ca^{2+} incubated with and without heparin-induced dissociation. Figure 2.1(e) shows the effect of $CaCl_2$ incubation without the additional step of Na_3PO_4 addition for the PAsp coated polyplexes with the ALL-Fect

concentrations of 0.047 and 0.063 μg/μL at 5 and 20 mM $CaCl_2$. Figure 2.1(f) shows the same samples submitted to the heparin-induced dissociation assay. The presence of $CaCl_2$ resulted in increased polyplex formation, indicating complete binding induced by $CaCl_2$ incubation. Different from the mineralized samples, Ca^{2+} incubated samples showed dissociation induced by the heparin; however, the pDNA bands are weaker than those observed in pDNA, and PAsp coated polyplex without $CaCl_2$, indicating only partial unpacking of the Ca^{2+} incubated polyplexes.

2.3.2 Particle Hydrodynamic Size and Zeta-potential Analysis

The effects of each particle fabrication step on hydrodynamic size, PDI and ζ-potential with 0.047 μg/μL and 0.063 μg/μL ALL-Fect are shown in Figure 2.2. The Ca^{+2} incubated samples were prepared with 10 mM $CaCl_2$, while the mineralized samples were prepared with the same $CaCl_2$ concentration and 1.1 mM Na_3PO_4. At 0.047 μg/μL (Figures 2.2 (a), (b), and (c)), the uncoated polyplexes show a hydrodynamic size of ~200 nm, PDI of 0.2, and ζ-potential of +10 mV. With the addition of the PAsp coating, there is a considerable increase in size (~3-fold) and PDI (~2-fold), as well as a shift of the ζ-potential to highly negative values (-55 mV). The $CaCl_2$ incubation caused a drastic increase in particle size to the micrometer range (~1360 nm), a PDI increase to ~0.4, and recovery of ζ-potential to close to neutral values (+5 mV). Mineralization resulted in non-significant size and PDI variations; however, ζ-potential shifted to negative value (-15 mV). At 0.063 μg/μL (Figures 2.2 (d), (e), and (f)), the uncoated polyplexes showed a hydrodynamic size of ~150 nm, PDI of ~0.1, and ζ-potential of +19 mV. Coating by PAsp did not significantly change the hydrodynamic particle size or PDI; however, the ζ-potential shifted to -34 mV. $CaCl_2$ incubation resulted in considerable particle size (~770 nm) and PDI increase (~0.2), as well as a recovery of the ζ-potential to values closer to the neutrality (-10 mV). The mineralization process further increased the hydrodynamic particle size, reaching the micrometer range (~1118 nm), with no significant variation in PDI, while the ζ-potential decreased to -19 mV.

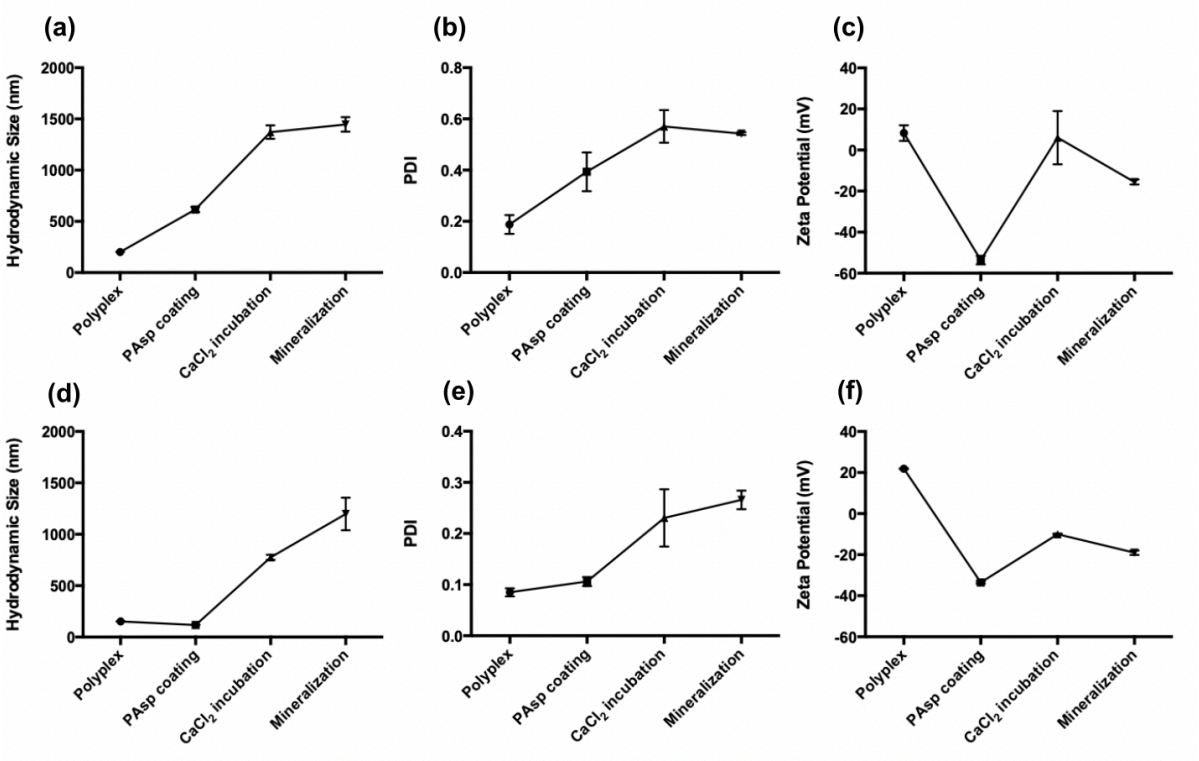

Figure 2.2 Hydrodynamic size, PDI and z-potential after each step of the particle fabrication process. (a) Hydrodynamic size, (b) PDI, and (c) z-potential after polyplex formation, PAsp coating, $CaCl_2$ incubation and mineralization at 0.047 µg/µL ALL-Fect. (d) Hydrodynamic size, (e) PDI, and (f) z-potential after polyplex formation, PAsp coating, $CaCl_2$ incubation and Mineralization at 0.063 µg/µL ALL-Fect.

2.3.3 Particle Morphology Analysis

The TEM images of the PAsp coated polyplexes before and after Ca^{+2} incubation and mineralization can be observed in Figures 2.3 (0.047 µg/µL ALL-Fect) and 2.4 (0.063 µg/µL ALL-Fect). The samples were fabricated following the same conditions as the samples used for hydrodynamic size analysis in Figure 2.2. The PAsp coated polyplexes with lower ALL-Fect concentration were composed of spherical diffuse particles with considerable

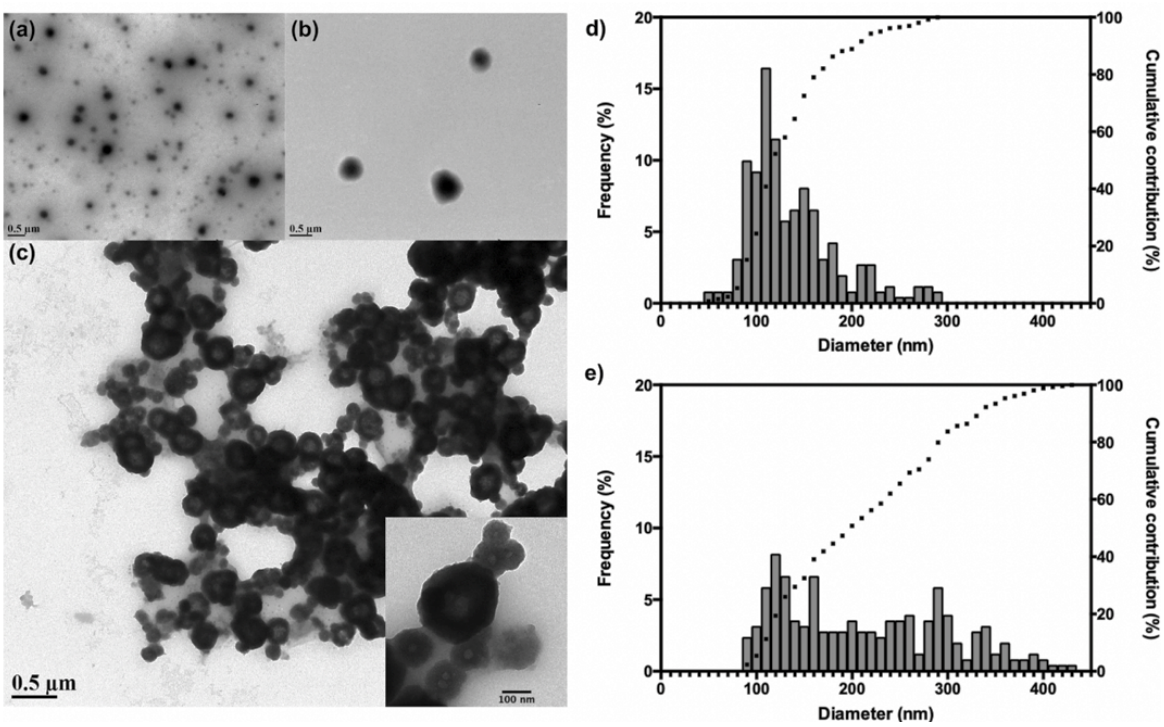

Figure 2.3 TEM images of (a)PAsp coated polyplexes, (b) CaCl2 incubated, PAsp coated polyplexes. and (c) mineralized PAsp coated polyplexes at ALL-Fect concentration of 0.047µg/µL. Size distribution diagram for PAsp coated polyplexes (d), and (e) mineralized PAsp coated polyplexes.

polydispersity, with submicron and nano-sized particles (Figure 2.3(a)), with the latter forming the most considerable portion of the sample. However, there was a considerable number of a submicron particles with sizes that reached up to ~300 nm. With incubation in 10 mM $CaCl_2$ (Figure 2.3(b)), less diffuse sub-micron particles were seen compared to the Ca^{+2}-free sample, probably due to the calcium interaction with the carboxylic groups of PAsp[48]. Figure 2.3(c) shows the mineralized polyplexes; the particles maintained their spherical shape, but a distinct heterogeneous morphology was present, observed as dark rings around a lighter core. Considerably polydispersity was evident with agglomeration and possibly some degree of aggregation, which might have been exasperated due to the drying process during sample preparation. While the shell-core morphology was readily evident on

larger particles at lower magnification, the same morphology was also present in smaller particles at high magnification, which is observed in the right lower corner of Figure 2.3(c).

Figures 2.3(d) and 2.3(e) show the particle size distribution obtained from TEM images of the polyplexes before and after mineralization, respectively. Before mineralization, the PAsp coated polyplexes presented ~25% of its population of particles with sizes up to 100 nm, 50% of the population with sizes up to 120 nm, and 90% of the sample is contained within the 200 nm limit. The distribution of particles peaked at 100 to 110 nm (16.5%). The mineralized sample showed an overall increase in particle size, with the disappearance of smaller particles (< 80 nm) and appearance of particles larger than 400 nm. Approximately 25% of its population was constituted by particles with sizes up to 130 nm, 50% by particles with sizes up to 200 nm, and 90% by particles with sizes up to 330 nm. The population of mineralized polyplexes has a maximum at 120 to 130 nm (8.1 %) and the particle size distribution is considerably homogeneous over the whole range of sizes.

With higher ALL-Fect concentration, the untreated polyplexes presented similar morphology to those in the sample with lower ALL-Fect concentration (Figure 2.4(a)). However, particles were smaller, reaching up to ~200 nm, and had more homogeneous size distribution in addition to the presence of fibrous structures. The calcium incubated sample showed considerable increase in size with the presence 200 nm plus particles, as well as agglomerates that reached ~400 nm in diameter (Figure 2.4(b). In this sample, nanoparticles (<100 nm) were only observed as part of agglomerates that were bigger than 200 nm. The mineralized sample showed a heterogeneous morphology consisting of multiple nuclei inside the mineralized matrix of spherical particles that were mostly smaller than 100 nm and agglomerated (Figure 2.4(c)). There was also presence of irregular particles that looked

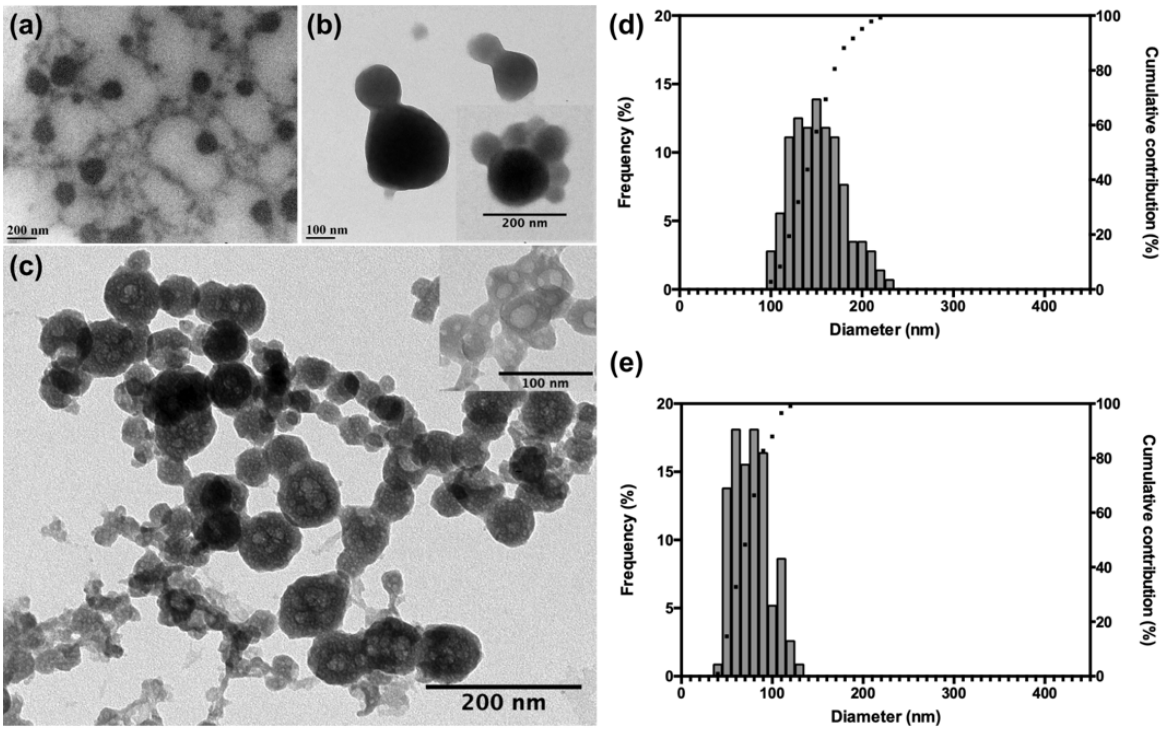

Figure 2.4 TEM images of (a) PAsp coated polyplexes, (b) $CaCl_2$ incubated, PAsp coated polyplexes. and (c) mineralized PAsp coated polyplexes at ALL-Fect concentration of 0.063 µg/µL. Size distribution diagram for PAsp coated polyplexes (d), and (e) mineralized PAsp coated polyplexes.

looked amorphous and aggregated (4(c), top right). Before mineralization (Figure 2.4(d)), 25% of the population was bellow ~130 nm, 50% was bellow 150 nm, and 90% of particles found were bellow 200 nm, reaching up to 230 nm in diameter (Figure 2.4(d). Mineralization resulted in considerable reduction of maximum particle size to (130 nm) and drastically increased in the presence of nanometric particles (~90%), with 50% of particles bellow 70 nm.

2.3.4 Particle Phase Analysis

Figure 2.5 shows the diffractogram of the mineralized polyplexes with same concentrations used for TEM (10 mM $CaCl_2$, 1.1 mM Na_3PO_4). The X-ray diffraction pattern of the mineralized sample shows weak peaks, with the presence of the (210) and (102) peaks

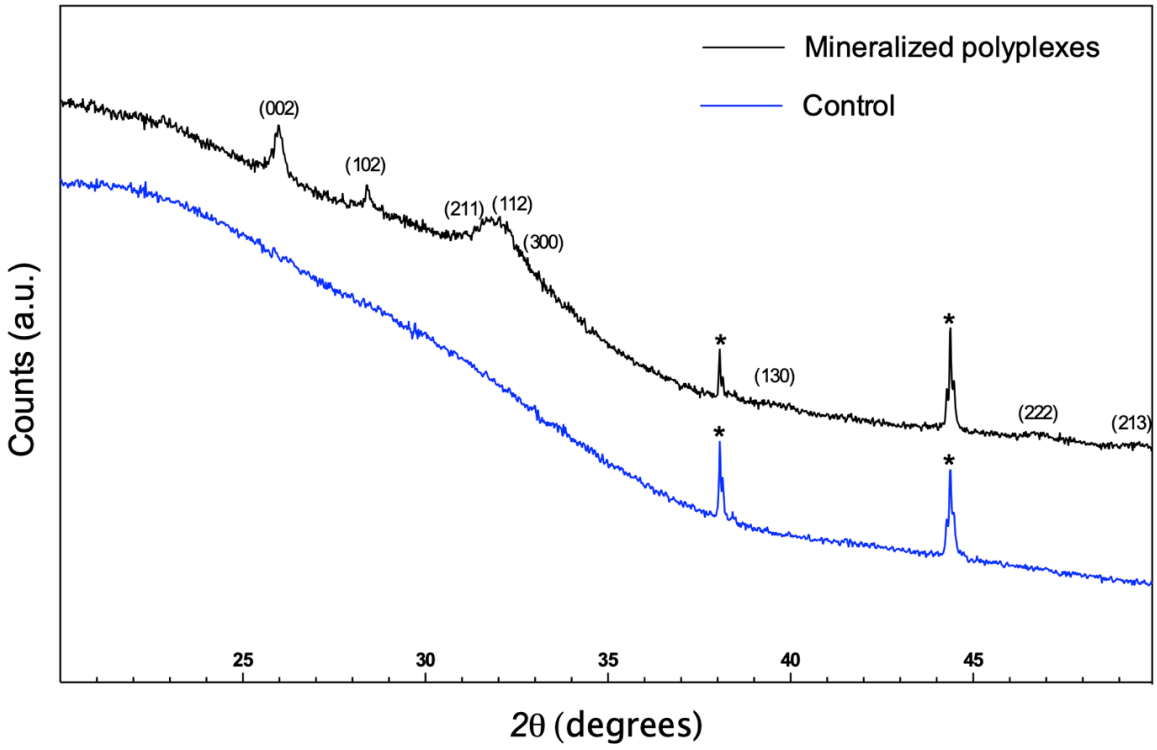

*Figure 2.5 X-ray diffraction analysis of the mineralized polyplexes and the control (precipitation reaction without polyplexes) at 10 mM $CaCl_2$ and 1.1 Na_3PO_4. Peaks relative to the substrate are indicated with *.*

in addition to the overlapping of the (211), (112) and (300) peaks. The (130), (222) and (213) peaks are also present, but they are extremely weak. The diffraction pattern is characteristic of hydroxyapatite with no presence of other crystallographic phases. The sample synthesized with same ionic composition without the presence of polyplexes shows a large amorphous band without the presence of intense peaks. Peaks from the analysis of the blank (glass substrate over an Al_2O_3 sample holder) are also indicated in Figure 2.5.

2.3.5 Transfection Efficiency

Figures 2.6 and 2.7 show the transfection efficiency of the mineralized and Ca^{+2} incubated polyplexes with 0.043 μg/μL and 0.067 μg/μL ALL-Fect, respectively, using MC3T3-E1 mouse osteoblastic cells. The effect of various concentrations of Ca^{2+} and PO_4^{3-}

on the transfection efficiency of polyplexes was assessed by the level of GFP expression as the GFP-positive population and mean fluorescent intensity (MFI) of each group. The free pGFP and untreated polyplexes (PAsp coated and uncoated) were used as controls, while PAsp coated polyplexes were incubated with Ca^{+2} at 5, 10 and 20 mM. The latter groups were compared with other mineralized samples with the same Ca^{2+} content and 0.7, 1.1, and 1.9 mM PO_4^{3-}. Due to excess Ca^{2+}, the increase in PO_4^{3-} concentration from 0.7 to 1.9 mM was expected to increase the amount of precipitated material. All mineralized samples from Figure 2.1 that showed increased robustness were considered as successfully mineralized and were utilized for the transfection efficiency studies (Figures 2.6(b) and 2.7(b)).

For both polycation contents (Figures 2.6(a) and 2.7(a)), PAsp coating lowered the transfection efficiency of polyplexes to levels comparable to that of free pGFP. However, transfection efficiency was drastically increased by incubation with $CaCl_2$. This increase was a lot more prominent for the samples with higher polycation content (~3-fold in GFP-positive population and 2-fold in MFI). Additionally, the Ca^{+2} incubated samples did not show a significant difference in transfection efficiency among each other, showing that a saturation was reached at $CaCl_2$ concentrations of 5 mM without any hinderance beyond this value. For most mineralized samples, a variation in transfection efficiency was observed both in the GFP-positive population and the MFI. No specific trend in transfection efficiency was evident as a consequence of phosphate increase across different Ca^{+2} concentrations. Depending on the Ca^{+2} and PO_4^{3-} concentrations, mineralization showed either no positive or negative effect (at low Ca^{+2} concentration) on transfection efficiency.

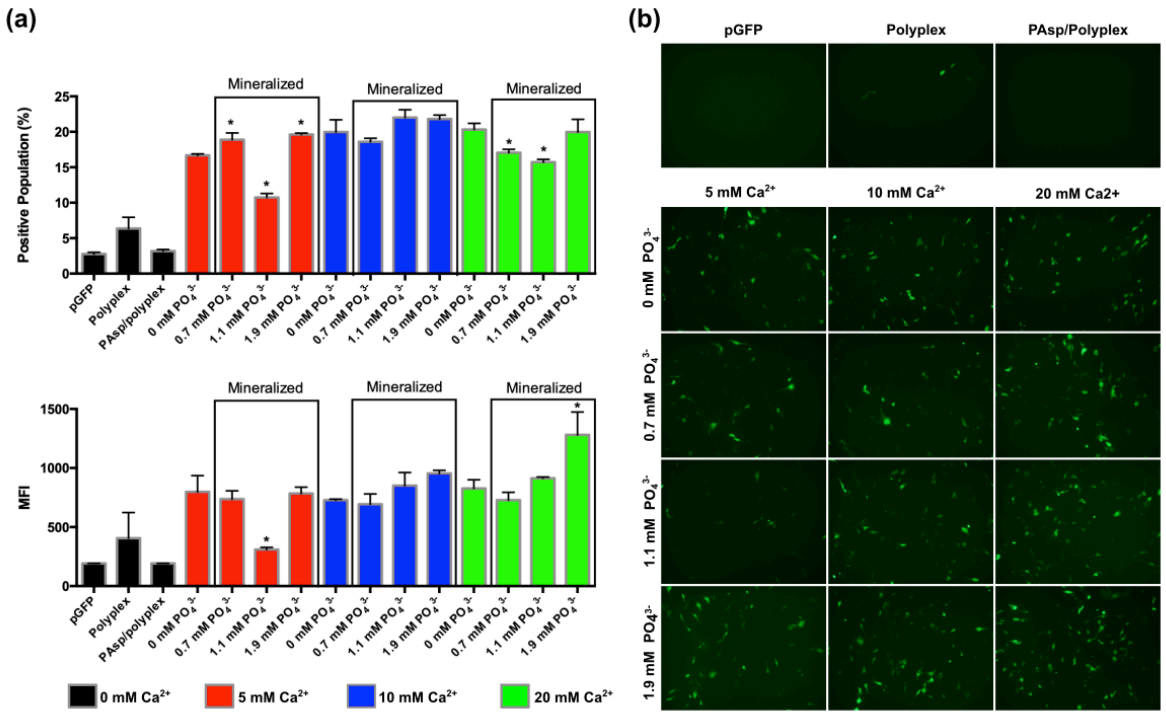

*Figure 2.6 Transfection efficiency of $CaCl_2$ incubated and mineralized polyplexes carrying pDNA encoding for GFP: (a) GFP-positive population and median fluorescence intensity of MC3T3-E1 cells transfected. (b) Fluorescence images from MC3T3-E1 cells with different Ca^{2+} and PO_4^{3-} contents. *p<0.05 compared with calcium incubated sample (0 mM $PO4^{3-}$) with same calcium concentration.*

The cellular uptake of various polyplexes is shown in Figure 2.8. The polyplexes were prepared with various $CaCl_2$ (5, 10, and 20 mM Ca^{2+}) and Na_3PO_4 (0.7, and 1.1 mM PO_4^{3-}) concentrations and uptake was based on pDNA-positive cell population (top) and MFI (bottom) using Cy3-labeled pDNA. The results showed that the free Cy3-labeled pDNA could not be taken up by cells without a carrier. The coating of polyplexes with PAsp resulted in a considerable lowering of the percentage of cells that took up polyplexes, however, for both samples, the resultant MFI was comparable to that of free pDNA under the experimental conditions. All samples containing calcium ($CaCl_2$ incubated or mineralized) showed close to 100% positive population; however, MFI varied slightly from sample to sample. Similar

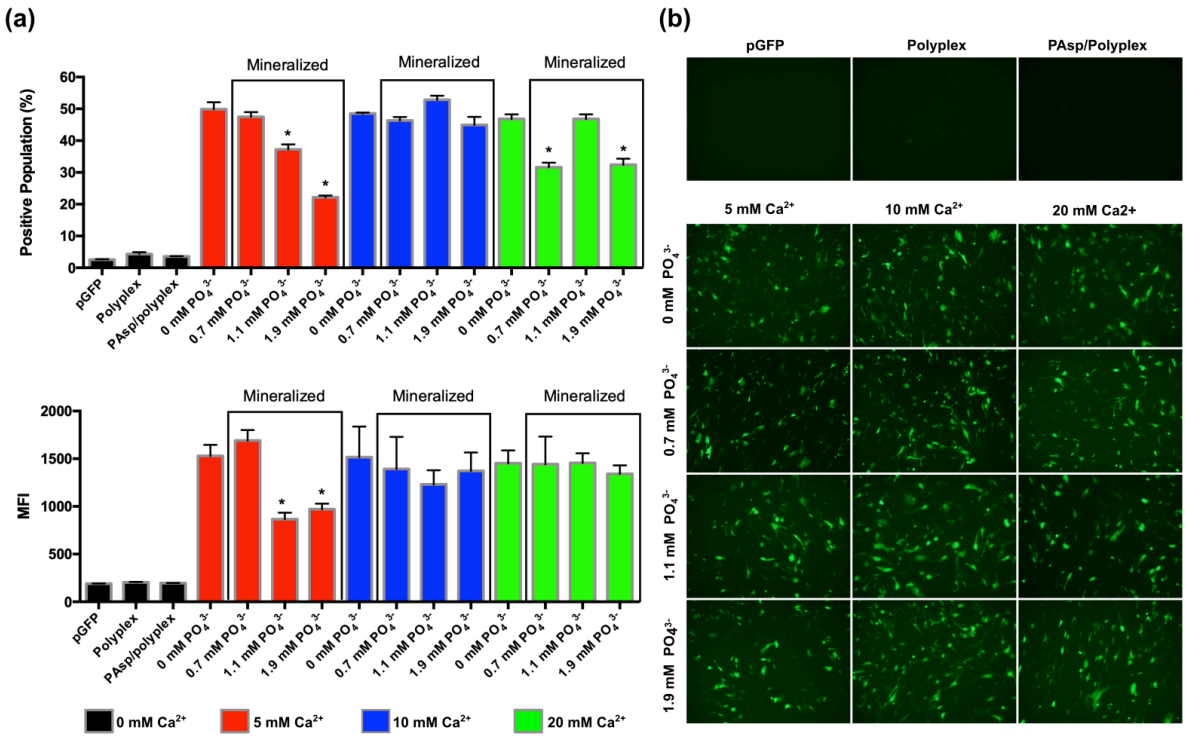

*Figure 2.7 Transfection efficiency of $CaCl_2$ incubated and mineralized polyplexes carrying pDNA encoding for GFP: (a) GFP-positive population and median fluorescence intensity of MC3T3-E1 cells transfected. (b) Fluorescence images from MC3T3-E1 cells with various Ca^{2+} and PO_4^{3-} contents. *p<0.05 compared with calcium incubated sample (0 mM $PO4^{3-}$) with same calcium concentration.*

to the transfection efficiency, the uptake did not significantly vary with the increase in Ca^{+2} concentration for non-mineralized samples. Uptake appeared to be slightly increased by mineralization, which was observed at every Ca^{+2} concentration depending on PO_4^{3-} concentration.

Figure 2.9 shows the transfection efficiency at days 4 and 9 using PAsp coated polyplexes mineralized at 5 mM $CaCl_2$ and 0.7 and 1.1 Na_3PO_4. These samples were chosen due to the possibility of inducing high and low transfection efficiency by the precipitation reaction at the same and Ca^{+2} concentration. Mineralized samples were less effective in

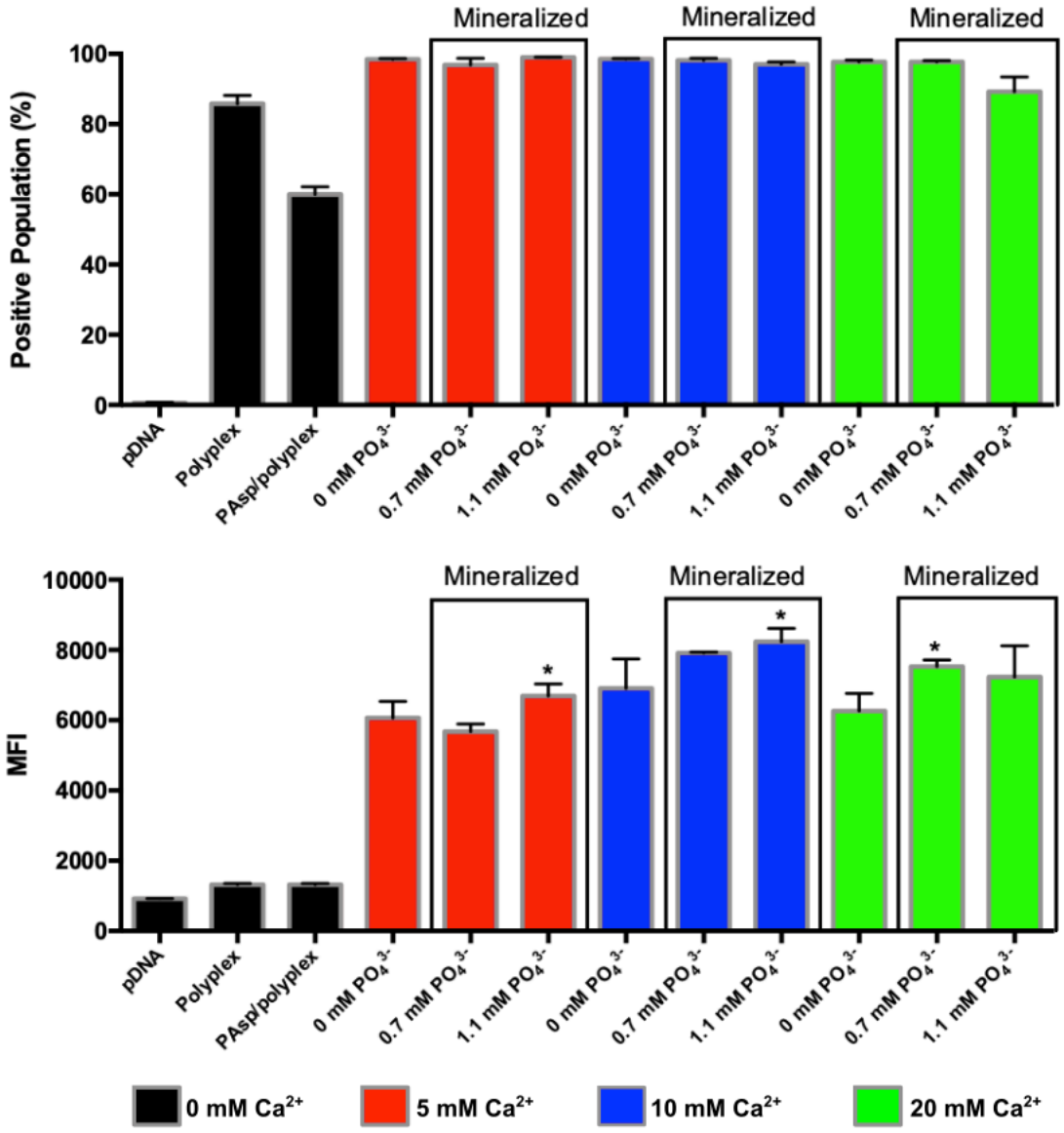

*Figure 2.8 Uptake of $CaCl_2$ incubated and mineralized polyplexes carrying Cy3-labeled pDNA: (a) Cy3-positive population and (b) MFI of transfected MC3T3-E1 cells. *p<05 compared with calcium incubated sample (0 mM $PO4^{3-}$) with same calcium concentration.*

transfecting the cells on days 4 and 9, and the transfection efficiency of the samples was significantly reduced on day 9, indicating that mineralization was not capable of sustaining expression. The experiment was not continued for more extended periods due to the significant decrease in transfection efficiency after 9 days.

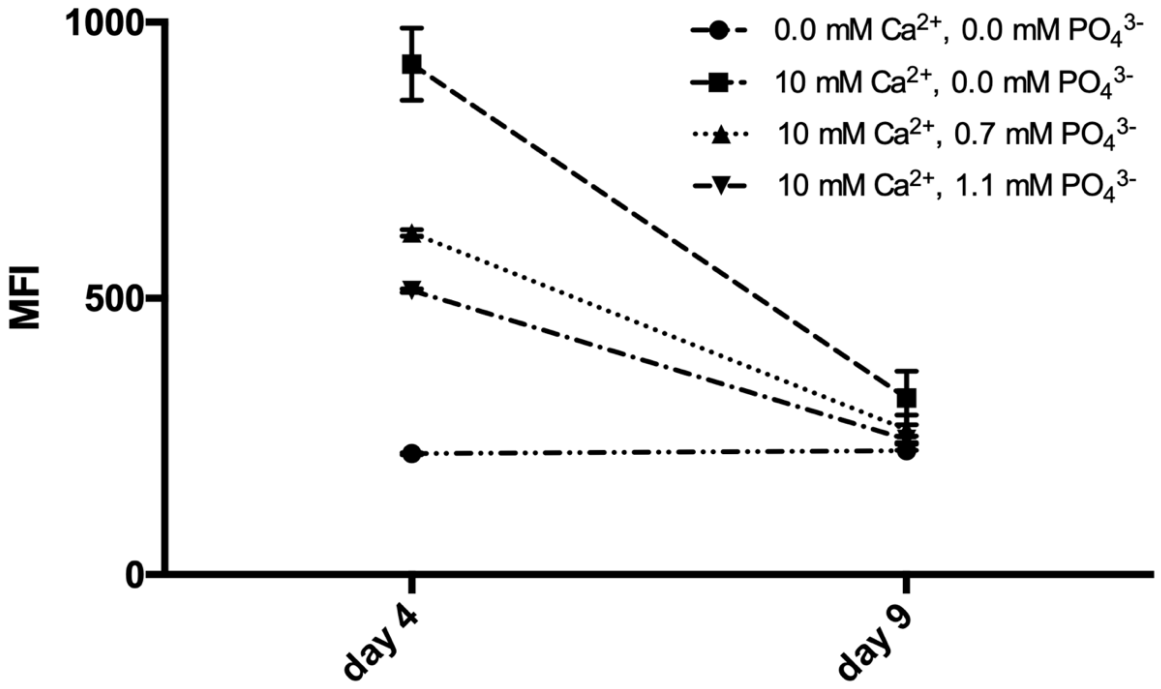

Figure 2.9 GFP transfection efficiency (MFI) at days 4 and 9 of unmineralized negatively charged polyplexes, calcium incubated polyplexes and mineralized polyplexes in MC3T3-E1 cells.

2.4 Discussion

Mineralization is a relatively simple process that can effectively be used to coat materials and render new properties. Particles, more specifically, are frequently used in applications demanding the intracellular delivery of therapeutic molecules. For a particle to efficiently cross biological barriers, mineralization must be performed with particular attention to parameters that control the growth of the mineral phase. Providing nucleation sites that thermodynamically favor heterogeneous nucleation allows nucleation to occur at low supersaturations, limiting uncontrolled mineral growth by lowering the availability of species after nucleation [53,54]. In practice, this is done by modifying the surface of particles with negatively charged functionalities that strongly interact with Ca^{+2} ions, lowering the energy barrier for nucleation and generating pre-nucleation polyelectrolyte/Ca^{2+} polyplexes

[48,55]. Polyplexes formed by complexation between cationic polymers and anionic nucleic acids might demand alternative strategies for mineralization since these must be anionic to allow mineralization. The polycationic content might be necessary for generating sufficient electrostatic attraction towards the anionic cell membrane, and once inside the cell, to escape the endo-lysosomal system and effectively reach the cytoplasm for RNA interference, or nucleus for gene expression [7,56]. We tried to circumvent this dilemma in the pDNA delivery to MC3T3-E1 mouse osteoblasts by first generating a positively charged core with an excess of the polycationic content and then adding a polyanion coating, capable of creating the necessary conditions for mineralization.

The first step in our study consisted in designing polyplexes susceptible to mineralization. This was accomplished by coating cationic polyplexes with the polyanion PAsp, whose electrostatic adsorption was readily observed by the shift in ζ-potential from positive to highly negative values (Figures 2.2(c) and (f)). We expected a given PAsp macromolecule to either adhere to the cationic polyplex to form anionic tricomponent polyplex, or, in the case of saturation, partially stay in the free form in solution. From the gel mobility assay, however, it appears that pDNA might be also present in solution as a consequence of the competition between PAsp and pDNA for PEI portion of ALL-Fect[57]. The free pDNA was less present at the higher transfection reagent concentration of 0.063 μg/μL (ALL-Fect:pDNA=10) than at the lower concentration of 0.047 μg/μL (ALL-Fect:pDNA=7.5) (Figure 2.1 (c)), which is likely a consequence of improved pDNA binding with more available ALL-fect. Also, the increase in particle size and PDI at lower PAsp amount might be indicative of particle structural rearrangement with unknown structure (PAsp could be either present as a coating or at the interior of the particle) and overall

negative surface charge. With higher polycation content, particles appear to be more stable (Figure 2.1 (c) and (d)), and therefore resistant to the to the loosening effect of PAsp, which might be responsible for the low PDI. Moreover, increased availability of the cationic content of the polyplex might result in a tightly attached PAsp layer, resulting in a less significant size change.

The choice of PAsp as a nucleator comes from the fact that aspartic acid residues are essential components in the mineral-regulating properties of proteins involved in bone formation, such as osteopontin[58]. PAsp is thought to act similarly to natural mineralizing proteins, stimulating nucleation when inserted onto a surface or inhibiting nucleation when in solution [49,59]. This ability to control growth makes PAsp an interesting choice for our particle system, favoring heterogeneous nucleation (precipitation of CaP as a coating) over homogeneous nucleation (CaP precipitation in solution)[60]. We opted for a convenient CaP precipitation protocol for the mineralization, adapted from Antonetti et al.[61], in which a $CaCl_2$ incubation step allows for increased Ca^{2+}/polyanion interaction before the reaction with Na_3PO_4. In comparison to the possibility of using metastable mineralizing solutions such as simulated body fluid[40], this two-step process allows for experimentation with a broader range of supersaturations since there is no need to reach a metastable state in which Ca^{+2} and PO_4^{-3} are present at the same time in solution. Also, this process can be more time-efficient compared to the mineralization using simulated body fluid, which in some cases can take up to 12 h [40]. Our protocol required 1 hour for mineralization after polyplex formation. Incubation time is a concern when working with polyplexes because of the change of properties during storage, which can frequently decrease the transfection efficiency [62].

The Ca^{2+} incubation step increased the particle size that was accompanied by an increase in PDI and ζ–potential to closer to neutral values (Figures 2.2(c) and (f)). This increase in size might be due to neutralization of the negative charges of the carboxylic acid by Ca^{2+}, affecting electrostatic stabilization, and/or collapsing of the PAsp layer at the particle surface, affecting steric stabilization[63], both being essential components involved in polyelectrolyte stabilization of nanoparticles. Ca^{2+}/PAsp interaction also seemed to be critical for better packaging of pDNA in the polyplexes (Figure 2.1e); Ca^{2+} can react with two carboxylic acid moieties from the same or different PAsp chains, generating physical crosslinks to increase polyplex integrity[64]. The same effect was not observed when Na^{+} was present and Ca^{2+} was absent (all samples were suspended in a 150 mM saline HEPES buffer, including controls), which is in agreement with reports from others[64]. The presence of Ca^{2+} might also result in decreased competition between PAsp and pDNA for the cationic portion of All-Fect[65]. However, when anionic heparin was present, competition for cationic components was still enough to promote partial dissociation of the polyplexes (Figure 2.1(f)).

Mineralization made the polyplexes resistant to heparin-induced dissociation, as expected. The change in ζ-potential observed at the mineralization step is another confirmation of Ca^{+2}/PO_4^{-3} condensation (Figure 2.2). Our results contrast with the findings of a study that reported the mineralization of polyplexes to reduce pDNA binding[39]. However, in that report, the polyplexes were cationic and did not contain the anionic functionalities needed for inducing mineralization[39]. Additionally, TEM images provided by the authors do not show particles with a contrast between the organic and inorganic phase, such as the observations on mineralized organic particles in other reports[55,66,67] or our TEM

images. It is well documented that while cationic surfaces can adsorb Ca/P particles homogeneously nucleated, they cannot effectively induce mineralization[68]. Others that performed the mineralization of anionic polyplexes in SBF also reported an increase in resistance to dissociation after mineralization; however, TEM was not performed for characterization of their mineralized shell[40]. In either case[39,40], Ca^{+2} incubated controls with the same Ca^{+2} concentration as mineralized samples were not reported.

Many intracellular applications might benefit from the robustness achieved through mineralization. Calcium phosphate or carbonate layers increase the robustness of polymeric micelles, avoiding drug leakage until the intracellular environment is reached [67,69–73]. The increased robustness proportioned by CaP was also used to drastically increase the encapsulation efficiency of hydrophilic drugs and nucleic acids by poly(D,L-co-glicolide)(PLGA) in a microemulsion method[74]. Since calcium-based minerals are acid labile and pH is low inside the endo-lysosome compartment, mineralization should not hinder the premature release of the drug[67,69–73]. Interestingly, it is proposed that viruses benefit from natural mineralized shells to survive off-body and increase infectivity between species, primarily through airways, taking benefit from improved robustness and adhesive properties and stealth capabilities from calcium-based minerals[30,75,76]. More importantly, biomimetics of this principle appears to translate into therapeutic applications using viral particles [20,30,31,33–35,77].

The TEM analysis of the particles mineralized with 10 mM $CaCl_2$ and 1.1 mM Na_3PO_4 shows morphologies characteristic of heterogeneous materials for both ALL-Fect compositions analysed. At 0.047 $\mu g/\mu L$ ALL-Fect the presence of dark rings around a lighter core gives strong evidence of a core-shell nanoarchitecture[66,78], with CaP coating the

polyplexes with a continuous spherical shell. The shell-core morphology is seen in particles of all ranges of sizes, which is an indication that both big and small particles are anionic and capable of undergoing mineralization. In most particles with this composition, the mineral layer represented 2/3 of the total particle diameter, which is an indication that mineralization at lower concentrations than 10 mM $CaCl_2$ and 1.1 Na_3PO_4 might be preferable for this polyplex composition and mineralization method. With an increase in ALL-Fect content to 0.063 μg/μL, the resultant morphology was also heterogeneous. Although, particles were considerably smaller and presented several cores per particle, which resulted in a granular morphology. It is not clear if more cores per particle result from more polyplexes per particle or simply a different organization of the mineral phase over a single polyplex. Particles with 0.063 μg/μL ALL-Fect also showed thinner mineral layers probably because of the smaller particle diameter and, accordingly, increased number of particles and a larger mineralizable area for the same calcium and phosphate supersaturations.

Interestingly, the sample with 0.063 μg/μL ALL-Fect showed a smaller single particle average size after mineralization (~70 nm compared to ~150 nm before treatment). This might be due to the shrinking of the soft polymeric organic core due to mineralization with a controlled growth of the mineral phase. Interestingly, a substantial size decrease and similar granular morphology were reported by other authors for the mineralization of hyaluronic acid nanoparticles[55]. To our knowledge, our work is the first to report the morphology of mineralized polyplexes.

By comparing the particle size analysis of mineralized samples by TEM to the hydrodynamic size by DLS, we conclude that agglomeration is responsible for the diameters measured that were, in both cases, greater than 1 μM. This might cause the collapsing of

the PAsp layer by the complexation with Ca^{2+} and neutralization of charges by ions in solution [63]. Accordingly, it could be beneficial to develop a synthesis reaction without using a saline buffer to control pH.

The X-ray diffraction pattern in Figure 2.5 is similar to that of a biological hydroxyapatite, with considerable peak broadening due to the amorphous quality of the sample, the inelastic scattering due to the small crystallite size and the equipment contribution[79] (Figure 2.5). The overlapping of the (211), (112) and (300) peaks is frequently observed for hydroxyapatite synthesized in the presence of organic templates[79,80]. The powder sample prepared without the presence of the PAsp-coated polyplexes shows a large amorphous band, and no recognizable crystallographic peaks. The difference between the two samples is an indication that PAsp is attached to the polyplexes and had an important role in promoting nucleation of hydroxyapatite. However, this assumption would have to be confirmed by a more in-depth crystallographic study of the samples. In this regard, cryoTEM of the nanoparticles would allow for recognition of crystalline spots on the nanoparticles with minimal influence of aging and drying of the particles [96]. Figure 2.10 summarizes our interpretation of the possible mechanisms involved in particle fabrication, as well as the final nanostructure.

Our results from transfection efficiency using Ca^{+2} incubated samples as controls led us to draw different conclusions from other authors regarding the role of mineralization in polyplexes. The Ca^{+2} treatment (5 to 20 mM $CaCl_2$) was sufficient to achieve high gene expression; however, the additional step of mineralization did not have a clear effect in improving transfection efficiency. Most mineralized groups were not significantly different from Ca^{+2} incubated controls regarding transfection efficiency, and the ones that showed

higher or lower significant values do not seem to follow any specific trend related to supersaturation levels. On the other hand, the polycation content was a critical factor for improving the transfection efficiency if $CaCl_2$ was present, which could be a consequence

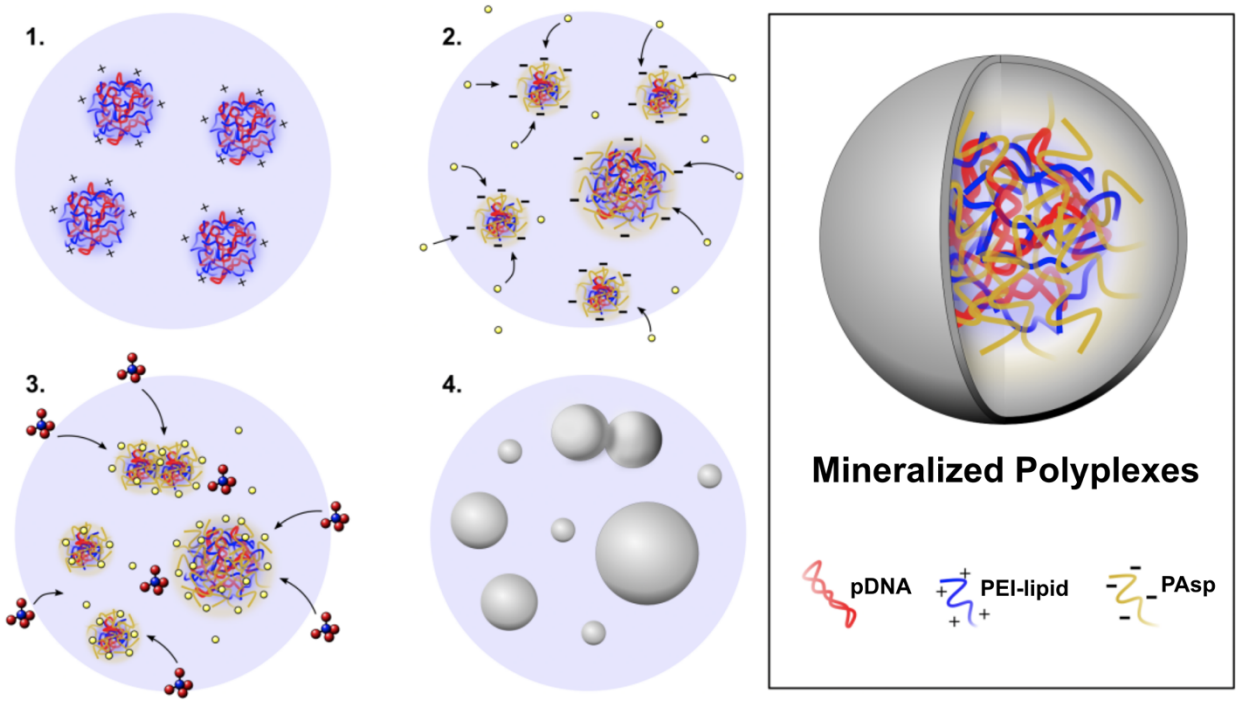

Figure 2.10 Steps leading to final structure of mineralized polyplexes: 1 – Positively charged polyplexes are formed by complexation of pDNA and the cationic PEI; 2 – Coating polyplexes with PAsp changes zeta-potential to negative, preparing particles to interact with Ca^{2+}, and leads to particle rearrangement and increase in PDI; 3 – Interaction with Ca^{2+} neutralizes part of the negative charges leading to aggregation of particles and increase in size and PDI, and concentration of Ca^{2+} around the particles ensures PAsp associated precipitation; 4 – Ionic reaction with PO_4^{3-} leads to calcium phosphate precipitation in association with the PAsp layer, increased negative surface charge and aggregation. The resulting morphology is schematically represented in the right.

of the increased efficiency of the escape mechanism proportioned by the modified PEI. The samples with lower PEI content benefited from high concentrations of $CaCl_2$, which is interesting considering that higher supersaturations will likely result in more mineral growth. Therefore, it might be useful to study the effect of higher calcium and phosphate concentrations in more detail for the highly negative polyplexes.

It is important to note that without comparing Ca^{+2} incubated to that of mineralized samples, one may misleadingly conclude that mineralization is the main factor contributing to transfection. Additionally, transfection with Ca^{+2} incubated polyplexes appears to be more reproducible across different concentrations of Ca^{2+}. The occurrence of nucleation and growth of the new CaP phase may cause variability in transfection efficiency and depend on many reaction parameters, such as reactants mixing rate, stirring mode and Ca/P ratio[81]. Uptake efficiency seems to be slightly favored by mineralization (Figure 2.8). However, we failed to achieve sustained transient transfection efficiency with mineralized samples after 9 days of incubation of the MC3T3-E1 cells. Ito et al. described prolongation of transient transfection efficiency with mineralized DNA/PEI/hyaluronic acid polyplexes for up to two weeks; however, they performed a different protocol for complexation, in which pDNA and hyaluronic acid were mixed before the addition of PEI for complexation and mineralization was performed by incubation in 1.5xSBF overnight in cold[40]. Chen et al. also mention a prolonged transfection effect in positively charged polyplexes in the presence of CaP[39]. Since none of the authors used calcium only incubated controls, it is impossible to know if the prolonged transfection effect could have been achieved with calcium incubation alone.

Changes observed in our polyplexes properties due to Ca^{+2} incubation include (i) rearrangement of polyplexes into larger agglomerated structures, (ii) increase in polyplex robustness, and (iii) change in ζ-potential from highly negative to near neutral values. With mineralization, the larger structures seem to be preserved, robustness is gained to the point of no dissociation under heparin incubation, and ζ-potential becomes more negative. While uptake by particles is commonly proposed to be highly favored by positive ζ-potentials[82,83], it seems that for our system, the negatively charged mineralized particles can be taken up as

efficiently. Other authors also found that negatively charged calcium phosphate particles can undergo efficient transfection efficiency in MC3T3-E1 cells[84] and other cell lines[18]. Regarding particle size, most authors report better results in uptake efficiency with small particles, with the frequently reported result of ~50 nm as the optimal result for particle uptake due to more favorable energetics for cell membrane folding and particle penetration[7]. However, large particle size does not necessarily inhibit uptake when other particle features are modified, such as shape[85]. Moreover, for the specific case of transfection efficiency using PEI, there are reports of complexation protocols that lead to increased transfection efficiency *in vitro* and *in vivo* by inducing drastic increases in size reaching close to, or more than 1 μm and changes in internal structure weaker binding to DNA[86,87].

Other authors that used PEI/pDNA positively charged polyplexes without adding polyanions found that Ca^{+2} incubation generated increased transfection efficiency due to decreased pDNA binding strength as a result of competition between the Ca^{2+} and PEI for the pDNA cargo[45,46]. In our system, Ca^{+2} helped to reach a more favorable pDNA binding by doing the opposite, i.e. an increase of binding strength, as previously discussed (Figure 2.1). It is possible that cationic polyplexes submitted to mineralization achieved high transfection efficiencies in other studies because of excess Ca^{2+} in solution after or during mineralization and not mineralization itself. However, the lack of Ca^{+2} treated polyplexes in these studies creates an ambiguity in the obtained outcomes and necessitates the use of Ca^{+2} incubation as a standard control in assessing mineralized polyplexes. It is important to note that most cell culture media have $CaCl_2$ and NaCl, which could be responsible for size increase and agglomeration, as shown here. Polyplexes were reported to rapidly increase

their size when incubated in cell culture media, which led to increases in transfection efficiency[87]. In our previous work, we achieved high transfection efficiency with the polyplexes described here when the complexation was made in cell culture medium[88,89]. It was proposed by other authors that the calcium and phosphate content from media was shown to be capable of interacting with nanoparticles and react to form a mineralized layer around particles if pH was basic and particles were negatively charged[90]. These are important considerations, as the surface chemistry can affect cell uptake mechanism[91,92]. Furthermore, it is common to prepare polyplexes in cell culture media and, in many cases, authors could be experiencing benefits from calcium incubation without knowing.

The benefits of mineralization on polyplex mediated gene delivery are yet to be understood entirely. It seems that mineralization can at least proportionate the same benefits as Ca^{+2} incubation if reaction parameters are optimized; however, if transfection improvement is desired for *in vitro* applications, a simple Ca^{+2} incubation step might be sufficient, as shown here. We did not study other possible benefits from performing mineralization. However, the properties explored by others in the development of therapeutic applications with mineralized virus particles *in vivo*, such as the increase in resistance to degradation during storage and increased adhesion to the mucosa in the airways[30–33] looks promising and could be applied to polyplexes. We theorize that polyplexes in applications undergoing harsh physical conditions or benefiting from mucosa adhesion might benefit from mineralization. Bone applications using gene therapy might also be of interest, especially considering the role of mineralized materials on reverse transfection[93–95]. However, future studies should rely on the measurements of pDNA binding, convincing

particle morphology characterization, and appropriate controls to separate benefits coming from mineralization and calcium interaction.

2.5 Conclusions

In this study, we report the fabrication and properties of mineralized PAsp coated polyplexes, as well as the effect of mineralization on transfection efficiency. The use of calcium incubated controls with the same $CaCl_2$ concentrations as the mineralized groups in this study was motivated by contradictory reports that do not allow for differentiation between the effects of mineralization or simply ionic incubation. To our knowledge, our study is the first to introduce this practice. We found that mineralization positively affects the transfection efficiency in MC3T3-E1 cells; however, this effect could be easily reproduced with a simple calcium incubation step, including particle size increase, improved pDNA binding, and adjustment of ζ-potential to less-negative values. Considering the unclear effect of mineralization in transfection efficiency and increased preparation time, we conclude that improvement of transfection efficiency through mineralization is not superior to calcium incubation. We emphasize that when exploring mineralization of polyplexes and possibly other types of particles, it is crucial to report controls submitted to calcium incubation to avoid misinterpretation of cause-and-effect relationships, and not overestimate the effects of mineralization on the transfection.

2.6 References

[1] M. H. Amer, *Molecular and Cellular Therapies* **2014**, *2*, 27.

[2] J. K. W. Lam, M. Y. T. Chow, Y. Zhang, S. W. S. Leung, *Molecular therapy. Nucleic acids* **2015**, *4*, e252.

[3] E. R. Balmayor, M. van Griensven, *Frontiers in Bioengineering and Biotechnology* **2015**, *3*, 9.

[4] A. Shahryari, M. Saghaeian Jazi, S. Mohammadi, H. Razavi Nikoo, Z. Nazari, E. S. Hosseini, I. Burtscher, S. J. Mowla, H. Lickert, *Frontiers in Genetics* **2019**, *10*, 868.

[5] J. D. Larsen, N. L. Ross, M. O. Sullivan, *The Journal of Gene Medicine* **2012**, *14*, 580.

[6] J. Slone, T. Huang, *npj Genomic Medicine* **2020**, *5*, 7.

[7] S. Behzadi, V. Serpooshan, W. Tao, M. A. Hamaly, M. Y. Alkawareek, E. C. Dreaden, D. Brown, A. M. Alkilany, O. C. Farokhzad, M. Mahmoudi, *Chemical Society Reviews* **2017**, *46*, 4218.

[8] K. Lundstrom, *Diseases (Basel, Switzerland)* **2018**, *6*, 42.

[9] S. E. Raper, N. Chirmule, F. S. Lee, N. A. Wivel, A. Bagg, G. Gao, J. M. Wilson, M. L. Batshaw, *Molecular Genetics and Metabolism* **2003**, *80*, 148.

[10] *Nature Biotechnology* **2020**, *38*, 910.

[11] C. L. Hardee, L. M. Arévalo-Soliz, B. D. Hornstein, L. Zechiedrich, *Genes* **2017**, *8*, 65.

[12] H. H. K. Xu, P. Wang, L. Wang, C. Bao, Q. Chen, M. D. Weir, L. C. Chow, L. Zhao, X. Zhou, M. A. Reynolds, *Bone Research* **2017**, *5*, 17056.

[13] F. L. Graham, A. J. van der Eb, *Virology* **1973**, *52*, 456.

[14] M. Jordan, A. Schallhorn, F. M. Wurm, *Nucleic Acids Research* **1996**, *24*, 596.

[15] D. Olton, J. Li, M. E. Wilson, T. Rogers, J. Close, L. Huang, P. N. Kumta, C. Sfeir, *Biomaterials* **2007**, *28*, 1267.

[16] L. Guo, L. Wang, R. Yang, R. Feng, Z. Li, X. Zhou, Z. Dong, G. Ghartey-Kwansah, M. Xu, M. Nishi, Q. Zhang, W. Isaacs, J. Ma, X. Xu, *Saudi Journal of Biological Sciences* **2017**, *24*, 622.

[17] J. Li, Y. Yang, L. Huang, *Journal of Controlled Release* **2012**, *158*, 108.

[18] S. Bisso, S. Mura, B. Castagner, P. Couvreur, J.-C. Leroux, *bioRxiv* **2019**, 621102.

[19] F. Pittella, K. Miyata, Y. Maeda, T. Suma, S. Watanabe, Q. Chen, R. J. Christie, K. Osada, N. Nishiyama, K. Kataoka, *Journal of Controlled Release* **2012**, *161*, 868.

[20] J. Chen, P. Gao, S. Yuan, R. Li, A. Ni, L. Chu, L. Ding, Y. Sun, X.-Y. Liu, Y. Duan, *ACS Nano* **2016**, *10*, 11548.

[21] J. Tang, C. B. Howard, S. M. Mahler, K. J. Thurecht, L. Huang, Z. P. Xu, *Nanoscale*

2018, *10*, 4258.

[22] Y. Wu, W. Gu, L. Li, C. Chen, Z. P. Xu, *Nanomaterials* **2019**, *9*, DOI 10.3390/nano9020159.

[23] K.-W. Huang, Y.-T. Lai, G.-J. Chern, S.-F. Huang, C.-L. Tsai, Y.-C. Sung, C.-C. Chiang, P.-B. Hwang, T.-L. Ho, R.-L. Huang, T.-Y. Shiue, Y. Chen, S.-K. Wang, *Biomacromolecules* **2018**, *19*, 2330.

[24] L. J. de Mello, G. R. R. Souza, E. Winter, A. H. Silva, F. Pittella, T. B. Creczynski-Pasa, *Nanotechnology* **2017**, *28*, 175101.

[25] M. S. Lee, J. E. Lee, E. Byun, N. W. Kim, K. Lee, H. Lee, S. J. Sim, D. S. Lee, J. H. Jeong, *Journal of Controlled Release* **2014**, *192*, 122.

[26] Y. Maeda, F. Pittella, T. Nomoto, H. Takemoto, N. Nishiyama, K. Miyata, K. Kataoka, *Macromolecular Rapid Communications* **2014**, *35*, 1211.

[27] L. N. Luong, K. M. McFalls, D. H. Kohn, *Biomaterials* **2009**, *30*, 6996.

[28] Y. Yazaki, A. Oyane, H. Tsurushima, H. Araki, Y. Sogo, A. Ito, A. Yamazaki, *Colloids and Surfaces B: Biointerfaces* **2014**, *122*, 465.

[29] B. Sun, K. K. Tran, H. Shen, *Biomaterials* **2009**, *30*, 6386.

[30] X. Wang, X. Liu, Y. Xiao, H. Hao, Y. Zhang, R. Tang, *Chemistry – A European Journal* **2018**, *24*, 11518.

[31] G. Wang, R.-Y. Cao, R. Chen, L. Mo, J.-F. Han, X. Wang, X. Xu, T. Jiang, Y.-Q. Deng, K. Lyu, S.-Y. Zhu, E.-D. Qin, R. Tang, C.-F. Qin, *Proceedings of the National Academy of Sciences* **2013**, *110*, 7619 LP.

[32] T. Sakoda, N. Kasahara, L. Kedes, M. Ohyanagi, *Experimental and clinical cardiology* **2007**, *12*, 133.

[33] X. Wang, D. Yang, S. Li, X. Xu, C.-F. Qin, R. Tang, *Biomaterials* **2016**, *106*, 286.

[34] Y.-W. Yang, C.-K. Chao, *The Journal of Gene Medicine* **2003**, *5*, 417.

[35] A. Fasbender, J. H. Lee, R. W. Walters, T. O. Moninger, J. Zabner, M. J. Welsh, *The Journal of Clinical Investigation* **1998**, *102*, 184.

[36] B. Neuhaus, B. Tosun, O. Rotan, A. Frede, A. M. Westendorf, M. Epple, *RSC Advances* **2016**, *6*, 18102.

[37] Y.-H. Lee, H.-C. Wu, C.-W. Yeh, C.-H. Kuan, H.-T. Liao, H.-C. Hsu, J.-C. Tsai, J.-S. Sun, T.-W. Wang, *Acta Biomaterialia* **2017**, *63*, 210.

[38] T. TENKUMO, O. ROTAN, V. SOKOLOVA, M. EPPLE, *Nano Biomedicine* **2013**, *5*,

64.

[39] P. Chen, Y. Liu, J. Zhao, X. Pang, P. Zhang, X. Hou, P. Chen, C. He, Z. Wang, Z. Chen, *Biomaterials Science* **2018**, *6*, 633.

[40] T. Ito, Y. Koyama, M. Otsuka, *Journal of Pharmaceutical Sciences* **2014**, *103*, 179.

[41] V. V Sokolova, I. Radtke, R. Heumann, M. Epple, *Biomaterials* **2006**, *27*, 3147.

[42] V. Sokolova, S. Neumann, A. Kovtun, S. Chernousova, R. Heumann, M. Epple, *Journal of Materials Science* **2010**, *45*, 4952.

[43] C. E. Pedraza, D. C. Bassett, M. D. McKee, V. Nelea, U. Gbureck, J. E. Barralet, *Biomaterials* **2008**, *29*, 3384.

[44] F. Bakan, G. Kara, M. Cokol Cakmak, M. Cokol, E. B. Denkbas, *Colloids and Surfaces B: Biointerfaces* **2017**, *158*, 175.

[45] S.-X. Xie, A. A. Baoum, N. A. Alhakamy, C. J. Berkland, *International Journal of Pharmaceutics* **2018**, *547*, 274.

[46] V. S. S. A. Ayyadevara, K.-H. Roh, *Drug Delivery* **2020**, *27*, 805.

[47] S. J. Lee, K. H. Min, H. J. Lee, A. N. Koo, H. P. Rim, B. J. Jeon, S. Y. Jeong, J. S. Heo, S. C. Lee, *Biomacromolecules* **2011**, *12*, 1224.

[48] Z. Zhou, L. Zhang, J. Li, Y. Shi, Z. Wu, H. Zheng, Z. Wang, W. Zhao, H. Pan, Q. Wang, X. Jin, X. Zhang, R. Tang, B. Fu, *Nanoscale* **2020**, DOI 10.1039/D0NR05640E.

[49] B. D. Quan, E. D. Sone, *Journal of the Royal Society, Interface* **2018**, *15*, 20180269.

[50] L. M. P. Vermeulen, S. C. De Smedt, K. Remaut, K. Braeckmans, *European Journal of Pharmaceutics and Biopharmaceutics* **2018**, *129*, 184.

[51] J. P. Clamme, J. Azoulay, Y. Mély, *Biophysical journal* **2003**, *84*, 1960.

[52] Z. Chen, Y. He, L. Zhang, Y. Li, *Journal of Materials Chemistry B* **2015**, *3*, 225.

[53] P. J. M. Smeets, A. R. Finney, W. J. E. M. Habraken, F. Nudelman, H. Friedrich, J. Laven, J. J. De Yoreo, P. M. Rodger, N. A. J. M. Sommerdijk, *Proceedings of the National Academy of Sciences* **2017**, *114*, E7882 LP.

[54] S. Karthika, T. K. Radhakrishnan, P. Kalaichelvi, *Crystal Growth & Design* **2016**, *16*, 6663.

[55] S.-Y. Han, H. S. Han, S. C. Lee, Y. M. Kang, I.-S. Kim, J. H. Park, *Journal of Materials Chemistry* **2011**, *21*, 7996.

[56] U. Lungwitz, M. Breunig, T. Blunk, A. Göpferich, *European Journal of Pharmaceutics*

and Biopharmaceutics **2005**, *60*, 247.

[57] P. L. Ma, M. Lavertu, F. M. Winnik, M. D. Buschmann, *Carbohydrate Polymers* **2017**, *176*, 167.

[58] K. M. Zurick, C. Qin, M. T. Bernards, *Journal of Biomedical Materials Research Part A* **2013**, *101A*, 1571.

[59] B. Cantaert, E. Beniash, F. C. Meldrum, *Journal of Materials Chemistry B* **2013**, *1*, 6586.

[60] X. Y. Liu, in (Eds.: K. Sato, Y. Furukawa, K.B.T.-A. in C.G.R. Nakajima), Elsevier Science B.V., Amsterdam, **2001**, pp. 42–61.

[61] M. Antonietti, M. Breulmann, C. G. Göltner, H. Cölfen, K. K. W. Wong, D. Walsh, S. Mann, *Chemistry – A European Journal* **1998**, *4*, 2493.

[62] Y. Sang, K. Xie, Y. Mu, Y. Lei, B. Zhang, S. Xiong, Y. Chen, N. Qi, *Cytotechnology* **2015**, *67*, 67.

[63] R. J. Nap, S. H. Park, I. Szleifer, *Soft Matter* **2018**, *14*, 2365.

[64] K. Huber, *The Journal of Physical Chemistry* **1993**, *97*, 9825.

[65] C. David, E. Companys, J. Galceran, J. L. Garcés, F. Mas, C. Rey-Castro, J. Salvador, J. Puy, *The Journal of Physical Chemistry B* **2007**, *111*, 10421.

[66] K. H. Min, H. J. Lee, K. Kim, I. C. Kwon, S. Y. Jeong, S. C. Lee, *Biomaterials* **2012**, *33*, 5788.

[67] B. Deng, M. Xia, J. Qian, R. Li, L. Li, J. Shen, G. Li, Y. Xie, *Molecular Pharmaceutics* **2017**, *14*, 1938.

[68] M. Tanahashi, T. Matsuda, *Journal of Biomedical Materials Research* **1997**, *34*, 305.

[69] Z. Wang, L. Wang, N. Prabhakar, Y. Xing, J. M. Rosenholm, J. Zhang, K. Cai, *Acta Biomaterialia* **2019**, *86*, 416.

[70] Y. Lv, H. Huang, B. Yang, H. Liu, Y. Li, J. Wang, *Carbohydrate Polymers* **2014**, *111*, 101.

[71] H. J. Lee, S. E. Kim, I. K. Kwon, C. Park, C. Kim, J. Yang, S. C. Lee, *Chemical Communications* **2010**, *46*, 377.

[72] B. J. Kim, K. H. Min, G. H. Hwang, H. J. Lee, S. Y. Jeong, E.-C. Kim, S. C. Lee, *Macromolecular Research* **2015**, *23*, 111.

[73] H. S. Han, J. Lee, H. R. Kim, S. Y. Chae, M. Kim, G. Saravanakumar, H. Y. Yoon, D. G. You, H. Ko, K. Kim, I. C. Kwon, J. C. Park, J. H. Park, *Journal of Controlled*

Release **2013**, *168*, 105.

[74] G. Dördelmann, D. Kozlova, S. Karczewski, R. Lizio, S. Knauer, M. Epple, *Journal of Materials Chemistry B* **2014**, *2*, 7250.

[75] H. Zhou, X. Wang, R. Tang, *Future Virology* **2018**, *13*, 79.

[76] H. Zhou, G. Wang, X. Wang, Z. Song, R. Tang, *Angewandte Chemie International Edition* **2017**, *56*, 12908.

[77] X. Wang, Y. Deng, S. Li, G. Wang, E. Qin, X. Xu, R. Tang, C. Qin, *Advanced Healthcare Materials* **2012**, *1*, 443.

[78] X. Zhou, X. Cheng, W. Feng, K. Qiu, L. Chen, W. Nie, Z. Yin, X. Mo, H. Wang, C. He, *Dalton Transactions* **2014**, *43*, 11834.

[79] S. M. Londoño-Restrepo, R. Jeronimo-Cruz, B. M. Millán-Malo, E. M. Rivera-Muñoz, M. E. Rodriguez-García, *Scientific Reports* **2019**, *9*, 5915.

[80] T. A. Dick, L. A. dos Santos, *Materials Science and Engineering C* **2017**, *77*, 874.

[81] D. Lee, K. Upadhye, P. N. Kumta, *Materials Science and Engineering: B* **2012**, *177*, 289.

[82] R. R. Arvizo, O. R. Miranda, M. A. Thompson, C. M. Pabelick, R. Bhattacharya, J. D. Robertson, V. M. Rotello, Y. S. Prakash, P. Mukherjee, *Nano Letters* **2010**, *10*, 2543.

[83] E. Fröhlich, *International journal of nanomedicine* **2012**, *7*, 5577.

[84] M. A. Khan, V. M. Wu, S. Ghosh, V. Uskoković, *Journal of Colloid and Interface Science* **2016**, *471*, 48.

[85] S. E. A. Gratton, P. A. Ropp, P. D. Pohlhaus, J. C. Luft, V. J. Madden, M. E. Napier, J. M. DeSimone, *Proceedings of the National Academy of Sciences* **2008**, *105*, 11613 LP.

[86] W. Zhang, X. Kang, B. Yuan, H. Wang, T. Zhang, M. Shi, Z. Zheng, Y. Zhang, C. Peng, X. Fan, H. Yang, Y. Shen, Y. Huang, *Theranostics* **2019**, *9*, 1580.

[87] D. Pezzoli, E. Giupponi, D. Mantovani, G. Candiani, *Scientific Reports* **2017**, *7*, 44134.

[88] P. Pankongadisak, E. Tsekoura, O. Suwantong, H. Uludağ, *International Journal of Biological Macromolecules* **2020**, *149*, 296.

[89] E. K. Tsekoura, T. Dick, P. Pankongadisak, D. Graf, Y. Boluk, H. Uludağ, *Pharmaceuticals* **2021**, *14*, 666.

[90] M. Ilett, O. Matar, F. Bamiduro, S. Sanchez-Segado, R. Brydson, A. Brown, N. Hondow, *Scientific Reports* **2020**, *10*, 5278.

[91] V. Francia, K. Yang, S. Deville, C. Reker-Smit, I. Nelissen, A. Salvati, *ACS nano* **2019**, *13*, 11107.

[92] A. Salvati, A. S. Pitek, M. P. Monopoli, K. Prapainop, F. B. Bombelli, D. R. Hristov, P. M. Kelly, C. Åberg, E. Mahon, K. A. Dawson, *Nature Nanotechnology* **2013**, *8*, 137.

[93] Y. Yazaki, A. Oyane, H. Tsurushima, H. Araki, Y. Sogo, A. Ito, A. Yamazaki, *Journal of Biomaterials Applications* **2013**, *28*, 937.

[94] Y. Yazaki, A. Oyane, Y. Sogo, A. Ito, A. Yamazaki, H. Tsurushima, *Biomaterials* **2011**, *32*, 4896.

[95] A. Oyane, Y. Yazaki, H. Araki, Y. Sogo, A. Ito, A. Yamazaki, H. Tsurushima, *Journal of Materials Science: Materials in Medicine* **2012**, *23*, 1011.

[96] A. Lotsari, A.K. Rajasekharan, M. Halvarsson, M. Andersson, Transformation of amorphous calcium phosphate to bone-like apatite, Nature Communications. 9 (2018) 4170. https://doi.org/10.1038/s41467-018-06570-x.

3. A Polyplex in a Shell: The Effect of Poly(aspartic acid)-Mediated Calcium Carbonate Mineralization on Polyplexes Properties and Transfection Efficiency

3.1 Introduction

After the early tragedies in gene therapy clinical trials and the recognition of the dangers viral vectors, non-viral gene carriers gained increased attention as a safer treatment option[1,2]. Development of non-viral vectors, however, constantly faces the challenge of creating engineered particles that can compete with viral vectors in their high transfection efficiency. It is no surprise that viral vectors are so efficient in transfecting the human cells: they are therapeutic variants of the natural viruses, selected by the nature since the eons to efficiently infect – and transfect– cells[3]. Accepting this natural advantage is perhaps the first step into creating non-viral virus inspired technologies.

One evolutionary advantage that could have given viruses a better environmental tolerance and infectivity is the capacity to self-mineralize[4–6]. Negatively charged protein domains of some viruses allow them to self-mineralize under naturally occurring supersaturated conditions[5,7]. The robust egg-like mineralized virus can spread over longer distances in a host-independent pathway and survive outside the host cell due to better

resistance to environmental factors until it reaches a host[4,6,8]. When reaching a host, many advantages may also be conferred due to mineralization, such as improved adhesion to nasal mucosal tissue and ablation of immune recognition which, for example, could have been an important factor in the interspecies infection by the influenza virus[9,10].

Many of the advantages mineralization provides to viral infection have been shown to be translatable into highly beneficial therapeutic technologies using viruses. In vitro mineralization seems to confer a collection of properties such as improved thermostability[11], increased cell adhesion and transfection[12–14], the possibility of alternative cell uptake pathways[15], modulation of immunological response[16] and increased systemic circulation time and tumor accumulation[17]. A thoughtful analysis of the body of literature reveals that these physical and biological properties are material specific, allowing any viral biological interaction to happen only inside the cell once the mineral layer is dissolved at the pH of the endosome. Therefore, it is presumable that the same benefits could be given to non-viral vectors upon mineralization.

To explore this possibility, we aim to develop a straightforward fabrication method for mineralized non-viral carriers for gene delivery. To do so, we first performed studies on a negatively charged tri-component polyplexes constituted of plasmid DNA (pDNA), a lipid-modified low molecular weight polyethyleneimine (PEI) and poly(aspartic acid) (pAsp). The polyplex system was then submitted to a mineralization reaction designed to synthesize a $CaCO_3$ shell around the polyplexes in a controlled way under short incubation times. We chose $CaCO_3$ as the inorganic component of the polyplexes due to its well stablished use as a drug delivery agent[18], and the fact that others have reported better transfection results with $CaCO_3$ instead of calcium phosphate due to reduced particle growth of co-precipitates for the

same reaction concentrations[19,20]. In this strategy, the lipid-modified PEI fills the role of forming the starting point of nanoparticle fabrication by self-assembling into polyplexes with pDNA and providing the proton sponge effect needed for endosomal rupture and escape[21] once inside the cells. The pAsp acts as the main component mediating the mineralization process. We used physicochemical characterization studies to discuss the mechanisms behind polyplex formation and pAsp mediated mineralization, and transfection studies on a mouse osteoblast progenitor cell line (MC3T3-E1) of the polyplexes and explain the resultant transfection properties.

3.2 Materials and Methods

3.2.1 Materials

A lipid-modified low molecular weight PEI (ALL-Fect) was provided by RJH Biosciences (Edmonton, AB). The gWIZ plasmids expressing Green Fluorescent Protein and with no protein expression were purchased from Aldevron (Fargo, ND) and used in the experiments below. Poly(aspartic acid) (pAsp) was purchased from Alamanda Polymers (Huntsville, Alabama, US). $CaCl_2$ and Na_2CO_3 used on the mineralization reaction, nuclease-free water, Hank's Balanced Salt Solution (HBSS), tissue culture media DMEM and F12, SYBR Green I nucleic acid gel stain, and antibiotic solutions Penicillin and Streptomycin were all from Life Technologies (Thermofisher). Heparin sodium salt was obtained from Sigma-Aldrich Corporation (St. Louis, MO) and fetal bovine serum (FBS) was purchased from PAA Laboratories, Inc. (Etobicoke, ON).

3.2.2 Poly(aspartic acid) mediated mineralization of polyplexes

First, pAsp coated polyplexes were fabricated by a two-step complexation method in sterile filtered water at room temperature (**Figure 3.1**). ALL-Fect (1.0 mg/mL) and pDNA (0.4 mg/mL) solutions were mixed in water for 15 s by pipetting and incubated at room temperature for 30 min to form positively charged polyplexes capable of adsorbing pAsp by opposite charge attraction. PAsp was added to the polyplexes in the form of a solution (0.4 mg/mL) under mixing for 15 s and incubated for a further 30 min at room temperature. The anionic pAsp coated polyplexes were then submitted to a mineralization reaction to precipitate $CaCO_3$ *in situ*. First, the prepared polyplex suspension was incubated with $CaCl_2$ for 30 min to allow Ca^{2+} sequestration by pAsp. After that, the suspension had its After that, the suspension had its volume doubled by fast addition of a Na_2CO_3 solution under mixing. Final concentrations ranged from 5 to 20 mM $CaCl_2$ and 0.7 to 1.9 mM Na_2CO_3 depending on the sample. The mineralized polyplexes were allowed to stand for 30 min and processed according to the experiments performed (see below).

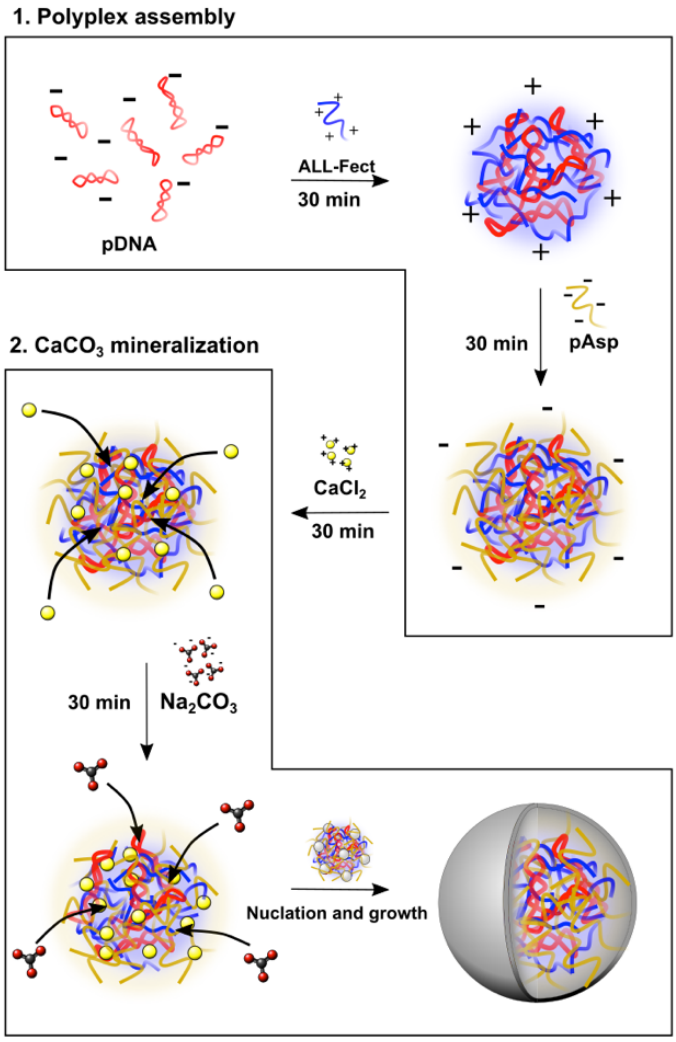

Figure 3.1 Scheme of the fabrication process of mineralized $CaCO_3$ mineralized polyplexes.

3.2.3 Particle size and z-potential analysis by light scattering

Dynamic light scattering (DLS) and electrophoretic light scattering (ELS) studies were carried using a Litesizer 500 (Anton Paar GmbH, Graz, Austria). Due to the self-assembled nature of the samples, the DLS analysis was done using samples at their native concentration in pure water. Samples for ELS analysis had their volume tripled with a 10 mM NaCl solution with pH=7.2 to create a stable ionic background and lower the effect of trace salts on the ζ-potential. DLS analysis was repeated 3 times on the same sample and ELS was repeated in 3

different samples of same composition. Because samples were always fabricated in small volumes, all analysis were made using 60 μL of sample in a low volume apparatus coupled to a dip cell.

3.2.4 Transmission electron microscopy

Samples for transmission electron microscopy (TEM) were prepared by first glow discharging carbon coated grids for 30 min to create a hydrophilic background for sample adsorption. A droplet of liquid suspension containing the sample was added to the grid and allowed to rest for 5 to 10 min depending on the sample, after which it was blotted out using paper filter and allowed to dry out for at least 24 h. The grids were analyzed using a 200kv JEOL 2100 Transmission Electron Microscope (Jeol, Tokio, Japan). Particle counting was done using the Fiji/ImageJ software.

3.2.5 Energy dispersive x-ray spectroscopy

A Bruker Nano scanning electron microscope was used to assess the chemical composition of the mineralized polyplexes using energy dispersive x-ray spectroscopy (EDS). The sample was purified by two steps of centrifugation in water and dried over a Si wafer overnight and analyzed.

3.2.6 Agarose gel retardation assay

To analyse the gain of robustness by polyplexes as a consequence of various $CaCl_2$ and Na_2CO_3 concentrations, mineralized and unmineralized samples were submitted to an agarose gel retardation assay. Incubation with heparin[22] at a final concentration of 0.7 mg/mL

for 1h was used to trigger dissociation of polyplexes and evaluate mineral protection by increase of robustness under many mineralizing concentrations. Finally, samples were electrophoresed in a 0.8% agarose gel in TAE buffer (40 mM Tris, 20 mM acetic acid, 1mM EDTA) containing SYBR Green I (10 μl) for 30 min under 100 mV at 0.3 μg of pDNA per well. The SYBR Green I-pDNA complex is fluorescent, and in case of pDNA release by polyplex dissociation, fluorescent bands shifts can be observed.

3.2.7 Cell Culture and transfection efficiency studies using flow cytometry

The stock cultures of MC3T3-E1 and MDA-MB 231 cells were grown in 75 cm^2 flasks with Dulbecco's Modified Eagle Medium:F12 medium (DMEM:F12=1:1) with 10% Fetal Bovine Serum (FBS), 0.1% Glutramax-1, 0.1% MEM NEAA, Penicillin (100 U/mL) and Streptomycin (100 μg/mL) in a humidified atmosphere with 95% air and 5% CO_2 at 37 ºC. When confluency was reached, cells were trypsinized and seeded into 24-well plates for the indicated studies. After ~50% confluence was reached inside the wells, the cells were treated with different types of polyplexes suspended in pure water (unmodified, calcium incubated, and mineralized polyplexes) to reach 0.5 μg/mL of gWIZ-GFP expression vector under the CMV promoter.

After 48h, cells were detached with trypsin, diluted 5x in complete culture medium with 10% FBS, washed using centrifugation and fixated with cold formaldehyde for 20 min, after which cells were washed again and suspended in PBS. Transfection efficiency was assessed by means of median fluorescence intensity (MFI) and positive population (%) due to green fluorescent protein (GFP) expression using an Attune NxT Flow Cytometer (Thermo Fisher Scientific, US).

3.2.8 Statistical Analysis

Results were represented as means ± standard deviation of values from experiments performed independently (n=3). One-way ANOVA followed by a Tukey-Kramer test was used to compare the means of different groups. Means were considered significantly different when $p<0.05$.

3.3 Results and Discussion

3.3.1 Initial characterization of pAsp-coated polyplexes

The first challenge for fabricating a mineralizable polyplex is developing a strategy to control its surface charge. We used two different ALL-Fect concentrations (0.0047 and 0.0063 μg/μL) to bind pDNA and form positively charged polyplexes with the ALL-Fect/pDNA ratios of 7.5 and 10. Then, DLS and ELS studies were performed to evaluate the changes in the charges of these polyplexes with pAsp coating (**Figure 3.2**). We chose to recharge the polyplexes by adsorption of the polyanion pAsp due to the large body of evidence describing its importance in mediating mineralization[23–30]. Furthermore, it has been reported that pAsp can mediate mineralization in an interesting way: if attached to a materials

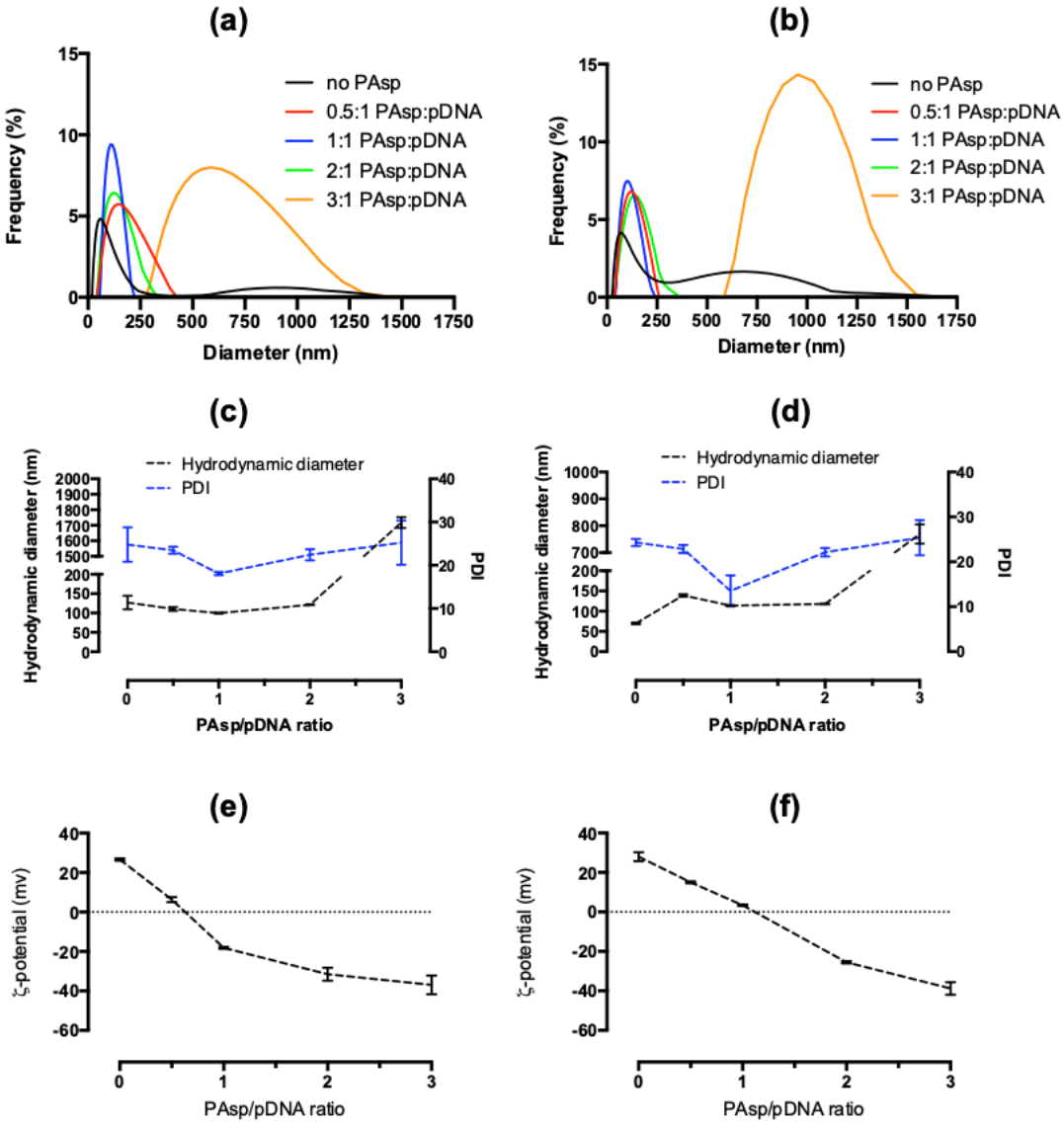

Figure 3.2 Effect of pAsp content analyzed by DLS and ELS: (a) Intensity weighted particle size distribution of polyplexes with ALL-Fect/pDNA=7.5 and pAsp/pDNA=(0.5–3); (b) Intensity weighted particle size distribution ALL-Fect/pDNA=10 and pAsp/pDNA=(0.5–3); (c) Hydrodynamic diameter and PDI of polyplexes with ALL-Fect/pDNA=7.5 and pAsp/pDNA=(0.5-3); (d) Hydrodynamic diameter and PDI of polyplexes with ALL-Fect/pDNA=10 and pAsp/pDNA=(0.5-3); (e) z-potential of ALL-Fect:pDNA=7.5 and pAsp/pDNA=(0.5-3) and (f) z-potential of ALL-Fect/pDNA=10 and pAsp/pDNA=(0.5-3).

surface, it induces mineralization, while when free in solution, it inhibits nucleation[26,27,31].

This capacity of playing antagonistic roles in nucleation – both of which useful for exerting

control over the mineralization process – was considered attractive for the mineralization of polyplexes.

Before pAsp adsorption, the unmodified cationic polyplexes presented two populations of particles recognizable by a narrow and intense peak and a wide peak extending over submicrometric ranges up to 1.5 μm (**Figures 3.2(a)** and **(b)**). The adsorption of pAsp led to the particles being found as a single population in all compositions. While pAsp/pDNA ratio of up to 2 led to a single peak population with small sizes, pAsp/pDNA = 3 yielded a wide peak similar to the one originally found at ALL-fect/pDNA polyplexeswith no pAsp, suppressing the presence of the smaller particle population. This effect created a "V-shaped" profile when plotting PDI over the whole pAsp/pDNA range with the smallest PDI at pAsp/pDNA = 1 for both ALL-Fect compositions. The hydrodynamic diameter stayed relatively stable over PAsp/pDNA = 0.5–2 for both cationic contents. The addition of pAsp to the originally positively charged polyplexes led to a gradually lowering of the ζ-potential (**Figure 3.2(e)** and **(f)**), indicating the adsorption of pAsp to the polyplexes.

Polyplexes, viruses or any other particulate particle subjected to supersaturated conditions will only be efficiently mineralized if specific surface characteristics are met. Using the classical nucleation theory (CNT) as a guide, we are looking for the lowering of the energy barrier for nucleation[32]. The energy barrier for nucleation is an Arrhenius type energy barrier, the crossing of which demands achievement of a certain thermodynamic driving force, which for ionic solutions is the chemical potential. Achieving such thermodynamic conditions on the polyplex favors heterogeneous nucleation, which, in opposition to homogeneous nucleation, and in the context of this work, means favoring nucleation of $CaCO_3$ in association with the polyplex, which is referred to as mineralization[30].

Materials can be mineralized by calcium based minerals if they are capable of binding Ca^{2+} to its surface by the action of negatively charged chemical groups[33,34]. The bound Ca^{2+} then act as nucleation sites, which upon reaction with counter ions in solution give origin to the mineral precipitate. In particulate materials, the achievement of a negative ζ-potential is a well-known requirement for effective mineralization[5,29,35].

For ALL-Fect:pDNA:pAsp = 1:7.5:1 there is a match between the lowest PDI and lowest hydrodynamic size, and considerable negative ζ-potential (approximately -20 mV). We named this polyplex composition as P1. At the higher polycationic content (ALL-Fect/pDNA = 10) the most favorable ζ-potential (-25 mV)/hydrodynamic size combination was achieved at pDNA:ALL-Fect:pAsp = 1:10:2. We named this polyplex composition as P2. P1 and P2 were selected as two possible mineralizable polyplex compositions with satisfactory particle size distribution. The simple attachment of polyanions capable of inducing mineralization by adsorption due to opposite charge proposed here contrasts with the much more laborious genetic manipulation needed for the charge manipulation of viruses for mineralized vaccine fabrication[11] or the chemical modification of polymeric agents for the fabrication of mineralizable micelles for cancer drug delivery[29,36,37].

We performed TEM analysis of the untreated and pAsp coated polyplexes P1 and P2 (**Figure 3.3**). The cationic polyplexes were found in two distinct morphologies (**Figure 3.3(a)** and **(c)**). The spherical particles most likely corresponded to the narrow, mostly nanometric population, while the wormlike assemblies, although having nanometric features, may have corresponded to the wide submicrometric peaks. DLS cannot be used to differentiate large

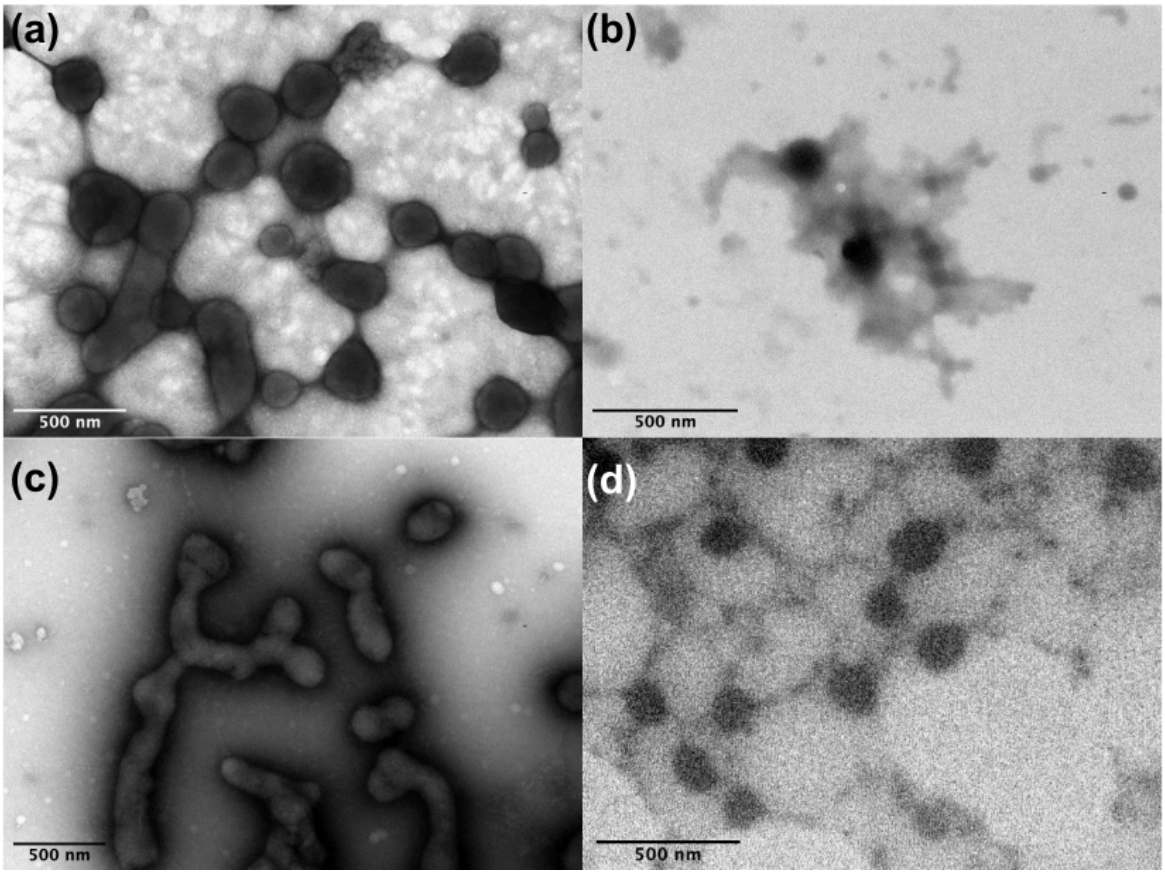

Figure 3.3 TEM images of :(a) uncoated polyplexes with pDNA:ALL-Fect=1:7.5 (stained); (b) pAsp coated polyplexes with pDNA:ALL-Fect:pAsp=1:7.5:1 (P1); (c) uncoated polyplexes with pDNA:ALL-Fect=1:10 (stained); and (b) pAsp coated polyplexes with pDNA:ALL-Fect:pAsp=1:10:2 (P2).

particles from elongated structures like the ones found [38], however, the wide, low intensity continuous peak might be an indication that particles form the wormlike structures by aggregating in polymeric assemblies, which would allow a wide range of possible sizes by joining of nanoparticles instead of particle growth. Indeed, the worm-like structures seemed to be formed by aggregated spherical particles.

When pAsp acid was added to the cationic polyplexes (**Figure 3.3(b)** and **(d))**, the samples showed spherical particles for both polyplex compositions. pAsp appeared to rearrange the wormlike structures observed into distinct nanoparticles, which agreed with the DLS data (**Figure 3.2(a)** and **(b)**), in which the wide frequency peaks were suppressed by

disassembly of the wormlike structures and stabilization of particles due to highly hydrophilic pAsp[39]. Considering the dependence of transfection efficiency on particle size, this could potentially be one of the factors influencing transfection efficiency in previous studies from our group when using lipid-modified PEIs in combination with other polyanions[40,41]. Size and shape are important features affecting particle uptake by cells[42–46], however the influence of these features on uptake and transfection efficiency seem to be highly dependent on the material forming the particles. While it is frequently regarded that 50 nm particles are optimally taken up by cells in experimental and computational studies[47], there are recent reports of improved transfection efficiency *in vitro* and *in vivo* with PEI polyplexes when using specific complexation protocols that increase sizes up to the micrometer [46,48].

The P1 and P2 also show presence of an amorphous background that may correspond to free polymer when pAsp is present. The amount of amorphous background seems to be less in P2. Differently from the samples in figures 3.3(a) and (c), the pAsp coated samples were not stained with uranyl acetate. From our experience, pAsp has some staining effect over the polyplexes. While this staining effect does not offer the same contrast that proper staining does, it allows observation of pAsp location in the sample. Accordingly, we believe that pAsp is contained on both the particles and amorphous background and, therefore, the presence of free pAsp in equilibrium with polyplex bound pAsp is a possibility. Apart from inducing mineralization when attached to materials surfaces, pAsp can potentially be inhibiting nucleation when free in solution[31], which could result in a mechanism favoring nucleation to happen over the polyplex. However, we cannot confirm the occurrence of this

phenomenon in this polyplex system without a more in-depth study specifically dedicated to this matter.

3.3.2 Calcium incubation and mineralization of polyplexes

After selecting P1 and P2 as the base compositions for mineralization, we first investigated the effect of Ca^{2+} adsorption by light scattering (**Figure 3.4**) to better understand the final properties of the mineralized polyplexes. Considering the important role of pAsp-Ca^{2+} binding on mineralization [30], it is ideal to have a method that allows the Ca^{2+} adsorption to occur freely in solution without the competing nucleation in the presence of Na_2CO_3. Again, using the CNT as a guide, the increased Ca^{2+} concentration around the particle would result in a stronger local thermodynamic driving force for nucleation. This effect, added to the lowering of the energy barrier for nucleation, could ensure effective mineralization.

P1 and P2 shared a tendency to increase the frequency of bigger particles as the $CaCl_2$ concentration was raised from 5 to 20 mM, however this was more prominent for P1 than for P2 (**Figure 3.4(a)** and **(b)**). Accordingly, P1 showed a more sensible hydrodynamic size and PDI increase with $CaCl_2$ compared to P2 (**Figure 3.4(c) and (d)).** P2 showed a decrease in PDI and stable hydrodynamic size up to 10 mM $CaCl_2$, over which both PDI and hydrodynamic size increased considerably. The differences in response to $CaCl_2$ are likely a consequence of the different ALL-Fect/pAsp ratios between P1 and P2 (7.5 and 5, respectively). Polyelectrolytes such as pAsp can work as steric and electrostatic dispersants, however the strong interaction with Ca^{2+} results in the formation of physical crosslink between the cation and carboxylate groups from pAsp, either from different macromolecules

or from the same one [49,50]. This results in a collapse of steric stabilization and partial neutralization of surface

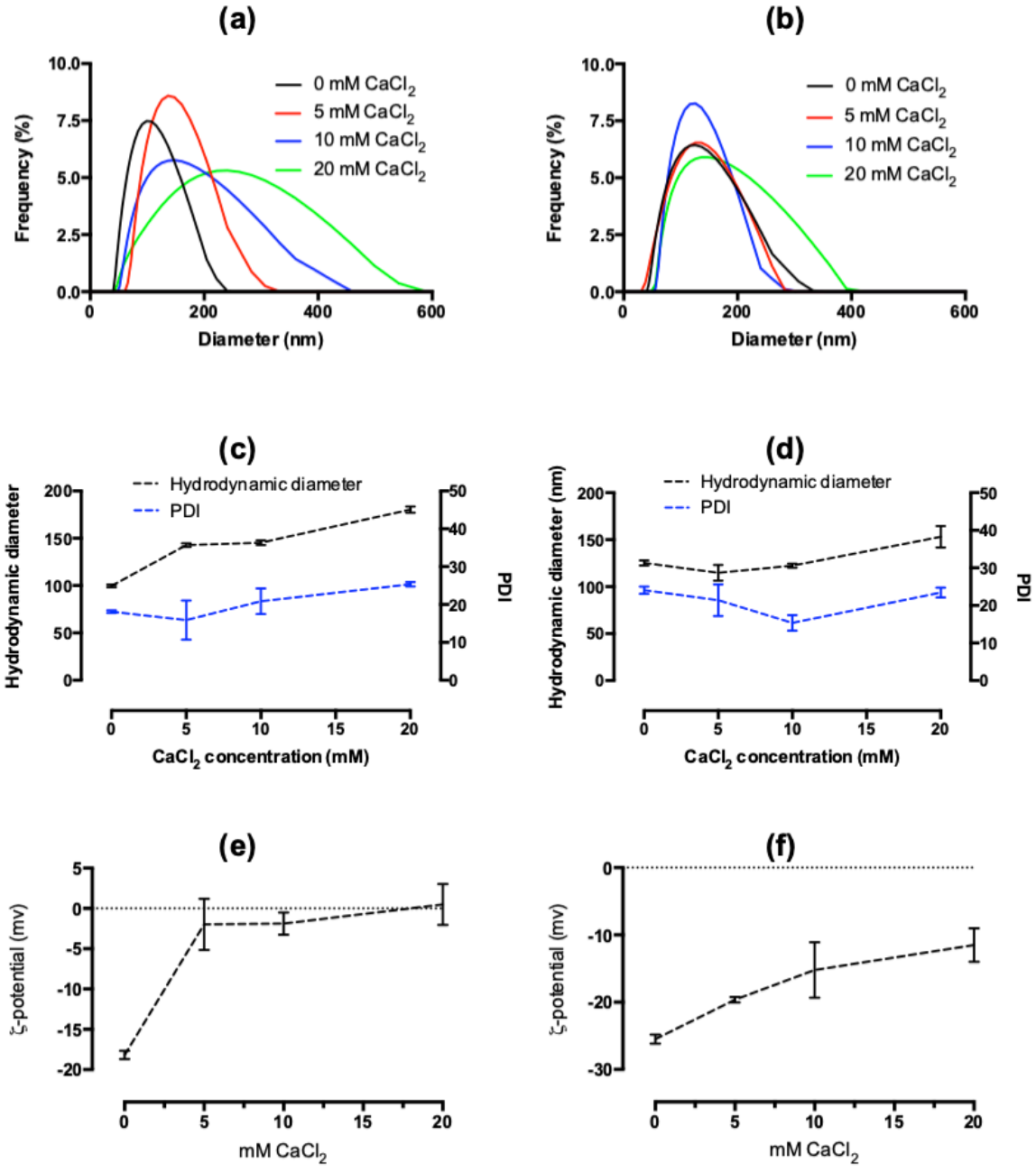

Figure 3.4 Effect of $CaCl_2$ incubation on pAsp coated polyplexes analyzed by ELS and DLS: (a) Intensity weighted particle size distribution of polyplexes with P1; (b) Intensity weighted particle size distribution of

P2; (c) Hydrodynamic diameter and PDI of polyplexes with ALL-P1; (d) P2; (e) z-potential of P1; and (f) z-potential of P2.

charge observed by ζ-potential shifts (**Figure 3.4(e)** and **(f)**). P1 underwent more efficient charge neutralization at 5 mM $CaCl_2$ (~2 mV), while P2 showed a much less abrupt variation in ζ-potential due to the higher pAsp content, having a negative ζ-potential up to 20 mM $CaCl_2$ (approximately -12 mV).

The effect of Ca^{2+} absorption on the morphology of P2 incubated with 10 mM $CaCl_2$ was studied by TEM (**Figure 3.5**). The addition of $CaCl_2$ increased the contrast in images, which is indicative of Ca^{2+} adsorption to the particles. There was also presence of agglomerates measuring up to 400 nm and a considerable amount of sub-100 nm particles. The free amorphous material observed in Figure 3.2 was not evident here; the interaction with Ca^{2+} might have led to further complexation that accounted for the particle size increase and formation of the new smaller particles by complexation.

Next, we mineralized P1 and P2 with 3 reaction compositions: 5 mM $CaCl_2$/0.7 mM Na_2CO_3, 10 mM $CaCl_2$/1.1 mM Na_2CO_3, and 20 mM $CaCl_2$/1.9 mM Na_2CO_3 (**Figure 3.6**). These compositions follow an increase in the amount of reactant species and, as a result, an increase in the amount of precipitated calcium carbonate was expected. Both P1 and P2 show a similar response to mineralization with the increase in supersaturations. An increase in the presence of bigger particles was observed (**Figures 3.6(a)** and **(b)**). The hydrodynamic diameter of P1 and P2 (**Figure** 3.6 (c) and (d)) showed a considerable increase even at the lowest reactants concentration used (P1 = 557 and P2 = 892 nm), and at 20 mM $CaCl_2$ and 1.9 mM Na_2CO_3, both polyplexes showed hydrodynamic sizes in the micrometer range (P1 = 1230 nm and P2 = 1331 nm). PDI values had large SDs, which makes difficult the

evaluation of a trend in values, but there seems to be a tendency for PDI to increase as supersaturation increased.

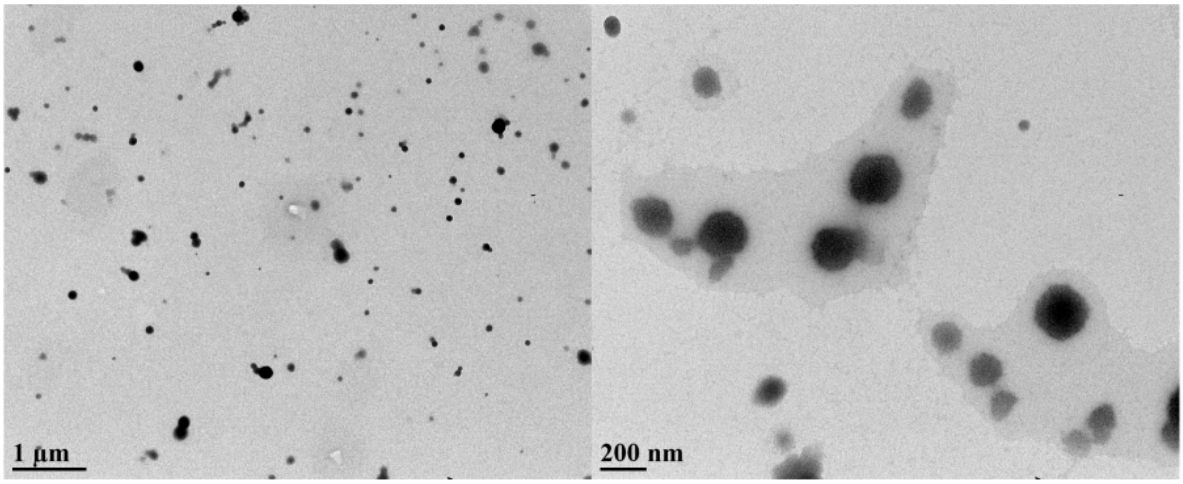

Figure 3.5 TEM of calcium incubated P1 (pDNA:ALL-Fect:pAsp=1:7.5:1)

All mineralized samples showed a negative ζ-potential as a consequence of Na_2CO_3 addition, which was directly influenced by the cationic/anionic ratios ALL-Fect/pAsp and Ca^{2+}/CO_3^{2-} ratios. This means that for the same mineralizing conditions, a higher ALL-Fect/pAsp ratio results in a less negative ζ-potential, and for the same polyplex composition, increasing Ca^{2+}/CO_3^{2-} results in a less negative ζ-potential. Having this control might be useful in the sense that ζ-potential of the pDNA:ALL-Fect:pAsp polyplex can be adjusted by the mineralizing composition and, if a certain mineralizing composition is considered ideal, ζ-potential can be adjusted by reformulating the polyplex composition. This effect could be potentially be used to modulate the binding strength of functional organic additives to the $CaCO_3$ external layer[51]. P1 and P2 with 5 mM $CaCl_2$ and 0.7 mM Na_2CO_3 have Ca^{2+}/CO_3^{2-} = 7.14 while the samples with 20 mM CaCl2 and 1.9 Na_2CO_3 have Ca^{2+}/CO_3^{2-} = 10.53 and, consequently, less negative ζ-potential.

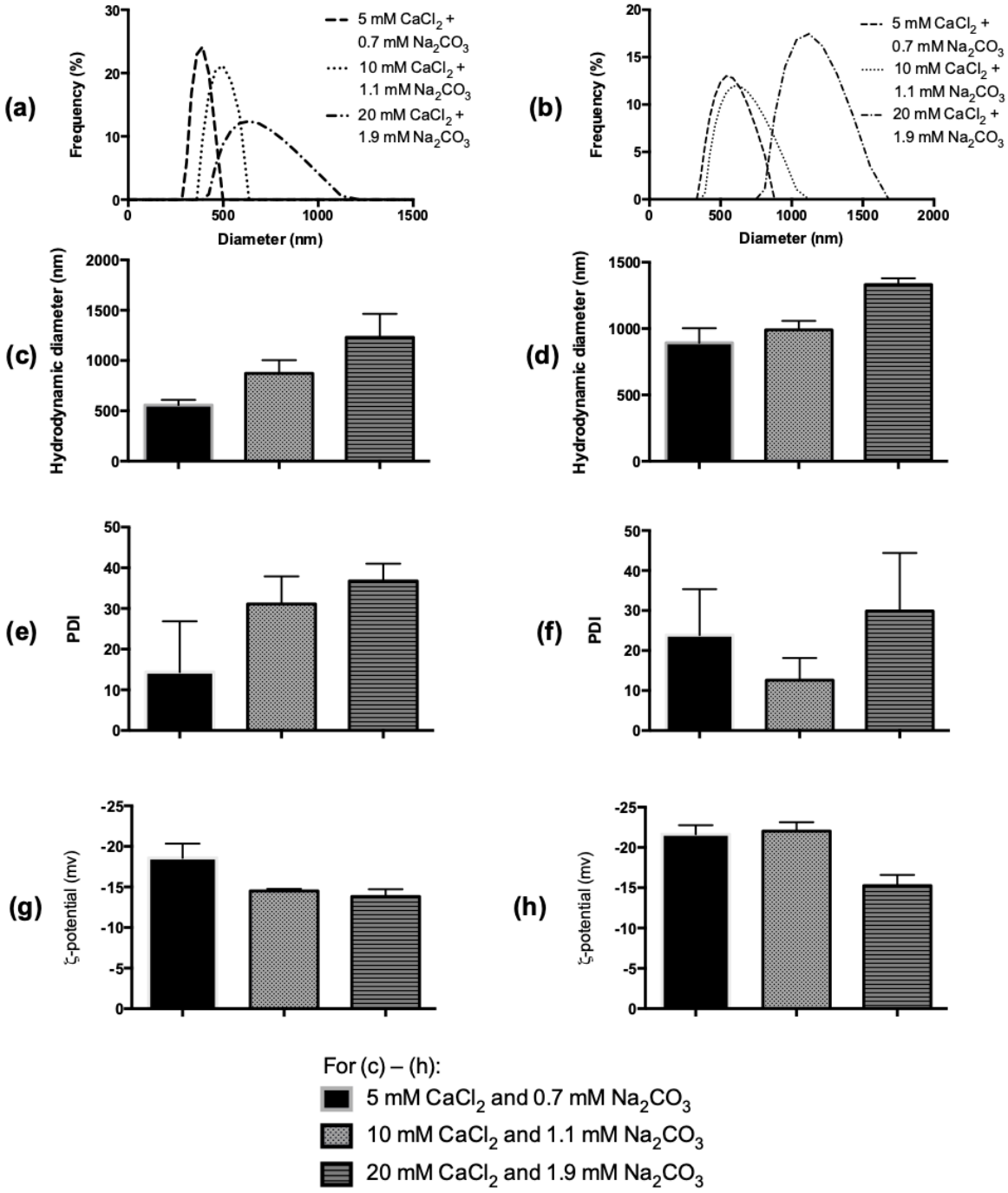

Figure 3.6 Effect of mineralized content on pAsp coated polyplexes analyzed by ELS and DLS: (a) Intensity weighted particle size distribution of P1; (b) Intensity weighted particle size distribution P2; (c) Hydrodynamic diameter and PDI of P1; (d) Hydrodynamic diameter and PDI of P2; (e) z-potential of P1; and (f) z-potential of P2.

Since polyplexes self-assemble and keep their integrity due to electrostatic attraction between the oppositely charged components, the stability of the mineralized polyplexes were investigated by exposing them to strong dissociative conditions. **Figure 3.7** shows a gel electrophoretic mobility study employing nine different $CaCl_2$ and Na_2CO_3 mineralizing compositions over P1 and P2, as well as calcium incubated and untreated controls. P1 and P2 dissociation was triggered by incubation in heparin, a negatively charged macromolecule capable of strongly binding to polycations, causing polyplex dissociation by competition with nucleotides[22,52,53]. Without heparin incubation, all polyplexes were stable except P1, which indicated some degree of pDNA dissociation due to pAsp action and recovery of stability by interaction with Ca^{2+}. After heparin incubation, all untreated polyplexes showed intense dissociation bands, while all mineralized samples seem to be completely protected against dissociation. We note that we incubated all samples with a 70-fold excess heparin to that of pDNA, which would dissociate most polyplexes made with traditional complexing agents. For example, it was reported that PEI and poly-L-lysine with optimal transfecting compositions dissociate with a heparin excess as low as 5 fold the amount of pDNA[54], and micelles capable of resisting dissociation by heparin were more resistant to nucleases and kept bioactivity after longer storage times[55]. Calcium incubated controls showed partial resistance against dissociation triggered by heparin, except by P1 incubated with 20 mM $CaCl_2$, that did not dissociate.

The mechanism behind protection by mineralization probably differs from the protection by Ca^{2+} binding. Mineralization probably provides a physical layer that protects the polyplexes, not allowing heparin to interact with the polyplexes. This protective effect is likely to be independent of heparin concentration. The mechanism behind protection by

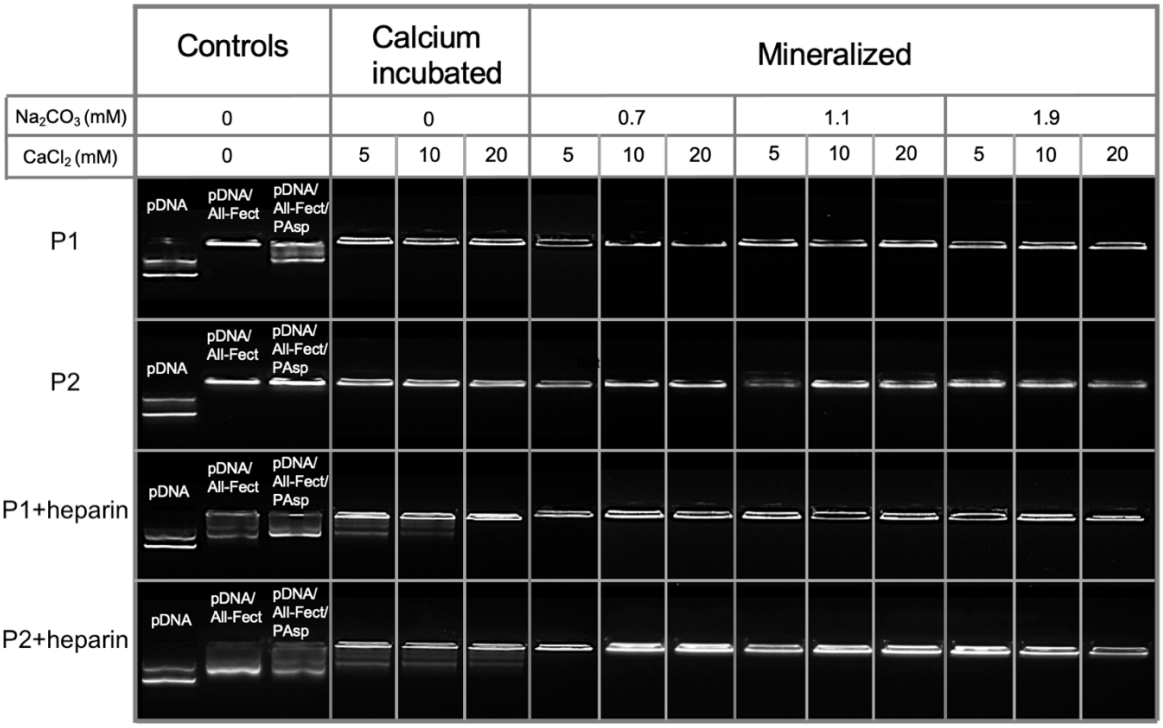

Figure 3.7Effect of mineralized content in the protection against heparin induced dissociation (0.7 mg/mL) analyzed by gel electrophoresis.

calcium binding is probably a bit more complex. It is possible that Ca^{2+} can make physical crosslinks with pAsp[49,56], increasing the robustness of the polyplexes. However, if heparin can reverse the crosslinks by binding to Ca^{2+}, which would demand excess of Ca^{2+} for a complete protective effect. In that case, calcium incubated polyplexes cannot be considered as robust as the mineralized ones, as they are still vulnerable to dissociation by competitive binding. P2 was probably more susceptible to dissociation due to the higher pAsp amount on its composition, which increases the polyanionic content of the polyplex and offers less free Ca^{2+} to sacrifice for binding with heparin. Interestingly, it was reported by others that incubation of cationic polyplexes with calcium salts show the opposite effect: Ca^{2+} in such case decreases pDNA binding of the polyplexes by competition with the polycation used[57,58]. This could explain why a decrease in pDNA binding was found recently when submitting

cationic polyplexes to mineralization[59]. Since the polyplexes were cationic, the authors probably failed to mineralize their polyplexes, precipitating particles by homogeneous nucleation, and the excess Ca^{2+} from the mineralization reaction caused decrease in pDNA binding. Furthermore, there is a large body of evidence showing that when drug carriers are mineralized, they become robust and need to be negatively charged to show that effect[29,35,37,60].

As all mineralizing concentrations tested were capable of resisting dissociation by heparin competition, we characterize the chemical composition of P1 mineralized with 10 mM $CaCl_2$ and 1.1 mM Na_2CO_3 as an intermediary composition of tested systems. **Figure 8(a)** shows the region used for the analysis and a rectangle containing 3 particles on the Si substrate used. Excluding the signal of the Si peaks, Ca, O, and C peaks were detected as expected as well as the Cl remaining from the synthesis reaction, which is another indication of effective mineralization (**Figure 3.8(b)**). We did not consider SEM for particle size counting because the samples were dried over the Si substrate, which, even after washing with centrifugation, could have led to size increase due to the prolonged drying process in the presence of traces of reactants. The particles were considerably smaller (~300 nm) than the hydrodynamic size found by DLS for the same polyplex composition mineralized under the same $CaCl_2$ and Na_2CO_3 concentrations (~800 nm). The particles are spherical and well dispersed, with no signs of agglomeration, which could be a consequence of the centrifugation and drying steps used to prepare the sample. It is interesting that, while this values drastically disagree with DLS from mineralized particles, they correlate better with the hydrodynamic sizes achieved for the calcium incubated samples with 5 mM $CaCl_2$ (P1=142.9 and P2=114.8). In **Figure 3.9**, there does not seem to be considerable particle

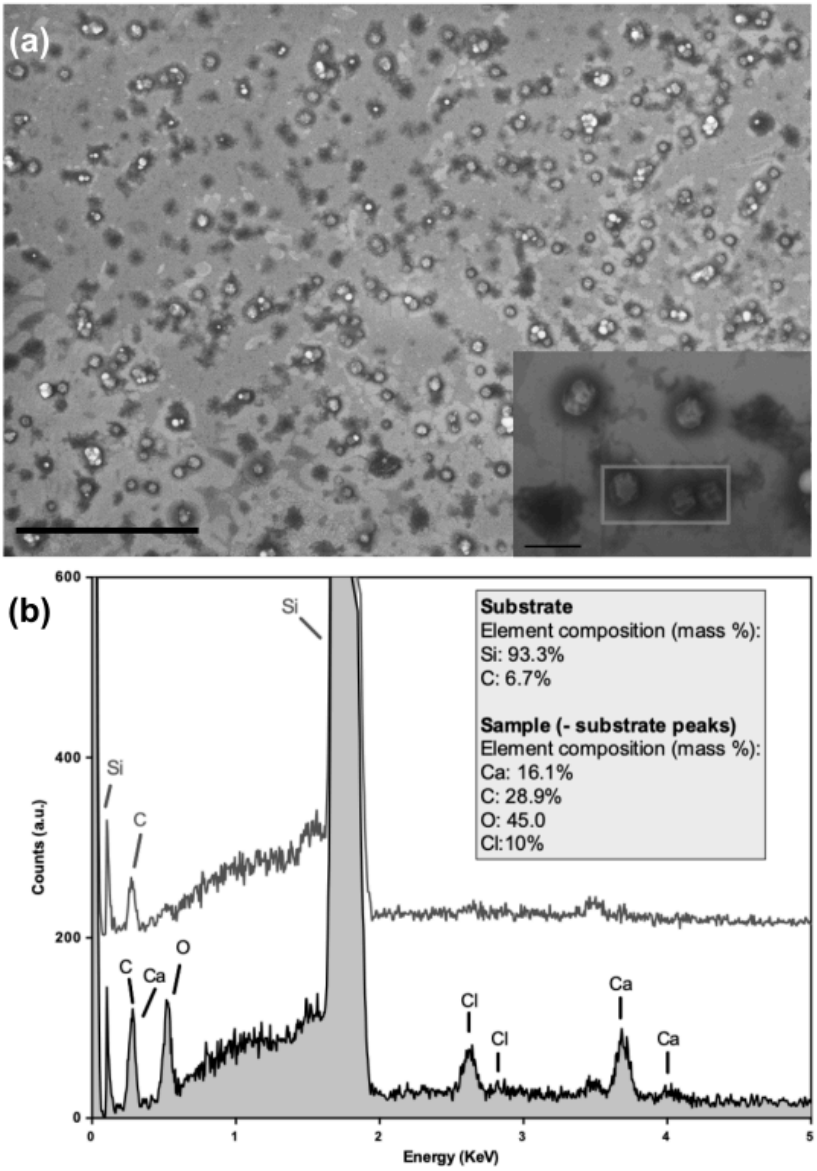

Figure 3.8 (a) Scanning Electron Microscopy (SEM) of particles prepared with pDNA:ALL-Fect:pAsp = 1:7.5:1 and mineralized with 10 mM $CaCl_2$ and 1.1 mM Na_2CO_3. Scale bars = 10 µm (lower magnification image) and = 1 µM (higher magnification image). (b) Electron dispersive x-ray spectroscopy (EDS) of the area highlighted on the higher magnification image and substrate without particles. Mass ratios of the elements are indicated.

agglomeration or aggregation and particles are well dispersed. Additionally, these particles showed no signs of excessive growth. The drastic difference in size between the two techniques (TEM vs hydrodynamic size by DLS) can be a consequence of the presence of

particle motion modes that are non-Brownian (possibly a consequence of agglomeration and sedimentation) not fulfilling the necessary sample characteristics for accurate measurements using DLS[38] as well as the way particle size is estimated depending on the technique (number weighted vs intensity weighted)[61].

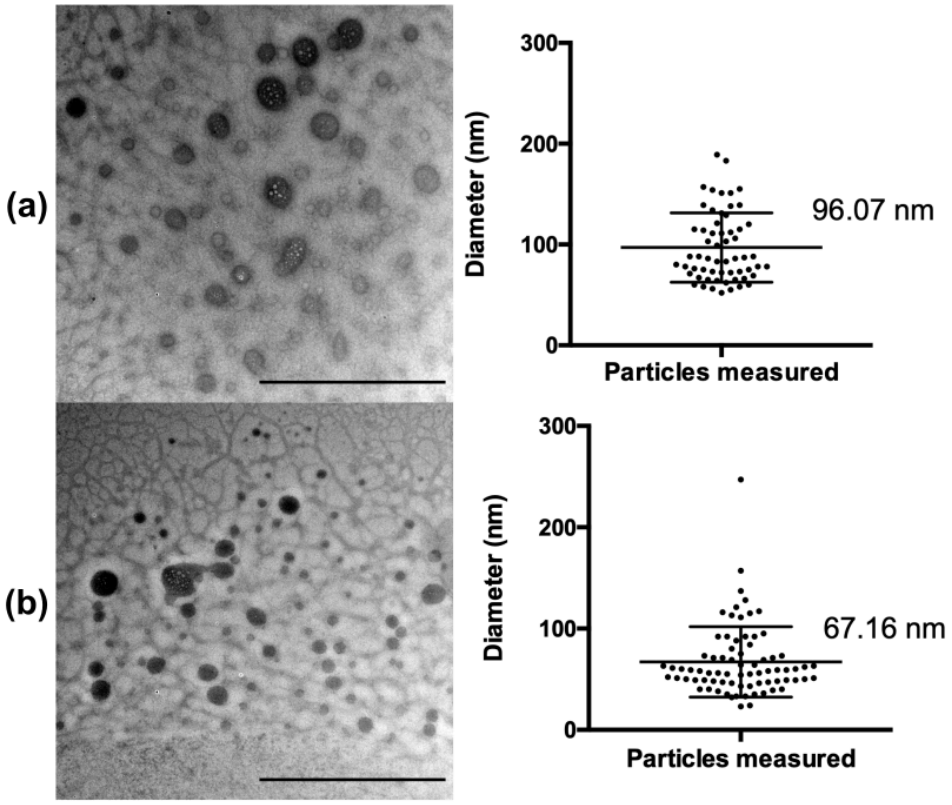

Figure 3.9 TEM images of polyplexes mineralized with 5 mM $CaCl_2$ and 0.7 mM Na_2PO_4: (a) P1 and particle sizes measured on the same image; and (b) P2 and particle sizes measured on the same image. Scale bars = 1 µm.

At higher magnification (**Figure 3.10**), the 'apparently' uniform particles at lower magnification showed an obvious heterogeneous morphology. Multiple cores embedded in a dense matrix was evident, which is likely the result of a complex interaction between the organic and inorganic components forming the particles during $CaCO_3$ nucleation and growth. Considering that the contrast of the denser mineral phase increases along the particle

radius towards its center, we presume that $CaCO_3$ is not restricted to the surface of the nanoparticle and forms an interconnected matrix inside. The cores vary in size, being smaller at the particles surfaces and increasing in size towards the center. The multiple cores are most likely organic (instead of hollow), and considering the already discussed properties of pAsp to mediate mineralization, we suspect they are possibly rich in polycationic content.

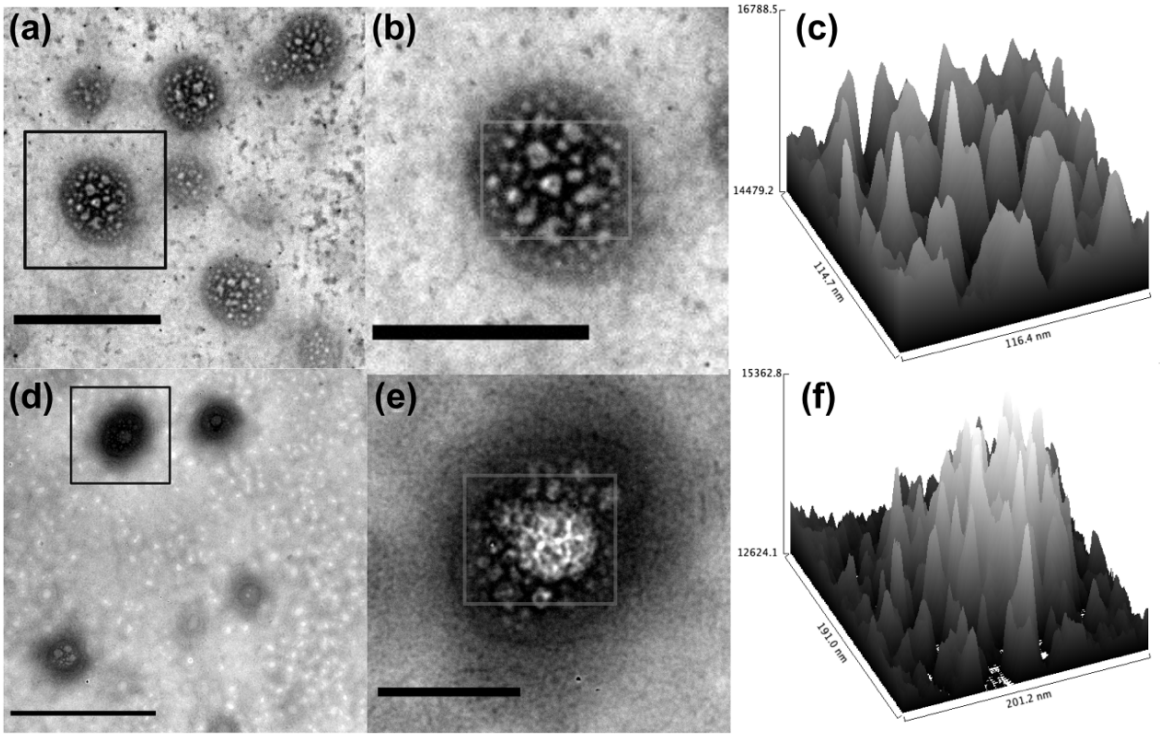

Figure 3.10 TEM images of mineralization using 5 mM $CaCl_2$ and 0.7 mM Na_2CO_3 of: (a) P1 (scale bar = 200 nm); (b) P1 at higher magnification (scale bar = 200 nm); (c) Inverse of Z-contrast values from the selected area in previous figure; (d) P2 (scale bar = 500 nm); (e) P2 at higher magnification (scale bar = 200 nm); (c) Inverse of Z-contrast values from the selected area in previous figure.

It seems that the main difference in morphology between P1 and P2 lies in how the size and number of cores evolve from the particle surface to the center. While both polyplex compositions show small multiple cores at the surface, P1 had the tendency to show multiple cores that were more homogeneous in size, and P2 more frequently showed just a few (one to three) bigger cores at its center. This difference can be observed by comparing **Figure**

3.10(a) and **(b)** with **Figure 3.10(d)** and **(e).** To better observe the difference in core distribution in the center of the nanoparticles, we plotted the gray scale values from the squares at the center of mineralized P1 in **Figure 3.10(c)** and P2 in **Figure 3.10(f)**, which can be interpreted as surface plots of the inverse of the Z contrast. While P1 showed multiple lower density peaks homogeneously distributed along the area chosen, P2 shows one main low-density peak with depressions on the main peak area, which is likely due to smaller more dense cores present closer to the surface.

Considering the two-step mineralization method used, in which incubation with $CaCl_2$ alone was allowed for 30 min before addition of Na_2CO_3, we suspect that Ca^{2+} adsorption on the particles surface and interior might be an important factor in achieving the interconnected mineral phase. Organic-inorganic interactions highly specific to our system might be at play. For example, pAsp is an important factor leading to infiltration of collagen by calcium phosphate during mineralization[25,31], however, how this phenomenon relates to our self-assembled particulate system in which pDNA is another anionic component in play and the majority of the polyplex body is formed by the lipid-modified PEI, which is also described to modulate final mineral morphology in its unmodified form[62], is unknown.

We proposed a possible nucleation and growth mechanism for the multiple core morphology observed based on a simple interpretation of the CNT and our results (**Figure 3.11**). We interpreted the smaller core size at the surface of the polyplexes as the indication of an increased nucleation rate on that site. This is consistent with the assumption that polyplexes have higher Ca^{2+} concentration than the reaction medium due to sequestration by pAsp. When Na_2CO_3 is added, CO_3^{2-} diffusion happens more easily in the reaction medium than inside the polyplex, generating a higher supersaturated state at the liquid/polyplex

interface, inducing nucleation by lowering of the energy barrier and local increase in the nucleation driving force. The continuous diffusion of CO_3^{2-} from the liquid/polyplex interface towards its center and excess Ca^{2+} available inside the polyplex volume feed the growth of $CaCO_3$ towards the polyplex center only until the growth of $CaCO_3$ at the surface leads to the formation of a shell and impediment of diffusion of ions. When that happens, growth can still happen by thickening of the mineral layer at the polyplex/liquid interface.

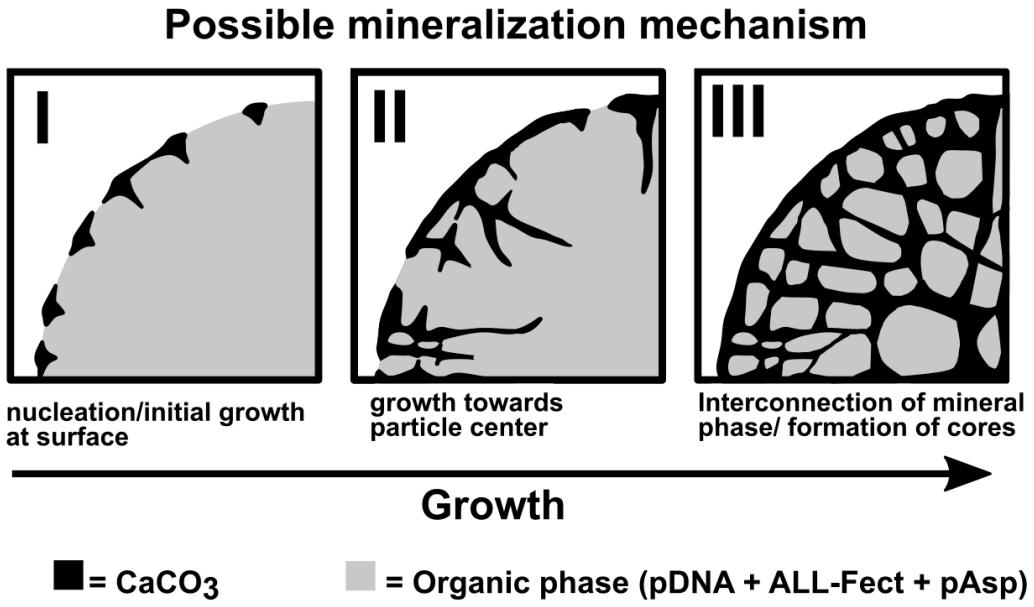

Figure 3.11 Proposed mechanism for mineralization.

3.3.3 Transfection Studies

As all $CaCl_2$ and Na_2CO_3 concentrations tested protected the polyplexes against dissociation by heparin, we considered all 18 mineralized samples to be "successfully mineralized", and therefore we employed all of them, including calcium incubated controls and untreated controls (P1 and P2 in pure water), in pGFP transfections in MC3T3-E1 cells, a mouse calvaria osteoblast precursor [63] (**Figure 3.12**). This cell line was chosen since mineralized polyplexes could be ideally suitable for gene therapy efforts with bone and

similar mineral-bearing tissues. Mineralization had an obvious effect in promoting GFP expression even at the lowest mineralizing concentrations; (i) in the absence of Ca^{+2}, no transfection was evident with the polyplexes and (ii) subsequent exposure to CO_3^{-2} enhanced the transfection efficiency. However, there seems to exist a dependency on the Ca^{2+}/CO_3^{2-} ratio used for mineralization. This dependency, to which clearly P1 is more sensible, is evident when we observe the decrease in transfection efficiency at the lowest $CaCl_2$ concentration used (5 mM) by the increase in $NaCO_3$ from 0.7 mM to 1.9 mM. The same dependency is confirmed when observing the transfection efficiency values achieved by mineralizing with 20 mM $CaCl_2$ and 1.9 mM Na_2CO_3 and the decay in transfection efficiency by lowering the $CaCl_2$ concentration. We propose that the optimal Ca^{2+}/CO_3^{2-} ratio to be at least 7.14 in this system (from P1 mineralized with 5 mM $CaCl_2$ and 0.7 mM Na_2CO_3).

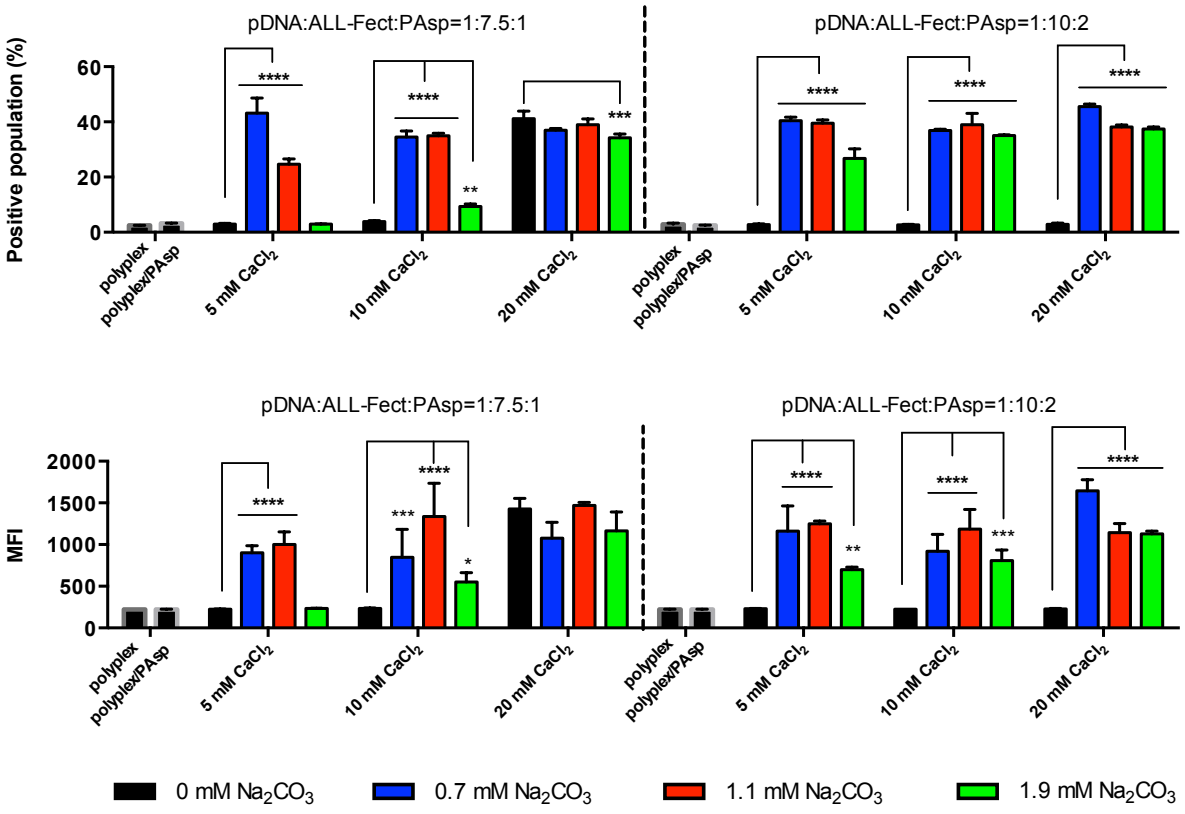

*Figure 3.12 Transfection efficiency of mineralized polyplexes on MC3T3 cells as the GFP positive population (top graphs) and the mean fluorescence intensity. (MFI, bottom graphs). The specific rations for the complexes prepared with pDNA, ALL-Fect and pAsp are indicated on top of each graph. $p \leq 0.05$ is indicated as *, $p \leq 0.001$ as ***, and $p \leq 0.0001$ as ****.*

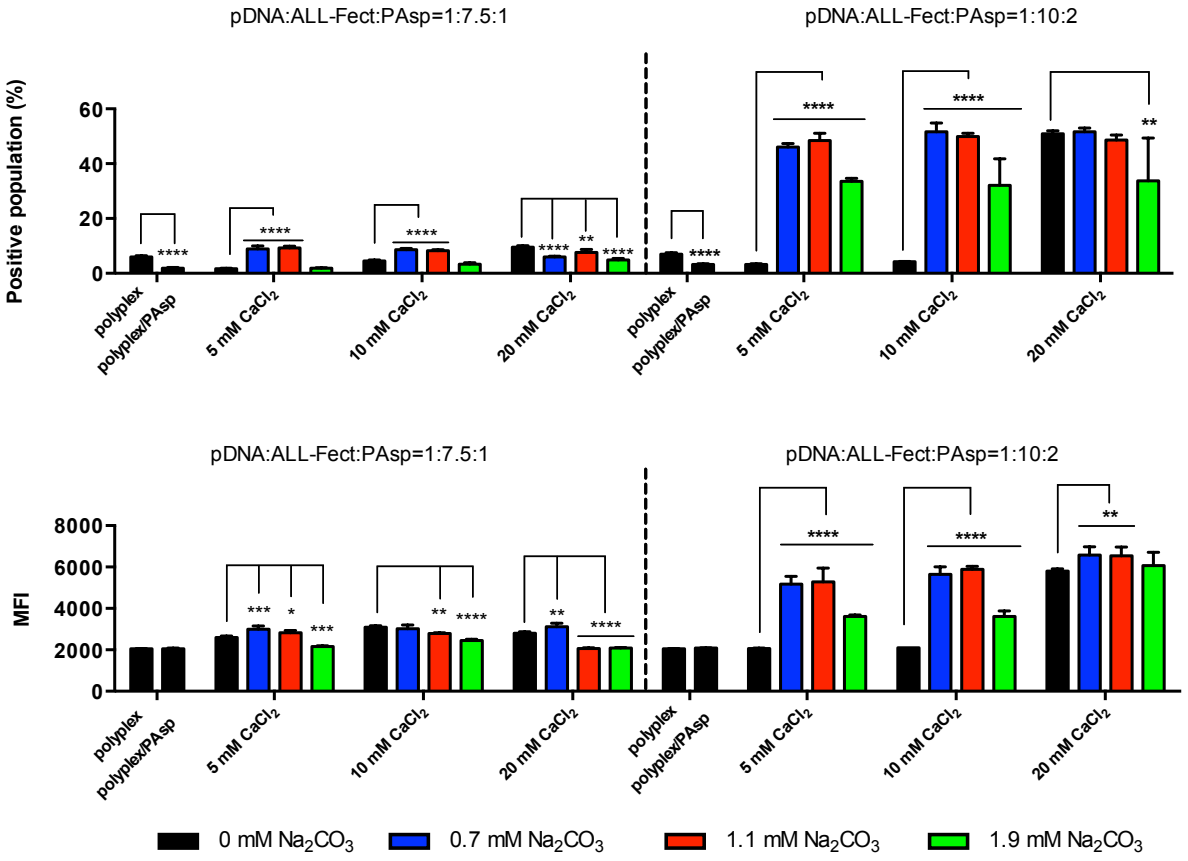

*Figure 3.13 Transfection efficiency of mineralized polyplexes on MDA-MB 231 cells as the GFP positive population (top graphs) and the mean fluorescence intensity. (MFI, bottom graphs). The specific rations for the complexes prepared with pDNA, ALL-Fect and pAsp are indicated on top of each graph. $p \leq 0.05$ is indicated as *, $p \leq 0.001$ as ***, and $p \leq 0.0001$ as ****.*

One of the calcium incubated controls in the absence of mineralization (P1, 20 mM $CaCl_2$) showed a very high transfection efficiency, comparable to the mineralized particles. This was the only calcium incubated sample to show protection against dissociation by heparin (**Figure 3.7**), indicating the formation of very stable particle. This presumably facilitated intracellular uptake of the nanoparticles making them withstand passage through

the cell membrane. Therefore, the heparin triggered dissociation of polyplexes could be an important tool to evaluate which polyplex formulations have potential to become efficient transfection agents when phenomena leading to increased robustness like the ones discussed here are in question. We most note that we were able to readily obtain transfection with the unmineralized polyplexes before[64] (unlike this study), but these studies employed polyplexes formed in tissue culture medium (with Ca^{2+} present) for short duration of time (30 min complexation vs 120 min here). It seems like robustness is the effect allowing transfection efficiency to happen and the calcium excess modulates transfection efficiency, since samples with intermediate robustness (calcium incubated samples except P1 incubated with 20 mM $CaCl_2$) did not show intermediate transfection efficiency, but when robustness is achieved without a considerable calcium excess for mineralized samples, transfection efficiency can be gradually increased by increasing the $CaCl_2$ concentration.

We also performed transfection in MDA-MB 231 cells (epithelial cell line from the breast adenocarcinoma) (**Figure 3.13**). This cell line was more sensible to the cationic content of the polyplexes, having a strong increase in transfection when ALL-Fect content was increased. Also, a decrease in transfection efficiency by the addition of pAsp was noted (polyplex vs polyplex pAsp). At the lower polycationic content (P1), increase in the number of cells transfected by mineralization did not translate into an as intense increase in the MFI. MDA-MB 231 transfection with P2 followed a similar profile of that observed in MC3T3 transfection with P1, in which calcium incubation at 20 mM $CaCl_2$ was capable of inducing transfection similar to that of the mineralized samples. Considering that this specific sample did not show complete inhibition of dissociation by heparin, it is possible that the dependency on robustness for transfection on the calcium incubated/mineralized system could vary from

cell line to cell line. MDA-MB 231 also show strong dependency of Ca^{2+}/CO_3^2, following a similar trend of decrease in transfection efficiency when Ca^{2+}/CO_3^{2-} is lower than 7.14.

It is interesting that mineralized samples were effective even being considerably anionic. Positive ζ-potential is frequently described as a pre-requisite for effective transfection efficiency[65]. Perhaps the surface charge effect is not as important to mineralized samples, and other specific mineral adhesion properties are at play, such as what is reported to mineralized viruses[15]. Other authors have also reported that increased intracellular calcium levels could increase transfection efficiency on its own, however it does not seem to be completely clear what is the mechanism behind such increase. It was observed that the effect of calcium is seen in a variety of cell lines, however the effect of calcium varied a lot depending on the cell line and type of lipoplex used[66]. Indeed, there are studies that suggest that an increase in cytosolic Ca^{2+} can increase endocytosis rates[67,68]. The effect of calcium has been recently highlighted in bone marrow-derived stem cells transfected with PEI/pDNA polyplexes[69]. It is also proposed that specific pDNA and polyplex interactions with Ca^{2+} resulting in smaller polyplex size might be one reason for improved transfection efficiency[57].

We believe that mineralization of the polyplexes could enable new applications based on the robustness of the mineral shell and specific mineral-biointeractions. The effects observed with mineralized viruses *in vivo* are perhaps what could be expected to be achieved with the synthetic vector, considering that these properties are believed to be materials specific[5]. Nucleotide vaccines using polyplexes could highly benefit on the thermostability gained through mineralization[11]. These, such as the recent mRNA vaccines used during COVID-19 global pandemic, would likely require storage under ultra-cold conditions. In that context, mineralization could lower costs related cold chains. Additionally, mineralized

vaccines have increased adhesion to mucosa and could increase local airway immunization when delivered through the nose, another property that could be useful dealing with the current pandemic[16]. Furthermore, mineralization of a COV-SARS-2 vaccine employing an adenovirus carrying the gene for the SARS-CoV-2 spike protein showed improved thermostability and was reported to induce higher levels of spike protein-specific antibody and T cell response[70]. The protective effect of the mineral shell could also prove to be useful in tissue engineering applications using gene activated matrices carrying polyplexes. In electrospinning, for example, polyplexes inside a spun fiber are subjected to several conditions that could reduce transfection efficiency, such as solvents, shear forces, temperature variation, and solvent drying inside a polymer matrix [64,71]. In this scenario, mineralized polyplexes are more likely to maintain efficiency until the gene activated matrix is employed.

3.4 Conclusions

Here, we reported an effective and straightforward mineralization strategy mediated by poly(aspartic acid) to fabricate robust $CaCO_3$ mineralized polyplexes, with preliminary biological work. The physicochemical and biological properties of the polyplexes have been found to highly dependent on the organic and inorganic cationic/anionic ratios ALL-Fect/pAsp and Ca^{2+}/CO_3^{2-}. An interesting morphology constituted of multiple organic cores on a mineral matrix was revealed by the TEM, which we presume is the consequence of $CaCO_3$ mineral growth towards the center of the polyplexes after nucleation at the surface. The mechanism behind the increase of transfection efficiency by mineralization seems to be highly dependent on the increase in robustness, and it is influenced by Ca^{2+}/CO_3^{2-} ratio and

polyplex composition, and seems to be dependent on the cell line used. We envisage the mineralized polyplexes becoming a promising robust gene carrier for applications that could benefit from increased Ca^{2+} intracellular levels or demanding outstanding protection. For example, mineralized polyplexes could be used in conjunction with material fabrication methods that are not friendly to unmineralized polyplexes to create novel gene activated matrices. It is also possible that some of the properties observed in mineralized vaccines employing viruses could be observed with mineralized polyplexes. However, it is first necessary to test the $CaCO_3$ mineralized polyplexes in a large variety of cell applications and better understand what the mechanisms behind the increase in transfection efficiency are, and how to better explore the new acquired properties through mineralization in novel applications, which we intent to do next.

3.5 References

[1] Glover, D. J., Lipps, H. J. & Jans, D. A. Towards safe, non-viral therapeutic gene expression in humans. *Nature Reviews Genetics* **6**, 299–310 (2005).

[2] Picanço-Castro, V. *et al*. Emerging patent landscape for non-viral vectors used for gene therapy. *Nature Biotechnology* **38**, 151–157 (2020).

[3] Baranowski, E., Ruiz-Jarabo, C. M., Pariente, N., Verdaguer, N. & Domingo, E. Evolution of Cell Recognition by Viruses: A Source of Biological Novelty with Medical Implications. *Advances in Virus Research* **62**, 19–111 (2003).

[4] Peng, X., Xu H FAU - Jones, B., Jones B FAU - Chen, S., Chen S FAU - Zhou, H. & Zhou, H. Silicified virus-like nanoparticles in an extreme thermal environment: implications for the preservation of viruses in the geological record. *Geobiology* **6**, 511–526 (2013).

[5] Wang, X. *et al*. Biomineralization State of Viruses and Their Biological Potential. *Chemistry – A European Journal* **24**, 11518–11529 (2018).

[6] Kyle, J. E., Pedersen, K. & Ferris, F. G. Virus Mineralization at Low pH in the Rio Tinto, Spain. *Geomicrobiology Journal* **25**, 338–345 (2008).

[7] Zhou, H., Wang, G., Wang, X., Song, Z. & Tang, R. Mineralized State of the Avian Influenza Virus in the Environment. *Angewandte Chemie International Edition* **56**, 12908–12912 (2017).

[8] De Wit, R. *et al*. Viruses Occur Incorporated in Biogenic High-Mg Calcite from Hypersaline Microbial Mats. *PLOS ONE* **10**, e0130552 (2015).

[9] Frede, A. *et al*. Local delivery of siRNA-loaded calcium phosphate nanoparticles abates pulmonary inflammation. *Nanomedicine: Nanotechnology, Biology and Medicine* **13**, 2395–2403 (2017).

[10] Zhou, H., Wang, X. & Tang, R. Could a mineralized state of avian flu virus be dangerous to humans? *Future Virology* **13**, 79–81 (2018).

[11] Wang, G. *et al*. Rational design of thermostable vaccines by engineered peptide-induced virus self-biomineralization under physiological conditions. *Proceedings of the National Academy of Sciences* **110**, 7619 LP – 7624 (2013).

[12] Sakoda, T., Kasahara, N., Kedes, L. & Ohyanagi, M. Calcium phosphate coprecipitation greatly enhances transduction of cardiac myocytes and vascular smooth muscle cells by lentivirus vectors. *Experimental and clinical cardiology* **12**, 133–138 (2007).

[13] Yang, Y.-W. & Chao, C.-K. Incorporation of calcium phosphate enhances recombinant adeno-associated virus-mediated gene therapy in diabetic mice. *The Journal of Gene Medicine* **5**, 417–424 (2003).

[14] Fasbender, A. *et al*. Incorporation of adenovirus in calcium phosphate precipitates enhances gene transfer to airway epithelia in vitro and in vivo. *The Journal of Clinical Investigation* **102**, 184–193 (1998).

[15] Wang, X. *et al*. Biomineralized vaccine nanohybrid for needle-free intranasal immunization. *Biomaterials* **106**, 286–294 (2016).

[16] Wang, X. *et al*. Vaccine Engineering with Dual-Functional Mineral Shell: A Promising Strategy to Overcome Preexisting Immunity. *Advanced Materials* **28**, 694–700 (2016).

[17] Huang, L.-L. *et al*. MnCaCs-Biomineralized Oncolytic Virus for Bimodal Imaging-Guided and Synergistically Enhanced Anticancer Therapy. *Nano Letters* **19**, 8002–8009 (2019).

[18] Maleki Dizaj, S. *et al*. An update on calcium carbonate nanoparticles as cancer drug/gene delivery system. *Expert Opinion on Drug Delivery* **16**, 331–345 (2019).

[19] Zhao, D., Wang, C.-Q., Zhuo, R.-X. & Cheng, S.-X. Modification of nanostructured calcium carbonate for efficient gene delivery. *Colloids and Surfaces B: Biointerfaces* **118**, 111–116 (2014).

[20] Chen, S., Li, F., Zhuo, R.-X. & Cheng, S.-X. Efficient non-viral gene delivery mediated by nanostructured calcium carbonate in solution-based transfection and solid-phase transfection. *Molecular BioSystems* **7**, 2841–2847 (2011).

[21] Rezvani Amin, Z., Rahimizadeh, M., Eshghi, H., Dehshahri, A. & Ramezani, M. The effect of cationic charge density change on transfection efficiency of polyethylenimine. *Iranian journal of basic medical sciences* **16**, 150–156 (2013).

[22] Clamme, J. P., Azoulay, J. & Mély, Y. Monitoring of the formation and dissociation of polyethylenimine/DNA complexes by two photon fluorescence correlation spectroscopy. *Biophysical journal* **84**, 1960–1968 (2003).

[23] Kim, D., Lee, B., Thomopoulos, S. & Jun, Y.-S. In Situ Evaluation of Calcium Phosphate Nucleation Kinetics and Pathways during Intra- and Extrafibrillar Mineralization of Collagen Matrices. *Crystal Growth & Design* **16**, 5359–5366 (2016).

[24] Min, K. H. *et al*. The tumor accumulation and therapeutic efficacy of doxorubicin carried in calcium phosphate-reinforced polymer nanoparticles. *Biomaterials* **33**, 5788–5797 (2012).

[25] Cantaert, B., Beniash, E. & Meldrum, F. C. The role of poly(aspartic acid) in the precipitation of calcium phosphate in confinement. *Journal of Materials Chemistry B* **1**, 6586–6595 (2013).

[26] Nudelman, F., Lausch, A. J., Sommerdijk, N. A. J. M. & Sone, E. D. In vitro models of collagen biomineralization. *Journal of Structural Biology* **183**, 258–269 (2013).

[27] Quan, B. D. & Sone, E. D. The effect of polyaspartate chain length on mediating biomimetic remineralization of collagenous tissues. *Journal of the Royal Society, Interface* **15**, 20180269 (2018).

[28] Lee, S. J. *et al*. Ketal Cross-Linked Poly(ethylene glycol)-Poly(amino acid)s Copolymer Micelles for Efficient Intracellular Delivery of Doxorubicin. *Biomacromolecules* **12**, 1224–1233 (2011).

[29] Kim, B. J. *et al*. Calcium carbonate-mineralized polymer nanoparticles for pH-responsive robust nanocarriers of docetaxel. *Macromolecular Research* **23**, 111–117 (2015).

[30] Zhou, Z. *et al*. Polyelectrolyte-calcium Complexes as a Pre-precursor Induce Biomimetic Mineralization of Collagen. *Nanoscale* (2020). doi:10.1039/D0NR05640E

[31] Nudelman, F. *et al*. The role of collagen in bone apatite formation in the presence of hydroxyapatite nucleation inhibitors. *Nature Materials* **9**, 1004–1009 (2010).

[32] Liu, X. Y. - Generic mechanism of heterogeneous nucleation and molecular interfacial effects. in (eds. Sato, K., Furukawa, Y. & Nakajima, K. B. T.-A. in C. G. R.) 42–61 (Elsevier Science B.V., 2001).

[33] Aizenberg, J., Black, A. J. & Whitesides, G. M. Oriented Growth of Calcite Controlled by Self-Assembled Monolayers of Functionalized Alkanethiols Supported on Gold and Silver. *Journal of the American Chemical Society* **121**, 4500–4509 (1999).

[34] Toworfe, G. K., Composto, R. J., Shapiro, I. M. & Ducheyne, P. Nucleation and growth of calcium phosphate on amine-, carboxyl- and hydroxyl-silane self-assembled monolayers. *Biomaterials* **27**, 631–642 (2006).

[35] Lv, Y. *et al*. A robust pH-sensitive drug carrier: Aqueous micelles mineralized by calcium phosphate based on chitosan. *Carbohydrate Polymers* **111**, 101–107 (2014).

[36] Han, S.-Y. *et al*. Mineralized hyaluronic acid nanoparticles as a robust drug carrier. *Journal of Materials Chemistry* **21**, 7996–8001 (2011).

[37] Lee, H. J. *et al*. Spatially mineralized self-assembled polymeric nanocarriers with enhanced robustness and controlled drug-releasing property. *Chemical Communications* **46**, 377–379 (2010).

[38] Stetefeld, J., McKenna, S. A. & Patel, T. R. Dynamic light scattering: a practical guide and applications in biomedical sciences. *Biophysical Reviews* **8**, 409–427 (2016).

[39] Wiśniewska, M., Ostolska, I. & Sternik, D. Impact of adsorption of poly(aspartic acid) and its copolymers with polyethylene glycol on thermal characteristic of Cr2O3. *Journal of Thermal Analysis and Calorimetry* **125**, 1171–1184 (2016).

[40] KC, R. B., Kucharski, C. & Uludağ, H. Additive nanocomplexes of cationic lipopolymers for improved non-viral gene delivery to mesenchymal stem cells. *Journal of Materials Chemistry B* **3**, 3972–3982 (2015).

[41] Parmar, M. B. *et al*. Combinational siRNA delivery using hyaluronic acid modified amphiphilic polyplexes against cell cycle and phosphatase proteins to inhibit growth and migration of triple-negative breast cancer cells. *Acta Biomaterialia* **66**, 294–309 (2018).

[42] Zheng, M. & Yu, J. The effect of particle shape and size on cellular uptake. *Drug Delivery and Translational Research* **6**, 67–72 (2016).

[43] Zhang, S., Li, J., Lykotrafitis, G., Bao, G. & Suresh, S. Size-Dependent Endocytosis of Nanoparticles. *Advanced Materials* **21**, 419–424 (2009).

[44] He, C., Hu, Y., Yin, L., Tang, C. & Yin, C. Effects of particle size and surface charge on cellular uptake and biodistribution of polymeric nanoparticles. *Biomaterials* **31**, 3657–3666 (2010).

[45] Arnida, Janát-Amsbury, M. M., Ray, A., Peterson, C. M. & Ghandehari, H. Geometry and surface characteristics of gold nanoparticles influence their biodistribution and uptake by macrophages. *European Journal of Pharmaceutics and Biopharmaceutics* **77**, 417–423 (2011).

[46] Pezzoli, D., Giupponi, E., Mantovani, D. & Candiani, G. Size matters for in vitro gene delivery: investigating the relationships among complexation protocol, transfection medium, size and sedimentation. *Scientific Reports* **7**, 44134 (2017).

[47] Behzadi, S. *et al*. Cellular uptake of nanoparticles: journey inside the cell. *Chemical Society Reviews* **46**, 4218–4244 (2017).

[48] Zhang, W. *et al*. Nano-Structural Effects on Gene Transfection: Large, Botryoid-Shaped Nanoparticles Enhance DNA Delivery via Macropinocytosis and Effective Dissociation. *Theranostics* **9**, 1580–1598 (2019).

[49] Nap, R. J., Park, S. H. & Szleifer, I. Competitive calcium ion binding to end-tethered weak polyelectrolytes. *Soft Matter* **14**, 2365–2378 (2018).

[50] Huber, K. Calcium-induced shrinking of polyacrylate chains in aqueous solution. *The Journal of Physical Chemistry* **97**, 9825–9830 (1993).

[51] Derkani, M. H. *et al*. Mechanisms of Surface Charge Modification of Carbonates in Aqueous Electrolyte Solutions. *Colloids and Interfaces* **3**, (2019).

[52] Ma, P. L., Lavertu, M., Winnik, F. M. & Buschmann, M. D. Stability and binding affinity of DNA/chitosan complexes by polyanion competition. *Carbohydrate Polymers* **176**, 167–176 (2017).

[53] Chen, Z., He, Y., Zhang, L. & Li, Y. Enhanced DNA release from disulfide-containing layered nanocomplexes by heparin-electrostatic competition. *Journal of Materials Chemistry B* **3**, 225–237 (2015).

[54] Park, J. H., Han, J. & Lee, M. Thymidine Kinase Gene Delivery Using Curcumin Loaded Peptide Micelles as a Combination Therapy for Glioblastoma. *Pharmaceutical Research* **32**, 528–537 (2015).

[55] Gwak, S.-J., Macks, C., Bae, S., Cecil, N. & Lee, J. S. Physicochemical stability and transfection efficiency of cationic amphiphilic copolymer/pDNA polyplexes for spinal cord injury repair. *Scientific Reports* **7**, 11247 (2017).

[56] Russo, R., Malinconico, M. & Santagata, G. Effect of Cross-Linking with Calcium Ions on the Physical Properties of Alginate Films. *Biomacromolecules* **8**, 3193–3197 (2007).

[57] Ayyadevara, V. S. S. A. & Roh, K.-H. Calcium enhances polyplex-mediated transfection efficiency of plasmid DNA in Jurkat cells. *Drug Delivery* **27**, 805–815 (2020).

[58] Xie, S.-X., Baoum, A. A., Alhakamy, N. A. & Berkland, C. J. Calcium enhances gene expression when using low molecular weight poly-l-lysine delivery vehicles. *International Journal of Pharmaceutics* **547**, 274–281 (2018).

[59] Chen, P. *et al*. The synthesis of amphiphilic polyethyleneimine/calcium phosphate

composites for bispecific T-cell engager based immunogene therapy. *Biomaterials Science* **6**, 633–641 (2018).

[60] Han, H. S. *et al*. Robust PEGylated hyaluronic acid nanoparticles as the carrier of doxorubicin: Mineralization and its effect on tumor targetability in vivo. *Journal of Controlled Release* **168**, 105–114 (2013).

[61] Farkas, N. & Kramar, J. A. Dynamic light scattering distributions by any means. *Journal of Nanoparticle Research* **23**, 120 (2021).

[62] Shkilnyy, A. *et al*. Poly(ethylene imine)-Controlled Calcium Phosphate Mineralization. *Langmuir* **24**, 2102–2109 (2008).

[63] Wang, D. *et al*. Isolation and Characterization of MC3T3-E1 Preosteoblast Subclones with Distinct In Vitro and In Vivo Differentiation/Mineralization Potential. *Journal of Bone and Mineral Research* **14**, 893–903 (1999).

[64] Tsekoura, E. K. *et al*. Delivery of Bioactive Gene Particles via Gelatin-Collagen-PEG-Based Electrospun Matrices. *Pharmaceuticals* **14**, 666 (2021).

[65] Gratton, S. E. A. *et al*. The effect of particle design on cellular internalization pathways. *Proceedings of the National Academy of Sciences* **105**, 11613 LP – 11618 (2008).

[66] Lam, A. M. I. & Cullis, P. R. Calcium enhances the transfection potency of plasmid DNA–cationic liposome complexes. *Biochimica et Biophysica Acta (BBA) - Biomembranes* **1463**, 279–290 (2000).

[67] Eliasson, L. *et al*. Endocytosis of secretory granules in mouse pancreatic beta-cells evoked by transient elevation of cytosolic calcium. *The Journal of physiology* **493 (Pt 3)**, 755–767 (1996).

[68] Epstein, R. J. *et al*. Extracellular calcium mimics the actions of platelet-derived growth factor on mouse fibroblasts. *Cell Growth Differentiation* **3**, 157–164 (1992).

[69] Acri, T., Laird, N. & Geary, S. Effects of calcium concentration on nonviral gene delivery to bone marrow-derived stem cells. *J Tissue Eng Regen Med* 2256–2265 (2019).

[70] Luo, S. *et al*. A Self-Biomineralized Novel Adenovirus Vectored COVID-19 Vaccine for Boosting Immunization of Mice. *Virologica Sinica* (2021). doi:10.1007/s12250-021-00434-3

[71] Xue, J., Wu, T., Dai, Y. & Xia, Y. Electrospinning and Electrospun Nanofibers: Methods, Materials, and Applications. *Chemical Reviews* **119**, 5298–5415 (2019).

4. General Discussion and Conclusions

In the face of recent reports that viruses can self-mineralize as an evolutionary advantage [1–4], benefiting from improved robustness and infectivity, and under the hypothesis that this benefit could be translated to non-viral gene carriers, in this thesis, polyplexes for pDNA delivery were mineralized. However, instead of employing known recipes for metastable supersaturated solutions, such as the one proposed by Kokubo [5], a polyplex-tailored mineralization strategy was presented. Freshly prepared polyplexes tend to reduce their transfection efficiency after long times of incubation [6], which makes the use of supersaturated metastable solutions inappropriate, as these demand long incubation times (hours or days). A time-efficient mineralization reaction is more convenient no matter the application. A short reaction time (1 hour) was achieved by performing two-step mineralization. The polyplexes were first incubated in a $CaCl_2$ solution for 30 min and then mineralized by addition of a saline buffered solution containing 0.7-1.9 mM Na_3PO_4 for calcium phosphate mineralization or a solution containing 0.7-1.9 mM Na_2CO_3 for calcium carbonate mineralization. The two-step process ensures efficient chelation of calcium ions by poly(aspartic acid) in the vicinity and possibly at the interior of the polyplexes, which was identified by the increase in contrast in calcium incubated polyplexes by TEM in Chapters 2 and 3.

The rationale adopted is that by limiting the supersaturated status of the system by using a very low concentration of the counter ions (PO_4^{3-} or CO_3^{2-}), well below stoichiometric values, it is possible to limit growth and homogeneous nucleation while benefiting from the increased efficiency in calcium chelation. The formation of polyelectrolyte/Ca^{2+} chelates is thought to be an important intermediate step in mineralization[7]. The assessment of changes

in hydrodynamic size, zeta potential, morphology, resistance to dissociation, and transfection efficiency as a consequence of each step of the fabrication method helped to generate an explanation for the phenomena behind the measurements made. Also, comparing mineralized samples with calcium incubated samples after recognition of the importance of the interaction of calcium ions and poly(aspartic acid) for transfection efficiency of polyplexes. A summary of the changes in properties as a consequence of each step of the fabrication can be found in Table 4-1.

Table 4-1 A summary of properties as a consequence of each step of the fabrication process.

	Hydrodynamic size	**Zeta potential**	**Resistance to dissociation**	**Morphology**	**Transfection Efficiency**
Coating with PAsp	Decreases: hydrophilic nature of PAsp helps to disperse polyplexes	Decreases (from positive to negative): PAsp adsorption at the surface of the polyplex changes the net surface charge from positive to negative.	Decreases: competition between PAsp and pDNA for PEI can reduce binding.	Changes from spheres + worm-like to just spheres: PAsp breaks apart worm-like structures due to its hydrophilic nature.	Decreases: Highly anionic particles without other uptake mechanisms do not have enough attraction towards the cell membrane to overcome the energy barrier for membrane folding.
Calcium incubation	Increases: Agglomeration due to collapse of steric and electrostatic stabilization with calcium binding.	Increases (from negative to neutral): partial charge neutralization due to Ca^{2+} binding with COO^- from PAsp	Increases: PAsp can chelate Ca^{2+}, generating physical crosslinks.	Increase in contrast: Calcium is located in the polyplexes.	High $CaCl_2$ or low $CaCl_2$ concentrations in the presence of a saline buffer promoted transfection: Increase in robustness
Mineralization	Increases: Agglomeration is followed by decantation.	Decreases (becomes more negative): Reaction with PO_4^{3-} or CO_3^{2-}.	Completely inhibits dissociation: Mineralization builds a physical barrier that protects the polyplex from heparin.	Heterogeneous: Presence of organic and inorganic components in the same particle.	Increases transfection at all $CaCl_2$ concentrations as long as a Ca^{2+}/PO_4^{3-} and Ca^{2+}/CO_3^{2-} lower limit is respected: The mineral layer readily promotes transfection due to increased

	robustness. Ca^{2+} excess might be necessary for particles not to become too negative.

The effect of ionic strength as a consequence of NaCl addition can be concluded by comparing Chapters 2 and 3. Polyplexes were mineralized following two different mineralization methods: method 1 – a calcium phosphate mineralization in a buffered salt solution containing 150 mM NaCl; and method 2 – a calcium carbonate mineralization reaction using only calcium and a carbonate salt. NaCl is found in the reaction media only as a byproduct of the chemical reaction $CaCl_2 + Na_2CO_3 \rightarrow NaCl + CaCO_3$ (maximum 1.4 to 3.8 mM NaCl). The removal of the buffered NaCl solution resulted in less agglomeration of the mineralized nanoparticles, which is clear when comparing TEMs and DLS from Chapters 2 and 3. However, it seems that NaCl modulates the effect of Ca^{2+}, improving its ability to increase transfection efficiency at lower concentrations, which can be concluded by comparing flow cytometry results from Chapters 2 and 3. While the modulation of the Ca^{2+}–driven increase of transfection effect by NaCl is an interesting phenomenon, definitely deserving a future in-depth investigation, it makes it difficult to fully isolate the effects of mineralization from that of Ca^{2+} binding. Additionally, for medical applications, due to the agglomeration effect caused by NaCl, observed by TEM in Chapter 2, particle mineralization in media with lower ionic strength seems preferable.

Without differentiating between the minerals precipitated, the increase of polyplex integrity (or robustness) due to calcium incubation or due to mineralization seems to be the main factor promoting transfection, and this effect was similar independently of the cell line transfected. Furthermore, calcium incubation or mineralization is not capable of significantly

sustaining transfection. For mineralized samples, while considerably negatively charged particles were still highly effective, calcium seems important to avoid loss of activity due to excess negative charge.

In Chapter 3, the cell lines MC3T3-E1 (fibroblast) and MDA-MB-231 (epithelial) were used for transfection efficiency studies using $CaCO_3$ mineralized polyplexes, which allow to make considerations about the effect of the cell-related parameters on transfection efficiency. While we were not interested on the effect off cell passage on transfection, other authors observed important outcomes when passage number was elevated. For MCT3T3-E1 cells, it was observed that cell proliferation can decrease as cell passage number increases [8], and osteogenesis decreases considerably above 30 passages [9]. We could not find studies on the effect of passage of MDA-MB-231, however for most cell lines, reduction of proliferation is frequently described [8–10], which could reduce transfection efficiency. Overall, it is well recognized that it is a good practice to work with cells with low passage number (bellow 20).

In our studies, the effects of calcium incubation and mineralization do not seem to depend significantly on the cell line used. We believe that transfection can be increased by a combination of factors that are consequence of physicochemical properties of the polyplexes, and not any specific Ca^{2+} receptor mediated mechanism. Improved robustness that can be turned off intracellularly [11]. Increased intracellular calcium concentration [12], and unspecific uptake as a consequence of the mineralized layer [13] are factors that have been recognized in the literature separately. A more detailed discussion on this topic can be found in Section 3.3.3 of this document.

4.1 The importance of surface charge for nucleation and materials fabrication

Electrostatic interactions are thought to be the main factor for calcium phosphate and carbonate heterogeneous nucleation [14]. Looking at the literature over the last decades, there is an absolute preference for using materials that contain acidic groups and are negatively charged [11,15–25]. This tradition might have started after early works utilizing polarized surfaces and coated substrates that could not mineralize positively charged surfaces [16,23,26–28]. However, recent work shows that functionalization with positively charged groups can be superior in nucleating calcium phosphate [29]. Therefore, there is still room for debate on ideal strategies for materials fabrication using mineralization.

In living organisms, mineralization happens in a complex scenario, in which extracellular proteins with acidic domains guide the formation of highly complex hard tissues with the action of electrostatic forces [30]. Positive charges on the collagen gap zone are thought to work as anchor sites for negatively charged complexes formed between liquid mineral precursors and proteins. This phenomenon is thought to direct intrafibrillar mineralization [14]. However, the overall mechanism for collagen intrafibrillar mineralization is still under debate, as a recent work was able to generate intrafibrillar mineralization with the action of a polycation, which indicates electrostatic forces are not enough to explain intrafibrillar mineralization [31,32]. A combination of positive and negative charges can also be an interesting strategy to improve mineralization efficiency in vitro [33]. However, in materials fabrication and comparative studies, traditionally, one type of surface charge modification is used at a time.

Using polarized surfaces, Yamashita [26] could only nucleate calcium phosphate over a negatively charged surface. The proposed mechanism is that nucleation sites for calcium phosphate could be created over a negative surface by the attraction of Ca^{2+} from solution,

and a positively charged surface could not nucleate calcium phosphate due to the lower charge density of the phosphate counter ions, which favors the adsorption of the more charge dense Cl^-. This explanation is in agreement with studies dedicated to selective adsorption of ions with different valences and diameters [34]. In the following years, the idea that positively charged surfaces cannot efficiently nucleate calcium phosphate was then reinforced by the publication of work by other authors using different surface modification techniques [23,27,28,35–38]. Most authors used classical concepts to explain the mechanism behind nucleation by a negatively charged surface: lowering of surface energy and local increase of supersaturation. In material fabrication studies, there is a noticeable predominance of the use of functionalization techniques to locate acidic groups over surfaces (mostly carboxylic acid groups), which is commonly confirmed by means of a negative zeta potential [15,16,39–41]. However, very recently, a study found more efficient mineralization with modification of a PEEK surface with positively charged groups [29]. It is possible that the different results from different groups might be a consequence of the different techniques used for surface functionalization, different experimental parameters, and the action of other factors that can influence nucleation.

To our knowledge, the only attempt to mineralize positively charged particles was performed in ref. [42], in a CaP precipitation reaction over positively charged polyplexes. Different from other studies (including this thesis), they found that mineralization increases the encapsulation of drugs or nucleic acids, and show TEMs of nanoparticles with an indication of organic and inorganic phases in the same nanoparticle [11,16,31,39,43,44]. Ref. [42] reports microparticles with homogeneous morphology and reduced DNA binding. Since mineralization is regarded as an efficient way of improving hydrophilic drug encapsulation

[31], a possible interpretation is that positively charged polyplexes could not be coated by CaP, and excess Ca^{2+} competes with the polycation used for pDNA biding. Interestingly, there are authors that found that positively charged polyplexes incubated with only $CaCl_2$ have reduced binding and increased transfection efficiency [45,46], characteristics that were also reported by ref. [42]. Ultimately, a study on the role of charge for the specific case of polyplexes is needed before drawing any conclusion.

4.2 Future perspectives and studies

As discussed in more detail in Chapter 1, calcium phosphate and calcium carbonate are highly safe materials routinely used in medical devices and as food additives, respectively. Drawbacks related to these materials are mostly a consequence of the inherent characteristic of continuous growth, which can lead to a low degree of reproducibility when used in the nanoparticulate form as a delivery tool. It is not clear if the mineralized polyplexes described here have the same drawbacks, given the early development of our mineralization protocols and lack of long-term studies on their stability. Nevertheless, solutions for this issue will be discussed below.

The first strategy for avoiding excessive growth is to work with the minimum concentration necessary for the extent of mineralization desired under the reaction time chosen, such as what was performed in this work. Again, short reaction times are beneficial to minimize any undesirable changes in polyplex properties (i.e., reduced transfection efficiency). While a particle size increase close to 1 μm has been reported as being beneficial for transfection efficiency *in vitro* [8] and in local administration *in vivo* [9] with PEI, for the general case of intravenous delivery of particles, small particle size, ranging from 50 to 100

nm is desired [10]. To further improve control over particle size, modification of the surface of the mineralized polyplexes might be explored with macromolecules that ideally play at least three roles:

(i) calcium binding, occupying sites for mineral growth;

(ii) steric and/or electrostatic stabilization to inhibit agglomeration and aggregation;

(iii) targeting of specific cell receptors, depending on the application.

For a powerful control over size, the synthesis of copolymers with a functionality capable of binding calcium and a long hydrophilic chain is indicated. The capacity to bind calcium ions is necessary either during mineralization or immediately after it, depending on the degree of affinity with calcium. In Chapter 1, it was observed that copolymers formed by organic polymers containing carboxylate groups, mainly poly(acrylic acid) and poly(aspartic acid), attached to poly(ethylene) glycol long chains, have a strong capability of stabilizing mineral particles when present during mineralization. Another possibility is to link bisphosphonate functionalities to the end of long hydrophilic chains. Bisphosphonates are a class of molecules that have very strong calcium binding strength due to the presence of two phosphate groups linked to the same carbon. In Chapter 1, where we reviewed the literature, it was observed that for bisphosphonate modified PEG, the most efficient strategy is to add this molecule immediately after mineralization. This is likely a consequence of the stronger calcium binding that leads to nucleation inhibition when present during mineralization. Since the mineralization reported here was performed under very low supersaturations, already under the presence of a highly negatively charged polyanion, in order to avoid competition, it might be more appropriate to use a bisphosphonate-modified hydrophilic molecule after

the mineralization process is over or to substitute the unmodified poly(aspartic acid) for a copolymer of poly(aspartic acid) and PEG.

Adding targeting functionalities is another challenge that could be tackled by the same strategy. This can be achieved by coupling molecules with strong calcium interaction (bisphosphonates, polyacrylic acid, and polyaspartic acid, among others) with targeting molecules. A whole library of mineral-interacting molecules to modify the mineralized polyplexes reported could then be built. These new compounds (a particle stabilizer and a targeting molecule) could be added at the same time if they had the same class of calcium binding molecule or at different times if they had different calcium binding strengths (one before and another after mineralization).

The route proposed here is to substitute poly(aspartic acid) with a poly(aspartic acid)-modified PEG that could potentially mediate mineralization and stabilize the particles concomitantly, following the addition of a bisphosphonate modified targeting molecule, such as described in Figure 4.1.

A few other studies as a continuation of this thesis are proposed:

1- A in-depth study of the effect of calcium in gene delivery utilizing polyplexes.

Other concentrations and other incubation protocols could be used in order to better access the effect of calcium. For example, calcium could be added before polyplex assembly or in between the steps of polyplex assembly and poly(aspartic acid) addition. A study of calcium-rich formulations for polyplex assembly in order to avoid the use of commercial cell

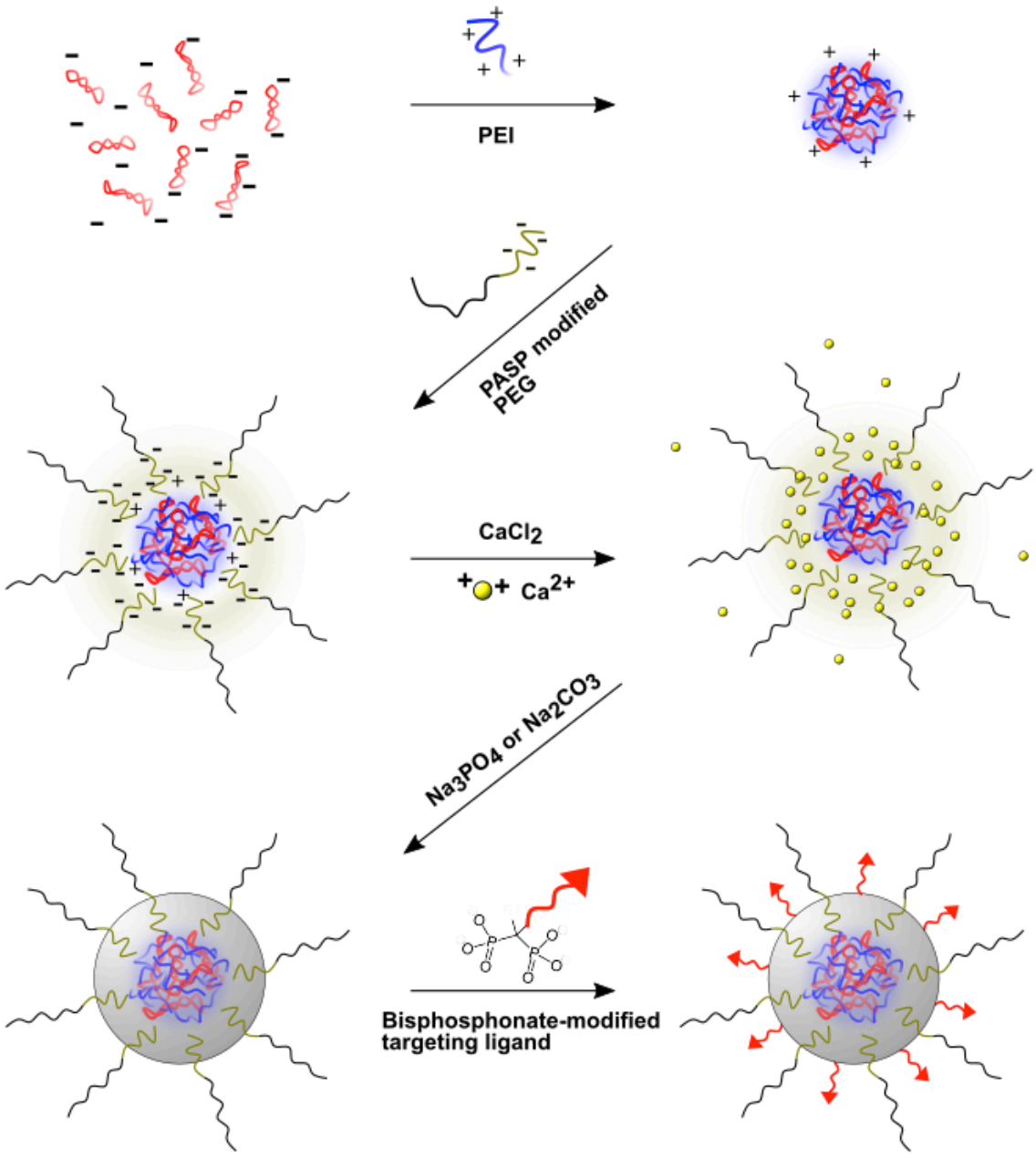

Figure 4.1 Fabrication of a PEG, targeting ligand-functionalized mineralized polyplex for gene delivery.

culture media is also proposed. It will be important to probe the role of calcium on cell binding and internalization of complexes, in addition to its direct effect in polyplex stabilization. Other authors have reported that increased intracellular calcium levels could increase transfection efficiency on its own, however it does not seem to be completely clear

what is the mechanism behind such increase. The effect of calcium is seen in a variety of cell lines, however the effect of calcium varied depending on the cell line and type of carrier used [11]. Indeed, there are studies that suggest that an increase in cytosolic Ca^{2+} can increase endocytosis rates, which could facilitate transfection [12,13]. The effect of calcium has been recently highlighted in bone marrow-derived stem cells transfected with PEI/pDNA polyplexes [14]. It is also proposed that specific pDNA and polyplex interactions with Ca^{2+} resulting in smaller polyplex size might be one reason for improved transfection efficiency [15].

2- ***Study of doping of the mineral phase with therapeutic ions or ions that control mineral solubility and/or have proved therapeutic effect***.

Intracellular delivery of strontium doped calcium phosphate improved markers related to bone regeneration in the co-delivery with pDNA [16] and manganese doped calcium phosphate [17] and carbonate [18] were capable of increasing cancer cell death by generating hydroxyl radicals via reaction with H_2O_2, which is produced in large amounts in cancer cells and tumors. Similar doping strategies could be used in the mineral portion of the mineralized polyplexes by adding soluble salts of the desired therapeutic ions during the mineralization reactions.

3- ***In vivo*** **administration of mineralized polyplexes.**

Mineralization gave viruses increased infection due to increased adhesion to mucosa from the airways and alternative cell uptake pathways [19]. This property was used in viral vaccination to increase local mucosal immunization by administration through airways [20],

which is theorized to be superior in avoiding infections to the respiratory system. Other authors also administered mineralized viral vectors intravenously in diverse applications such as cancer treatment and immunization against the SARS-CoV-2 virus with improved results compared to unmineralized viruses. The Table II in Chapter one can be consulted for more in vivo studies utilizing mineralized viruses. If the improved adhesion to airways by mineralization is materials specific, theoretically it could be observed in non-viral mineralized vectors such as the ones described in this thesis.

4- Study of the protective effect of mineralized polyplexes and incorporation in gene-activated matrices.

In this thesis, mineralization protected the polyplexes against dissociation in aqueous media. For viral vectors, it is observed that mineralization is also capable of providing improved thermostability [21,22]. A more in-depth study of the protective effect of mineralization over polyplexes against heat and other chemicals and physical conditions could be useful to expand the applications of polyplexes by incorporation in gene activated matrices. As an example, mineralization could preserve polyplex function when incorporated into electro-spun mats during the process of electrospinning, in which the use of elevated temperatures, organic solvents, and the drying process and entrapment inside the polymer fiber would be required. Maybe, mineralized polyplexes could be used in electrospinning and other fabrication methods dispersed on the same way as nanometric hydroxyapatite and other inorganic particulate materials currently in use[23].

Calcium incubation and mineralization might have an important role depending on the application desired and might open new applications for the use of polyplexes. If the same

benefits observed with mineralized viruses can be achieved with mineralized polyplexes, such as improved thermostability, improved adhesion to airways, and better immunization in vaccination, mineralized polyplexes could be a safer option compared to mineralized viruses.

4.3 References

[1] H. Zhou, G. Wang, X. Wang, Z. Song, R. Tang, Mineralized State of the Avian Influenza Virus in the Environment, Angewandte Chemie International Edition. 56 (2017) 12908–12912. https://doi.org/10.1002/anie.201705769.

[2] J.E. Kyle, K. Pedersen, F.G. Ferris, Virus Mineralization at Low pH in the Rio Tinto, Spain, Geomicrobiology Journal. 25 (2008) 338–345. https://doi.org/10.1080/01490450802402703.

[3] X. Peng, B. Xu H FAU - Jones, S. Jones B FAU - Chen, H. Chen S FAU - Zhou, H. Zhou, Silicified virus-like nanoparticles in an extreme thermal environment: implications for the preservation of viruses in the geological record, Geobiology. 6 (2013) 511–526.

[4] R. De Wit, P. Gautret, Y. Bettarel, C. Roques, C. Marlière, M. Ramonda, T. Nguyen Thanh, H. Tran Quang, T. Bouvier, Viruses Occur Incorporated in Biogenic High-Mg Calcite from Hypersaline Microbial Mats, PLOS ONE. 10 (2015) e0130552. https://doi.org/10.1371/journal.pone.0130552.

[5] T. Kokubo, H. Takadama, How useful is SBF in predicting in vivo bone bioactivity?, Biomaterials. 27 (2006) 2907–2915. https://doi.org/https://doi.org/10.1016/j.biomaterials.2006.01.017.

[6] Y. Sang, K. Xie, Y. Mu, Y. Lei, B. Zhang, S. Xiong, Y. Chen, N. Qi, Salt ions and related parameters affect PEI-DNA particle size and transfection efficiency in Chinese hamster ovary cells, Cytotechnology. 67 (2015) 67–74. https://doi.org/10.1007/s10616-013-9658-z.

[7] Z. Zhou, L. Zhang, J. Li, Y. Shi, Z. Wu, H. Zheng, Z. Wang, W. Zhao, H. Pan, Q. Wang, X. Jin, X. Zhang, R. Tang, B. Fu, Polyelectrolyte-calcium Complexes as a Pre-precursor Induce Biomimetic Mineralization of Collagen, Nanoscale. (2020). https://doi.org/10.1039/D0NR05640E.

[8] W.J. Peterson, K.H. Tachiki, D.T. Yamaguchi, Serial passage of MC3T3-E1 cells down-regulates proliferation during osteogenesis in vitro, Cell Proliferation. 37 (2004) 325–336. https://doi.org/https://doi.org/10.1111/j.1365-2184.2004.00316.x.

[9] X.-Z. Yan, W. Yang, F. Yang, M. Kersten-Niessen, J.A. Jansen, S.K. Both, Effects of Continuous Passaging on Mineralization of MC3T3-E1 Cells with Improved Osteogenic Culture Protocol, Tissue Engineering Part C: Methods. 20 (2013) 198–204. https://doi.org/10.1089/ten.tec.2012.0412.

[10] J. Cao, X. Wu, X. Qin, Z. Li, Uncovering the Effect of Passage Number on HT29 Cell Line Based on the Cell Metabolomic Approach, Journal of Proteome Research. 20 (2021) 1582–1590. https://doi.org/10.1021/acs.jproteome.0c00806.

[11] S.J. Lee, K.H. Min, H.J. Lee, A.N. Koo, H.P. Rim, B.J. Jeon, S.Y. Jeong, J.S. Heo, S.C. Lee, Ketal Cross-Linked Poly(ethylene glycol)-Poly(amino acid)s Copolymer Micelles for Efficient Intracellular Delivery of Doxorubicin, Biomacromolecules. 12 (2011) 1224–1233. https://doi.org/10.1021/bm101517x.

[12] L. Eliasson, P. Proks, C. Ammälä, F.M. Ashcroft, K. Bokvist, E. Renström, P. Rorsman, P.A. Smith, Endocytosis of secretory granules in mouse pancreatic beta-cells evoked by transient elevation of cytosolic calcium, The Journal of Physiology. 493 (Pt 3 (1996) 755–767. https://doi.org/10.1113/jphysiol.1996.sp021420.

[13] X. Wang, X. Liu, Y. Xiao, H. Hao, Y. Zhang, R. Tang, Biomineralization State of Viruses and Their Biological Potential, Chemistry – A European Journal. 24 (2018) 11518–11529. https://doi.org/10.1002/chem.201705936.

[14] F. Nudelman, K. Pieterse, A. George, P.H.H. Bomans, H. Friedrich, L.J. Brylka, P.A.J. Hilbers, G. de With, N.A.J.M. Sommerdijk, The role of collagen in bone apatite formation in the presence of hydroxyapatite nucleation inhibitors, Nature Materials. 9 (2010) 1004–1009. https://doi.org/10.1038/nmat2875.

[15] G. Wang, R.-Y. Cao, R. Chen, L. Mo, J.-F. Han, X. Wang, X. Xu, T. Jiang, Y.-Q. Deng, K. Lyu, S.-Y. Zhu, E.-D. Qin, R. Tang, C.-F. Qin, Rational design of thermostable vaccines by engineered peptide-induced virus self-biomineralization under physiological conditions, Proceedings of the National Academy of Sciences. 110 (2013) 7619–7624. https://doi.org/10.1073/pnas.1300233110.

[16] B.J. Kim, K.H. Min, G.H. Hwang, H.J. Lee, S.Y. Jeong, E.-C. Kim, S.C. Lee, Calcium carbonate-mineralized polymer nanoparticles for pH-responsive robust nanocarriers of docetaxel, Macromolecular Research. 23 (2015) 111–117. https://doi.org/10.1007/s13233-015-3020-6.

[17] D. Barati, J.D. Walters, S.R. Pajoum Shariati, S. Moeinzadeh, E. Jabbari, Effect of Organic Acids on Calcium Phosphate Nucleation and Osteogenic Differentiation of Human Mesenchymal Stem Cells on Peptide Functionalized Nanofibers, Langmuir. 31 (2015) 5130–5140. https://doi.org/10.1021/acs.langmuir.5b00615.

[18] K.K. Perkin, J.L. Turner, K.L. Wooley, S. Mann, Fabrication of Hybrid

Nanocapsules by Calcium Phosphate Mineralization of Shell Cross-Linked Polymer Micelles and Nanocages, Nano Letters. 5 (2005) 1457–1461. https://doi.org/10.1021/nl050817w.

[19] L.-L. Huang, X. Li, J. Zhang, Q.R. Zhao, M.J. Zhang, A.-A. Liu, D.-W. Pang, H.-Y. Xie, MnCaCs-Biomineralized Oncolytic Virus for Bimodal Imaging-Guided and Synergistically Enhanced Anticancer Therapy, Nano Letters. 19 (2019) 8002–8009. https://doi.org/10.1021/acs.nanolett.9b03193.

[20] J. Chen, P. Gao, S. Yuan, R. Li, A. Ni, L. Chu, L. Ding, Y. Sun, X.-Y. Liu, Y. Duan, Oncolytic Adenovirus Complexes Coated with Lipids and Calcium Phosphate for Cancer Gene Therapy, ACS Nano. 10 (2016) 11548–11560. https://doi.org/10.1021/acsnano.6b06182.

[21] H. Jiang, X.-Y. Liu, G. Zhang, Y. Li, Kinetics and Template Nucleation of Self-Assembled Hydroxyapatite Nanocrystallites by Chondroitin Sulfate, Journal of Biological Chemistry . 280 (2005) 42061–42066. https://doi.org/10.1074/jbc.M412280200.

[22] S. Wang, Y. Yang, R. Wang, X. Kong, X. Wang, Mineralization of calcium phosphate controlled by biomimetic self-assembled peptide monolayers via surface electrostatic potentials, Bioactive Materials. 5 (2020) 387–397. https://doi.org/https://doi.org/10.1016/j.bioactmat.2020.03.003.

[23] M. Tanahashi, T. Matsuda, Surface functional group dependence on apatite formation on self-assembled monolayers in a simulated body fluid, Journal of Biomedical Materials Research. 34 (1997) 305–315. https://doi.org/10.1002/(SICI)1097-4636(19970305)34:3<305::AID-JBM5>3.0.CO;2-O.

[24] K.H. Min, H.J. Lee, K. Kim, I.C. Kwon, S.Y. Jeong, S.C. Lee, The tumor accumulation and therapeutic efficacy of doxorubicin carried in calcium phosphate-reinforced polymer nanoparticles, Biomaterials. 33 (2012) 5788–5797. https://doi.org/https://doi.org/10.1016/j.biomaterials.2012.04.057.

[25] Z. Xu, L. Shi, D. Hu, B. Hu, M. Yang, L. Zhu, Formation of hierarchical bone-like apatites on silk microfiber templates: Via biomineralization, RSC Advances. 6 (2016) 76426–76433. https://doi.org/10.1039/c6ra17199k.

[26] K. Yamashita, N. Oikawa, T. Umegaki, Acceleration and Deceleration of Bone-Like Crystal Growth on Ceramic Hydroxyapatite by Electric Poling, Chemistry of Materials. 8 (1996) 2697–2700. https://doi.org/10.1021/cm9602858.

[27] Y. Xie, X. Liu, P.K. Chu, C. Ding, Nucleation and growth of calcium–phosphate on Ca-implanted titanium surface, Surface Science. 600 (2006) 651–656. https://doi.org/https://doi.org/10.1016/j.susc.2005.11.016.

[28] M. OHGAKI, S. NAKAMURA, T. OKURA, K. YAMASHITA, Enhanced

Mineralization on Electrically Polarized Hydroxyapatite Ceramics in Culture Medium, Journal of the Ceramic Society of Japan. 108 (2000) 1037–1040. https://doi.org/10.2109/jcersj.108.1263_1037.

[29] E. Buck, S. Lee, Q. Gao, S.D. Tran, F. Tamimi, L.S. Stone, M. Cerruti, The Role of Surface Chemistry in the Osseointegration of PEEK Implants, ACS Biomaterials Science & Engineering. 8 (2022) 1506–1521. https://doi.org/10.1021/acsbiomaterials.1c01434.

[30] F. Nudelman, A.J. Lausch, N.A.J.M. Sommerdijk, E.D. Sone, In vitro models of collagen biomineralization, Journal of Structural Biology. 183 (2013) 258–269. https://doi.org/10.1016/j.jsb.2013.04.003.

[31] G. Dördelmann, D. Kozlova, S. Karczewski, R. Lizio, S. Knauer, M. Epple, Calcium phosphate increases the encapsulation efficiency of hydrophilic drugs (proteins, nucleic acids) into poly(d,l-lactide-co-glycolide acid) nanoparticles for intracellular delivery, Journal of Materials Chemistry B. 2 (2014) 7250–7259. https://doi.org/10.1039/C4TB00922C.

[32] L. Niu, S.E. Jee, K. Jiao, L. Tonggu, M. Li, L. Wang, Y. Yang, J. Bian, L. Breschi, S.S. Jang, J. Chen, D.H. Pashley, F.R. Tay, Collagen intrafibrillar mineralization as a result of the balance between osmotic equilibrium and electroneutrality, Nature Materials. 16 (2017) 370–378. https://doi.org/10.1038/nmat4789.

[33] M. Tavafoghi, N. Brodusch, R. Gauvin, M. Cerruti, Hydroxyapatite formation on graphene oxide modified with amino acids: arginine versus glutamic acid, Journal of The Royal Society Interface. 13 (2016) 20150986. https://doi.org/10.1098/rsif.2015.0986.

[34] M. Valiskó, D. Boda, D. Gillespie, Selective Adsorption of Ions with Different Diameter and Valence at Highly Charged Interfaces, The Journal of Physical Chemistry C. 111 (2007) 15575–15585. https://doi.org/10.1021/jp073703c.

[35] P. Zhu, Y. Masuda, K. Koumoto, The effect of surface charge on hydroxyapatite nucleation, Biomaterials. 25 (2004) 3915–3921. https://doi.org/https://doi.org/10.1016/j.biomaterials.2003.10.022.

[36] G.K. Toworfe, R.J. Composto, I.M. Shapiro, P. Ducheyne, Nucleation and growth of calcium phosphate on amine-, carboxyl- and hydroxyl-silane self-assembled monolayers, Biomaterials. 27 (2006) 631–642. https://doi.org/https://doi.org/10.1016/j.biomaterials.2005.06.017.

[37] S. Bodhak, S. Bose, A. Bandyopadhyay, Role of surface charge and wettability on early stage mineralization and bone cell–materials interactions of polarized hydroxyapatite, Acta Biomaterialia. 5 (2009) 2178–2188. https://doi.org/https://doi.org/10.1016/j.actbio.2009.02.023.

[38] I. HIRATA, M. AKAMATSU, E. FUJII, S. POOLTHONG, M. OKAZAKI, Chemical analyses of hydroxyapatite formation on SAM surfaces modified with COOH, NH₂, CH₃, and OH functions, Dental Materials Journal. 29 (2010) 438–445. https://doi.org/10.4012/dmj.2010-017.

[39] H.J. Lee, S.E. Kim, I.K. Kwon, C. Park, C. Kim, J. Yang, S.C. Lee, Spatially mineralized self-assembled polymeric nanocarriers with enhanced robustness and controlled drug-releasing property, Chemical Communications. 46 (2010) 377–379. https://doi.org/10.1039/B913732G.

[40] H.S. Han, J. Lee, H.R. Kim, S.Y. Chae, M. Kim, G. Saravanakumar, H.Y. Yoon, D.G. You, H. Ko, K. Kim, I.C. Kwon, J.C. Park, J.H. Park, Robust PEGylated hyaluronic acid nanoparticles as the carrier of doxorubicin: Mineralization and its effect on tumor targetability in vivo, Journal of Controlled Release. 168 (2013) 105–114. https://doi.org/https://doi.org/10.1016/j.jconrel.2013.02.022.

[41] Y. Lv, H. Huang, B. Yang, H. Liu, Y. Li, J. Wang, A robust pH-sensitive drug carrier: Aqueous micelles mineralized by calcium phosphate based on chitosan, Carbohydrate Polymers. 111 (2014) 101–107. https://doi.org/https://doi.org/10.1016/j.carbpol.2014.04.082.

[42] P. Chen, Y. Liu, J. Zhao, X. Pang, P. Zhang, X. Hou, P. Chen, C. He, Z. Wang, Z. Chen, The synthesis of amphiphilic polyethyleneimine/calcium phosphate composites for bispecific T-cell engager based immunogene therapy, Biomaterials Science. 6 (2018) 633–641. https://doi.org/10.1039/C7BM01143A.

[43] T. A. Dick, H. Uludağ, Mineralized polyplexes for gene delivery: Improvement of transfection efficiency as a consequence of calcium incubation and not mineralization, Materials Science and Engineering: C. 129 (2021) 112419. https://doi.org/https://doi.org/10.1016/j.msec.2021.112419.

[44] T. Atz Dick, H. Uludağ, A Polyplex in a Shell: The Effect of Poly(aspartic acid)-Mediated Calcium Carbonate Mineralization on Polyplexes Properties and Transfection Efficiency, Molecular Pharmaceutics. (2022). https://doi.org/10.1021/acs.molpharmaceut.1c00909.

[45] S.-X. Xie, A.A. Baoum, N.A. Alhakamy, C.J. Berkland, Calcium enhances gene expression when using low molecular weight poly-l-lysine delivery vehicles, International Journal of Pharmaceutics. 547 (2018) 274–281. https://doi.org/https://doi.org/10.1016/j.ijpharm.2018.05.067.

[46] V.S.S.A. Ayyadevara, K.-H. Roh, Calcium enhances polyplex-mediated transfection efficiency of plasmid DNA in Jurkat cells, Drug Delivery. 27 (2020) 805–815. https://doi.org/10.1080/10717544.2020.1770371.

[47] D. Pezzoli, E. Giupponi, D. Mantovani, G. Candiani, Size matters for in vitro gene delivery: investigating the relationships among complexation protocol, transfection medium, size and sedimentation, Scientific Reports. 7 (2017) 44134.

https://doi.org/10.1038/srep44134.

[48] W. Zhang, X. Kang, B. Yuan, H. Wang, T. Zhang, M. Shi, Z. Zheng, Y. Zhang, C. Peng, X. Fan, H. Yang, Y. Shen, Y. Huang, Nano-Structural Effects on Gene Transfection: Large, Botryoid-Shaped Nanoparticles Enhance DNA Delivery via Macropinocytosis and Effective Dissociation, Theranostics. 9 (2019) 1580–1598. https://doi.org/10.7150/thno.30302.

[49] S. Behzadi, V. Serpooshan, W. Tao, M.A. Hamaly, M.Y. Alkawareek, E.C. Dreaden, D. Brown, A.M. Alkilany, O.C. Farokhzad, M. Mahmoudi, Cellular uptake of nanoparticles: journey inside the cell, Chemical Society Reviews. 46 (2017) 4218–4244. https://doi.org/10.1039/C6CS00636A.

[50] A.M.I. Lam, P.R. Cullis, Calcium enhances the transfection potency of plasmid DNA–cationic liposome complexes, Biochimica et Biophysica Acta (BBA) - Biomembranes. 1463 (2000) 279–290. https://doi.org/https://doi.org/10.1016/S0005-2736(99)00219-9.

[51] R.J. Epstein, B.J. Druker, J.C. Irminger, S.D. Jones, T.M. Roberts, C.D. Stiles, Extracellular calcium mimics the actions of platelet-derived growth factor on mouse fibroblasts, Cell Growth Differentiation. 3 (1992) 157–164. http://cgd.aacrjournals.org/cgi/content/abstract/3/3/157.

[52] T. Acri, N. Laird, S. Geary, Effects of calcium concentration on nonviral gene delivery to bone marrow-derived stem cells., J Tissue Eng Regen Med. (2019) 2256–2265.

[53] R. Khalifehzadeh, H. Arami, DNA-Templated Strontium-Doped Calcium Phosphate Nanoparticles for Gene Delivery in Bone Cells, ACS Biomaterials Science and Engineering. 5 (2019) 3201–3211. https://doi.org/10.1021/acsbiomaterials.8b01587.

[54] L.-H. Fu, Y.-R. Hu, C. Qi, T. He, S. Jiang, C. Jiang, J. He, J. Qu, J. Lin, P. Huang, Biodegradable Manganese-Doped Calcium Phosphate Nanotheranostics for Traceable Cascade Reaction-Enhanced Anti-Tumor Therapy, ACS Nano. 13 (2019) 13985–13994. https://doi.org/10.1021/acsnano.9b05836.

[55] H. Zhou, X. Wang, R. Tang, Could a mineralized state of avian flu virus be dangerous to humans?, Future Virology. 13 (2018) 79–81. https://doi.org/10.2217/fvl-2017-0142.

[56] X. Wang, D. Yang, S. Li, X. Xu, C.-F. Qin, R. Tang, Biomineralized vaccine nanohybrid for needle-free intranasal immunization, Biomaterials. 106 (2016) 286–294. https://doi.org/https://doi.org/10.1016/j.biomaterials.2016.08.035.

[57] S. Luo, P. Zhang, P. Zou, C. Wang, B. Liu, C. Wu, T. Li, L. Zhang, Y. Zhang, C. Li, A Self-Biomineralized Novel Adenovirus Vectored COVID-19 Vaccine for Boosting Immunization of Mice, Virologica Sinica. (2021).

https://doi.org/10.1007/s12250-021-00434-3.

[58] A.A. Shitole, P.W. Raut, N. Sharma, P. Giram, A.P. Khandwekar, B. Garnaik, Electrospun polycaprolactone/hydroxyapatite/ZnO nanofibers as potential biomaterials for bone tissue regeneration, Journal of Materials Science: Materials in Medicine. 30 (2019) 51. https://doi.org/10.1007/s10856-019-6255-5.

References

Chapter 1

[1] M.H. Amer, Gene therapy for cancer: present status and future perspective, Molecular and Cellular Therapies. 2 (2014) 27. https://doi.org/10.1186/2052-8426-2-27.

[2] M. Cucchiarini, A.L. McNulty, R.L. Mauck, L.A. Setton, F. Guilak, H. Madry, Advances in combining gene therapy with cell and tissue engineering-based approaches to enhance healing of the meniscus, Osteoarthritis and Cartilage. 24 (2016) 1330–1339. https://doi.org/https://doi.org/10.1016/j.joca.2016.03.018.

[3] C.E. Dunbar, K.A. High, J.K. Joung, D.B. Kohn, K. Ozawa, M. Sadelain, Gene therapy comes of age, Science. 359 (2018) eaan4672. https://doi.org/10.1126/science.aan4672.

[4] T. Friedmann, R. Roblin, Gene Therapy for Human Genetic Disease?, Science. 175 (1972) 949 LP – 955. https://doi.org/10.1126/science.175.4025.949.

[5] S.M. Elbashir, J. Harborth, W. Lendeckel, A. Yalcin, K. Weber, T. Tuschl, Duplexes of 21-nucleotide RNAs mediate RNA interference in cultured mammalian cells, Nature. 411 (2001) 494–498. https://doi.org/10.1038/35078107.

[6] A.P. McCaffrey, L. Meuse, T.-T.T. Pham, D.S. Conklin, G.J. Hannon, M.A. Kay, RNA interference in adult mice, Nature. 418 (2002) 38–39. https://doi.org/10.1038/418038a.

[7] D. Grimm, M.A. Kay, Therapeutic application of RNAi: is mRNA targeting finally ready for prime time?, The Journal of Clinical Investigation. 117 (2007) 3633–3641. https://doi.org/10.1172/JCI34129.

[8] C.L. Hardee, L.M. Arévalo-Soliz, B.D. Hornstein, L. Zechiedrich, Advances in Non-Viral DNA Vectors for Gene Therapy, Genes. 8 (2017) 65. https://doi.org/10.3390/genes8020065.

[9] S.E. Raper, N. Chirmule, F.S. Lee, N.A. Wivel, A. Bagg, G. Gao, J.M. Wilson, M.L. Batshaw, Fatal systemic inflammatory response syndrome in a ornithine transcarbamylase deficient patient following adenoviral gene transfer, Molecular Genetics and Metabolism. 80 (2003) 148–158. https://doi.org/https://doi.org/10.1016/j.ymgme.2003.08.016.

[10] V. Picanço-Castro, C.G. Pereira, D.T. Covas, G.S. Porto, A. Athanassiadou, M.L. Figueiredo, Emerging patent landscape for non-viral vectors used for gene therapy, Nature Biotechnology. 38 (2020) 151–157. https://doi.org/10.1038/s41587-019-

0402-x.

[11] Z. Xiong, C.S. Alves, J. Wang, A. Li, J. Liu, M. Shen, J. Rodrigues, H. Tomás, X. Shi, Zwitterion-functionalized dendrimer-entrapped gold nanoparticles for serum-enhanced gene delivery to inhibit cancer cell metastasis, Acta Biomaterialia. 99 (2019) 320–329. https://doi.org/10.1016/j.actbio.2019.09.005.

[12] K. Bates, K. Kostarelos, Carbon nanotubes as vectors for gene therapy: Past achievements, present challenges and future goals, Advanced Drug Delivery Reviews. 65 (2013) 2023–2033. https://doi.org/https://doi.org/10.1016/j.addr.2013.10.003.

[13] J. Dobson, Gene therapy progress and prospects: magnetic nanoparticle-based gene delivery, Gene Therapy. 13 (2006) 283–287. https://doi.org/10.1038/sj.gt.3302720.

[14] H. Lv, S. Zhang, B. Wang, S. Cui, J. Yan, Toxicity of cationic lipids and cationic polymers in gene delivery, Journal of Controlled Release. 114 (2006) 100–109. https://doi.org/https://doi.org/10.1016/j.jconrel.2006.04.014.

[15] R. Khalifehzadeh, H. Arami, Biodegradable calcium phosphate nanoparticles for cancer therapy, Advances in Colloid and Interface Science. 279 (2020). https://doi.org/10.1016/j.cis.2020.102157.

[16] W. Habraken, P. Habibovic, M. Epple, M. Bohner, Calcium phosphates in biomedical applications: materials for the future?, Materials Today. 19 (2016) 69–87. https://doi.org/https://doi.org/10.1016/j.mattod.2015.10.008.

[17] L. Guo, L. Wang, R. Yang, R. Feng, Z. Li, X. Zhou, Z. Dong, G. Ghartey-Kwansah, M. Xu, M. Nishi, Q. Zhang, W. Isaacs, J. Ma, X. Xu, Optimizing conditions for calcium phosphate mediated transient transfection, Saudi Journal of Biological Sciences. 24 (2017) 622–629. https://doi.org/https://doi.org/10.1016/j.sjbs.2017.01.034.

[18] Y. Wu, W. Gu, J. Tang, Z.P. Xu, Devising new lipid-coated calcium phosphate/carbonate hybrid nanoparticles for controlled release in endosomes for efficient gene delivery, Journal of Materials Chemistry B. 5 (2017) 7194–7203. https://doi.org/10.1039/c7tb01635b.

[19] C.-Q. Wang, M.-Q. Gong, J.-L. Wu, R.-X. Zhuo, S.-X. Cheng, Dual-functionalized calcium carbonate based gene delivery system for efficient gene delivery, RSC Advances. 4 (2014) 38623–38629. https://doi.org/10.1039/C4RA05468G.

[20] Y. Fang, M. Vadlamudi, Y. Huang, X. Guo, Lipid-Coated, pH-Sensitive Magnesium Phosphate Particles for Intracellular Protein Delivery, Pharmaceutical Research. 36 (2019) 81. https://doi.org/10.1007/s11095-019-2607-6.

[21] G. Bhakta, V. Nurcombe, A. Maitra, A. Shrivastava, DNA-encapsulated magnesium phosphate nanoparticles elicit both humoral and cellular immune

responses in mice, Results in Immunology. 4 (2014) 46–53. https://doi.org/10.1016/j.rinim.2014.04.001.

[22] L. Jin, X. Zeng, M. Liu, Y. Deng, N. He, Current Progress in Gene Delivery Technology Based on Chemical Methods and Nano-carriers, Theranostics. 4 (2014) 240–255. https://doi.org/10.7150/thno.6914.

[23] V. Di Mauro, M. Iafisco, N. Salvarani, M. Vacchiano, P. Carullo, G.B. Ramírez-Rodríguez, T. Patrício, A. Tampieri, M. Miragoli, D. Catalucci, Bioinspired negatively charged calcium phosphate nanocarriers for cardiac delivery of MicroRNAs, Nanomedicine. 11 (2016) 891–906. https://doi.org/10.2217/nnm.16.26.

[24] K.-W. Huang, Y.-T. Lai, G.-J. Chern, S.-F. Huang, C.-L. Tsai, Y.-C. Sung, C.-C. Chiang, P.-B. Hwang, T.-L. Ho, R.-L. Huang, T.-Y. Shiue, Y. Chen, S.-K. Wang, Galactose Derivative-Modified Nanoparticles for Efficient siRNA Delivery to Hepatocellular Carcinoma, Biomacromolecules. 19 (2018) 2330–2339. https://doi.org/10.1021/acs.biomac.8b00358.

[25] C. Qiu, W. Wei, J. Sun, H.-T. Zhang, J.-S. Ding, J.-C. Wang, Q. Zhang, Systemic delivery of siRNA by hyaluronan-functionalized calcium phosphate nanoparticles for tumor-targeted therapy, Nanoscale. 8 (2016) 13033–13044. https://doi.org/10.1039/C6NR04034A.

[26] J. Chen, P. Gao, S. Yuan, R. Li, A. Ni, L. Chu, L. Ding, Y. Sun, X.-Y. Liu, Y. Duan, Oncolytic Adenovirus Complexes Coated with Lipids and Calcium Phosphate for Cancer Gene Therapy, ACS Nano. 10 (2016) 11548–11560. https://doi.org/10.1021/acsnano.6b06182.

[27] R. Becker, W. Döring, Kinetische Behandlung der Keimbildung in übersättigten Dämpfen, Annalen Der Physik. 416 (1935) 719–752. https://doi.org/10.1002/andp.19354160806.

[28] J. Frenkel, A General Theory of Heterophase Fluctuations and Pretransition Phenomena, The Journal of Chemical Physics. 7 (1939) 538–547. https://doi.org/10.1063/1.1750484.

[29] M. Volmer, A. Weber, Keimbildung in übersättigten Gebilden, Zeitschrift Für Physikalische Chemie. 119U (1926) 277–301. https://doi.org/https://doi.org/10.1515/zpch-1926-11927.

[30] W.J.E.M. Habraken, J. Tao, L.J. Brylka, H. Friedrich, L. Bertinetti, A.S. Schenk, A. Verch, V. Dmitrovic, P.H.H. Bomans, P.M. Frederik, J. Laven, P. van der Schoot, B. Aichmayer, G. de With, J.J. DeYoreo, N.A.J.M. Sommerdijk, Ion-association complexes unite classical and non-classical theories for the biomimetic nucleation of calcium phosphate, Nature Communications. 4 (2013) 1507. https://doi.org/10.1038/ncomms2490.

[31] P.G. Vekilov, The two-step mechanism of nucleation of crystals in solution, Nanoscale. 2 (2010) 2346–2357. https://doi.org/10.1039/C0NR00628A.

[32] D. Gebauer, M. Kellermeier, J.D. Gale, L. Bergström, H. Cölfen, Pre-nucleation clusters as solute precursors in crystallisation, Chemical Society Reviews. 43 (2014) 2348–2371. https://doi.org/10.1039/C3CS60451A.

[33] P.J.M. Smeets, A.R. Finney, W.J.E.M. Habraken, F. Nudelman, H. Friedrich, J. Laven, J.J. De Yoreo, P.M. Rodger, N.A.J.M. Sommerdijk, A classical view on nonclassical nucleation, Proceedings of the National Academy of Sciences. 114 (2017) E7882 LP-E7890. https://doi.org/10.1073/pnas.1700342114.

[34] D. Gebauer, A. Völkel, H. Cölfen, Stable Prenucleation Calcium Carbonate Clusters, Science. 322 (2008) 1819 LP – 1822. https://doi.org/10.1126/science.1164271.

[35] A.S. Posner, F. Betts, Synthetic amorphous calcium phosphate and its relation to bone mineral structure, Accounts of Chemical Research. 8 (1975) 273–281. https://doi.org/10.1021/ar50092a003.

[36] A. Dey, P.H.H. Bomans, F.A. Müller, J. Will, P.M. Frederik, G. de With, N.A.J.M. Sommerdijk, The role of prenucleation clusters in surface-induced calcium phosphate crystallization, Nature Materials. 9 (2010) 1010–1014. https://doi.org/10.1038/nmat2900.

[37] K. Onuma, A. Ito, Cluster Growth Model for Hydroxyapatite, Chemistry of Materials. 10 (1998) 3346–3351. https://doi.org/10.1021/cm980062c.

[38] O. Bertran, G. Revilla-López, J. Casanovas, L.J. del Valle, P. Turon, J. Puiggalí, C. Alemán, Dissolving Hydroxyolite: A DNA Molecule into Its Hydroxyapatite Mold, Chemistry – A European Journal. 22 (2016) 6631–6636. https://doi.org/10.1002/chem.201600703.

[39] D. Zhao, C.-Q. Wang, R.-X. Zhuo, S.-X. Cheng, Modification of nanostructured calcium carbonate for efficient gene delivery, Colloids and Surfaces B: Biointerfaces. 118 (2014) 111–116. https://doi.org/https://doi.org/10.1016/j.colsurfb.2014.03.007.

[40] J. Li, Y. Yang, L. Huang, Calcium phosphate nanoparticles with an asymmetric lipid bilayer coating for siRNA delivery to the tumor, Journal of Controlled Release. 158 (2012) 108–114. https://doi.org/https://doi.org/10.1016/j.jconrel.2011.10.020.

[41] L. Pham, H. Ye, F.-L. Cosset, S.J. Russell, K.-W. Peng, Concentration of viral vectors by co-precipitation with calcium phosphate, The Journal of Gene Medicine. 3 (2001) 188–194. https://doi.org/10.1002/1521-2254(2000)9999:9999<::AID-JGM159>3.0.CO;2-9.

[42] J. Zhao, P. Chen, G. Chen, X.J. Pang, P. Huang, X. Hou, Z. Wang, C.-Y. He, Z.-Y. Chen, Controllable synthesis of calcium silicate nanoparticles through one-step microemulsion method for drug and gene delivery, Nanoscience and Nanotechnology Letters. 9 (2017) 1720–1723. https://doi.org/10.1166/nnl.2017.2391.

[43] J. Tang, C.B. Howard, S.M. Mahler, K.J. Thurecht, L. Huang, Z.P. Xu, Enhanced delivery of siRNA to triple negative breast cancer cells in vitro and in vivo through functionalizing lipid-coated calcium phosphate nanoparticles with dual target ligands, Nanoscale. 10 (2018) 4258–4266. https://doi.org/10.1039/C7NR08644J.

[44] M. Puddu, N. Broguiere, D. Mohn, M. Zenobi-Wong, W.J. Stark, R.N. Grass, Magnetically deliverable calcium phosphate nanoparticles for localized gene expression, RSC Advances. 5 (2015) 9997–10004. https://doi.org/10.1039/C4RA13413C.

[45] C. Zelmer, L.P. Zweifel, L.E. Kapinos, I. Craciun, Z.P. Güven, C.G. Palivan, R.Y.H. Lim, Organelle-specific targeting of polymersomes into the cell nucleus, Proceedings of the National Academy of Sciences. 117 (2020) 2770 LP – 2778. https://doi.org/10.1073/pnas.1916395117.

[46] Y. Zeng, B.R. Cullen, RNA interference in human cells is restricted to the cytoplasm, RNA (New York, N.Y.). 8 (2002) 855–860. https://doi.org/10.1017/s1355838202020071.

[47] M.M. Munye, A.D. Tagalakis, J.L. Barnes, R.E. Brown, R.J. McAnulty, S.J. Howe, S.L. Hart, Minicircle DNA Provides Enhanced and Prolonged Transgene Expression Following Airway Gene Transfer, Scientific Reports. 6 (2016) 23125. https://doi.org/10.1038/srep23125.

[48] B.D. Hornstein, D. Roman, L.M. Arévalo-Soliz, M.A. Engevik, L. Zechiedrich, Effects of Circular DNA Length on Transfection Efficiency by Electroporation into HeLa Cells, PLOS ONE. 11 (2016) e0167537. https://doi.org/10.1371/journal.pone.0167537.

[49] P. Kreiss, P. Mailhe, D. Scherman, B. Pitard, B. Cameron, R. Rangara, O. Aguerre-Charriol, M. Airiau, J. Crouzet, Plasmid DNA size does not affect the physicochemical properties of lipoplexes but modulates gene transfer efficiency, Nucleic Acids Research. 27 (1999) 3792–3798. https://doi.org/10.1093/nar/27.19.3792.

[50] J. Mairhofer, R. Grabherr, Rational Vector Design for Efficient Non-viral Gene Delivery: Challenges Facing the Use of Plasmid DNA, Molecular Biotechnology. 39 (2008) 97–104. https://doi.org/10.1007/s12033-008-9046-7.

[51] S.N. Tammam, H.M.E. Azzazy, H.G. Breitinger, A. Lamprecht, Chitosan Nanoparticles for Nuclear Targeting: The Effect of Nanoparticle Size and Nuclear Localization Sequence Density, Molecular Pharmaceutics. 12 (2015) 4277–4289.

https://doi.org/10.1021/acs.molpharmaceut.5b00478.

[52] S.N. Tammam, H.M.E. Azzazy, A. Lamprecht, How successful is nuclear targeting by nanocarriers?, Journal of Controlled Release. 229 (2016) 140–153. https://doi.org/https://doi.org/10.1016/j.jconrel.2016.03.022.

[53] J.D. Larsen, N.L. Ross, M.O. Sullivan, Requirements for the nuclear entry of polyplexes and nanoparticles during mitosis, The Journal of Gene Medicine. 14 (2012) 580–589. https://doi.org/10.1002/jgm.2669.

[54] J.K.W. Lam, M.Y.T. Chow, Y. Zhang, S.W.S. Leung, siRNA Versus miRNA as Therapeutics for Gene Silencing, Molecular Therapy. Nucleic Acids. 4 (2015) e252–e252. https://doi.org/10.1038/mtna.2015.23.

[55] G. Sahay, D.Y. Alakhova, A. V Kabanov, Endocytosis of nanomedicines, Journal of Controlled Release : Official Journal of the Controlled Release Society. 145 (2010) 182–195. https://doi.org/10.1016/j.jconrel.2010.01.036.

[56] F. Niedergang, Phagocytosis, in: R.A. Bradshaw, P.D.B.T.-E. of C.B. Stahl (Eds.), Academic Press, Waltham, 2016: pp. 751–757. https://doi.org/https://doi.org/10.1016/B978-0-12-394447-4.20073-4.

[57] T.U. Wani, S.N. Raza, N.A. Khan, Nanoparticle opsonization: forces involved and protection by long chain polymers, Polymer Bulletin. 77 (2020) 3865–3889. https://doi.org/10.1007/s00289-019-02924-7.

[58] J.A. Champion, A. Walker, S. Mitragotri, Role of particle size in phagocytosis of polymeric microspheres, Pharmaceutical Research. 25 (2008) 1815–1821. https://doi.org/10.1007/s11095-008-9562-y.

[59] C. He, Y. Hu, L. Yin, C. Tang, C. Yin, Effects of particle size and surface charge on cellular uptake and biodistribution of polymeric nanoparticles, Biomaterials. 31 (2010) 3657–3666. https://doi.org/https://doi.org/10.1016/j.biomaterials.2010.01.065.

[60] J.A. Swanson, S. Yoshida, Macropinocytosis, in: R.A. Bradshaw, P.D.B.T.-E. of C.B. Stahl (Eds.), Academic Press, Waltham, 2016: pp. 758–765. https://doi.org/https://doi.org/10.1016/B978-0-12-394447-4.20084-9.

[61] W. Zhang, X. Kang, B. Yuan, H. Wang, T. Zhang, M. Shi, Z. Zheng, Y. Zhang, C. Peng, X. Fan, H. Yang, Y. Shen, Y. Huang, Nano-Structural Effects on Gene Transfection: Large, Botryoid-Shaped Nanoparticles Enhance DNA Delivery via Macropinocytosis and Effective Dissociation, Theranostics. 9 (2019) 1580–1598. https://doi.org/10.7150/thno.30302.

[62] X.-Y. Sun, Q.-Z. Gan, J.-M. Ouyang, Size-dependent cellular uptake mechanism and cytotoxicity toward calcium oxalate on Vero cells, Scientific Reports. 7 (2017) 41949. https://doi.org/10.1038/srep41949.

[63] J. Mercer, A. Helenius, Virus entry by macropinocytosis, Nature Cell Biology. 11 (2009) 510–520. https://doi.org/10.1038/ncb0509-510.

[64] M. Kaksonen, A. Roux, Mechanisms of clathrin-mediated endocytosis, Nature Reviews Molecular Cell Biology. 19 (2018) 313–326. https://doi.org/10.1038/nrm.2017.132.

[65] F.P. G., W.S. E., P.D. S., L.M. P., Caveolin, Caveolae, and Endothelial Cell Function, Arteriosclerosis, Thrombosis, and Vascular Biology. 23 (2003) 1161–1168. https://doi.org/10.1161/01.ATV.0000070546.16946.3A.

[66] S. Kumari, S. MG, S. Mayor, Endocytosis unplugged: multiple ways to enter the cell, Cell Research. 20 (2010) 256–275. https://doi.org/10.1038/cr.2010.19.

[67] P. Foroozandeh, A.A. Aziz, Insight into Cellular Uptake and Intracellular Trafficking of Nanoparticles, Nanoscale Research Letters. 13 (2018) 339. https://doi.org/10.1186/s11671-018-2728-6.

[68] S. Behzadi, V. Serpooshan, W. Tao, M.A. Hamaly, M.Y. Alkawareek, E.C. Dreaden, D. Brown, A.M. Alkilany, O.C. Farokhzad, M. Mahmoudi, Cellular uptake of nanoparticles: journey inside the cell, Chemical Society Reviews. 46 (2017) 4218–4244. https://doi.org/10.1039/C6CS00636A.

[69] Y.-B. Hu, E.B. Dammer, R.-J. Ren, G. Wang, The endosomal-lysosomal system: from acidification and cargo sorting to neurodegeneration, Translational Neurodegeneration. 4 (2015) 18. https://doi.org/10.1186/s40035-015-0041-1.

[70] D.Y.E. Olton, J.M. Close, C.S. Sfeir, P.N. Kumta, Intracellular trafficking pathways involved in the gene transfer of nano-structured calcium phosphate-DNA particles, Biomaterials. 32 (2011) 7662–7670. https://doi.org/https://doi.org/10.1016/j.biomaterials.2011.01.043.

[71] C. Zhou, B. Yu, X. Yang, T. Huo, L.J. Lee, R.F. Barth, R.J. Lee, Lipid-coated nano-calcium-phosphate (LNCP) for gene delivery, International Journal of Pharmaceutics. 392 (2010) 201–208. https://doi.org/10.1016/j.ijpharm.2010.03.012.

[72] L.M.P. Vermeulen, S.C. De Smedt, K. Remaut, K. Braeckmans, The proton sponge hypothesis: Fable or fact?, European Journal of Pharmaceutics and Biopharmaceutics. 129 (2018) 184–190. https://doi.org/https://doi.org/10.1016/j.ejpb.2018.05.034.

[73] L. Wang, J. Lu, F. Xu, F. Zhang, Dynamics of crystallization and dissolution of calcium orthophosphates at the near-molecular level, Chinese Science Bulletin. 56 (2011) 713–721. https://doi.org/10.1007/s11434-010-4184-2.

[74] A.E. Nel, L. Mädler, D. Velegol, T. Xia, E.M. V Hoek, P. Somasundaran, F. Klaessig, V. Castranova, M. Thompson, Understanding biophysicochemical

interactions at the nano–bio interface, Nature Materials. 8 (2009) 543–557. https://doi.org/10.1038/nmat2442.

[75] W. Hu, C. Peng, M. Lv, X. Li, Y. Zhang, N. Chen, C. Fan, Q. Huang, Protein Corona-Mediated Mitigation of Cytotoxicity of Graphene Oxide, ACS Nano. 5 (2011) 3693–3700. https://doi.org/10.1021/nn200021j.

[76] V. Serpooshan, M. Mahmoudi, M. Zhao, K. Wei, S. Sivanesan, K. Motamedchaboki, A. V Malkovskiy, A.B. Goldstone, J.E. Cohen, P.C. Yang, J. Rajadas, D. Bernstein, Y.J. Woo, P. Ruiz-Lozano, Protein Corona Influences Cell–Biomaterial Interactions in Nanostructured Tissue Engineering Scaffolds, Advanced Functional Materials. 25 (2015) 4379–4389. https://doi.org/10.1002/adfm.201500875.

[77] M.P. Monopoli, C. Åberg, A. Salvati, K.A. Dawson, Biomolecular coronas provide the biological identity of nanosized materials, Nature Nanotechnology. 7 (2012) 779–786. https://doi.org/10.1038/nnano.2012.207.

[78] A. Salvati, A.S. Pitek, M.P. Monopoli, K. Prapainop, F.B. Bombelli, D.R. Hristov, P.M. Kelly, C. Åberg, E. Mahon, K.A. Dawson, Transferrin-functionalized nanoparticles lose their targeting capabilities when a biomolecule corona adsorbs on the surface, Nature Nanotechnology. 8 (2013) 137–143. https://doi.org/10.1038/nnano.2012.237.

[79] S. Tenzer, D. Docter, J. Kuharev, A. Musyanovych, V. Fetz, R. Hecht, F. Schlenk, D. Fischer, K. Kiouptsi, C. Reinhardt, K. Landfester, H. Schild, M. Maskos, S.K. Knauer, R.H. Stauber, Rapid formation of plasma protein corona critically affects nanoparticle pathophysiology, Nature Nanotechnology. 8 (2013) 772–781. https://doi.org/10.1038/nnano.2013.181.

[80] F.S.M. Tekie, M. Hajiramezanali, P. Geramifar, M. Raoufi, R. Dinarvand, M. Soleimani, F. Atyabi, Controlling evolution of protein corona: a prosperous approach to improve chitosan-based nanoparticle biodistribution and half-life, Scientific Reports. 10 (2020) 9664. https://doi.org/10.1038/s41598-020-66572-y.

[81] S. Kaga, N.P. Truong, L. Esser, D. Senyschyn, A. Sanyal, R. Sanyal, J.F. Quinn, T.P. Davis, L.M. Kaminskas, M.R. Whittaker, Influence of Size and Shape on the Biodistribution of Nanoparticles Prepared by Polymerization-Induced Self-Assembly, Biomacromolecules. 18 (2017) 3963–3970. https://doi.org/10.1021/acs.biomac.7b00995.

[82] C. Carnovale, G. Bryant, R. Shukla, V. Bansal, Identifying Trends in Gold Nanoparticle Toxicity and Uptake: Size, Shape, Capping Ligand, and Biological Corona, ACS Omega. 4 (2019) 242–256. https://doi.org/10.1021/acsomega.8b03227.

[83] A. Lesniak, F. Fenaroli, M.P. Monopoli, C. Åberg, K.A. Dawson, A. Salvati, Effects of the Presence or Absence of a Protein Corona on Silica Nanoparticle

Uptake and Impact on Cells, ACS Nano. 6 (2012) 5845–5857. https://doi.org/10.1021/nn300223w.

[84] M. Lundqvist, J. Stigler, T. Cedervall, T. Berggård, M.B. Flanagan, I. Lynch, G. Elia, K. Dawson, The Evolution of the Protein Corona around Nanoparticles: A Test Study, ACS Nano. 5 (2011) 7503–7509. https://doi.org/10.1021/nn202458g.

[85] S. Zhang, J. Li, G. Lykotrafitis, G. Bao, S. Suresh, Size-Dependent Endocytosis of Nanoparticles, Advanced Materials. 21 (2009) 419–424. https://doi.org/10.1002/adma.200801393.

[86] H. Yuan, C. Huang, S. Zhang, Virus-inspired design principles of nanoparticle-based bioagents, PloS One. 5 (2010) e13495–e13495. https://doi.org/10.1371/journal.pone.0013495.

[87] B.D. Chithrani, A.A. Ghazani, W.C.W. Chan, Determining the Size and Shape Dependence of Gold Nanoparticle Uptake into Mammalian Cells, Nano Letters. 6 (2006) 662–668. https://doi.org/10.1021/nl052396o.

[88] F. Osaki, T. Kanamori, S. Sando, T. Sera, Y. Aoyama, A Quantum Dot Conjugated Sugar Ball and Its Cellular Uptake. On the Size Effects of Endocytosis in the Subviral Region, Journal of the American Chemical Society. 126 (2004) 6520–6521. https://doi.org/10.1021/ja048792a.

[89] F. Lu, S.-H. Wu, Y. Hung, C.-Y. Mou, Size Effect on Cell Uptake in Well-Suspended, Uniform Mesoporous Silica Nanoparticles, Small. 5 (2009) 1408–1413. https://doi.org/10.1002/smll.200900005.

[90] B.D. Chithrani, W.C.W. Chan, Elucidating the Mechanism of Cellular Uptake and Removal of Protein-Coated Gold Nanoparticles of Different Sizes and Shapes, Nano Letters. 7 (2007) 1542–1550. https://doi.org/10.1021/nl070363y.

[91] S.-H. Wang, C.-W. Lee, A. Chiou, P.-K. Wei, Size-dependent endocytosis of gold nanoparticles studied by three-dimensional mapping of plasmonic scattering images, Journal of Nanobiotechnology. 8 (2010) 33. https://doi.org/10.1186/1477-3155-8-33.

[92] M. Wu, H. Guo, L. Liu, Y. Liu, L. Xie, Size-dependent cellular uptake and localization profiles of silver nanoparticles, International Journal of Nanomedicine. 14 (2019) 4247–4259. https://doi.org/10.2147/IJN.S201107.

[93] N. Hoshyar, S. Gray, H. Han, G. Bao, The effect of nanoparticle size on in vivo pharmacokinetics and cellular interaction, Nanomedicine. 11 (2016) 673–692. https://doi.org/10.2217/nnm.16.5.

[94] J.M. Caster, S.K. Yu, A.N. Patel, N.J. Newman, Z.J. Lee, S.B. Warner, K.T. Wagner, K.C. Roche, X. Tian, Y. Min, A.Z. Wang, Effect of particle size on the biodistribution, toxicity, and efficacy of drug-loaded polymeric nanoparticles in

chemoradiotherapy, Nanomedicine: Nanotechnology, Biology and Medicine. 13 (2017) 1673–1683. https://doi.org/https://doi.org/10.1016/j.nano.2017.03.002.

[95] D. Pezzoli, E. Giupponi, D. Mantovani, G. Candiani, Size matters for in vitro gene delivery: investigating the relationships among complexation protocol, transfection medium, size and sedimentation, Scientific Reports. 7 (2017) 44134. https://doi.org/10.1038/srep44134.

[96] L. Li, W.-S. Xi, Q. Su, Y. Li, G.-H. Yan, Y. Liu, H. Wang, A. Cao, Unexpected Size Effect: The Interplay between Different-Sized Nanoparticles in Their Cellular Uptake, Small. 15 (2019) 1901687. https://doi.org/10.1002/smll.201901687.

[97] N. Hao, L. Li, Q. Zhang, X. Huang, X. Meng, Y. Zhang, D. Chen, F. Tang, L. Li, The shape effect of PEGylated mesoporous silica nanoparticles on cellular uptake pathway in Hela cells, Microporous and Mesoporous Materials. 162 (2012) 14–23. https://doi.org/https://doi.org/10.1016/j.micromeso.2012.05.040.

[98] X. Xie, J. Liao, X. Shao, Q. Li, Y. Lin, The Effect of shape on Cellular Uptake of Gold Nanoparticles in the forms of Stars, Rods, and Triangles, Scientific Reports. 7 (2017) 3827. https://doi.org/10.1038/s41598-017-04229-z.

[99] S.E.A. Gratton, P.A. Ropp, P.D. Pohlhaus, J.C. Luft, V.J. Madden, M.E. Napier, J.M. DeSimone, The effect of particle design on cellular internalization pathways, Proceedings of the National Academy of Sciences. 105 (2008) 11613 LP – 11618. https://doi.org/10.1073/pnas.0801763105.

[100] P.M. Favi, M. Gao, L. Johana Sepúlveda Arango, S.P. Ospina, M. Morales, J.J. Pavon, T.J. Webster, Shape and surface effects on the cytotoxicity of nanoparticles: Gold nanospheres versus gold nanostars, Journal of Biomedical Materials Research Part A. 103 (2015) 3449–3462. https://doi.org/10.1002/jbm.a.35491.

[101] Arnida, A. Malugin, H. Ghandehari, Cellular uptake and toxicity of gold nanoparticles in prostate cancer cells: a comparative study of rods and spheres, Journal of Applied Toxicology. 30 (2010) 212–217. https://doi.org/10.1002/jat.1486.

[102] Arnida, M.M. Janát-Amsbury, A. Ray, C.M. Peterson, H. Ghandehari, Geometry and surface characteristics of gold nanoparticles influence their biodistribution and uptake by macrophages, European Journal of Pharmaceutics and Biopharmaceutics. 77 (2011) 417–423. https://doi.org/https://doi.org/10.1016/j.ejpb.2010.11.010.

[103] E. Fröhlich, The role of surface charge in cellular uptake and cytotoxicity of medical nanoparticles, International Journal of Nanomedicine. 7 (2012) 5577–5591. https://doi.org/10.2147/IJN.S36111.

[104] V. Sokolova, S. Neumann, A. Kovtun, S. Chernousova, R. Heumann, M. Epple, An outer shell of positively charged poly(ethyleneimine) strongly increases the transfection efficiency of calcium phosphate/DNA nanoparticles, Journal of

Materials Science. 45 (2010) 4952–4957. https://doi.org/10.1007/s10853-009-4159-3.

[105] S.M. Moghimi, P. Symonds, J.C. Murray, A.C. Hunter, G. Debska, A. Szewczyk, A two-stage poly(ethylenimine)-mediated cytotoxicity: implications for gene transfer/therapy, Molecular Therapy. 11 (2005) 990–995. https://doi.org/https://doi.org/10.1016/j.ymthe.2005.02.010.

[106] B. Wang, L. Zhang, S.C. Bae, S. Granick, Nanoparticle-induced surface reconstruction of phospholipid membranes, Proceedings of the National Academy of Sciences. 105 (2008) 18171 LP – 18175. https://doi.org/10.1073/pnas.0807296105.

[107] E.C. Cho, J. Xie, P.A. Wurm, Y. Xia, Understanding the Role of Surface Charges in Cellular Adsorption versus Internalization by Selectively Removing Gold Nanoparticles on the Cell Surface with a I2/KI Etchant, Nano Letters. 9 (2009) 1080–1084. https://doi.org/10.1021/nl803487r.

[108] J. Lin, H. Zhang, Z. Chen, Y. Zheng, Penetration of Lipid Membranes by Gold Nanoparticles: Insights into Cellular Uptake, Cytotoxicity, and Their Relationship, ACS Nano. 4 (2010) 5421–5429. https://doi.org/10.1021/nn1010792.

[109] T. Wang, J. Bai, X. Jiang, G.U. Nienhaus, Cellular Uptake of Nanoparticles by Membrane Penetration: A Study Combining Confocal Microscopy with FTIR Spectroelectrochemistry, ACS Nano. 6 (2012) 1251–1259. https://doi.org/10.1021/nn203892h.

[110] K. Xiao, Y. Li, J. Luo, J.S. Lee, W. Xiao, A.M. Gonik, R.G. Agarwal, K.S. Lam, The effect of surface charge on in vivo biodistribution of PEG-oligocholic acid based micellar nanoparticles, Biomaterials. 32 (2011) 3435–3446. https://doi.org/10.1016/j.biomaterials.2011.01.021.

[111] Y. Yamamoto, Y. Nagasaki, Y. Kato, Y. Sugiyama, K. Kataoka, Long-circulating poly(ethylene glycol)–poly(d,l-lactide) block copolymer micelles with modulated surface charge, Journal of Controlled Release. 77 (2001) 27–38. https://doi.org/https://doi.org/10.1016/S0168-3659(01)00451-5.

[112] K. Kobayashi, J. Wei, R. Iida, K. Ijiro, K. Niikura, Surface engineering of nanoparticles for therapeutic applications, Polymer Journal. 46 (2014) 460–468. https://doi.org/10.1038/pj.2014.40.

[113] S.T. Kim, K. Saha, C. Kim, V.M. Rotello, The Role of Surface Functionality in Determining Nanoparticle Cytotoxicity, Accounts of Chemical Research. 46 (2013) 681–691. https://doi.org/10.1021/ar3000647.

[114] D.F. Moyano, M. Goldsmith, D.J. Solfiell, D. Landesman-Milo, O.R. Miranda, D. Peer, V.M. Rotello, Nanoparticle hydrophobicity dictates immune response, Journal of the American Chemical Society. 134 (2012) 1520–5126.

[115] M. Samadi Moghaddam, M. Heiny, V.P. Shastri, Enhanced cellular uptake of nanoparticles by increasing the hydrophobicity of poly(lactic acid) through copolymerization with cell-membrane-lipid components, Chemical Communications. 51 (2015) 14605–14608. https://doi.org/10.1039/C5CC06397C.

[116] H.-Y. Lee, S.H.R. Shin, L.L. Abezgauz, S.A. Lewis, A.M. Chirsan, D.D. Danino, K.J.M. Bishop, Integration of Gold Nanoparticles into Bilayer Structures via Adaptive Surface Chemistry, Journal of the American Chemical Society. 135 (2013) 5950–5953. https://doi.org/10.1021/ja400225n.

[117] Z. Luo, Y. Dai, H. Gao, Development and application of hyaluronic acid in tumor targeting drug delivery, Acta Pharmaceutica Sinica. B. 9 (2019) 1099–1112. https://doi.org/10.1016/j.apsb.2019.06.004.

[118] R.B. KC, C. Kucharski, H. Uludağ, Additive nanocomplexes of cationic lipopolymers for improved non-viral gene delivery to mesenchymal stem cells, Journal of Materials Chemistry B. 3 (2015) 3972–3982. https://doi.org/10.1039/C4TB02101K.

[119] L. Sánchez-del-Campo, M.F. Montenegro, J. Cabezas-Herrera, J.N. Rodríguez-López, The critical role of alpha-folate receptor in the resistance of melanoma to methotrexate, Pigment Cell & Melanoma Research. 22 (2009) 588–600. https://doi.org/10.1111/j.1755-148X.2009.00586.x.

[120] G.L. Zwicke, G. Ali Mansoori, C.J. Jeffery, Utilizing the folate receptor for active targeting of cancer nanotherapeutics, Nano Reviews. 3 (2012) 18496. https://doi.org/10.3402/nano.v3i0.18496.

[121] B. Frigerio, C. Bizzoni, G. Jansen, C.P. Leamon, G.J. Peters, P.S. Low, L.H. Matherly, M. Figini, Folate receptors and transporters: biological role and diagnostic/therapeutic targets in cancer and other diseases, Journal of Experimental & Clinical Cancer Research. 38 (2019) 125. https://doi.org/10.1186/s13046-019-1123-1.

[122] Z. Jiang, J. Guan, J. Qian, C. Zhan, Peptide ligand-mediated targeted drug delivery of nanomedicines, Biomaterials Science. 7 (2019) 461–471. https://doi.org/10.1039/C8BM01340C.

[123] D.A. Richards, A. Maruani, V. Chudasama, Antibody fragments as nanoparticle targeting ligands: a step in the right direction, Chemical Science. 8 (2017) 63–77. https://doi.org/10.1039/C6SC02403C.

[124] Z. Zhou, H. Li, K. Wang, Q. Guo, C. Li, H. Jiang, Y. Hu, D. Oupicky, M. Sun, Bioreducible Cross-Linked Hyaluronic Acid/Calcium Phosphate Hybrid Nanoparticles for Specific Delivery of siRNA in Melanoma Tumor Therapy, ACS Applied Materials & Interfaces. 9 (2017) 14576–14589. https://doi.org/10.1021/acsami.6b15347.

[125] M.S. Lee, J.E. Lee, E. Byun, N.W. Kim, K. Lee, H. Lee, S.J. Sim, D.S. Lee, J.H. Jeong, Target-specific delivery of siRNA by stabilized calcium phosphate nanoparticles using dopa–hyaluronic acid conjugate, Journal of Controlled Release. 192 (2014) 122–130. https://doi.org/https://doi.org/10.1016/j.jconrel.2014.06.049.

[126] J.E. Lee, Y. Yin, S.Y. Lim, E.S. Kim, J. Jung, D. Kim, J.W. Park, M.S. Lee, J.H. Jeong, J.E. Lee, Y. Yin, S.Y. Lim, E.S. Kim, J. Jung, D. Kim, J.W. Park, M.S. Lee, J.H. Jeong, Enhanced Transfection of Human Mesenchymal Stem Cells Using a Hyaluronic Acid/Calcium Phosphate Hybrid Gene Delivery System, Polymers. 11 (2019) 798. https://doi.org/10.3390/polym11050798.

[127] Y. Yang, Y. Hu, Y. Wang, J. Li, F. Liu, L. Huang, Nanoparticle Delivery of Pooled siRNA for Effective Treatment of Non-Small Cell Lung Caner, Molecular Pharmaceutics. 9 (2012) 2280–2289. https://doi.org/10.1021/mp300152v.

[128] Y. Yang, J. Li, F. Liu, L. Huang, Systemic delivery of siRNA via LCP nanoparticle efficiently inhibits lung metastasis, Molecular Therapy. 20 (2012) 609–615. https://doi.org/10.1038/mt.2011.270.

[129] M. Hu, Y. Wang, L. Xu, S. An, Y. Tang, X. Zhou, J. Li, R. Liu, L. Huang, Relaxin gene delivery mitigates liver metastasis and synergizes with check point therapy, Nature Communications. 10 (2019). https://doi.org/10.1038/s41467-019-10893-8.

[130] T.J. Goodwin, Y. Zhou, S.N. Musetti, R. Liu, L. Huang, Local and transient gene expression primes the liver to resist cancer metastasis, Science Translational Medicine. 8 (2016) 364ra153 LP-364ra153. https://doi.org/10.1126/scitranslmed.aag2306.

[131] C.-H. Liu, G.-J. Chern, F.-F. Hsu, K.-W. Huang, Y.-C. Sung, H.-C. Huang, J.T. Qiu, S.-K. Wang, C.-C. Lin, C.-H. Wu, H.-C. Wu, J.-Y. Liu, Y. Chen, A multifunctional nanocarrier for efficient TRAIL-based gene therapy against hepatocellular carcinoma with desmoplasia in mice, Hepatology. 67 (2018) 899–913. https://doi.org/10.1002/hep.29513.

[132] K.-W. Huang, F.-F. Hsu, J.T. Qiu, G.-J. Chern, Y.-A. Lee, C.-C. Chang, Y.-T. Huang, Y.-C. Sung, C.-C. Chiang, R.-L. Huang, C.-C. Lin, T.K. Dinh, H.-C. Huang, Y.-C. Shih, D. Alson, C.-Y. Lin, Y.-C. Lin, P.-C. Chang, S.-Y. Lin, Y. Chen, Highly efficient and tumor-selective nanoparticles for dual-targeted immunogene therapy against cancer, Science Advances. 6 (2020) eaax5032. https://doi.org/10.1126/sciadv.aax5032.

[133] Y. Wu, W. Gu, Z.P. Xu, Enhanced combination cancer therapy using lipid-calcium carbonate/phosphate nanoparticles as a targeted delivery platform, Nanomedicine. 14 (2019) 77–92. https://doi.org/10.2217/nnm-2018-0252.

[134] V. Sokolova, Z. Shi, S. Huang, Y. Du, M. Kopp, A. Frede, T. Knuschke, J. Buer, D. Yang, J. Wu, A.M. Westendorf, M. Epple, Delivery of the TLR ligand poly(I:C) to liver cells in vitro and in vivo by calcium phosphate nanoparticles leads to a

pronounced immunostimulation, Acta Biomaterialia. 64 (2017) 401–410. https://doi.org/10.1016/j.actbio.2017.09.037.

[135] S. Li, B. Wang, S. Jiang, Y. Pan, Y. Shi, W. Kong, Y. Shan, Surface-Functionalized Silica-Coated Calcium Phosphate Nanoparticles Efficiently Deliver DNA-Based HIV-1 Trimeric Envelope Vaccines against HIV-1, ACS Applied Materials & Interfaces. 13 (2021) 53630–53645. https://doi.org/10.1021/acsami.1c16989.

[136] F.L. Graham, A.J. van der Eb, A new technique for the assay of infectivity of human adenovirus 5 DNA, Virology. 52 (1973) 456–467. https://doi.org/https://doi.org/10.1016/0042-6822(73)90341-3.

[137] F.L. Graham, This Week's Citation Classic - A new technique for the assay of infectivity of human adenovirus 5 DNA., (1988) 1. http://garfield.library.upenn.edu/classics1988/A1988Q713500001.pdf.

[138] M. Jordan, A. Schallhorn, F.M. Wurm, Transfecting Mammalian Cells: Optimization of Critical Parameters Affecting Calcium-Phosphate Precipitate Formation, Nucleic Acids Research. 24 (1996) 596–601. https://doi.org/10.1093/nar/24.4.596.

[139] B. Goetze, B. Grunewald, S. Baldassa, M. Kiebler, Chemically controlled formation of a DNA/calcium phosphate coprecipitate: Application for transfection of mature hippocampal neurons, Journal of Neurobiology. 60 (2004) 517–525. https://doi.org/10.1002/neu.20073.

[140] D. Olton, J. Li, M.E. Wilson, T. Rogers, J. Close, L. Huang, P.N. Kumta, C. Sfeir, Nanostructured calcium phosphates (NanoCaPs) for non-viral gene delivery: Influence of the synthesis parameters on transfection efficiency, Biomaterials. 28 (2007) 1267–1279. https://doi.org/https://doi.org/10.1016/j.biomaterials.2006.10.026.

[141] M.A. Khan, V.M. Wu, S. Ghosh, V. Uskoković, Gene delivery using calcium phosphate nanoparticles: Optimization of the transfection process and the effects of citrate and poly(l-lysine) as additives, Journal of Colloid and Interface Science. 471 (2016) 48–58. https://doi.org/https://doi.org/10.1016/j.jcis.2016.03.007.

[142] L. Wang, G.H. Nancollas, Calcium orthophosphates: crystallization and dissolution, Chemical Reviews. 108 (2008) 4628–4669. https://doi.org/10.1021/cr0782574.

[143] H.-B. Pan, B.W. Darvell, Calcium Phosphate Solubility: The Need for Re-Evaluation, Crystal Growth & Design. 9 (2009) 639–645. https://doi.org/10.1021/cg801118v.

[144] J. Jeong, J.H. Kim, J.H. Shim, N.S. Hwang, C.Y. Heo, Bioactive calcium phosphate materials and applications in bone regeneration, Biomaterials Research. 23 (2019) 4. https://doi.org/10.1186/s40824-018-0149-3.

[145] D.J. HADJIDAKIS, I.I. ANDROULAKIS, Bone Remodeling, Annals of the New York Academy of Sciences. 1092 (2006) 385–396. https://doi.org/10.1196/annals.1365.035.

[146] S. Shekhar, A. Roy, D. Hong, P.N. Kumta, Nanostructured silicate substituted calcium phosphate (NanoSiCaPs) nanoparticles — Efficient calcium phosphate based non-viral gene delivery systems, Materials Science and Engineering: C. 69 (2016) 486–495. https://doi.org/https://doi.org/10.1016/j.msec.2016.06.076.

[147] X. Huang, D. Andina, J. Ge, A. Labarre, J.-C. Leroux, B. Castagner, Characterization of Calcium Phosphate Nanoparticles Based on a PEGylated Chelator for Gene Delivery, ACS Applied Materials & Interfaces. 9 (2017) 10435–10445. https://doi.org/10.1021/acsami.6b15925.

[148] S. Chen, F. Li, R.-X. Zhuo, S.-X. Cheng, Efficient non-viral gene delivery mediated by nanostructured calcium carbonate in solution-based transfection and solid-phase transfection, Molecular BioSystems. 7 (2011) 2841–2847. https://doi.org/10.1039/C1MB05147D.

[149] G. Bhakta, S. Mitra, A. Maitra, DNA encapsulated magnesium and manganous phosphate nanoparticles: potential non-viral vectors for gene delivery, Biomaterials. 26 (2005) 2157–2163. https://doi.org/https://doi.org/10.1016/j.biomaterials.2004.06.039.

[150] E. V Giger, B. Castagner, J. Räikkönen, J. Mönkkönen, J.-C. Leroux, siRNA Transfection with Calcium Phosphate Nanoparticles Stabilized with PEGylated Chelators, Advanced Healthcare Materials. 2 (2013) 134–144. https://doi.org/10.1002/adhm.201200088.

[151] F. Pittella, K. Miyata, Y. Maeda, T. Suma, S. Watanabe, Q. Chen, R.J. Christie, K. Osada, N. Nishiyama, K. Kataoka, Pancreatic cancer therapy by systemic administration of VEGF siRNA contained in calcium phosphate/charge-conversional polymer hybrid nanoparticles, Journal of Controlled Release. 161 (2012) 868–874. https://doi.org/https://doi.org/10.1016/j.jconrel.2012.05.005.

[152] J. Li, Y.-C. Chen, Y.-C. Tseng, S. Mozumdar, L. Huang, Biodegradable calcium phosphate nanoparticle with lipid coating for systemic siRNA delivery, Journal of Controlled Release. 142 (2010) 416–421. https://doi.org/https://doi.org/10.1016/j.jconrel.2009.11.008.

[153] B. Sun, K.K. Tran, H. Shen, Enabling customization of non-viral gene delivery systems for individual cell types by surface-induced mineralization, Biomaterials. 30 (2009) 6386–6393. https://doi.org/https://doi.org/10.1016/j.biomaterials.2009.08.006.

[154] B. Neuhaus, B. Tosun, O. Rotan, A. Frede, A.M. Westendorf, M. Epple, Nanoparticles as transfection agents: a comprehensive study with ten different cell lines, RSC Advances. 6 (2016) 18102–18112.

https://doi.org/10.1039/C5RA25333K.

[155] T. A. Dick, H. Uludağ, Mineralized polyplexes for gene delivery: Improvement of transfection efficiency as a consequence of calcium incubation and not mineralization, Materials Science and Engineering: C. 129 (2021) 112419. https://doi.org/https://doi.org/10.1016/j.msec.2021.112419.

[156] L.-L. Huang, X. Li, J. Zhang, Q.R. Zhao, M.J. Zhang, A.-A. Liu, D.-W. Pang, H.-Y. Xie, MnCaCs-Biomineralized Oncolytic Virus for Bimodal Imaging-Guided and Synergistically Enhanced Anticancer Therapy, Nano Letters. 19 (2019) 8002–8009. https://doi.org/10.1021/acs.nanolett.9b03193.

[157] F. Pittella, H. Cabral, Y. Maeda, P. Mi, S. Watanabe, H. Takemoto, H.J. Kim, N. Nishiyama, K. Miyata, K. Kataoka, Systemic siRNA delivery to a spontaneous pancreatic tumor model in transgenic mice by PEGylated calcium phosphate hybrid micelles, Journal of Controlled Release. 178 (2014) 18–24. https://doi.org/https://doi.org/10.1016/j.jconrel.2014.01.008.

[158] J. Chen, X. Sun, R. Shao, Y. Xu, J. Gao, W. Liang, VEGF siRNA delivered by polycation liposome-encapsulated calcium phosphate nanoparticles for tumor angiogenesis inhibition in breast cancer, International Journal of Nanomedicine. 12 (2017) 6075–6088. https://doi.org/10.2147/IJN.S142739.

[159] S. Bisso, S. Mura, B. Castagner, P. Couvreur, J.-C. Leroux, Dual delivery of nucleic acids and PEGylated-bisphosphonates via calcium phosphate nanoparticles, BioRxiv. (2019) 621102. https://doi.org/10.1101/621102.

[160] R.-Q. Cai, D.-Z. Liu, H. Cui, Y. Cheng, M. Liu, B.-L. Zhang, Q.-B. Mei, S.-Y. Zhou, Charge reversible calcium phosphate lipid hybrid nanoparticle for siRNA delivery, Oncotarget; Vol 8, No 26. (2017). https://www.oncotarget.com/article/17484/text/.

[161] A. Frede, B. Neuhaus, R. Klopfleisch, C. Walker, J. Buer, W. Müller, M. Epple, A.M. Westendorf, Colonic gene silencing using siRNA-loaded calcium phosphate/PLGA nanoparticles ameliorates intestinal inflammation in vivo, Journal of Controlled Release. 222 (2016) 86–96. https://doi.org/https://doi.org/10.1016/j.jconrel.2015.12.021.

[162] T. Tenkumo, J.R. Vanegas Sáenz, K. Nakamura, Y. Shimizu, V. Sokolova, M. Epple, Y. Kamano, H. Egusa, T. Sugaya, K. Sasaki, Prolonged release of bone morphogenetic protein-2 in vivo by gene transfection with DNA-functionalized calcium phosphate nanoparticle-loaded collagen scaffolds, Materials Science and Engineering: C. 92 (2018) 172–183. https://doi.org/10.1016/J.MSEC.2018.06.047.

[163] T. Devarasu, R. Saad, A. Ouadi, B. Frisch, E. Robinet, P. Laquerriere, J.-C. Voegel, T. Baumert, J. Ogier, F. Meyer, Potent calcium phosphate nanoparticle surface coating for in vitro and in vivo siRNA delivery: a step toward multifunctional nanovectors, Journal of Materials Chemistry B. 1 (2013) 4692–4700.

https://doi.org/10.1039/C3TB20557F.

[164] T. Acri, N. Laird, L. Jaidev, D. Meyerholz, A. Salem, K. Shin, Nonviral Gene Delivery Embedded in Biomimetically Mineralized Matrices for Bone Tissue Engineering, Tissue Engineering Part A. 27 (2021) 1074–1083.

[165] W. Zhang, H. Tsurushima, A. Oyane, Y. Yazaki, Y. Sogo, A. Ito, A. Matsumura, BMP-2 gene-fibronectin-apatite composite layer enhances bone formation, Journal of Biomedical Science. 18 (2011) 62. https://doi.org/10.1186/1423-0127-18-62.

[166] X. Wang, D. Yang, S. Li, X. Xu, C.-F. Qin, R. Tang, Biomineralized vaccine nanohybrid for needle-free intranasal immunization, Biomaterials. 106 (2016) 286–294. https://doi.org/https://doi.org/10.1016/j.biomaterials.2016.08.035.

[167] L.J. de Mello, G.R.R. Souza, E. Winter, A.H. Silva, F. Pittella, T.B. Creczynski-Pasa, Knockdown of antiapoptotic genes in breast cancer cells by siRNA loaded into hybrid nanoparticles, Nanotechnology. 28 (2017) 175101. https://doi.org/10.1088/1361-6528/aa6283.

[168] E. V Giger, J. Puigmartí-Luis, R. Schlatter, B. Castagner, P.S. Dittrich, J.-C. Leroux, Gene delivery with bisphosphonate-stabilized calcium phosphate nanoparticles, Journal of Controlled Release. 150 (2011) 87–93. https://doi.org/https://doi.org/10.1016/j.jconrel.2010.11.012.

[169] Y. Kakizawa, K. Kataoka, Block Copolymer Self-Assembly into Monodispersive Nanoparticles with Hybrid Core of Antisense DNA and Calcium Phosphate, Langmuir. 18 (2002) 4539–4543. https://doi.org/10.1021/la011736s.

[170] J.S. Suk, Q. Xu, N. Kim, J. Hanes, L.M. Ensign, PEGylation as a strategy for improving nanoparticle-based drug and gene delivery, Advanced Drug Delivery Reviews. 99 (2016) 28–51. https://doi.org/https://doi.org/10.1016/j.addr.2015.09.012.

[171] K. Knop, R. Hoogenboom, D. Fischer, U.S. Schubert, Poly(ethylene glycol) in Drug Delivery: Pros and Cons as Well as Potential Alternatives, Angewandte Chemie International Edition. 49 (2010) 6288–6308. https://doi.org/10.1002/anie.200902672.

[172] Y. Kakizawa, K. Miyata, S. Furukawa, K. Kataoka, Size-Controlled Formation of a Calcium Phosphate-Based Organic–Inorganic Hybrid Vector for Gene Delivery Using Poly(ethylene glycol)-block-poly(aspartic acid), Advanced Materials. 16 (2004) 699–702. https://doi.org/10.1002/adma.200305782.

[173] F. Pittella, M. Zhang, Y. Lee, H.J. Kim, T. Tockary, K. Osada, T. Ishii, K. Miyata, N. Nishiyama, K. Kataoka, Enhanced endosomal escape of siRNA-incorporating hybrid nanoparticles from calcium phosphate and PEG-block charge-conversional polymer for efficient gene knockdown with negligible cytotoxicity, Biomaterials. 32 (2011) 3106–3114.

https://doi.org/https://doi.org/10.1016/j.biomaterials.2010.12.057.

[174] Y. Maeda, F. Pittella, T. Nomoto, H. Takemoto, N. Nishiyama, K. Miyata, K. Kataoka, Fine-Tuning of Charge-Conversion Polymer Structure for Efficient Endosomal Escape of siRNA-Loaded Calcium Phosphate Hybrid Micelles, Macromolecular Rapid Communications. 35 (2014) 1211–1215. https://doi.org/10.1002/marc.201400049.

[175] M. Khansarizadeh, A. Mokhtarzadeh, M. Rashedinia, S.M. Taghdisi, P. Lari, K.H. Abnous, M. Ramezani, Identification of possible cytotoxicity mechanism of polyethylenimine by proteomics analysis, Human & Experimental Toxicology. 35 (2015) 377–387. https://doi.org/10.1177/0960327115591371.

[176] M.-E. Halatsch, R.E. Kast, A. Dwucet, M. Hlavac, T. Heiland, M.-A. Westhoff, K.-M. Debatin, C.R. Wirtz, M.D. Siegelin, G. Karpel-Massler, Bcl-2/Bcl-xL inhibition predominantly synergistically enhances the anti-neoplastic activity of a low-dose CUSP9 repurposed drug regime against glioblastoma, British Journal of Pharmacology. 176 (2019) 3681–3694. https://doi.org/10.1111/bph.14773.

[177] M.-E. Halatsch, R.E. Kast, A. Dwucet, C.R. Wirtz, M. Siegelin, G. Karpel-Massler, EXTH-54. Bcl-2/Bcl-xL INHIBITION SYNERGISTICALLY ENHANCES THE ANTI-NEOPLASTIC ACTIVITY OF CUSP9 AGAINST GLIOBLASTOMA CELLS IN VITRO, Neuro-Oncology. 20 (2018) vi96–vi96. https://doi.org/10.1093/neuonc/noy148.402.

[178] S. Kehr, T. Haydn, A. Bierbrauer, B. Irmer, M. Vogler, S. Fulda, Targeting BCL-2 proteins in pediatric cancer: Dual inhibition of BCL-XL and MCL-1 leads to rapid induction of intrinsic apoptosis, Cancer Letters. (2020). https://doi.org/https://doi.org/10.1016/j.canlet.2020.02.041.

[179] Q. Zhou, Y. Wang, J. Xiang, Y. Piao, Z. Zhou, J. Tang, X. Liu, Y. Shen, Stabilized calcium phosphate hybrid nanocomposite using a benzoxaborole-containing polymer for pH-responsive siRNA delivery, Biomaterials Science. 6 (2018) 3178–3188. https://doi.org/10.1039/c8bm00575c.

[180] L. Forte, S. Sarda, P. Torricelli, C. Combes, F. Brouillet, O. Marsan, F. Salamanna, M. Fini, E. Boanini, A. Bigi, Multifunctionalization Modulates Hydroxyapatite Surface Interaction with Bisphosphonate: Antiosteoporotic and Antioxidative Stress Materials, ACS Biomaterials Science & Engineering. 5 (2019) 3429–3439. https://doi.org/10.1021/acsbiomaterials.9b00795.

[181] M.T. Drake, B.L. Clarke, S. Khosla, Bisphosphonates: mechanism of action and role in clinical practice, Mayo Clinic Proceedings. 83 (2008) 1032–1045. https://doi.org/10.4065/83.9.1032.

[182] S. Cremers, M.T. Drake, F.H. Ebetino, J.P. Bilezikian, R.G.G. Russell, Pharmacology of bisphosphonates, British Journal of Clinical Pharmacology. 85 (2019) 1052–1062. https://doi.org/10.1111/bcp.13867.

[183] D.D. Waller, J. Park, Y.S. Tsantrizos, Inhibition of farnesyl pyrophosphate (FPP) and/or geranylgeranyl pyrophosphate (GGPP) biosynthesis and its implication in the treatment of cancers, Critical Reviews in Biochemistry and Molecular Biology. 54 (2019) 41–60. https://doi.org/10.1080/10409238.2019.1568964.

[184] S.S. Virtanen, H.K. Väänänen, P.L. Härkönen, P.T. Lakkakorpi, Alendronate Inhibits Invasion of PC-3 Prostate Cancer Cells by Affecting the Mevalonate Pathway, Cancer Research. 62 (2002) 2708 LP – 2714. http://cancerres.aacrjournals.org/content/62/9/2708.abstract.

[185] Y. Liu, C. Du, Y. Zhang, S. Zhao, L. Zhao, P. Li, F. Hu, L. Zhu, Y. Liu, D. Pang, Y. Zhao, Bisphosphonate and risk of cancer recurrence: protocol for a systematic review, meta-analysis and trial sequential analysis of randomised controlled trials, BMJ Open. 5 (2015) e007215–e007215. https://doi.org/10.1136/bmjopen-2014-007215.

[186] T.L. Rogers, I. Holen, Tumour macrophages as potential targets of bisphosphonates, Journal of Translational Medicine. 9 (2011) 177. https://doi.org/10.1186/1479-5876-9-177.

[187] G. Mattheolabakis, L. Milane, A. Singh, M.M. Amiji, Hyaluronic acid targeting of CD44 for cancer therapy: from receptor biology to nanomedicine, Journal of Drug Targeting. 23 (2015) 605–618. https://doi.org/10.3109/1061186X.2015.1052072.

[188] A. Fakhari, C. Berkland, Applications and emerging trends of hyaluronic acid in tissue engineering, as a dermal filler and in osteoarthritis treatment, Acta Biomaterialia. 9 (2013) 7081–7092. https://doi.org/https://doi.org/10.1016/j.actbio.2013.03.005.

[189] J.. Lee, J.E.; Yin, Y.; Lim, S.Y.; Kim, E.S.; Jung, J.; Kim, D.; Park, J.W.; Lee, M.S.; Jeong, Enhanced Transfection of Human Mesenchymal Stem Cells Using a Hyaluronic Acid/Calcium Phosphate Hybrid Gene Delivery System, Polymers. 11 (2019) 798.

[190] A.H. Hofman, I.A. van Hees, J. Yang, M. Kamperman, Bioinspired Underwater Adhesives by Using the Supramolecular Toolbox, Advanced Materials. 30 (2018) 1704640. https://doi.org/10.1002/adma.201704640.

[191] H.Y. Nam, K.H. Min, D.E. Kim, J.R. Choi, H.J. Lee, S.C. Lee, Mussel-inspired poly(L-DOPA)-templated mineralization for calcium phosphate-assembled intracellular nanocarriers, Colloids and Surfaces B: Biointerfaces. 157 (2017) 215–222. https://www.scopus.com/inward/record.uri?eid=2-s2.0-85020258647&doi=10.1016%2Fj.colsurfb.2017.05.077&partnerID=40&md5=e8ec80d84e58d34fc8f985fbcb24a1fd.

[192] M. Ullah, D.D. Liu, A.S. Thakor, Mesenchymal Stromal Cell Homing: Mechanisms and Strategies for Improvement, IScience. 15 (2019) 421–438. https://doi.org/10.1016/j.isci.2019.05.004.

[193] J. Zhang, X. Sun, R. Shao, W. Liang, J. Gao, J. Chen, Polycation liposomes combined with calcium phosphate nanoparticles as a non-viral carrier for siRNA delivery, Journal of Drug Delivery Science and Technology. 30 (2015) 1–6. https://doi.org/https://doi.org/10.1016/j.jddst.2015.09.005.

[194] B. Sun, M. Gillard, Y. Wu, P. Wu, Z.P. Xu, W. Gu, Bisphosphonate Stabilized Calcium Phosphate Nanoparticles for Effective Delivery of Plasmid DNA to Macrophages, ACS Applied Bio Materials. 3 (2020) 986–996. https://doi.org/10.1021/acsabm.9b00994.

[195] J. Tang, L. Li, C.B. Howard, S.M. Mahler, L. Huang, Z.P. Xu, Preparation of optimized lipid-coated calcium phosphate nanoparticles for enhanced in vitro gene delivery to breast cancer cells, Journal of Materials Chemistry B. 3 (2015) 6805–6812. https://doi.org/10.1039/C5TB00912J.

[196] S. Karthika, T.K. Radhakrishnan, P. Kalaichelvi, A Review of Classical and Nonclassical Nucleation Theories, Crystal Growth & Design. 16 (2016) 6663–6681. https://doi.org/10.1021/acs.cgd.6b00794.

[197] K.R. Baillargeon, K. Meserve, S. Faulkner, S. Watson, H. Butts, P. Deighan, A.E. Gerdon, Precipitation SELEX: identification of DNA aptamers for calcium phosphate materials synthesis, Chemical Communications. 53 (2017) 1092–1095. https://doi.org/10.1039/c6cc08687j.

[198] M.B. Parmar, D.N. Meenakshi Sundaram, R.B. K.C., R. Maranchuk, H. Montazeri Aliabadi, J.C. Hugh, R. Löbenberg, H. Uludağ, Combinational siRNA delivery using hyaluronic acid modified amphiphilic polyplexes against cell cycle and phosphatase proteins to inhibit growth and migration of triple-negative breast cancer cells, Acta Biomaterialia. 66 (2018) 294–309. https://doi.org/https://doi.org/10.1016/j.actbio.2017.11.036.

[199] M.A. López-Quintela, Synthesis of nanomaterials in microemulsions: formation mechanisms and growth control, Current Opinion in Colloid & Interface Science. 8 (2003) 137–144. https://doi.org/https://doi.org/10.1016/S1359-0294(03)00019-0.

[200] M. de Dios, F. Barroso, C. Tojo, M.A. López-Quintela, Simulation of the kinetics of nanoparticle formation in microemulsions, Journal of Colloid and Interface Science. 333 (2009) 741–748. https://doi.org/https://doi.org/10.1016/j.jcis.2009.01.032.

[201] R. Jain, D. Shukla, A. Mehra, Coagulation of Nanoparticles in Reverse Micellar Systems: A Monte Carlo Model, Langmuir. 21 (2005) 11528–11533. https://doi.org/10.1021/la0523208.

[202] T. Hirai, H. Sato, I. Komasawa, Mechanism of Formation of CdS and ZnS Ultrafine Particles in Reverse Micelles, Industrial & Engineering Chemistry Research. 33 (1994) 3262–3266. https://doi.org/10.1021/ie00036a048.

[203] S. Bisht, G. Bhakta, S. Mitra, A. Maitra, pDNA loaded calcium phosphate nanoparticles: highly efficient non-viral vector for gene delivery, International Journal of Pharmaceutics. 288 (2005) 157–168. https://doi.org/https://doi.org/10.1016/j.ijpharm.2004.07.035.

[204] N.I. Ponomareva, T.D. Poprygina, S.I. Karpov, M. V Lesovoi, B.L. Agapov, Microemulsion method for producing hydroxyapatite, Russian Journal of General Chemistry. 80 (2010) 905–908. https://doi.org/10.1134/S1070363210050063.

[205] X. He, T. Liu, Y. Chen, D. Cheng, X. Li, Y. Xiao, Y. Feng, Calcium carbonate nanoparticle delivering vascular endothelial growth factor-C siRNA effectively inhibits lymphangiogenesis and growth of gastric cancer in vivo, Cancer Gene Therapy. 15 (2008) 193–202. https://doi.org/10.1038/sj.cgt.7701122.

[206] G. Bhakta, A. Shrivastava, A. Maitra, Magnesium phosphate nanoparticles can be efficiently used in vitro and in vivo as non-viral vectors for targeted gene delivery, Journal of Biomedical Nanotechnology. 5 (2009) 106–114. https://doi.org/10.1166/jbn.2009.029.

[207] I. Roy, S. Mitra, A. Maitra, S. Mozumdar, Calcium phosphate nanoparticles as novel non-viral vectors for targeted gene delivery, International Journal of Pharmaceutics. 250 (2003) 25–33. https://doi.org/https://doi.org/10.1016/S0378-5173(02)00452-0.

[208] C. Tojo, M. de Dios, F. Barroso, Surfactant Effects on Microemulsion-Based Nanoparticle Synthesis, Materials (Basel, Switzerland). 4 (2010) 55–72. https://doi.org/10.3390/ma4010055.

[209] M. Soleimani Zohr Shiri, W. Henderson, M.R. Mucalo, A Review of The Lesser-Studied Microemulsion-Based Synthesis Methodologies Used for Preparing Nanoparticle Systems of The Noble Metals, Os, Re, Ir and Rh, Materials (Basel, Switzerland). 12 (2019) 1896. https://doi.org/10.3390/ma12121896.

[210] S. Hou, H. Ma, Y. Ji, W. Hou, N. Jia, A Calcium Phosphate Nanoparticle-Based Biocarrier for Efficient Cellular Delivery of Antisense Oligodeoxynucleotides, ACS Applied Materials & Interfaces. 5 (2013) 1131–1136. https://doi.org/10.1021/am3028926.

[211] K. Lee, M.H. Oh, M.S. Lee, Y.S. Nam, T.G. Park, J.H. Jeong, Stabilized calcium phosphate nano-aggregates using a dopa-chitosan conjugate for gene delivery, International Journal of Pharmaceutics. 445 (2013) 196–202. https://doi.org/https://doi.org/10.1016/j.ijpharm.2013.01.014.

[212] R. Paliwal, R.J. Babu, S. Palakurthi, Nanomedicine Scale-up Technologies: Feasibilities and Challenges, AAPS PharmSciTech. 15 (2014) 1527–1534. https://doi.org/10.1208/s12249-014-0177-9.

[213] Y. Wu, W. Gu, L. Li, C. Chen, Z.P. Xu, Enhancing PD-1 gene silence in T

lymphocytes by comparing the delivery performance of two inorganic nanoparticle platforms, Nanomaterials. 9 (2019). https://doi.org/10.3390/nano9020159.

[214] Z. Zhou, C. Kennell, J.-Y. Lee, Y.-K. Leung, P. Tarapore, Calcium phosphate-polymer hybrid nanoparticles for enhanced triple negative breast cancer treatment via co-delivery of paclitaxel and miR-221/222 inhibitors, Nanomedicine: Nanotechnology, Biology and Medicine. 13 (2017) 403–410. https://doi.org/https://doi.org/10.1016/j.nano.2016.07.016.

[215] S. Li, Q. Li, J. Lü, Q. Zhao, D. Li, L. Shen, Z. Wang, J. Liu, D. Xie, W.C. Cho, S. Xu, Z. Yu, Targeted Inhibition of miR-221/222 Promotes Cell Sensitivity to Cisplatin in Triple-Negative Breast Cancer MDA-MB-231 Cells , Frontiers in Genetics . 10 (2020) 1278. https://www.frontiersin.org/article/10.3389/fgene.2019.01278.

[216] K. Taylor, C.B. Howard, M.L. Jones, I. Sedliarou, J. MacDiarmid, H. Brahmbhatt, T.P. Munro, S.M. Mahler, Nanocell targeting using engineered bispecific antibodies, MAbs. 7 (2015) 53–65. https://doi.org/10.4161/19420862.2014.985952.

[217] Y. Wu, W. Gu, J. Li, C. Chen, Z.P. Xu, Silencing PD-1 and PD-L1 with nanoparticle-delivered small interfering RNA increases cytotoxicity of tumor-infiltrating lymphocytes, Nanomedicine. 14 (2019) 955–967. https://doi.org/10.2217/nnm-2018-0237.

[218] N. Kang, G.J. Gores, V.H. Shah, Hepatic stellate cells: partners in crime for liver metastases?, Hepatology (Baltimore, Md.). 54 (2011) 707–713. https://doi.org/10.1002/hep.24384.

[219] S.J. Turley, V. Cremasco, J.L. Astarita, Immunological hallmarks of stromal cells in the tumour microenvironment, Nature Reviews Immunology. 15 (2015) 669–682. https://doi.org/10.1038/nri3902.

[220] D.F. Mardhian, G. Storm, R. Bansal, J. Prakash, Nano-targeted relaxin impairs fibrosis and tumor growth in pancreatic cancer and improves the efficacy of gemcitabine in vivo, Journal of Controlled Release. 290 (2018) 1–10. https://doi.org/https://doi.org/10.1016/j.jconrel.2018.09.031.

[221] I.S. Zeelenberg, L. Ruuls-Van Stalle, E. Roos, The Chemokine Receptor CXCR4 Is Required for Outgrowth of Colon Carcinoma Micrometastases, Cancer Research. 63 (2003) 3833 LP – 3839. http://cancerres.aacrjournals.org/content/63/13/3833.abstract.

[222] E.M. García-Cuesta, C.A. Santiago, J. Vallejo-Díaz, Y. Juarranz, J.M. Rodríguez-Frade, M. Mellado, The Role of the CXCL12/CXCR4/ACKR3 Axis in Autoimmune Diseases, Frontiers in Endocrinology. 10 (2019) 585. https://doi.org/10.3389/fendo.2019.00585.

[223] A.A. D'Souza, P. V Devarajan, Asialoglycoprotein receptor mediated hepatocyte targeting — Strategies and applications, Journal of Controlled Release. 203 (2015) 126–139. https://doi.org/https://doi.org/10.1016/j.jconrel.2015.02.022.

[224] S. von Karstedt, A. Montinaro, H. Walczak, Exploring the TRAILs less travelled: TRAIL in cancer biology and therapy, Nature Reviews Cancer. 17 (2017) 352–366. https://doi.org/10.1038/nrc.2017.28.

[225] N. Takata, Y. Ohshima, M. Suzuki-Karasaki, Y. Yoshida, Y. Tokuhashi, Y. Suzuki-Karasaki, Mitochondrial Ca2+ removal amplifies TRAIL cytotoxicity toward apoptosis-resistant tumor cells via promotion of multiple cell death modalities, International Journal of Oncology. 51 (2017) 193–203. https://doi.org/10.3892/ijo.2017.4020.

[226] Y. Ohshima, N. Takata, Suzuki-Karasaki, Y. M., Yoshida, Y. Tokuhashi, Y. Suzuki-Karasaki, Disrupting mitochondrial Ca2+ homeostasis causes tumor-selective TRAIL sensitization through mitochondrial network abnormalities, International Journal of Oncology. 51 (2017) 1146–1158.

[227] K.N. Prasad, B. Kumar, X.-D. Yan, A.J. Hanson, W.C. Cole, α-Tocopheryl Succinate, the Most Effective Form of Vitamin E for Adjuvant Cancer Treatment: A Review, Journal of the American College of Nutrition. 22 (2003) 108–117. https://doi.org/10.1080/07315724.2003.10719283.

[228] J. Meerak, S.P. Wanichwecharungruang, T. Palaga, Enhancement of immune response to a DNA vaccine against Mycobacterium tuberculosis Ag85B by incorporation of an autophagy inducing system, Vaccine. 31 (2013) 784–790. https://doi.org/https://doi.org/10.1016/j.vaccine.2012.11.075.

[229] T. Kokubo, H. Takadama, How useful is SBF in predicting in vivo bone bioactivity?, Biomaterials. 27 (2006) 2907–2915. https://doi.org/https://doi.org/10.1016/j.biomaterials.2006.01.017.

[230] J. Si, Z. Cui, Q. Wang, Q. Liu, C. Liu, Biomimetic composite scaffolds based on mineralization of hydroxyapatite on electrospun poly(ε-caprolactone)/nanocellulose fibers, Carbohydrate Polymers. 143 (2016) 270–278. https://doi.org/10.1016/j.carbpol.2016.02.015.

[231] Z. Xu, L. Shi, D. Hu, B. Hu, M. Yang, L. Zhu, Formation of hierarchical bone-like apatites on silk microfiber templates: Via biomineralization, RSC Advances. 6 (2016) 76426–76433. https://doi.org/10.1039/c6ra17199k.

[232] K.H. Park, S.-J. Kim, Y.-H. Jeong, H.-J. Moon, H.-J. Song, Y.-J. Park, Fabrication and biological properties of calcium phosphate/chitosan composite coating on titanium in modified SBF, Materials Science and Engineering: C. 90 (2018) 113–118. https://doi.org/https://doi.org/10.1016/j.msec.2018.04.060.

[233] X. Wang, J. Yang, C.M. Andrei, L. Soleymani, K. Grandfield, Biomineralization

of calcium phosphate revealed by in situ liquid-phase electron microscopy, Communications Chemistry. 1 (2018) 80. https://doi.org/10.1038/s42004-018-0081-4.

[234] K. Shin, T. Acri, S. Geary, A.K. Salem, Biomimetic Mineralization of Biomaterials Using Simulated Body Fluids for Bone Tissue Engineering and Regenerative Medicine<sup/>, Tissue Engineering. Part A. 23 (2017) 1169–1180. https://doi.org/10.1089/ten.TEA.2016.0556.

[235] F. Nudelman, N.A.J.M. Sommerdijk, Biomineralization as an Inspiration for Materials Chemistry, Angewandte Chemie International Edition. 51 (2012) 6582–6596. https://doi.org/10.1002/anie.201106715.

[236] R. Khalifehzadeh, H. Arami, DNA-Templated Strontium-Doped Calcium Phosphate Nanoparticles for Gene Delivery in Bone Cells, ACS Biomaterials Science and Engineering. 5 (2019) 3201–3211. https://doi.org/10.1021/acsbiomaterials.8b01587.

[237] A. Aimaiti, A. Maimaitiyiming, X. Boyong, K. Aji, C. Li, L. Cui, Low-dose strontium stimulates osteogenesis but high-dose doses cause apoptosis in human adipose-derived stem cells via regulation of the ERK1/2 signaling pathway, Stem Cell Research & Therapy. 8 (2017) 282. https://doi.org/10.1186/s13287-017-0726-8.

[238] V. Nardone, S. Fabbri, F. Marini, R. Zonefrati, G. Galli, A. Carossino, A. Tanini, M.L. Brandi, Osteodifferentiation of Human Preadipocytes Induced by Strontium Released from Hydrogels, International Journal of Biomaterials. 2012 (2012) 865291. https://doi.org/10.1155/2012/865291.

[239] B.G. Mohan, S. Suresh Babu, H.K. Varma, A. John, In vitro evaluation of bioactive strontium-based ceramic with rabbit adipose-derived stem cells for bone tissue regeneration, Journal of Materials Science: Materials in Medicine. 24 (2013) 2831–2844. https://doi.org/10.1007/s10856-013-5018-y.

[240] H. Shen, J. Tan, W.M. Saltzman, Surface-mediated gene transfer from nanocomposites of controlled texture, Nature Materials. 3 (2004) 569–574. https://doi.org/10.1038/nmat1179.

[241] B. Sun, K.K. Tran, H. Shen, Enabling customization of non-viral gene delivery systems for individual cell types by surface-induced mineralization, Biomaterials. 30 (2009) 6386–6393. https://doi.org/10.1016/j.biomaterials.2009.08.006.

[242] L.N. Luong, K.M. McFalls, D.H. Kohn, Gene delivery via DNA incorporation within a biomimetic apatite coating, Biomaterials. 30 (2009) 6996–7004. https://doi.org/https://doi.org/10.1016/j.biomaterials.2009.09.001.

[243] B. Sun, H. Shen, Correlation of the composition of biominerals with their ability of stimulating intracellular DNA sensors and inflammatory cytokines, Biomaterials.

54 (2015) 106–115. https://doi.org/https://doi.org/10.1016/j.biomaterials.2015.03.013.

[244] S. Choi, X. Yu, L. Jongpaiboonkit, S.J. Hollister, W.L. Murphy, Inorganic coatings for optimized non-viral transfection of stem cells, Scientific Reports. 3 (2013) 1567. https://doi.org/10.1038/srep01567.

[245] B. Sun, M. Yi, C.C. Yacoob, H.T. Nguyen, H. Shen, Effect of surface chemistry on gene transfer efficiency mediated by surface-induced DNA-doped nanocomposites, Acta Biomaterialia. 8 (2012) 1109–1116. https://doi.org/https://doi.org/10.1016/j.actbio.2011.12.005.

[246] M. Tanahashi, T. Matsuda, Surface functional group dependence on apatite formation on self-assembled monolayers in a simulated body fluid, Journal of Biomedical Materials Research. 34 (1997) 305–315. https://doi.org/10.1002/(SICI)1097-4636(19970305)34:3<305::AID-JBM5>3.0.CO;2-O.

[247] J. Aizenberg, A.J. Black, G.M. Whitesides, Oriented Growth of Calcite Controlled by Self-Assembled Monolayers of Functionalized Alkanethiols Supported on Gold and Silver, Journal of the American Chemical Society. 121 (1999) 4500–4509. https://doi.org/10.1021/ja984254k.

[248] I. HIRATA, M. AKAMATSU, E. FUJII, S. POOLTHONG, M. OKAZAKI, Chemical analyses of hydroxyapatite formation on SAM surfaces modified with COOH, NH₂, CH₃, and OH functions, Dental Materials Journal. 29 (2010) 438–445. https://doi.org/10.4012/dmj.2010-017.

[249] G.K. Toworfe, R.J. Composto, I.M. Shapiro, P. Ducheyne, Nucleation and growth of calcium phosphate on amine-, carboxyl- and hydroxyl-silane self-assembled monolayers, Biomaterials. 27 (2006) 631–642. https://doi.org/https://doi.org/10.1016/j.biomaterials.2005.06.017.

[250] Y. Yazaki, A. Oyane, H. Tsurushima, H. Araki, Y. Sogo, A. Ito, A. Yamazaki, Improved gene transfer efficiency of a DNA-lipid-apatite composite layer by controlling the layer molecular composition, Colloids and Surfaces B: Biointerfaces. 122 (2014) 465–471. https://doi.org/https://doi.org/10.1016/j.colsurfb.2014.07.001.

[251] B. Sun, H. Shen, Controlling Surface-Induced Nanocomposites by Lipoplexes for Enhanced Gene Transfer, Journal of Nanomaterials. 2015 (2015) 784836. https://doi.org/10.1155/2015/784836.

[252] A. Oyane, Y. Yazaki, H. Araki, Y. Sogo, A. Ito, A. Yamazaki, H. Tsurushima, Fabrication of a DNA-lipid-apatite composite layer for efficient and area-specific gene transfer, Journal of Materials Science: Materials in Medicine. 23 (2012) 1011–1019. https://doi.org/10.1007/s10856-012-4581-y.

[253] C. Gao, S. Peng, P. Feng, C. Shuai, Bone biomaterials and interactions with stem cells, Bone Research. 5 (2017) 17059. https://doi.org/10.1038/boneres.2017.59.

[254] R. Langer, J.P. Vacanti, Tissue engineering, Science. 260 (1993) 920 LP – 926. https://doi.org/10.1126/science.8493529.

[255] A. Oyane, H. Tsurushima, A. Ito, Novel gene-transferring scaffolds having a cell adhesion molecule–DNA–apatite nanocomposite surface, Gene Therapy. 14 (2007) 1750–1753. https://doi.org/10.1038/sj.gt.3303041.

[256] Y. Yazaki, A. Oyane, Y. Sogo, A. Ito, A. Yamazaki, H. Tsurushima, Area-Specific Cell Stimulation via Surface-Mediated Gene Transfer Using Apatite-Based Composite Layers, International Journal of Molecular Sciences . 16 (2015). https://doi.org/10.3390/ijms16048294.

[257] Y. Yazaki, A. Oyane, Y. Sogo, A. Ito, A. Yamazaki, H. Tsurushima, Control of gene transfer on a DNA–fibronectin–apatite composite layer by the incorporation of carbonate and fluoride ions, Biomaterials. 32 (2011) 4896–4902. https://doi.org/https://doi.org/10.1016/j.biomaterials.2011.03.021.

[258] Y. Yazaki, A. Oyane, H. Tsurushima, H. Araki, Y. Sogo, A. Ito, A. Yamazaki, Coprecipitation of DNA-lipid complexes with apatite and comparison with superficial adsorption for gene transfer applications, Journal of Biomaterials Applications. 28 (2013) 937–945. https://doi.org/10.1177/0885328213486706.

[259] V. V Sokolova, I. Radtke, R. Heumann, M. Epple, Effective transfection of cells with multi-shell calcium phosphate-DNA nanoparticles, Biomaterials. 27 (2006) 3147–3153. https://doi.org/https://doi.org/10.1016/j.biomaterials.2005.12.030.

[260] V. Sokolova, L. Rojas-Sánchez, N. Białas, N. Schulze, M. Epple, Calcium phosphate nanoparticle-mediated transfection in 2D and 3D mono- and co-culture cell models, Acta Biomaterialia. 84 (2019) 391–401. https://doi.org/10.1016/J.ACTBIO.2018.11.051.

[261] T. Tenkumo, J.R. Vanegas Sáenz, K. Nakamura, Y. Shimizu, V. Sokolova, M. Epple, Y. Kamano, H. Egusa, T. Sugaya, K. Sasaki, Prolonged release of bone morphogenetic protein-2 in vivo by gene transfection with DNA-functionalized calcium phosphate nanoparticle-loaded collagen scaffolds, Materials Science and Engineering: C. 92 (2018) 172–183. https://doi.org/https://doi.org/10.1016/j.msec.2018.06.047.

[262] L.J. del Valle, O. Bertran, G. Chaves, G. Revilla-López, M. Rivas, M.T. Casas, J. Casanovas, P. Turon, J. Puiggalí, C. Alemán, DNA adsorbed on hydroxyapatite surfaces, Journal of Materials Chemistry B. 2 (2014) 6953–6966. https://doi.org/10.1039/C4TB01184H.

[263] M. Okazaki, Y. Yoshida, S. Yamaguchi, M. Kaneno, J.C. Elliott, Affinity binding phenomena of DNA onto apatite crystals, Biomaterials. 22 (2001) 2459–2464.

https://doi.org/10.1016/S0142-9612(00)00433-6.

[264] F. Bakan, G. Kara, M. Cokol Cakmak, M. Cokol, E.B. Denkbas, Synthesis and characterization of amino acid-functionalized calcium phosphate nanoparticles for siRNA delivery, Colloids and Surfaces B: Biointerfaces. 158 (2017) 175–181. https://doi.org/https://doi.org/10.1016/j.colsurfb.2017.06.028.

[265] Y. Kan, Q. Tan, G. Wu, W. Si, Y. Chen, Study of DNA adsorption on mica surfaces using a surface force apparatus, Scientific Reports. 5 (2015) 8442. https://doi.org/10.1038/srep08442.

[266] M. Banik, T. Basu, Calcium phosphate nanoparticles: a study of their synthesis, characterization and mode of interaction with salmon testis DNA, Dalton Transactions. 43 (2014) 3244–3259. https://doi.org/10.1039/C3DT52522H.

[267] C.E. Pedraza, D.C. Bassett, M.D. McKee, V. Nelea, U. Gbureck, J.E. Barralet, The importance of particle size and DNA condensation salt for calcium phosphate nanoparticle transfection, Biomaterials. 29 (2008) 3384–3392. https://doi.org/https://doi.org/10.1016/j.biomaterials.2008.04.043.

[268] Y.-H. Lee, H.-C. Wu, C.-W. Yeh, C.-H. Kuan, H.-T. Liao, H.-C. Hsu, J.-C. Tsai, J.-S. Sun, T.-W. Wang, Enzyme-crosslinked gene-activated matrix for the induction of mesenchymal stem cells in osteochondral tissue regeneration, Acta Biomaterialia. 63 (2017) 210–226. https://doi.org/https://doi.org/10.1016/j.actbio.2017.09.008.

[269] A. Frede, B. Neuhaus, T. Knuschke, M. Wadwa, S. Kollenda, R. Klopfleisch, W. Hansen, J. Buer, D. Bruder, M. Epple, A.M. Westendorf, Local delivery of siRNA-loaded calcium phosphate nanoparticles abates pulmonary inflammation, Nanomedicine: Nanotechnology, Biology and Medicine. 13 (2017) 2395–2403. https://doi.org/https://doi.org/10.1016/j.nano.2017.08.001.

[270] T. Tenkumo, J.R. Vanegas Sáenz, Y. Takada, M. Takahashi, O. Rotan, V. Sokolova, M. Epple, K. Sasaki, Gene transfection of human mesenchymal stem cells with a nano-hydroxyapatite–collagen scaffold containing DNA-functionalized calcium phosphate nanoparticles, Genes to Cells. 21 (2016) 682–695. https://doi.org/10.1111/gtc.12374.

[271] C. Hadjicharalambous, D. Kozlova, V. Sokolova, M. Epple, M. Chatzinikolaidou, Calcium phosphate nanoparticles carrying BMP-7 plasmid DNA induce an osteogenic response in MC3T3-E1 pre-osteoblasts, Journal of Biomedical Materials Research Part A. 103 (2015) 3834–3842. https://doi.org/10.1002/jbm.a.35527.

[272] J.R. Vanegas Sáenz, T. Tenkumo, Y. Kamano, H. Egusa, K. Sasaki, Amiloride-enhanced gene transfection of octa-arginine functionalized calcium phosphate nanoparticles, PLOS ONE. 12 (2017) e0188347. https://doi.org/10.1371/journal.pone.0188347.

[273] D. Dutta, J.G. Donaldson, Search for inhibitors of endocytosis: Intended specificity and unintended consequences, Cellular Logistics. 2 (2012) 203–208. https://doi.org/10.4161/cl.23967.

[274] L. Qin, Y. Sun, P. Liu, Q. Wang, B. Han, Y. Duan, F127/Calcium phosphate hybrid nanoparticles: a promising vector for improving siRNA delivery and gene silencing, Journal of Biomaterials Science, Polymer Edition. 24 (2013) 1757–1766. https://doi.org/10.1080/09205063.2013.801702.

[275] C. Chen, H. Han, W. Yang, X. Ren, X. Kong, Polyethyleneimine-modified calcium carbonate nanoparticles for p53 gene delivery , Regenerative Biomaterials. 3 (2016) 57–63. https://doi.org/10.1093/rb/rbv029.

[276] D. Kozlova, S. Chernousova, T. Knuschke, J. Buer, A.M. Westendorf, M. Epple, Cell targeting by antibody-functionalized calcium phosphate nanoparticles, Journal of Materials Chemistry. 22 (2012) 396–404. https://doi.org/10.1039/C1JM14683A.

[277] Y. Yin, M.S. Lee, J.E. Lee, S.Y. Lim, E.S. Kim, J. Jeong, D. Kim, J. Kim, D.S. Lee, J.H. Jeong, Effective systemic siRNA delivery using dual-layer protected long-circulating nanohydrogel containing an inorganic core, Biomaterials Science. 7 (2019) 3297–3306. https://doi.org/10.1039/c9bm00369j.

[278] M. Antonietti, M. Breulmann, C.G. Göltner, H. Cölfen, K.K.W. Wong, D. Walsh, S. Mann, Inorganic/Organic Mesostructures with Complex Architectures: Precipitation of Calcium Phosphate in the Presence of Double-Hydrophilic Block Copolymers, Chemistry – A European Journal. 4 (1998) 2493–2500. https://doi.org/10.1002/(SICI)1521-3765(19981204)4:12<2493::AID-CHEM2493>3.0.CO;2-V.

[279] H.T. Schmidt, A.E. Ostafin, Liposome Directed Growth of Calcium Phosphate Nanoshells, Advanced Materials. 14 (2002) 532–535. https://doi.org/10.1002/1521-4095(20020404)14:7<532::AID-ADMA532>3.0.CO;2-4.

[280] K.K. Perkin, J.L. Turner, K.L. Wooley, S. Mann, Fabrication of Hybrid Nanocapsules by Calcium Phosphate Mineralization of Shell Cross-Linked Polymer Micelles and Nanocages, Nano Letters. 5 (2005) 1457–1461. https://doi.org/10.1021/nl050817w.

[281] H.J. Lee, S.E. Kim, I.K. Kwon, C. Park, C. Kim, J. Yang, S.C. Lee, Spatially mineralized self-assembled polymeric nanocarriers with enhanced robustness and controlled drug-releasing property, Chemical Communications. 46 (2010) 377–379. https://doi.org/10.1039/B913732G.

[282] S.-Y. Han, H.S. Han, S.C. Lee, Y.M. Kang, I.-S. Kim, J.H. Park, Mineralized hyaluronic acid nanoparticles as a robust drug carrier, Journal of Materials Chemistry. 21 (2011) 7996–8001. https://doi.org/10.1039/C1JM10466G.

[283] K.H. Min, H.J. Lee, K. Kim, I.C. Kwon, S.Y. Jeong, S.C. Lee, The tumor accumulation and therapeutic efficacy of doxorubicin carried in calcium phosphate-reinforced polymer nanoparticles, Biomaterials. 33 (2012) 5788–5797. https://doi.org/https://doi.org/10.1016/j.biomaterials.2012.04.057.

[284] H.S. Han, J. Lee, H.R. Kim, S.Y. Chae, M. Kim, G. Saravanakumar, H.Y. Yoon, D.G. You, H. Ko, K. Kim, I.C. Kwon, J.C. Park, J.H. Park, Robust PEGylated hyaluronic acid nanoparticles as the carrier of doxorubicin: Mineralization and its effect on tumor targetability in vivo, Journal of Controlled Release. 168 (2013) 105–114. https://doi.org/https://doi.org/10.1016/j.jconrel.2013.02.022.

[285] Y. Lv, H. Huang, B. Yang, H. Liu, Y. Li, J. Wang, A robust pH-sensitive drug carrier: Aqueous micelles mineralized by calcium phosphate based on chitosan, Carbohydrate Polymers. 111 (2014) 101–107. https://doi.org/https://doi.org/10.1016/j.carbpol.2014.04.082.

[286] B.J. Kim, K.H. Min, G.H. Hwang, H.J. Lee, S.Y. Jeong, E.-C. Kim, S.C. Lee, Calcium carbonate-mineralized polymer nanoparticles for pH-responsive robust nanocarriers of docetaxel, Macromolecular Research. 23 (2015) 111–117. https://doi.org/10.1007/s13233-015-3020-6.

[287] B. Deng, M. Xia, J. Qian, R. Li, L. Li, J. Shen, G. Li, Y. Xie, Calcium Phosphate-Reinforced Reduction-Sensitive Hyaluronic Acid Micelles for Delivering Paclitaxel in Cancer Therapy, Molecular Pharmaceutics. 14 (2017) 1938–1949. https://doi.org/10.1021/acs.molpharmaceut.7b00025.

[288] Y. Li, K. Xiao, W. Zhu, W. Deng, K.S. Lam, Stimuli-responsive cross-linked micelles for on-demand drug delivery against cancers, Advanced Drug Delivery Reviews. 66 (2014) 58–73. https://doi.org/https://doi.org/10.1016/j.addr.2013.09.008.

[289] S.J. Lee, K.H. Min, H.J. Lee, A.N. Koo, H.P. Rim, B.J. Jeon, S.Y. Jeong, J.S. Heo, S.C. Lee, Ketal Cross-Linked Poly(ethylene glycol)-Poly(amino acid)s Copolymer Micelles for Efficient Intracellular Delivery of Doxorubicin, Biomacromolecules. 12 (2011) 1224–1233. https://doi.org/10.1021/bm101517x.

[290] X. Wang, Y. Deng, S. Li, G. Wang, E. Qin, X. Xu, R. Tang, C. Qin, Biomineralization-Based Virus Shell-Engineering: Towards Neutralization Escape and Tropism Expansion, Advanced Healthcare Materials. 1 (2012) 443–449. https://doi.org/10.1002/adhm.201200034.

[291] T. Sakoda, N. Kasahara, L. Kedes, M. Ohyanagi, Calcium phosphate coprecipitation greatly enhances transduction of cardiac myocytes and vascular smooth muscle cells by lentivirus vectors, Experimental and Clinical Cardiology. 12 (2007) 133–138. https://pubmed.ncbi.nlm.nih.gov/18650994.

[292] H. Zhou, G. Wang, X. Wang, Z. Song, R. Tang, Mineralized State of the Avian Influenza Virus in the Environment, Angewandte Chemie International Edition. 56

(2017) 12908–12912. https://doi.org/10.1002/anie.201705769.

[293] X. Wang, X. Liu, Y. Xiao, H. Hao, Y. Zhang, R. Tang, Biomineralization State of Viruses and Their Biological Potential, Chemistry – A European Journal. 24 (2018) 11518–11529. https://doi.org/10.1002/chem.201705936.

[294] H. Zhou, X. Wang, R. Tang, Could a mineralized state of avian flu virus be dangerous to humans?, Future Virology. 13 (2018) 79–81. https://doi.org/10.2217/fvl-2017-0142.

[295] A. Fasbender, J.H. Lee, R.W. Walters, T.O. Moninger, J. Zabner, M.J. Welsh, Incorporation of adenovirus in calcium phosphate precipitates enhances gene transfer to airway epithelia in vitro and in vivo., The Journal of Clinical Investigation. 102 (1998) 184–193. https://doi.org/10.1172/JCI2732.

[296] Y.-W. Yang, C.-K. Chao, Incorporation of calcium phosphate enhances recombinant adeno-associated virus-mediated gene therapy in diabetic mice, The Journal of Gene Medicine. 5 (2003) 417–424. https://doi.org/10.1002/jgm.353.

[297] K. Toyoda, J.J. Andresen, J. Zabner, F.M. Faraci, D.D. Heistad, Calcium phosphate precipitates augment adenovirus-mediated gene transfer to blood vessels in vitro and in vivo, Gene Therapy. 7 (2000) 1284–1291. https://doi.org/10.1038/sj.gt.3301214.

[298] G. Wang, R.-Y. Cao, R. Chen, L. Mo, J.-F. Han, X. Wang, X. Xu, T. Jiang, Y.-Q. Deng, K. Lyu, S.-Y. Zhu, E.-D. Qin, R. Tang, C.-F. Qin, Rational design of thermostable vaccines by engineered peptide-induced virus self-biomineralization under physiological conditions, Proceedings of the National Academy of Sciences. 110 (2013) 7619 LP – 7624. https://doi.org/10.1073/pnas.1300233110.

[299] C.S. Schneider, Q. Xu, N.J. Boylan, J. Chisholm, B.C. Tang, B.S. Schuster, A. Henning, L.M. Ensign, E. Lee, P. Adstamongkonkul, B.W. Simons, S.-Y.S. Wang, X. Gong, T. Yu, M.P. Boyle, J.S. Suk, J. Hanes, Nanoparticles that do not adhere to mucus provide uniform and long-lasting drug delivery to airways following inhalation, Science Advances. 3 (2017) e1601556. https://doi.org/10.1126/sciadv.1601556.

[300] T. Ito, Y. Koyama, M. Otsuka, Preparation of Calcium Phosphate Nanocapsule Including Deoxyribonucleic Acid–Polyethyleneimine–Hyaluronic Acid Ternary Complex for Durable Gene Delivery, Journal of Pharmaceutical Sciences. 103 (2014) 179–184. https://doi.org/10.1002/jps.23768.

[301] P. Chen, Y. Liu, J. Zhao, X. Pang, P. Zhang, X. Hou, P. Chen, C. He, Z. Wang, Z. Chen, The synthesis of amphiphilic polyethyleneimine/calcium phosphate composites for bispecific T-cell engager based immunogene therapy, Biomaterials Science. 6 (2018) 633–641. https://doi.org/10.1039/C7BM01143A.

[302] T.M. Acri, N.Z. Laird, S.M. Geary, A.K. Salem, K. Shin, Effects of calcium

concentration on nonviral gene delivery to bone marrow-derived stem cells, Journal of Tissue Engineering and Regenerative Medicine. 13 (2019) 2256–2265. https://doi.org/10.1002/term.2971.

[303] S.-X. Xie, A.A. Baoum, N.A. Alhakamy, C.J. Berkland, Calcium enhances gene expression when using low molecular weight poly-l-lysine delivery vehicles, International Journal of Pharmaceutics. 547 (2018) 274–281. https://doi.org/https://doi.org/10.1016/j.ijpharm.2018.05.067.

[304] R.R. Rao, J. He, J.K. Leach, Biomineralized composite substrates increase gene expression with nonviral delivery, Journal of Biomedical Materials Research Part A. 94A (2010) 344–354. https://doi.org/10.1002/jbm.a.32690.

[305] Z. Zhou, L. Zhang, J. Li, Y. Shi, Z. Wu, H. Zheng, Z. Wang, W. Zhao, H. Pan, Q. Wang, X. Jin, X. Zhang, R. Tang, B. Fu, Polyelectrolyte-calcium Complexes as a Pre-precursor Induce Biomimetic Mineralization of Collagen, Nanoscale. (2020). https://doi.org/10.1039/D0NR05640E.

[306] T. TENKUMO, O. ROTAN, V. SOKOLOVA, M. EPPLE, Protamine Increases Transfection Efficiency and Cell Viability after Transfection with Calcium Phosphate Nanoparticles, Nano Biomedicine. 5 (2013) 64–74. https://doi.org/10.11344/nano.5.64.

[307] X. Wang, S. Masse, G. Laurent, C. Hélary, T. Coradin, Impact of Polyethylenimine Conjugation Mode on the Cell Transfection Efficiency of Silica Nanovectors, Langmuir. 31 (2015) 11078–11085. https://doi.org/10.1021/acs.langmuir.5b02616.

[308] F. Yang, J. Yang D FAU - Tu, Q. Tu J FAU - Zheng, L. Zheng Q FAU - Cai, L. Cai L FAU - Wang, L. Wang, Strontium enhances osteogenic differentiation of mesenchymal stem cells and in vivo bone formation by activating Wnt/catenin signaling., STEM CELLS. 29 (2011) 981–991. 10.1002/stem.646.

[309] T. Gonzalez-Fernandez, B.N. Sathy, C. Hobbs, G.M. Cunniffe, H.O. McCarthy, N.J. Dunne, V. Nicolosi, F.J. O'Brien, D.J. Kelly, Mesenchymal stem cell fate following non-viral gene transfection strongly depends on the choice of delivery vector, Acta Biomaterialia. 55 (2017) 226–238. https://doi.org/https://doi.org/10.1016/j.actbio.2017.03.044.

[310] Y. Li, C. Yang, H. Zhao, S. Qu, X. Li, Y. Li, New Developments of Ti-Based Alloys for Biomedical Applications, Materials (Basel, Switzerland). 7 (2014) 1709–1800. https://doi.org/10.3390/ma7031709.

[311] K. Indira, U.K. Mudali, T. Nishimura, N. Rajendran, A Review on TiO2 Nanotubes: Influence of Anodization Parameters, Formation Mechanism, Properties, Corrosion Behavior, and Biomedical Applications, Journal of Bio- and Tribo-Corrosion. 1 (2015) 28. https://doi.org/10.1007/s40735-015-0024-x.

[312] J. Yun, J. Wu, C. Aparicio, J.K. Hon Tsoi, Y. Wang, A. Fok, Enzyme-Mediated

Mineralization of TiO2 Nanotubes Subjected to Different Heat Treatments, Crystal Growth & Design. 19 (2019) 7112–7121. https://doi.org/10.1021/acs.cgd.9b00966.

[313] N.-C. Huang, Q. Ji, T. Yamazaki, W. Nakanishi, N. Hanagata, K. Ariga, S. Hsu, Gene transfer on inorganic/organic hybrid silica nanosheets, Physical Chemistry Chemical Physics. 17 (2015) 25455–25462. https://doi.org/10.1039/C5CP03483C.

[314] P. Pankongadisak, E. Tsekoura, O. Suwantong, H. Uludağ, Electrospun gelatin matrices with bioactive pDNA polyplexes, International Journal of Biological Macromolecules. 149 (2020) 296–308. https://doi.org/https://doi.org/10.1016/j.ijbiomac.2020.01.252.

[315] M. Hellfritzsch, R. Scherließ, Mucosal Vaccination via the Respiratory Tract, Pharmaceutics. 11 (2019) 375. https://doi.org/10.3390/pharmaceutics11080375.

Chapter 2

[1] M. H. Amer, *Molecular and Cellular Therapies* **2014**, *2*, 27.

[2] J. K. W. Lam, M. Y. T. Chow, Y. Zhang, S. W. S. Leung, *Molecular therapy. Nucleic acids* **2015**, *4*, e252.

[3] E. R. Balmayor, M. van Griensven, *Frontiers in Bioengineering and Biotechnology* **2015**, *3*, 9.

[4] A. Shahryari, M. Saghaeian Jazi, S. Mohammadi, H. Razavi Nikoo, Z. Nazari, E. S. Hosseini, I. Burtscher, S. J. Mowla, H. Lickert, *Frontiers in Genetics* **2019**, *10*, 868.

[5] J. D. Larsen, N. L. Ross, M. O. Sullivan, *The Journal of Gene Medicine* **2012**, *14*, 580.

[6] J. Slone, T. Huang, *npj Genomic Medicine* **2020**, *5*, 7.

[7] S. Behzadi, V. Serpooshan, W. Tao, M. A. Hamaly, M. Y. Alkawareek, E. C. Dreaden, D. Brown, A. M. Alkilany, O. C. Farokhzad, M. Mahmoudi, *Chemical Society Reviews* **2017**, *46*, 4218.

[8] K. Lundstrom, *Diseases (Basel, Switzerland)* **2018**, *6*, 42.

[9] S. E. Raper, N. Chirmule, F. S. Lee, N. A. Wivel, A. Bagg, G. Gao, J. M. Wilson, M. L. Batshaw, *Molecular Genetics and Metabolism* **2003**, *80*, 148.

[10] *Nature Biotechnology* **2020**, *38*, 910.

[11] C. L. Hardee, L. M. Arévalo-Soliz, B. D. Hornstein, L. Zechiedrich, *Genes* **2017**, *8*, 65.

[12] H. H. K. Xu, P. Wang, L. Wang, C. Bao, Q. Chen, M. D. Weir, L. C. Chow, L. Zhao, X. Zhou, M. A. Reynolds, *Bone Research* **2017**, *5*, 17056.

[13] F. L. Graham, A. J. van der Eb, *Virology* **1973**, *52*, 456.

[14] M. Jordan, A. Schallhorn, F. M. Wurm, *Nucleic Acids Research* **1996**, *24*, 596.

[15] D. Olton, J. Li, M. E. Wilson, T. Rogers, J. Close, L. Huang, P. N. Kumta, C. Sfeir, *Biomaterials* **2007**, *28*, 1267.

[16] L. Guo, L. Wang, R. Yang, R. Feng, Z. Li, X. Zhou, Z. Dong, G. Ghartey-Kwansah, M. Xu, M. Nishi, Q. Zhang, W. Isaacs, J. Ma, X. Xu, *Saudi Journal of Biological Sciences* **2017**, *24*, 622.

[17] J. Li, Y. Yang, L. Huang, *Journal of Controlled Release* **2012**, *158*, 108.

[18] S. Bisso, S. Mura, B. Castagner, P. Couvreur, J.-C. Leroux, *bioRxiv* **2019**, 621102.

[19] F. Pittella, K. Miyata, Y. Maeda, T. Suma, S. Watanabe, Q. Chen, R. J. Christie, K. Osada, N. Nishiyama, K. Kataoka, *Journal of Controlled Release* **2012**, *161*, 868.

[20] J. Chen, P. Gao, S. Yuan, R. Li, A. Ni, L. Chu, L. Ding, Y. Sun, X.-Y. Liu, Y. Duan, *ACS Nano* **2016**, *10*, 11548.

[21] J. Tang, C. B. Howard, S. M. Mahler, K. J. Thurecht, L. Huang, Z. P. Xu, *Nanoscale* **2018**, *10*, 4258.

[22] Y. Wu, W. Gu, L. Li, C. Chen, Z. P. Xu, *Nanomaterials* **2019**, *9*, DOI 10.3390/nano9020159.

[23] K.-W. Huang, Y.-T. Lai, G.-J. Chern, S.-F. Huang, C.-L. Tsai, Y.-C. Sung, C.-C. Chiang, P.-B. Hwang, T.-L. Ho, R.-L. Huang, T.-Y. Shiue, Y. Chen, S.-K. Wang, *Biomacromolecules* **2018**, *19*, 2330.

[24] L. J. de Mello, G. R. R. Souza, E. Winter, A. H. Silva, F. Pittella, T. B. Creczynski-Pasa, *Nanotechnology* **2017**, *28*, 175101.

[25] M. S. Lee, J. E. Lee, E. Byun, N. W. Kim, K. Lee, H. Lee, S. J. Sim, D. S. Lee, J. H. Jeong, *Journal of Controlled Release* **2014**, *192*, 122.

[26] Y. Maeda, F. Pittella, T. Nomoto, H. Takemoto, N. Nishiyama, K. Miyata, K. Kataoka, *Macromolecular Rapid Communications* **2014**, *35*, 1211.

[27] L. N. Luong, K. M. McFalls, D. H. Kohn, *Biomaterials* **2009**, *30*, 6996.

[28] Y. Yazaki, A. Oyane, H. Tsurushima, H. Araki, Y. Sogo, A. Ito, A. Yamazaki, *Colloids and Surfaces B: Biointerfaces* **2014**, *122*, 465.

[29] B. Sun, K. K. Tran, H. Shen, *Biomaterials* **2009**, *30*, 6386.

[30] X. Wang, X. Liu, Y. Xiao, H. Hao, Y. Zhang, R. Tang, *Chemistry – A European Journal* **2018**, *24*, 11518.

[31] G. Wang, R.-Y. Cao, R. Chen, L. Mo, J.-F. Han, X. Wang, X. Xu, T. Jiang, Y.-Q. Deng, K. Lyu, S.-Y. Zhu, E.-D. Qin, R. Tang, C.-F. Qin, *Proceedings of the National Academy of Sciences* **2013**, *110*, 7619 LP.

[32] T. Sakoda, N. Kasahara, L. Kedes, M. Ohyanagi, *Experimental and clinical cardiology* **2007**, *12*, 133.

[33] X. Wang, D. Yang, S. Li, X. Xu, C.-F. Qin, R. Tang, *Biomaterials* **2016**, *106*, 286.

[34] Y.-W. Yang, C.-K. Chao, *The Journal of Gene Medicine* **2003**, *5*, 417.

[35] A. Fasbender, J. H. Lee, R. W. Walters, T. O. Moninger, J. Zabner, M. J. Welsh, *The Journal of Clinical Investigation* **1998**, *102*, 184.

[36] B. Neuhaus, B. Tosun, O. Rotan, A. Frede, A. M. Westendorf, M. Epple, *RSC Advances* **2016**, *6*, 18102.

[37] Y.-H. Lee, H.-C. Wu, C.-W. Yeh, C.-H. Kuan, H.-T. Liao, H.-C. Hsu, J.-C. Tsai, J.-S. Sun, T.-W. Wang, *Acta Biomaterialia* **2017**, *63*, 210.

[38] T. TENKUMO, O. ROTAN, V. SOKOLOVA, M. EPPLE, *Nano Biomedicine* **2013**, *5*, 64.

[39] P. Chen, Y. Liu, J. Zhao, X. Pang, P. Zhang, X. Hou, P. Chen, C. He, Z. Wang, Z. Chen, *Biomaterials Science* **2018**, *6*, 633.

[40] T. Ito, Y. Koyama, M. Otsuka, *Journal of Pharmaceutical Sciences* **2014**, *103*, 179.

[41] V. V Sokolova, I. Radtke, R. Heumann, M. Epple, *Biomaterials* **2006**, *27*, 3147.

[42] V. Sokolova, S. Neumann, A. Kovtun, S. Chernousova, R. Heumann, M. Epple, *Journal of Materials Science* **2010**, *45*, 4952.

[43] C. E. Pedraza, D. C. Bassett, M. D. McKee, V. Nelea, U. Gbureck, J. E. Barralet, *Biomaterials* **2008**, *29*, 3384.

[44] F. Bakan, G. Kara, M. Cokol Cakmak, M. Cokol, E. B. Denkbas, *Colloids and Surfaces B: Biointerfaces* **2017**, *158*, 175.

[45] S.-X. Xie, A. A. Baoum, N. A. Alhakamy, C. J. Berkland, *International Journal of Pharmaceutics* **2018**, *547*, 274.

[46] V. S. S. A. Ayyadevara, K.-H. Roh, *Drug Delivery* **2020**, *27*, 805.

[47] S. J. Lee, K. H. Min, H. J. Lee, A. N. Koo, H. P. Rim, B. J. Jeon, S. Y. Jeong, J. S. Heo, S. C. Lee, *Biomacromolecules* **2011**, *12*, 1224.

[48] Z. Zhou, L. Zhang, J. Li, Y. Shi, Z. Wu, H. Zheng, Z. Wang, W. Zhao, H. Pan, Q. Wang, X. Jin, X. Zhang, R. Tang, B. Fu, *Nanoscale* **2020**, DOI 10.1039/D0NR05640E.

[49] B. D. Quan, E. D. Sone, *Journal of the Royal Society, Interface* **2018**, *15*, 20180269.

[50] L. M. P. Vermeulen, S. C. De Smedt, K. Remaut, K. Braeckmans, *European Journal of Pharmaceutics and Biopharmaceutics* **2018**, *129*, 184.

[51] J. P. Clamme, J. Azoulay, Y. Mély, *Biophysical journal* **2003**, *84*, 1960.

[52] Z. Chen, Y. He, L. Zhang, Y. Li, *Journal of Materials Chemistry B* **2015**, *3*, 225.

[53] P. J. M. Smeets, A. R. Finney, W. J. E. M. Habraken, F. Nudelman, H. Friedrich, J. Laven, J. J. De Yoreo, P. M. Rodger, N. A. J. M. Sommerdijk, *Proceedings of the National Academy of Sciences* **2017**, *114*, E7882 LP.

[54] S. Karthika, T. K. Radhakrishnan, P. Kalaichelvi, *Crystal Growth & Design* **2016**, *16*, 6663.

[55] S.-Y. Han, H. S. Han, S. C. Lee, Y. M. Kang, I.-S. Kim, J. H. Park, *Journal of Materials Chemistry* **2011**, *21*, 7996.

[56] U. Lungwitz, M. Breunig, T. Blunk, A. Göpferich, *European Journal of Pharmaceutics and Biopharmaceutics* **2005**, *60*, 247.

[57] P. L. Ma, M. Lavertu, F. M. Winnik, M. D. Buschmann, *Carbohydrate Polymers* **2017**, *176*, 167.

[58] K. M. Zurick, C. Qin, M. T. Bernards, *Journal of Biomedical Materials Research Part A* **2013**, *101A*, 1571.

[59] B. Cantaert, E. Beniash, F. C. Meldrum, *Journal of Materials Chemistry B* **2013**, *1*, 6586.

[60] X. Y. Liu, in (Eds.: K. Sato, Y. Furukawa, K.B.T.-A. in C.G.R. Nakajima), Elsevier Science B.V., Amsterdam, **2001**, pp. 42–61.

[61] M. Antonietti, M. Breulmann, C. G. Göltner, H. Cölfen, K. K. W. Wong, D. Walsh, S. Mann, *Chemistry – A European Journal* **1998**, *4*, 2493.

[62] Y. Sang, K. Xie, Y. Mu, Y. Lei, B. Zhang, S. Xiong, Y. Chen, N. Qi, *Cytotechnology* **2015**, *67*, 67.

[63] R. J. Nap, S. H. Park, I. Szleifer, *Soft Matter* **2018**, *14*, 2365.

[64] K. Huber, *The Journal of Physical Chemistry* **1993**, *97*, 9825.

[65] C. David, E. Companys, J. Galceran, J. L. Garcés, F. Mas, C. Rey-Castro, J.

Salvador, J. Puy, *The Journal of Physical Chemistry B* **2007**, *111*, 10421.

[66] K. H. Min, H. J. Lee, K. Kim, I. C. Kwon, S. Y. Jeong, S. C. Lee, *Biomaterials* **2012**, *33*, 5788.

[67] B. Deng, M. Xia, J. Qian, R. Li, L. Li, J. Shen, G. Li, Y. Xie, *Molecular Pharmaceutics* **2017**, *14*, 1938.

[68] M. Tanahashi, T. Matsuda, *Journal of Biomedical Materials Research* **1997**, *34*, 305.

[69] Z. Wang, L. Wang, N. Prabhakar, Y. Xing, J. M. Rosenholm, J. Zhang, K. Cai, *Acta Biomaterialia* **2019**, *86*, 416.

[70] Y. Lv, H. Huang, B. Yang, H. Liu, Y. Li, J. Wang, *Carbohydrate Polymers* **2014**, *111*, 101.

[71] H. J. Lee, S. E. Kim, I. K. Kwon, C. Park, C. Kim, J. Yang, S. C. Lee, *Chemical Communications* **2010**, *46*, 377.

[72] B. J. Kim, K. H. Min, G. H. Hwang, H. J. Lee, S. Y. Jeong, E.-C. Kim, S. C. Lee, *Macromolecular Research* **2015**, *23*, 111.

[73] H. S. Han, J. Lee, H. R. Kim, S. Y. Chae, M. Kim, G. Saravanakumar, H. Y. Yoon, D. G. You, H. Ko, K. Kim, I. C. Kwon, J. C. Park, J. H. Park, *Journal of Controlled Release* **2013**, *168*, 105.

[74] G. Dördelmann, D. Kozlova, S. Karczewski, R. Lizio, S. Knauer, M. Epple, *Journal of Materials Chemistry B* **2014**, *2*, 7250.

[75] H. Zhou, X. Wang, R. Tang, *Future Virology* **2018**, *13*, 79.

[76] H. Zhou, G. Wang, X. Wang, Z. Song, R. Tang, *Angewandte Chemie International Edition* **2017**, *56*, 12908.

[77] X. Wang, Y. Deng, S. Li, G. Wang, E. Qin, X. Xu, R. Tang, C. Qin, *Advanced Healthcare Materials* **2012**, *1*, 443.

[78] X. Zhou, X. Cheng, W. Feng, K. Qiu, L. Chen, W. Nie, Z. Yin, X. Mo, H. Wang, C. He, *Dalton Transactions* **2014**, *43*, 11834.

[79] S. M. Londoño-Restrepo, R. Jeronimo-Cruz, B. M. Millán-Malo, E. M. Rivera-Muñoz, M. E. Rodriguez-García, *Scientific Reports* **2019**, *9*, 5915.

[80] T. A. Dick, L. A. dos Santos, *Materials Science and Engineering C* **2017**, *77*, 874.

[81] D. Lee, K. Upadhye, P. N. Kumta, *Materials Science and Engineering: B* **2012**, *177*, 289.

[82] R. R. Arvizo, O. R. Miranda, M. A. Thompson, C. M. Pabelick, R. Bhattacharya, J. D. Robertson, V. M. Rotello, Y. S. Prakash, P. Mukherjee, *Nano Letters* **2010**, *10*, 2543.

[83] E. Fröhlich, *International journal of nanomedicine* **2012**, *7*, 5577.

[84] M. A. Khan, V. M. Wu, S. Ghosh, V. Uskoković, *Journal of Colloid and Interface Science* **2016**, *471*, 48.

[85] S. E. A. Gratton, P. A. Ropp, P. D. Pohlhaus, J. C. Luft, V. J. Madden, M. E. Napier, J. M. DeSimone, *Proceedings of the National Academy of Sciences* **2008**, *105*, 11613 LP.

[86] W. Zhang, X. Kang, B. Yuan, H. Wang, T. Zhang, M. Shi, Z. Zheng, Y. Zhang, C. Peng, X. Fan, H. Yang, Y. Shen, Y. Huang, *Theranostics* **2019**, *9*, 1580.

[87] D. Pezzoli, E. Giupponi, D. Mantovani, G. Candiani, *Scientific Reports* **2017**, *7*, 44134.

[88] P. Pankongadisak, E. Tsekoura, O. Suwantong, H. Uludağ, *International Journal of Biological Macromolecules* **2020**, *149*, 296.

[89] E. K. Tsekoura, T. Dick, P. Pankongadisak, D. Graf, Y. Boluk, H. Uludağ, *Pharmaceuticals* **2021**, *14*, 666.

[90] M. Ilett, O. Matar, F. Bamiduro, S. Sanchez-Segado, R. Brydson, A. Brown, N. Hondow, *Scientific Reports* **2020**, *10*, 5278.

[91] V. Francia, K. Yang, S. Deville, C. Reker-Smit, I. Nelissen, A. Salvati, *ACS nano* **2019**, *13*, 11107.

[92] A. Salvati, A. S. Pitek, M. P. Monopoli, K. Prapainop, F. B. Bombelli, D. R. Hristov, P. M. Kelly, C. Åberg, E. Mahon, K. A. Dawson, *Nature Nanotechnology* **2013**, *8*, 137.

[93] Y. Yazaki, A. Oyane, H. Tsurushima, H. Araki, Y. Sogo, A. Ito, A. Yamazaki, *Journal of Biomaterials Applications* **2013**, *28*, 937.

[94] Y. Yazaki, A. Oyane, Y. Sogo, A. Ito, A. Yamazaki, H. Tsurushima, *Biomaterials* **2011**, *32*, 4896.

[95] A. Oyane, Y. Yazaki, H. Araki, Y. Sogo, A. Ito, A. Yamazaki, H. Tsurushima, *Journal of Materials Science: Materials in Medicine* **2012**, *23*, 1011.

[96] A. Lotsari, A.K. Rajasekharan, M. Halvarsson, M. Andersson, Transformation of amorphous calcium phosphate to bone-like apatite, Nature Communications. 9 (2018) 4170. https://doi.org/10.1038/s41467-018-06570-x.

Chapter 3

[1] Glover, D. J., Lipps, H. J. & Jans, D. A. Towards safe, non-viral therapeutic gene expression in humans. *Nature Reviews Genetics* **6**, 299–310 (2005).

[2] Picanço-Castro, V. *et al*. Emerging patent landscape for non-viral vectors used for gene therapy. *Nature Biotechnology* **38**, 151–157 (2020).

[3] Baranowski, E., Ruiz-Jarabo, C. M., Pariente, N., Verdaguer, N. & Domingo, E. Evolution of Cell Recognition by Viruses: A Source of Biological Novelty with Medical Implications. *Advances in Virus Research* **62**, 19–111 (2003).

[4] Peng, X., Xu H FAU - Jones, B., Jones B FAU - Chen, S., Chen S FAU - Zhou, H. & Zhou, H. Silicified virus-like nanoparticles in an extreme thermal environment: implications for the preservation of viruses in the geological record. *Geobiology* **6**, 511–526 (2013).

[5] Wang, X. *et al*. Biomineralization State of Viruses and Their Biological Potential. *Chemistry – A European Journal* **24**, 11518–11529 (2018).

[6] Kyle, J. E., Pedersen, K. & Ferris, F. G. Virus Mineralization at Low pH in the Rio Tinto, Spain. *Geomicrobiology Journal* **25**, 338–345 (2008).

[7] Zhou, H., Wang, G., Wang, X., Song, Z. & Tang, R. Mineralized State of the Avian Influenza Virus in the Environment. *Angewandte Chemie International Edition* **56**, 12908–12912 (2017).

[8] De Wit, R. *et al*. Viruses Occur Incorporated in Biogenic High-Mg Calcite from Hypersaline Microbial Mats. *PLOS ONE* **10**, e0130552 (2015).

[9] Frede, A. *et al*. Local delivery of siRNA-loaded calcium phosphate nanoparticles abates pulmonary inflammation. *Nanomedicine: Nanotechnology, Biology and Medicine* **13**, 2395–2403 (2017).

[10] Zhou, H., Wang, X. & Tang, R. Could a mineralized state of avian flu virus be dangerous to humans? *Future Virology* **13**, 79–81 (2018).

[11] Wang, G. *et al*. Rational design of thermostable vaccines by engineered peptide-induced virus self-biomineralization under physiological conditions. *Proceedings of the National Academy of Sciences* **110**, 7619 LP – 7624 (2013).

[12] Sakoda, T., Kasahara, N., Kedes, L. & Ohyanagi, M. Calcium phosphate coprecipitation greatly enhances transduction of cardiac myocytes and vascular smooth muscle cells by lentivirus vectors. *Experimental and clinical cardiology* **12**, 133–138 (2007).

[13] Yang, Y.-W. & Chao, C.-K. Incorporation of calcium phosphate enhances

recombinant adeno-associated virus-mediated gene therapy in diabetic mice. *The Journal of Gene Medicine* **5**, 417–424 (2003).

[14] Fasbender, A. *et al*. Incorporation of adenovirus in calcium phosphate precipitates enhances gene transfer to airway epithelia in vitro and in vivo. *The Journal of Clinical Investigation* **102**, 184–193 (1998).

[15] Wang, X. *et al*. Biomineralized vaccine nanohybrid for needle-free intranasal immunization. *Biomaterials* **106**, 286–294 (2016).

[16] Wang, X. *et al*. Vaccine Engineering with Dual-Functional Mineral Shell: A Promising Strategy to Overcome Preexisting Immunity. *Advanced Materials* **28**, 694–700 (2016).

[17] Huang, L.-L. *et al*. MnCaCs-Biomineralized Oncolytic Virus for Bimodal Imaging-Guided and Synergistically Enhanced Anticancer Therapy. *Nano Letters* **19**, 8002–8009 (2019).

[18] Maleki Dizaj, S. *et al*. An update on calcium carbonate nanoparticles as cancer drug/gene delivery system. *Expert Opinion on Drug Delivery* **16**, 331–345 (2019).

[19] Zhao, D., Wang, C.-Q., Zhuo, R.-X. & Cheng, S.-X. Modification of nanostructured calcium carbonate for efficient gene delivery. *Colloids and Surfaces B: Biointerfaces* **118**, 111–116 (2014).

[20] Chen, S., Li, F., Zhuo, R.-X. & Cheng, S.-X. Efficient non-viral gene delivery mediated by nanostructured calcium carbonate in solution-based transfection and solid-phase transfection. *Molecular BioSystems* **7**, 2841–2847 (2011).

[21] Rezvani Amin, Z., Rahimizadeh, M., Eshghi, H., Dehshahri, A. & Ramezani, M. The effect of cationic charge density change on transfection efficiency of polyethylenimine. *Iranian journal of basic medical sciences* **16**, 150–156 (2013).

[22] Clamme, J. P., Azoulay, J. & Mély, Y. Monitoring of the formation and dissociation of polyethylenimine/DNA complexes by two photon fluorescence correlation spectroscopy. *Biophysical journal* **84**, 1960–1968 (2003).

[23] Kim, D., Lee, B., Thomopoulos, S. & Jun, Y.-S. In Situ Evaluation of Calcium Phosphate Nucleation Kinetics and Pathways during Intra- and Extrafibrillar Mineralization of Collagen Matrices. *Crystal Growth & Design* **16**, 5359–5366 (2016).

[24] Min, K. H. *et al*. The tumor accumulation and therapeutic efficacy of doxorubicin carried in calcium phosphate-reinforced polymer nanoparticles. *Biomaterials* **33**, 5788–5797 (2012).

[25] Cantaert, B., Beniash, E. & Meldrum, F. C. The role of poly(aspartic acid) in the precipitation of calcium phosphate in confinement. *Journal of Materials Chemistry*

B **1**, 6586–6595 (2013).

[26] Nudelman, F., Lausch, A. J., Sommerdijk, N. A. J. M. & Sone, E. D. In vitro models of collagen biomineralization. *Journal of Structural Biology* **183**, 258–269 (2013).

[27] Quan, B. D. & Sone, E. D. The effect of polyaspartate chain length on mediating biomimetic remineralization of collagenous tissues. *Journal of the Royal Society, Interface* **15**, 20180269 (2018).

[28] Lee, S. J. *et al*. Ketal Cross-Linked Poly(ethylene glycol)-Poly(amino acid)s Copolymer Micelles for Efficient Intracellular Delivery of Doxorubicin. *Biomacromolecules* **12**, 1224–1233 (2011).

[29] Kim, B. J. *et al*. Calcium carbonate-mineralized polymer nanoparticles for pH-responsive robust nanocarriers of docetaxel. *Macromolecular Research* **23**, 111–117 (2015).

[30] Zhou, Z. *et al*. Polyelectrolyte-calcium Complexes as a Pre-precursor Induce Biomimetic Mineralization of Collagen. *Nanoscale* (2020). doi:10.1039/D0NR05640E

[31] Nudelman, F. *et al*. The role of collagen in bone apatite formation in the presence of hydroxyapatite nucleation inhibitors. *Nature Materials* **9**, 1004–1009 (2010).

[32] Liu, X. Y. - Generic mechanism of heterogeneous nucleation and molecular interfacial effects. in (eds. Sato, K., Furukawa, Y. & Nakajima, K. B. T.-A. in C. G. R.) 42–61 (Elsevier Science B.V., 2001).

[33] Aizenberg, J., Black, A. J. & Whitesides, G. M. Oriented Growth of Calcite Controlled by Self-Assembled Monolayers of Functionalized Alkanethiols Supported on Gold and Silver. *Journal of the American Chemical Society* **121**, 4500–4509 (1999).

[34] Toworfe, G. K., Composto, R. J., Shapiro, I. M. & Ducheyne, P. Nucleation and growth of calcium phosphate on amine-, carboxyl- and hydroxyl-silane self-assembled monolayers. *Biomaterials* **27**, 631–642 (2006).

[35] Lv, Y. *et al*. A robust pH-sensitive drug carrier: Aqueous micelles mineralized by calcium phosphate based on chitosan. *Carbohydrate Polymers* **111**, 101–107 (2014).

[36] Han, S.-Y. *et al*. Mineralized hyaluronic acid nanoparticles as a robust drug carrier. *Journal of Materials Chemistry* **21**, 7996–8001 (2011).

[37] Lee, H. J. *et al*. Spatially mineralized self-assembled polymeric nanocarriers with enhanced robustness and controlled drug-releasing property. *Chemical Communications* **46**, 377–379 (2010).

[38] Stetefeld, J., McKenna, S. A. & Patel, T. R. Dynamic light scattering: a practical guide and applications in biomedical sciences. *Biophysical Reviews* **8**, 409–427 (2016).

[39] Wiśniewska, M., Ostolska, I. & Sternik, D. Impact of adsorption of poly(aspartic acid) and its copolymers with polyethylene glycol on thermal characteristic of Cr2O3. *Journal of Thermal Analysis and Calorimetry* **125**, 1171–1184 (2016).

[40] KC, R. B., Kucharski, C. & Uludağ, H. Additive nanocomplexes of cationic lipopolymers for improved non-viral gene delivery to mesenchymal stem cells. *Journal of Materials Chemistry B* **3**, 3972–3982 (2015).

[41] Parmar, M. B. *et al*. Combinational siRNA delivery using hyaluronic acid modified amphiphilic polyplexes against cell cycle and phosphatase proteins to inhibit growth and migration of triple-negative breast cancer cells. *Acta Biomaterialia* **66**, 294–309 (2018).

[42] Zheng, M. & Yu, J. The effect of particle shape and size on cellular uptake. *Drug Delivery and Translational Research* **6**, 67–72 (2016).

[43] Zhang, S., Li, J., Lykotrafitis, G., Bao, G. & Suresh, S. Size-Dependent Endocytosis of Nanoparticles. *Advanced Materials* **21**, 419–424 (2009).

[44] He, C., Hu, Y., Yin, L., Tang, C. & Yin, C. Effects of particle size and surface charge on cellular uptake and biodistribution of polymeric nanoparticles. *Biomaterials* **31**, 3657–3666 (2010).

[45] Arnida, Janát-Amsbury, M. M., Ray, A., Peterson, C. M. & Ghandehari, H. Geometry and surface characteristics of gold nanoparticles influence their biodistribution and uptake by macrophages. *European Journal of Pharmaceutics and Biopharmaceutics* **77**, 417–423 (2011).

[46] Pezzoli, D., Giupponi, E., Mantovani, D. & Candiani, G. Size matters for in vitro gene delivery: investigating the relationships among complexation protocol, transfection medium, size and sedimentation. *Scientific Reports* **7**, 44134 (2017).

[47] Behzadi, S. *et al*. Cellular uptake of nanoparticles: journey inside the cell. *Chemical Society Reviews* **46**, 4218–4244 (2017).

[48] Zhang, W. *et al*. Nano-Structural Effects on Gene Transfection: Large, Botryoid-Shaped Nanoparticles Enhance DNA Delivery via Macropinocytosis and Effective Dissociation. *Theranostics* **9**, 1580–1598 (2019).

[49] Nap, R. J., Park, S. H. & Szleifer, I. Competitive calcium ion binding to end-tethered weak polyelectrolytes. *Soft Matter* **14**, 2365–2378 (2018).

[50] Huber, K. Calcium-induced shrinking of polyacrylate chains in aqueous solution. *The Journal of Physical Chemistry* **97**, 9825–9830 (1993).

[51] Derkani, M. H. *et al*. Mechanisms of Surface Charge Modification of Carbonates in Aqueous Electrolyte Solutions. *Colloids and Interfaces* **3**, (2019).

[52] Ma, P. L., Lavertu, M., Winnik, F. M. & Buschmann, M. D. Stability and binding affinity of DNA/chitosan complexes by polyanion competition. *Carbohydrate Polymers* **176**, 167–176 (2017).

[53] Chen, Z., He, Y., Zhang, L. & Li, Y. Enhanced DNA release from disulfide-containing layered nanocomplexes by heparin-electrostatic competition. *Journal of Materials Chemistry B* **3**, 225–237 (2015).

[54] Park, J. H., Han, J. & Lee, M. Thymidine Kinase Gene Delivery Using Curcumin Loaded Peptide Micelles as a Combination Therapy for Glioblastoma. *Pharmaceutical Research* **32**, 528–537 (2015).

[55] Gwak, S.-J., Macks, C., Bae, S., Cecil, N. & Lee, J. S. Physicochemical stability and transfection efficiency of cationic amphiphilic copolymer/pDNA polyplexes for spinal cord injury repair. *Scientific Reports* **7**, 11247 (2017).

[56] Russo, R., Malinconico, M. & Santagata, G. Effect of Cross-Linking with Calcium Ions on the Physical Properties of Alginate Films. *Biomacromolecules* **8**, 3193–3197 (2007).

[57] Ayyadevara, V. S. S. A. & Roh, K.-H. Calcium enhances polyplex-mediated transfection efficiency of plasmid DNA in Jurkat cells. *Drug Delivery* **27**, 805–815 (2020).

[58] Xie, S.-X., Baoum, A. A., Alhakamy, N. A. & Berkland, C. J. Calcium enhances gene expression when using low molecular weight poly-l-lysine delivery vehicles. *International Journal of Pharmaceutics* **547**, 274–281 (2018).

[59] Chen, P. *et al*. The synthesis of amphiphilic polyethyleneimine/calcium phosphate composites for bispecific T-cell engager based immunogene therapy. *Biomaterials Science* **6**, 633–641 (2018).

[60] Han, H. S. *et al*. Robust PEGylated hyaluronic acid nanoparticles as the carrier of doxorubicin: Mineralization and its effect on tumor targetability in vivo. *Journal of Controlled Release* **168**, 105–114 (2013).

[61] Farkas, N. & Kramar, J. A. Dynamic light scattering distributions by any means. *Journal of Nanoparticle Research* **23**, 120 (2021).

[62] Shkilnyy, A. *et al*. Poly(ethylene imine)-Controlled Calcium Phosphate Mineralization. *Langmuir* **24**, 2102–2109 (2008).

[63] Wang, D. *et al*. Isolation and Characterization of MC3T3-E1 Preosteoblast Subclones with Distinct In Vitro and In Vivo Differentiation/Mineralization Potential. *Journal of Bone and Mineral Research* **14**, 893–903 (1999).

[64] Tsekoura, E. K. *et al*. Delivery of Bioactive Gene Particles via Gelatin-Collagen-PEG-Based Electrospun Matrices. *Pharmaceuticals* **14**, 666 (2021).

[65] Gratton, S. E. A. *et al*. The effect of particle design on cellular internalization pathways. *Proceedings of the National Academy of Sciences* **105**, 11613 LP – 11618 (2008).

[66] Lam, A. M. I. & Cullis, P. R. Calcium enhances the transfection potency of plasmid DNA–cationic liposome complexes. *Biochimica et Biophysica Acta (BBA) - Biomembranes* **1463**, 279–290 (2000).

[67] Eliasson, L. *et al*. Endocytosis of secretory granules in mouse pancreatic beta-cells evoked by transient elevation of cytosolic calcium. *The Journal of physiology* **493 (Pt 3)**, 755–767 (1996).

[68] Epstein, R. J. *et al*. Extracellular calcium mimics the actions of platelet-derived growth factor on mouse fibroblasts. *Cell Growth Differentiation* **3**, 157–164 (1992).

[69] Acri, T., Laird, N. & Geary, S. Effects of calcium concentration on nonviral gene delivery to bone marrow-derived stem cells. *J Tissue Eng Regen Med* 2256–2265 (2019).

[70] Luo, S. *et al*. A Self-Biomineralized Novel Adenovirus Vectored COVID-19 Vaccine for Boosting Immunization of Mice. *Virologica Sinica* (2021). doi:10.1007/s12250-021-00434-3

[71] Xue, J., Wu, T., Dai, Y. & Xia, Y. Electrospinning and Electrospun Nanofibers: Methods, Materials, and Applications. *Chemical Reviews* **119**, 5298–5415 (2019).

Chapter 4

[1] H. Zhou, G. Wang, X. Wang, Z. Song, R. Tang, Mineralized State of the Avian Influenza Virus in the Environment, Angewandte Chemie International Edition. 56 (2017) 12908–12912. https://doi.org/10.1002/anie.201705769.

[2] J.E. Kyle, K. Pedersen, F.G. Ferris, Virus Mineralization at Low pH in the Rio Tinto, Spain, Geomicrobiology Journal. 25 (2008) 338–345. https://doi.org/10.1080/01490450802402703.

[3] X. Peng, B. Xu H FAU - Jones, S. Jones B FAU - Chen, H. Chen S FAU - Zhou, H. Zhou, Silicified virus-like nanoparticles in an extreme thermal environment: implications for the preservation of viruses in the geological record, Geobiology. 6 (2013) 511–526.

[4] R. De Wit, P. Gautret, Y. Bettarel, C. Roques, C. Marlière, M. Ramonda, T. Nguyen Thanh, H. Tran Quang, T. Bouvier, Viruses Occur Incorporated in Biogenic High-

Mg Calcite from Hypersaline Microbial Mats, PLOS ONE. 10 (2015) e0130552. https://doi.org/10.1371/journal.pone.0130552.

[5] T. Kokubo, H. Takadama, How useful is SBF in predicting in vivo bone bioactivity?, Biomaterials. 27 (2006) 2907–2915. https://doi.org/https://doi.org/10.1016/j.biomaterials.2006.01.017.

[6] Y. Sang, K. Xie, Y. Mu, Y. Lei, B. Zhang, S. Xiong, Y. Chen, N. Qi, Salt ions and related parameters affect PEI-DNA particle size and transfection efficiency in Chinese hamster ovary cells, Cytotechnology. 67 (2015) 67–74. https://doi.org/10.1007/s10616-013-9658-z.

[7] Z. Zhou, L. Zhang, J. Li, Y. Shi, Z. Wu, H. Zheng, Z. Wang, W. Zhao, H. Pan, Q. Wang, X. Jin, X. Zhang, R. Tang, B. Fu, Polyelectrolyte-calcium Complexes as a Pre-precursor Induce Biomimetic Mineralization of Collagen, Nanoscale. (2020). https://doi.org/10.1039/D0NR05640E.

[8] W.J. Peterson, K.H. Tachiki, D.T. Yamaguchi, Serial passage of MC3T3-E1 cells down-regulates proliferation during osteogenesis in vitro, Cell Proliferation. 37 (2004) 325–336. https://doi.org/https://doi.org/10.1111/j.1365-2184.2004.00316.x.

[9] X.-Z. Yan, W. Yang, F. Yang, M. Kersten-Niessen, J.A. Jansen, S.K. Both, Effects of Continuous Passaging on Mineralization of MC3T3-E1 Cells with Improved Osteogenic Culture Protocol, Tissue Engineering Part C: Methods. 20 (2013) 198–204. https://doi.org/10.1089/ten.tec.2012.0412.

[10] J. Cao, X. Wu, X. Qin, Z. Li, Uncovering the Effect of Passage Number on HT29 Cell Line Based on the Cell Metabolomic Approach, Journal of Proteome Research. 20 (2021) 1582–1590. https://doi.org/10.1021/acs.jproteome.0c00806.

[11] S.J. Lee, K.H. Min, H.J. Lee, A.N. Koo, H.P. Rim, B.J. Jeon, S.Y. Jeong, J.S. Heo, S.C. Lee, Ketal Cross-Linked Poly(ethylene glycol)-Poly(amino acid)s Copolymer Micelles for Efficient Intracellular Delivery of Doxorubicin, Biomacromolecules. 12 (2011) 1224–1233. https://doi.org/10.1021/bm101517x.

[12] L. Eliasson, P. Proks, C. Ammälä, F.M. Ashcroft, K. Bokvist, E. Renström, P. Rorsman, P.A. Smith, Endocytosis of secretory granules in mouse pancreatic beta-cells evoked by transient elevation of cytosolic calcium, The Journal of Physiology. 493 (Pt 3 (1996) 755–767. https://doi.org/10.1113/jphysiol.1996.sp021420.

[13] X. Wang, X. Liu, Y. Xiao, H. Hao, Y. Zhang, R. Tang, Biomineralization State of Viruses and Their Biological Potential, Chemistry – A European Journal. 24 (2018) 11518–11529. https://doi.org/10.1002/chem.201705936.

[14] F. Nudelman, K. Pieterse, A. George, P.H.H. Bomans, H. Friedrich, L.J. Brylka, P.A.J. Hilbers, G. de With, N.A.J.M. Sommerdijk, The role of collagen in bone apatite formation in the presence of hydroxyapatite nucleation inhibitors, Nature Materials. 9 (2010) 1004–1009. https://doi.org/10.1038/nmat2875.

[15] G. Wang, R.-Y. Cao, R. Chen, L. Mo, J.-F. Han, X. Wang, X. Xu, T. Jiang, Y.-Q. Deng, K. Lyu, S.-Y. Zhu, E.-D. Qin, R. Tang, C.-F. Qin, Rational design of thermostable vaccines by engineered peptide-induced virus self-biomineralization under physiological conditions, Proceedings of the National Academy of Sciences. 110 (2013) 7619–7624. https://doi.org/10.1073/pnas.1300233110.

[16] B.J. Kim, K.H. Min, G.H. Hwang, H.J. Lee, S.Y. Jeong, E.-C. Kim, S.C. Lee, Calcium carbonate-mineralized polymer nanoparticles for pH-responsive robust nanocarriers of docetaxel, Macromolecular Research. 23 (2015) 111–117. https://doi.org/10.1007/s13233-015-3020-6.

[17] D. Barati, J.D. Walters, S.R. Pajoum Shariati, S. Moeinzadeh, E. Jabbari, Effect of Organic Acids on Calcium Phosphate Nucleation and Osteogenic Differentiation of Human Mesenchymal Stem Cells on Peptide Functionalized Nanofibers, Langmuir. 31 (2015) 5130–5140. https://doi.org/10.1021/acs.langmuir.5b00615.

[18] K.K. Perkin, J.L. Turner, K.L. Wooley, S. Mann, Fabrication of Hybrid Nanocapsules by Calcium Phosphate Mineralization of Shell Cross-Linked Polymer Micelles and Nanocages, Nano Letters. 5 (2005) 1457–1461. https://doi.org/10.1021/nl050817w.

[19] L.-L. Huang, X. Li, J. Zhang, Q.R. Zhao, M.J. Zhang, A.-A. Liu, D.-W. Pang, H.-Y. Xie, MnCaCs-Biomineralized Oncolytic Virus for Bimodal Imaging-Guided and Synergistically Enhanced Anticancer Therapy, Nano Letters. 19 (2019) 8002–8009. https://doi.org/10.1021/acs.nanolett.9b03193.

[20] J. Chen, P. Gao, S. Yuan, R. Li, A. Ni, L. Chu, L. Ding, Y. Sun, X.-Y. Liu, Y. Duan, Oncolytic Adenovirus Complexes Coated with Lipids and Calcium Phosphate for Cancer Gene Therapy, ACS Nano. 10 (2016) 11548–11560. https://doi.org/10.1021/acsnano.6b06182.

[21] H. Jiang, X.-Y. Liu, G. Zhang, Y. Li, Kinetics and Template Nucleation of Self-Assembled Hydroxyapatite Nanocrystallites by Chondroitin Sulfate, Journal of Biological Chemistry . 280 (2005) 42061–42066. https://doi.org/10.1074/jbc.M412280200.

[22] S. Wang, Y. Yang, R. Wang, X. Kong, X. Wang, Mineralization of calcium phosphate controlled by biomimetic self-assembled peptide monolayers via surface electrostatic potentials, Bioactive Materials. 5 (2020) 387–397. https://doi.org/https://doi.org/10.1016/j.bioactmat.2020.03.003.

[23] M. Tanahashi, T. Matsuda, Surface functional group dependence on apatite formation on self-assembled monolayers in a simulated body fluid, Journal of Biomedical Materials Research. 34 (1997) 305–315. https://doi.org/10.1002/(SICI)1097-4636(19970305)34:3<305::AID-JBM5>3.0.CO;2-O.

[24] K.H. Min, H.J. Lee, K. Kim, I.C. Kwon, S.Y. Jeong, S.C. Lee, The tumor

accumulation and therapeutic efficacy of doxorubicin carried in calcium phosphate-reinforced polymer nanoparticles, Biomaterials. 33 (2012) 5788–5797. https://doi.org/https://doi.org/10.1016/j.biomaterials.2012.04.057.

[25] Z. Xu, L. Shi, D. Hu, B. Hu, M. Yang, L. Zhu, Formation of hierarchical bone-like apatites on silk microfiber templates: Via biomineralization, RSC Advances. 6 (2016) 76426–76433. https://doi.org/10.1039/c6ra17199k.

[26] K. Yamashita, N. Oikawa, T. Umegaki, Acceleration and Deceleration of Bone-Like Crystal Growth on Ceramic Hydroxyapatite by Electric Poling, Chemistry of Materials. 8 (1996) 2697–2700. https://doi.org/10.1021/cm9602858.

[27] Y. Xie, X. Liu, P.K. Chu, C. Ding, Nucleation and growth of calcium–phosphate on Ca-implanted titanium surface, Surface Science. 600 (2006) 651–656. https://doi.org/https://doi.org/10.1016/j.susc.2005.11.016.

[28] M. OHGAKI, S. NAKAMURA, T. OKURA, K. YAMASHITA, Enhanced Mineralization on Electrically Polarized Hydroxyapatite Ceramics in Culture Medium, Journal of the Ceramic Society of Japan. 108 (2000) 1037–1040. https://doi.org/10.2109/jcersj.108.1263_1037.

[29] E. Buck, S. Lee, Q. Gao, S.D. Tran, F. Tamimi, L.S. Stone, M. Cerruti, The Role of Surface Chemistry in the Osseointegration of PEEK Implants, ACS Biomaterials Science & Engineering. 8 (2022) 1506–1521. https://doi.org/10.1021/acsbiomaterials.1c01434.

[30] F. Nudelman, A.J. Lausch, N.A.J.M. Sommerdijk, E.D. Sone, In vitro models of collagen biomineralization, Journal of Structural Biology. 183 (2013) 258–269. https://doi.org/10.1016/j.jsb.2013.04.003.

[31] G. Dördelmann, D. Kozlova, S. Karczewski, R. Lizio, S. Knauer, M. Epple, Calcium phosphate increases the encapsulation efficiency of hydrophilic drugs (proteins, nucleic acids) into poly(d,l-lactide-co-glycolide acid) nanoparticles for intracellular delivery, Journal of Materials Chemistry B. 2 (2014) 7250–7259. https://doi.org/10.1039/C4TB00922C.

[32] L. Niu, S.E. Jee, K. Jiao, L. Tonggu, M. Li, L. Wang, Y. Yang, J. Bian, L. Breschi, S.S. Jang, J. Chen, D.H. Pashley, F.R. Tay, Collagen intrafibrillar mineralization as a result of the balance between osmotic equilibrium and electroneutrality, Nature Materials. 16 (2017) 370–378. https://doi.org/10.1038/nmat4789.

[33] M. Tavafoghi, N. Brodusch, R. Gauvin, M. Cerruti, Hydroxyapatite formation on graphene oxide modified with amino acids: arginine versus glutamic acid, Journal of The Royal Society Interface. 13 (2016) 20150986. https://doi.org/10.1098/rsif.2015.0986.

[34] M. Valiskó, D. Boda, D. Gillespie, Selective Adsorption of Ions with Different Diameter and Valence at Highly Charged Interfaces, The Journal of Physical

Chemistry C. 111 (2007) 15575–15585. https://doi.org/10.1021/jp073703c.

[35] P. Zhu, Y. Masuda, K. Koumoto, The effect of surface charge on hydroxyapatite nucleation, Biomaterials. 25 (2004) 3915–3921. https://doi.org/https://doi.org/10.1016/j.biomaterials.2003.10.022.

[36] G.K. Toworfe, R.J. Composto, I.M. Shapiro, P. Ducheyne, Nucleation and growth of calcium phosphate on amine-, carboxyl- and hydroxyl-silane self-assembled monolayers, Biomaterials. 27 (2006) 631–642. https://doi.org/https://doi.org/10.1016/j.biomaterials.2005.06.017.

[37] S. Bodhak, S. Bose, A. Bandyopadhyay, Role of surface charge and wettability on early stage mineralization and bone cell–materials interactions of polarized hydroxyapatite, Acta Biomaterialia. 5 (2009) 2178–2188. https://doi.org/https://doi.org/10.1016/j.actbio.2009.02.023.

[38] I. HIRATA, M. AKAMATSU, E. FUJII, S. POOLTHONG, M. OKAZAKI, Chemical analyses of hydroxyapatite formation on SAM surfaces modified with COOH, NH₂, CH₃, and OH functions, Dental Materials Journal. 29 (2010) 438–445. https://doi.org/10.4012/dmj.2010-017.

[39] H.J. Lee, S.E. Kim, I.K. Kwon, C. Park, C. Kim, J. Yang, S.C. Lee, Spatially mineralized self-assembled polymeric nanocarriers with enhanced robustness and controlled drug-releasing property, Chemical Communications. 46 (2010) 377–379. https://doi.org/10.1039/B913732G.

[40] H.S. Han, J. Lee, H.R. Kim, S.Y. Chae, M. Kim, G. Saravanakumar, H.Y. Yoon, D.G. You, H. Ko, K. Kim, I.C. Kwon, J.C. Park, J.H. Park, Robust PEGylated hyaluronic acid nanoparticles as the carrier of doxorubicin: Mineralization and its effect on tumor targetability in vivo, Journal of Controlled Release. 168 (2013) 105–114. https://doi.org/https://doi.org/10.1016/j.jconrel.2013.02.022.

[41] Y. Lv, H. Huang, B. Yang, H. Liu, Y. Li, J. Wang, A robust pH-sensitive drug carrier: Aqueous micelles mineralized by calcium phosphate based on chitosan, Carbohydrate Polymers. 111 (2014) 101–107. https://doi.org/https://doi.org/10.1016/j.carbpol.2014.04.082.

[42] P. Chen, Y. Liu, J. Zhao, X. Pang, P. Zhang, X. Hou, P. Chen, C. He, Z. Wang, Z. Chen, The synthesis of amphiphilic polyethyleneimine/calcium phosphate composites for bispecific T-cell engager based immunogene therapy, Biomaterials Science. 6 (2018) 633–641. https://doi.org/10.1039/C7BM01143A.

[43] T. A. Dick, H. Uludağ, Mineralized polyplexes for gene delivery: Improvement of transfection efficiency as a consequence of calcium incubation and not mineralization, Materials Science and Engineering: C. 129 (2021) 112419. https://doi.org/https://doi.org/10.1016/j.msec.2021.112419.

[44] T. Atz Dick, H. Uludağ, A Polyplex in a Shell: The Effect of Poly(aspartic acid)-

Mediated Calcium Carbonate Mineralization on Polyplexes Properties and Transfection Efficiency, Molecular Pharmaceutics. (2022). https://doi.org/10.1021/acs.molpharmaceut.1c00909.

[45] S.-X. Xie, A.A. Baoum, N.A. Alhakamy, C.J. Berkland, Calcium enhances gene expression when using low molecular weight poly-l-lysine delivery vehicles, International Journal of Pharmaceutics. 547 (2018) 274–281. https://doi.org/https://doi.org/10.1016/j.ijpharm.2018.05.067.

[46] V.S.S.A. Ayyadevara, K.-H. Roh, Calcium enhances polyplex-mediated transfection efficiency of plasmid DNA in Jurkat cells, Drug Delivery. 27 (2020) 805–815. https://doi.org/10.1080/10717544.2020.1770371.

[47] D. Pezzoli, E. Giupponi, D. Mantovani, G. Candiani, Size matters for in vitro gene delivery: investigating the relationships among complexation protocol, transfection medium, size and sedimentation, Scientific Reports. 7 (2017) 44134. https://doi.org/10.1038/srep44134.

[48] W. Zhang, X. Kang, B. Yuan, H. Wang, T. Zhang, M. Shi, Z. Zheng, Y. Zhang, C. Peng, X. Fan, H. Yang, Y. Shen, Y. Huang, Nano-Structural Effects on Gene Transfection: Large, Botryoid-Shaped Nanoparticles Enhance DNA Delivery via Macropinocytosis and Effective Dissociation, Theranostics. 9 (2019) 1580–1598. https://doi.org/10.7150/thno.30302.

[49] S. Behzadi, V. Serpooshan, W. Tao, M.A. Hamaly, M.Y. Alkawareek, E.C. Dreaden, D. Brown, A.M. Alkilany, O.C. Farokhzad, M. Mahmoudi, Cellular uptake of nanoparticles: journey inside the cell, Chemical Society Reviews. 46 (2017) 4218–4244. https://doi.org/10.1039/C6CS00636A.

[50] A.M.I. Lam, P.R. Cullis, Calcium enhances the transfection potency of plasmid DNA–cationic liposome complexes, Biochimica et Biophysica Acta (BBA) - Biomembranes. 1463 (2000) 279–290. https://doi.org/https://doi.org/10.1016/S0005-2736(99)00219-9.

[51] R.J. Epstein, B.J. Druker, J.C. Irminger, S.D. Jones, T.M. Roberts, C.D. Stiles, Extracellular calcium mimics the actions of platelet-derived growth factor on mouse fibroblasts, Cell Growth Differentiation. 3 (1992) 157–164. http://cgd.aacrjournals.org/cgi/content/abstract/3/3/157.

[52] T. Acri, N. Laird, S. Geary, Effects of calcium concentration on nonviral gene delivery to bone marrow-derived stem cells., J Tissue Eng Regen Med. (2019) 2256–2265.

[53] R. Khalifehzadeh, H. Arami, DNA-Templated Strontium-Doped Calcium Phosphate Nanoparticles for Gene Delivery in Bone Cells, ACS Biomaterials Science and Engineering. 5 (2019) 3201–3211. https://doi.org/10.1021/acsbiomaterials.8b01587.

[54] L.-H. Fu, Y.-R. Hu, C. Qi, T. He, S. Jiang, C. Jiang, J. He, J. Qu, J. Lin, P. Huang, Biodegradable Manganese-Doped Calcium Phosphate Nanotheranostics for Traceable Cascade Reaction-Enhanced Anti-Tumor Therapy, ACS Nano. 13 (2019) 13985–13994. https://doi.org/10.1021/acsnano.9b05836.

[55] H. Zhou, X. Wang, R. Tang, Could a mineralized state of avian flu virus be dangerous to humans?, Future Virology. 13 (2018) 79–81. https://doi.org/10.2217/fvl-2017-0142.

[56] X. Wang, D. Yang, S. Li, X. Xu, C.-F. Qin, R. Tang, Biomineralized vaccine nanohybrid for needle-free intranasal immunization, Biomaterials. 106 (2016) 286–294. https://doi.org/https://doi.org/10.1016/j.biomaterials.2016.08.035.

[57] S. Luo, P. Zhang, P. Zou, C. Wang, B. Liu, C. Wu, T. Li, L. Zhang, Y. Zhang, C. Li, A Self-Biomineralized Novel Adenovirus Vectored COVID-19 Vaccine for Boosting Immunization of Mice, Virologica Sinica. (2021). https://doi.org/10.1007/s12250-021-00434-3.

[58] A.A. Shitole, P.W. Raut, N. Sharma, P. Giram, A.P. Khandwekar, B. Garnaik, Electrospun polycaprolactone/hydroxyapatite/ZnO nanofibers as potential biomaterials for bone tissue regeneration, Journal of Materials Science: Materials in Medicine. 30 (2019) 51. https://doi.org/10.1007/s10856-019-6255-5.